11-1-1980

Green River Basin Optimization-Simulation Model

H. Yazicigil

G. H. Toebes

M. H. Houck

TECHNICAL REPORT 137

GREEN RIVER BASIN OPTIMIZATION-SIMULATION MODEL

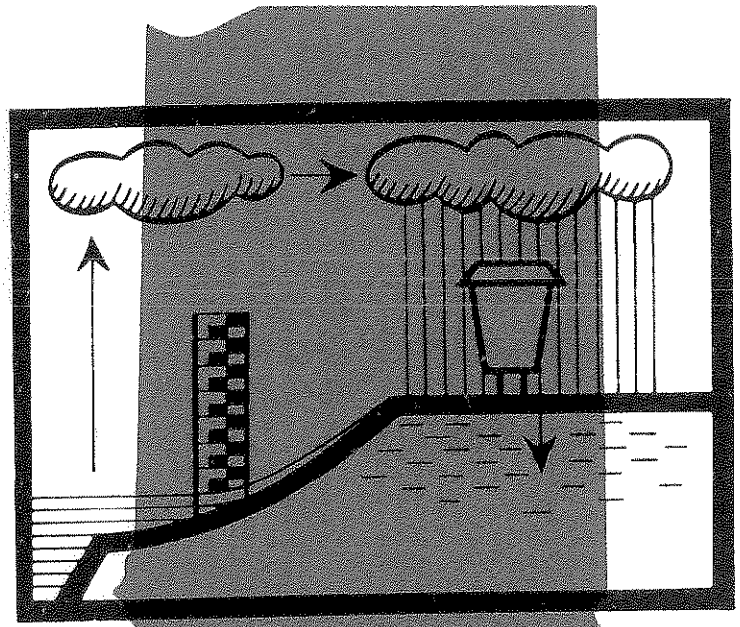

by

H. Yazicigil

G. H. Toebes

M. H. Houck

November 1980

PURDUE UNIVERSITY
WATER RESOURCES RESEARCH CENTER
WEST LAFAYETTE, INDIANA

Water Resources Research Center
Purdue University
West Lafayette, Indiana 47907

Evolutionary Approach to Reservoir Systems Management Using Forecasts

GREEN RIVER BASIN
OPTIMIZATION-SIMULATION MODEL

by

Hasan Yazicigil
Gerrit H. Toebes
Mark H. Houck

The work upon which this publication is based was supported in part by funds provided by the United States Department of the Interior, Office of Water Research and Technology, Project No. OWRT-B-094-IND, Washington, D. C., as authorized by the Water Research and Development Act of 1978 (PL95-467).

Completion Report for
Matching Grant Project OWRT-B-094-IND
Agreement No. 14-34-0001-8084

Purdue University Water Resources Research Center
Technical Report No. 137
November 1980

ADDENDA AND ERRATA

The following attributions are to be added in the text of Report #137:

* after deleting line 6 of page 5 (i.e. "are discussed herein."), read: "were discussed in detail by Tao et al. (1975), Toebes et al. (1976), and Rao et al. (1977). Only a brief summary of these studies is found herein."

* after deleting the sentence -- "In this chapter, ... are discussed." -- in lines 8, 9 and 10 of page 17, read: "The theoretical aspects of MIL model as well as parameter estimation methods and their application to the GRB system are discussed in detail by Yazicigil et al. (1979). Results from that study are summarized in this chapter."

* insert below the heading "7.1.1 Descriptive Component" on page 177: "Conclusions about the segmented models are discussed in detail by Yazicigil et al. (1979) and are summarized below for completeness." End of paragraph.

* Add to the Title of the Fig. 2.1 (pg 6): (From Tao et al., 1975)

* Add to the Titles of the Tables 2.1 (pg 7) and 2.2 (pg 11) and the Fig. 2.3 (pg 12): (From Rao et al., 1977)

* Add to the Titles of Fig. 2.2 (pg 8), and Tables 2.3 (pg 13), 2.4 (pg 14), 2.5 (pg 16):(From Toebes et al., 1976)

* Add to the Titles of Fig. 3.1 and 3.2 (pg 18), 3.3 (pg. 31), 3.4 (pg 35), 3.5 (pg 36), 3.6 (pg 38), 3.7 (pg 40), 3.8 (pg 43) and Tables 3.1 (pg 26), 3.2 (pg 42), 3.3 (pg 42): (From Yazicigil et al., 1979)

PAGE	LINE	CHANGE FROM	TO
19	last	system change	system may change
22	14	paramter u	parameter u
23	Eq. 3.16	$\sum_{i=}^{n} \sum_{j=0}^{k=1} Up_i(j)$	$\sum_{i=}^{n} \sum_{j=0}^{k-1} Up_i(j)$
	Eq. 3.17	i = i, 2, ...	i = i, 2, ...n
25	Equation	[....]	[....] (3.20)
	Eq. 3.20	(3.20)	(3.2])
36	Heading	GRBSYS1 - OLS	GRBSYS1 - CLS
45	24	have develop-d	have developed

PAGE	LINE	CHANGE FROM	TO
51	16	normative component	prescriptive component
55	21	reservoir inflow	reservoir inflows
57	3	must equal the	must be equal to the
	12	$RO^*(t+1)$	$R)(t+1)^*$
58	8	upper bond	upper bound
61	6	where RO(t+1) is	where $\dot{RO}(t+1)$ is
63	13	constrain set	constraint set
66	17	many reservoir	many reservoirs
76	12	GRB reservoir	GRB reservoirs
95	3	Z_2 - values	Z_2 values
116	11	namely 38.4%	namely -38.4%
159	19	$RO^*(t+1))$	$RO(t+1)^*)$
162	6	potential conditions	potential editions
166	18	four four tributary	four tributary

PREFACE AND ACKNOWLEDGMENTS

This report is the seventeenth in a series of publications that record the development of a family of models intended as an aid in the daily operation of and related long-range studies for a four-reservoir system in the Green River Basin, Kentucky. The system is operated by the Reservoir Regulation Section, Louisville District Office, Corps of Engineers. Inter-system coordination is provided by the Reservoir Control Center staff of the Cincinnatti Division Office, Corps of Engineers. Through the years the work has been funded by the Office of Water Resources Research and Technology (OWRT), Department of the Interior; by the Corps of Engineers, Department of the Army; and by Purdue University, West Lafayette, Indiana, via research fund matching arrangements. This Report No. 137 and its companion Report No. 136 represent the Completion Report of an OWRT Matching Grant Project B-094-IND. Report No. 137 text is substantially the same as the Ph.D. thesis by Hasan Yazicigil, entitled "Optimal Operation of a Reservoir System Using Forecasts."

The authors appreciate the opportunities for meaningful work made possible by the research funds provided by the above-named sponsors. They appreciate the sustained administrative support offered by Dr. Dan Wiersma, Director of the Purdue Water Resources Research Center. They owe gratitude to all who worked on previously reported project results incorporated in this study and whose contributions may be inferred from the earlier reports referenced herein.

The reported work would not have been possible without the ready support from Corps of Engineers' staff members, especially Mr. Robert A. Biel, Chief, Reservoir Regulation Section, Louisville, and Mr. Ronald A. Yates, Chief, Reservoir Control Center, Cincinnatti.

We thank Mrs. Kathy Scholl for her typing of this report.

ABSTRACT

The present study concerns the optimal operation of an existing multi-purpose multireservoir system using forecasts. An optimization-simulation model was constructed for a system of four flood control reservoirs in the Green River Basin, Kentucky, having recreation and low-flow augmentation as secondary objectives. The resulting model, called GRBOPM2, is designed for use in real-time as well as in long-run operations studies.

GRBOPM2 consists of descriptive and prescriptive components. Its descriptive component consists of a segmented model comprising nine multi-input linear (MIL) models of the river system downstream of the four reservoirs. The prescriptive component is largely in the form of an operating policy algorithm that involves repeated solution of a mathematical program. The optimization technique employed to solve the mathematical program is Linear Programming.

Each of the nine MIL model components of the segmented model represents a routing model for a reach between control stations. These models accept reach inflow, gaged tributary inflow(s), and rainfall over the ungaged side inflow area as inputs. Their outputs are the reach outflows. Three approaches to MIL-model construction were investigated. The results showed that a constrained linear systems estimation method gave better results than the ordinary least-squares method. The addition of an error model further improved the forecasting performance of the models.

The development of the operating policy component involved an investigation of goals and priorities for reservoir operation. To that end the state variables of the system associated with the reservoirs and with the control stations were divided into time-varying target or ideal values or ranges. Deviations from the ideal state vector were then divided into various zones and different penalties

were associated with different zones. By aggregating these penalties over an operating horizon, most of the goals and priorities for reservoir operation were commensurated into a overall system's measure of effectiveness.

The use of GRBOPM2 model in long-run reservoir operations studies has been demonstrated; system's responses under various operating and hydrologic conditions were obtained. In particular, trade-off curves between various system's objectives were generated both for the winter and summer seasons by using historical hydrologic as well as synthetic model input data.

The use of GRBOPM2 in real-time operations has been discussed also. It involves the use of forecast data during an operating horizon and the performing of sensitivity analyses of operating decisions with respect to changes in those forecasts. The results obtained from the model are represented in an integrated set of graphs and tables that appropriately shows the recommended optimal release decisions and the resulting state of the system at the reservoirs and control stations throughout the operating horizon.

The GRBOPM2 model, besides being computationally efficient, is flexible to allow the examination of the operation of a complex reservoir-river system for a variety of operational policies. Specific to the approach in designing the GRBOPM2 algorithm is that penalty weights and target levels and zones are among the input variables for each time step. This provides for the flexibility needed in real-time operations.

TABLE OF CONTENTS

LIST OF TABLES

LIST OF FIGURES

Page

Page

I. INTRODUCTION

1.1 ORIGIN AND SCOPE OF THE STUDY

Initial efforts to support and improve the planning and operation of reservoir systems by use of digital computation and the systems-analytic approaches it supports, commenced some two decades ago. Early in this evolution the attention of academic researchers shifted to methodology development. The application of systems analysis tools tended to be restricted to hypothetical problems. Even where real hydrologic data were used, the examined systems and their operation tended to be far removed from actual operations problems.

By contrast the work done in this area by staff of federal agencies tended towards generalizing proven planning and analysis methods. Outstanding and widely known results were produced by the staff of the Hydrologic Engineering Center, Corps of Engineers, for example. Until relatively recently efforts by practitioners involved few if any of the optimization tools promoted by analytical researchers. Notable exceptions are the efforts undertaken by Tennessee Valley Authority and Central Valley Project staffs.

A number of researchers have recognized for some time that reservoir systems are too complex to adequately model their operation within the framework of typical optimization models. They concluded that it would be necessary to account for numerous system and systems operation characteristics by means of a simulation model constructed on the basis of historical operations of the system in question. Such a simulation model might then be combined profitably with a formal optimization model in the effort to facilitate the reservoir systems operations task and to improve the analysis of such operations as well as related planning-type studies.

The work reported herein deals, in a case-study context, with the problem of grafting a reservoir operation's optimization model onto a reservoir

simulation model. Its origins are found in a five-reservoir systems operations study undertaken for the Upper-Wabash Basin in Indiana. Its emphasis was on incorporating existing operation rules into a simulation model and on maintaining a linear simulation model structure in order to facilitate the use of linear programming in the attempt to obtain a workable prescriptive operations model.

The case study system that was involved in the present study is a group of four flood control reservoirs in the Green River Basin, Kentucky. This system is regulated by the Reservoir Control Section at the Louisville District Office of the Corps of Engineers. Starting in 1974 with data digitization efforts, a model building effort has been maintained since then. Much of that work, reported in some 15 reports, does underlie and is incorporated in the present study, the result of which is a "second iteration Green River Basin (Reservoir) Operations Model" or GRBOPM2, for short. This model family is now ready for testing by the aboved-named agency staff. The structure and the visualized potential of GRBOPM2 are detailed herein.

1.2 ORGANIZATION OF AND GUIDELINES FOR THE STUDY

The GRBOPM2 model may be thought of as being divided into an optimization algorithm that imposes all necessary field operations constraints and a descriptive model of the simulation type, having a time step of one day, and called GRBSYS. GRBSYS is composed of sub-models, each of which is linear.

GRBSYS is used to generate the short-run consequences of recent and forecasted precipitation and past and proposed future releases from the four reservoirs. The releases constitute the four decision variables of the optimization component of the overall model, called GRBOPM2.

From the outset the principle was adopted that the weights selected to commensurate and hence to aggregate all operations effects should be part of a daily systems specification vector. Reservoir operators in their role as

decision makers when it comes to real-time operations should be able to readily alter these weights if the model is to be an effective aid in such operations.

II. DESCRIPTION OF THE GREEN RIVER BASIN SYSTEM AND ITS DATA BASE

The general information needed for the operations study of GRB system is rather varied and it covers data on hydrology as well as man-made structures. Description of the basin, and the characteristics and availability of the data are discussed herein.

2.1 DESCRIPTION OF BASIN

The Green River Basin, covering 9,230 mi^2 and roughly rectangular in shape, lies largely in West-Central Kentucky (see Figure 2.1). It is a subbasin of the Ohio River. The terrain is gently rolling with 300 ft. high hills and 150 ft. deep river valleys. The region is subject to frequent temperature changes and occasional intense precipitation caused by storms originating in the Gulf of Mexico. Late winter and early spring are the periods of high run-off. Although localized summer storms can be intense, they do not lead to basin wide flooding. The average annual precipitation is 47 inches.

2.2 STREAMS AND RESERVOIRS

Data related to streams and reservoirs in the Green River Basin are shown in Table 2.1. There are six main tributaries of the Green River; among these the Barren River is the principal tributary. It is about 139 miles long and has a 2262 square mile drainage area.

There are four reservoirs in the Green River Basin; namely, Green, Nolin, Barren, and Rough Reservoirs. The locations of these reservoirs are shown also in Figure 2.1. The four reservoirs have considerable storage space, ranging from 13 to 20 inches of runoff.

A schematic representation or systems graph of the reservoir-river system is shown in Figure 2.2. It portrays the relative locations of the reservoirs

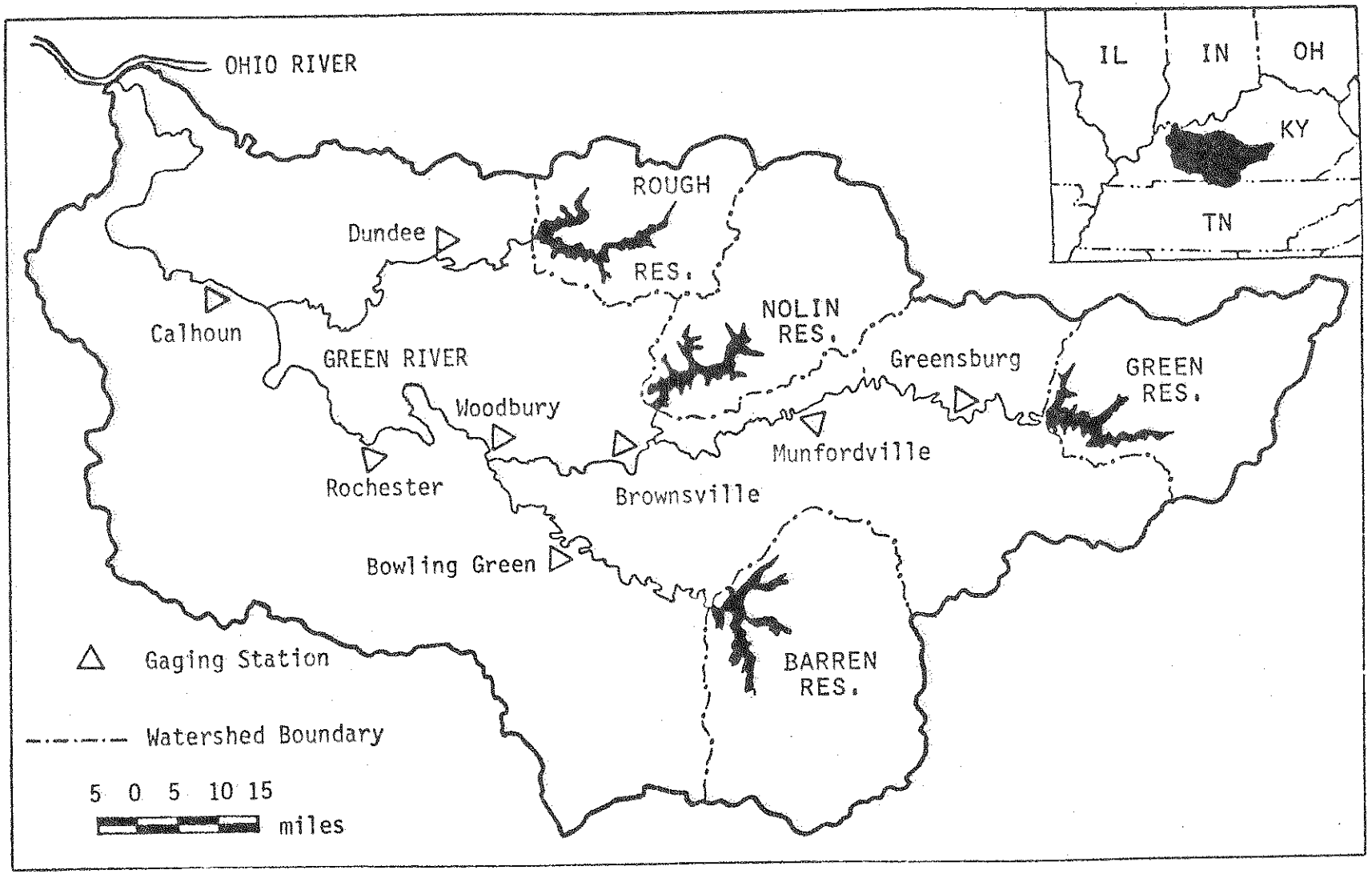

FIGURE 2.1 Green River Basin Reservoir System, Ky.

Table 2.1 Pertinent Data for Streams and Reservoirs in the Green River Basin, Kentucky

Miles Above Mouth of Green River	Stream	Length (miles)	Drainage Area (sq. mi)	Reservoirs			
				Miles Above Mouth of Stream	Controlled Drainage Area (sq. mi)	Storage Capacity (inches)	Year Finished
-	Green River	370	9229	305.7	682	19.89	1968
28.4	Panther Creek	about 59	374	-	-	-	-
55.0	Pond River	about 100	799	-	-	-	-
71.3	Rough River	157	1081	89.2	454	13.81	1960
108.6	Mud River	55	375	-	-	-	-
149.5	Barren River	139	2262	79.2	940	16.26	1964
183.5	Nolin River	125	727	7.8	703	16.25	1963

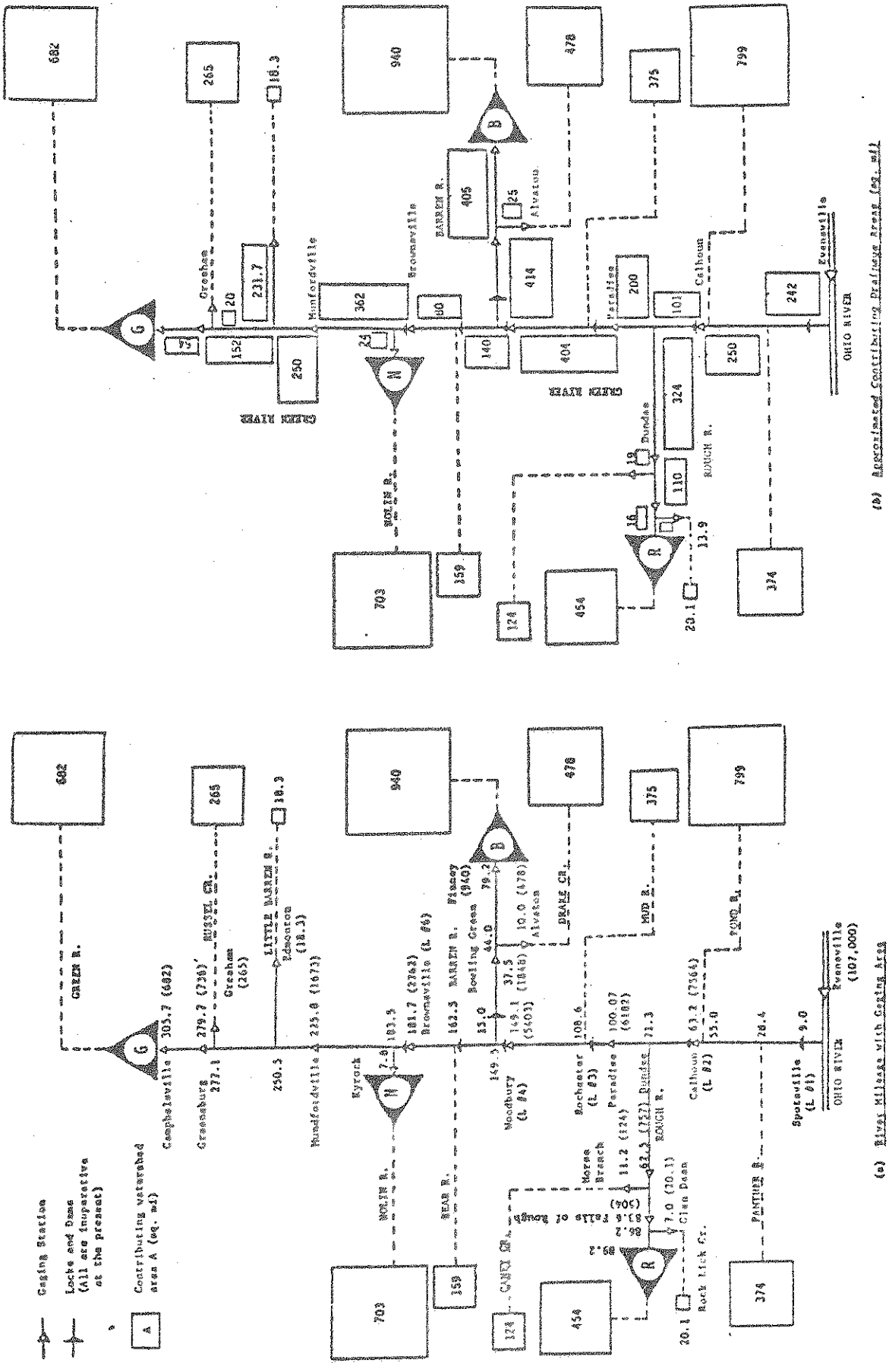

Figure 2.2 Systems Graph of the Green River Basin Reservoir System

and of the gaging stations. It also shows the approximate sizes of their contributing drainage areas.

2.3 OPERATION OF THE GRB RESERVOIR SYSTEM

The model developed for this study is intended as an aid in the operation of the four GRB reservoirs. Past operations of these reservoirs have been described in detail elsewhere (Toebes, Rukvichai, Lin, 1976; and Toebes and Rukvichai, 1978). The Corps of Engineers, U. S. Army is the agency responsible for the operation of the reservoirs in the basin.

The primary objective in the operation of each of the GRB reservoirs is flood control in the Green River Basin and in the downstream area of the Ohio River. The secondary objectives include recreation, low flow augmentation, and water quality.

2.4 RESERVOIR CHARACTERISTICS

In order to build an optimization-simulation model for the Green River Basin reservoirs, the storage-elevation-surface area relationships were needed. These functions expressed in polynomial equations were already developed by Rukvichai (1977) for each of the GRB reservoirs:

$$S = \sum_{m=0}^{M} a_m E^m \tag{2.1}$$

$$A = \sum_{m=0}^{M} b_m E^m \tag{2.2}$$

where S = reservoir storage in ac-ft; A = reservoir surface area in acres; E = reservoir elevation in ft above mean sea level; a_m = polynomial coefficient of m^{th} order for storage; b_m = polynomial coefficient of m^{th} order for surface area; M = maximum order of the equations.

Equations 2.1 and 2.2 were fitted to the data of each reservoir by the least squares criterion in order to estimate the polynomial coefficients a_m

and b_m. The estimated parameters along with the regression criterion, R^2, are given in Table 2.2. Figure 2.3 shows the data for the storage-elevation-surface area relationships plots against the fitted polynomial curves. The plots confirm the accuracy of the fitting as shown by the regression coefficients of 99.99% in Table 2.2.

2.5 GAGING STATION, STREAMFLOW, AND PRECIPITATION DATA

In order to build the flow simulation component of the GRBOPM2 model, the GRB reservoir-river system was decomposed into components that are largely determined by the location of gaging stations. Some of these gaging stations are being used as the system's main or local control stations; they are given substantial weight in operating the four reservoirs.

In the Green River Basin, there are 27 gaging stations. Most of them are being operated by the United States Geological Survey. Some are operated by the Corps of Engineers. The locations of these gaging stations in the Green River Basin together with the period of data availability and principal statistics, are shown in Table 2.3.

The quality of these daily discharge data ranges, as rated by the USGS, from excellent to fair (95 percent of daily discharges are within 5 to 15 percent). The accuracy of these data depends primarily on the stability of the stage-discharge relationships at gaging stations and the accuracy of observations of the stages, reasonably frequent measurements of discharge, and interpretation of records. Often substantial loss of accuracy is caused by backwater effects. The use of a base gage and auxiliary gages does not fully compensate for flow field dynamics. At most gaging stations, the stage-discharge relationship is also affected by ice flow during the winter.

There are 43 stations located in the Green River Basin at which daily climatological data, including precipitation data, are recorded. Table 2.4

Table 2.2 Fitted Polynomial Equation Coefficients for Storage-Elevation-Surface Area Relationships for Green River Basin Reservoirs

Reservoir	Storage-Elevation Curves			Surface Area-Elevation Curves		
	R^2 M	Order m	a_m	R^2 M	Order m	b_m
Rough River Reservoir	99.99 / 3	0	-2.9600244×10^{7}	99.99 / 3	0	-2.2472623×10^{6}
		1	2.0403855×10^{5}		1	1.3940344×10^{4}
		2	-4.7077855×10^{2}		2	-2.9010603×10
		3	3.6337791×10^{-1}		3	2.0283986×10^{-2}
Nolin River Reservoir	99.99 / 4	0	1.1336309×10^{7}	99.99 / 4	0	3.3093375×10^{6}
		1	-1.2486259×10^{5}		1	-2.5466376×10^{4}
		2	5.1156465×10^{2}		2	7.3745794×10
		3	$-9.2321451 \times 10^{-1}$		3	$-9.5615399 \times 10^{-2}$
		4	6.1925434×10^{-4}		4	4.7091808×10^{-5}
Barren River Reservoir	99.99 / 4	0	3.1485398×10^{8}	99.99 / 4	0	1.3213236×10^{7}
		1	-2.2776856×10^{6}		1	-9.6959031×10^{4}
		2	6.2387489×10^{3}		2	2.6651810×10^{2}
		3	-7.6931803		3	$-3.2576203 \times 10^{-1}$
		4	3.6155171×10^{-3}		4	1.4972358×10^{-4}
Green River Reservoir	99.99 / 4	0	6.4768566×10^{8}	99.99 / 4	0	-6.7981049×10^{7}
		1	-4.0663433×10^{6}		1	3.9095999×10^{5}
		2	9.5991164×10^{3}		2	-8.4081127×10^{2}
		3	-1.0106039×10		3	8.0097941×10^{-1}
		4	4.0069600×10^{-3}		4	$-2.8494495 \times 10^{-4}$

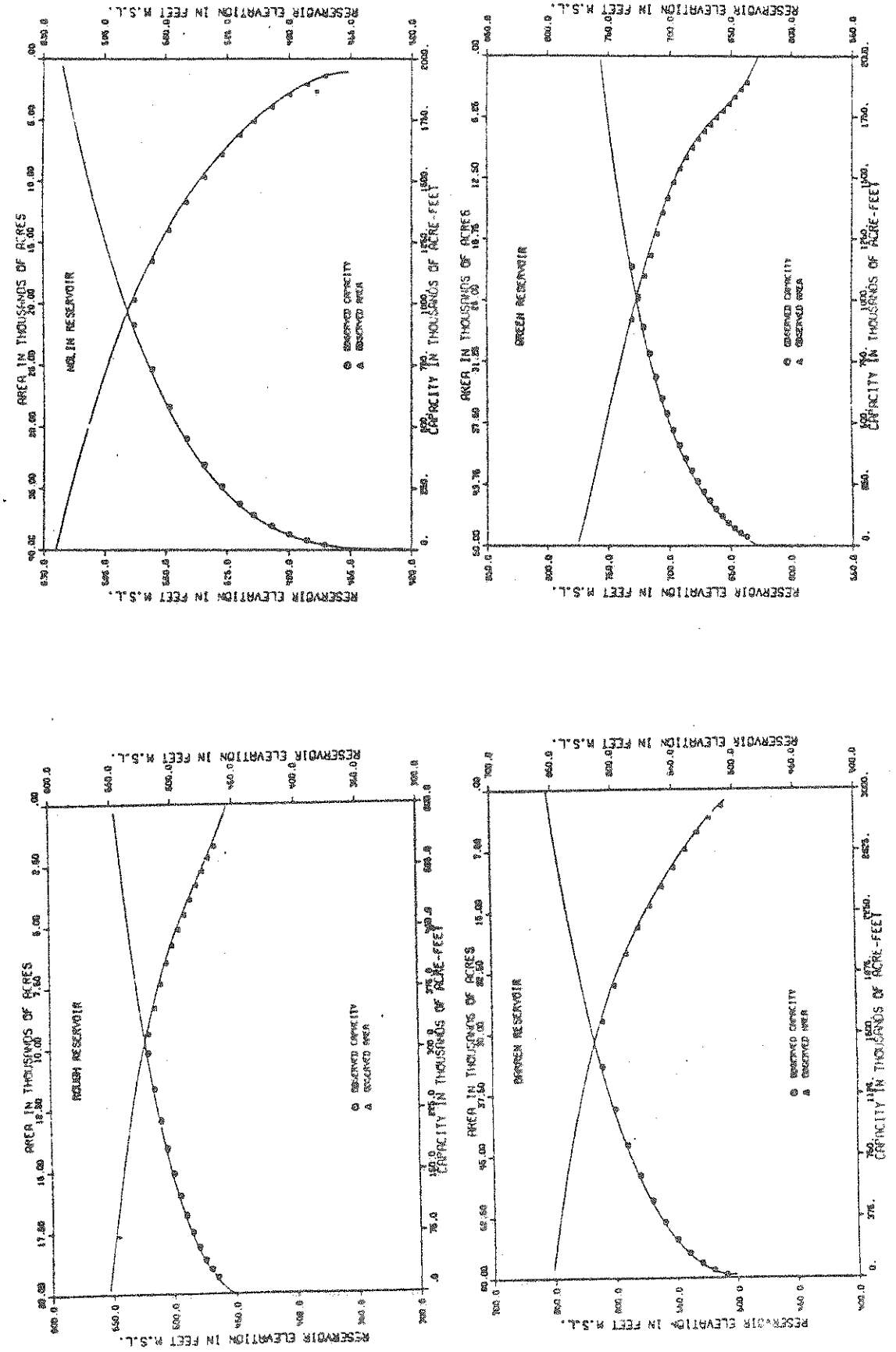

Figure 2.3 Storage-Elevation-Surface Area Curves for Green River Basin Reservoirs

Table 2.3 Availability of Streamflow Data for the Green River Basin

Flow Segment Number	USGS Number	Station Name	Stream Name	Drainage Area Sq. Mi.	Discontinued as of 1972	Period of Data Availability	Statistics of Discharge, cfs			Period of Statistics
							Mean	Max	Min.	
1	3316500	Paradise	Green River	6182	no	1961-1972	8600	107000	250	1939-1950, 1960-1972
2	3317500	Westview	North Fork Rough River	42	no	1955-1972	35.8	3890	0	1954-1972
3	331820	Glen Dean	Rock Lick Creek	20	yes	1957-1971	24.9	8720	0	1956-1971
4	3318500	Falls of Rough	Rough River	504	no	1949-1972	711		6	1939-1972
5	3318800	Horse Branch	Caney Creek	124	no	1957-1972	157	10000	0	1956-1972
6	3319000	Dundee	Rough	757	no	1941-1972	963	20000	8.1	1939-1972
7	3320000	Calhoun	Green River at Lock 2	7564	no	1931-1972	10620	208000	280	1930-1972
8	3305000	McKinney	Green River	22.4	no	1952-1973	30.7	13700	0	1951-1972
9	3306000	Campbellsville	Green River	682	no	1964-1974	907	29200	0.83	1930-1932, 1963-1972
10	3306500	Greensburg	Green River	736	no	1940-1974	1081	60600	0.4	1939-1972
11	3307000	Columbia	Russell Creek	188	no	1940-1974	272	16700	0.4	1939-1972
12	3307100	Gresham	Russell Creek	265	no	1965-1974	411	13500	5.2	1964-1972
13	3307500	Edmonton	South Fork Little Barren River	18.3	no	1942-1972	26.3	2970	0	1941-1972
14	3308500	Munfordville	Green River	1673	no	1938-1974	2575	76800	39	1915-1922, 1927-1931 1936-1937, 1937-1972
15	3309500	Hodgenville	McDougal Creek	5.34	yes	1954-1971	7.01	2890	0	1953-1971
16	3310000	Hodgenville	North Fork Nolin River	36.4	no	1942-1973	46.3	9380	0	1941-1972
18	3310400	Priceville	Bacon Creek	85.4	no	1960-1974	51.1	2610	4.4	1959-1972
19	3311000	Kyrock	Nolin River	707	no	1961-1974	836	22700	0	1930-1932, 1939-1950 1960-1972
20	3311500	Brownsville	Green River at Lock 6	2762	no	1939-1974	4092	120000	120	1924-1931, 1936-1937 1938-1972
21	3313000	Finney	Barren River	940	no	1961-1974	1383	78000	20	1941-1950, 1960-1972
22	3313700	Franklin	West Fork Drakes Creek	110	no	1969-1974	----	9930	6.3	1968-1972
23	3314500	Bowling Green	Barren River	1848	no	1939-1974	2397	85000	44	1938-1972
24	3315500	Woodbury	Green River at Lock 4	5403	no	1938-1974	7719	205000	200	1936-1937, 1937-1972
25	3320500	Apex	Pond River	194	no	1942-1974	257	21800	0	1940-1972
26	3322000	Evansville	Ohio River	107000	no	1964-1972	130300	1410000	---	1936-1972
27	3314000	Alvaton	Drakes Creek	478	yes	1965-1971	688	96400	9	1939-1971

Table 2.4 List of Climatological Stations and Daily Precipitation Data Availability

Precip Segment Number	NWS NO.	Name of Station	Operated by	Location		Period of Precip Data availability
				Lat.	Long.	
32	422	Barren River Res.	NWS	36-54	86-08	1964 - 1972
33	490	Beaver Dam	NWS	37-25	86-52	1964 - 1972
34	854	Bonnieville	NWS	37-23	85-54	1964 - 1966
35	909	Bowling Green Airport	NWS	36-58	86-26	1964 - 1972
36	1047	Brownsville	NWS	37-12	86-16	1964 - 1972
37	1227	Calhoun Lock 2	NWS	37-32	87-16	1964 - 1972
38	1256	Campbellsvile	NWS	37-20	85-21	1964 - 1972
39	1294	Caneyville	NWS	37-25	86-30	1964 - 1972
40	1406	Cecilia	NWS	37-40	85-57	1964 - 1972
41	2358	Dundee	NWS	37-33	86-43	1964 - 1972
42	2366	Dunmor	NWS	37-05	87-00	1964 - 1972
43	2469	Edmonton	NWS	37-00	85-37	1964 - 1972
44	3036	Franklin 1 E	NWS	36-43	86-34	1964 - 1972
45	3246	Glasgow WKAY	NWS	37-00	85-55	1964 - 1972
46	3252	Glendale 1 E	NWS	37-36	85-54	1964 - 1972
47	3430	Greensburg	NWS	37-15	85-30	1964 - 1972
48	3451	Greenville 2 W	NWS	37-12	87-12	1964 - 1972
49	3652	Hartford 6 NW	NWS	37-32	86-54	1964 - 1972
50	3929	Hodgenville-Lincoln National Park	NWS	37-32	85-44	1967 - 1972
51	4165	Irvington	NWS	37-53	86-17	1964 - 1972
52	4703	Lietchfield 2 N	NWS	37-31	86-16	1964 - 1972
53	4755	Liberty	NWS	37-21	84-55	1964 - 1972
54	5067	Madisonville 1 SE	NWS	37-19	87-29	1964 - 1972
55	5097	Mammoth Cave Park	NWS	37-11	86-05	1964 - 1972
56	5438	Millerstown	NWS	37-27	86-03	1964 - 1972
57	5684	Munfordville	NWS	37-16	85-53	1964 - 1972
58	5834	Nolin River Res.	NWS	37-17	86-15	1965 - 1972
59	6155	Paradise Steam Plant	NWS	37-16	86-59	1964 - 1972
60	6882	Rochester Lock 3	NWS	37-13	86-54	1964 - 1972
61	6988	Rough River Dam	NWS	37-37	86-30	1965 - 1972
62	7049	Russelville	NWS	36-52	86-53	1964 - 1972
63	7215	Scottsville 3 SSW	NWS	36-44	86-13	1964 - 1972
64	7234	Sebree	NWS	37-36	87-32	1964 - 1965
65	7800	Summer Shade	NWS	36-53	85-43	1964 - 1972
66	8824	Woodbury Lock 4	NWS	37-11	86-38	1964 - 1972
67		Green River (Dam)	COE			1966 - 1972
68		Merrimac	COE			1968 - 1072
69		Russel Spring	COE			1967 - 1972
70		Argyle	COE			1968 - 1972
71		Buffalo	COE			1964 - 1972
72		Lafayette	COE			1963 - 1973
73		Barren Dam	COE			1973 - 1973
74		Nolin Dam	COE			1973 - 1973

Remark - The data were obtained from the source indicated in the "Operated by" column.

lists these stations, their location, and the availability of daily data. Thirty-five of these stations are being operated by the National Weather Service and data could be obtained in digitized form from NWS. The remaining Corps of Engineers station records were in written form and were digitized for the GRB model studies.

Daily rainfall and runoff data were stored in a data base in the form of permanent files (disc) and magnetic tapes. The data base is designed such that the data can be retrieved and used in an efficient and systematic manner. More details concerning the construction and the uses of the GRB Data Base can be found elsewhere (Toebes, Rukvichai, and Lin, 1976; Steven, Rao, Toebes, and Chassiakos, 1978).

The optimization-simulation model developed for the GRB system incorporates an operating policy component. In order to develop that component all past operations data for the GRB system were analyzed. These data consist of reservoir elevations and releases which were obtained from so called Dam Tender Reports. Like the rainfall and runoff data, these data were also stored in the GRB Data Base.

2.6 STAGE-DISCHARGE RELATIONSHIPS

The regulation schedules for GRB reservoirs given in Appendix A show that each reservoir has one or two local control stations. They are gaging stations at Glen Dean and Horse Branch (used in operating Rough Reservoir), Alvaton (for Barren Reservoir), Munfordville (for Nolin Reservoir), and Gresham (for Green Reservoir). The stages at these gaging stations dictate the maximum allowable releases from each reservoir during critical flood periods. Since the model uses flow data, it is necessary to convert stage data into flow data. This requires a set of equations representing the stage-discharge rating curves of the gaging stations at Gresham, Alvaton, and Munfordville. Glen Dean and

Horse Branch data were already in the form of flow data. The three rating equations of which the parameters were estimated by the least squares method, are shown in Table 2.5.

Table 2.5 Stage-Discharge Relationships for GRB Local Control Stations

Local Control Stations	Stage-Discharge Equations	Range
Munfordville	$Q = \left(\frac{S}{0.10213}\right)^{(1/0.5667)}$	
Alvaton	$Q = \left(\frac{S}{0.5041}\right)^{(1/0.4018)}$	$S \leq 27$
	$Q = \left(\frac{S}{1.3377}\right)^{(1/0.3017)}$	$S > 27$
Gresham	$Q = \left(\frac{S}{1.1388}\right)^{(1/0.3094)}$	

III. MULTI-INPUT LINEAR MODEL

A multi-input linear "MIL" model, is a correlative linear model. It enables one to utilize directly and simultaneously all relevant data series for the purpose of constructing a "black-box" systems model. The systems components to which the modeling techniques were applied in this study are river reaches and their corresponding watersheds. Thus the data series of interest are: tributary inflows, precipitation data, and the river reach inflow. The model can accept multiple tributary and rainfall inputs. In this chapter, the theoretical aspects of MIL model as well as parameter estimation methods and their application to the GRB system are discussed.

3.1 THEORETICAL ASPECTS

Adopting an MIL model of a system amounts to assuming that the output is linearly related to the inputs. Consider a hypothetical river reach shown in Figure 3.1. The inputs to the reach during the time periods t are: reach inflow $I(t)$; tributary inflows $T_r(t)$, $r = 1, 2, \ldots, s$; and rainfall measured at n raingages $P_i(t)$, $i = 1, 2, \ldots n$. The reach outflow is the streamflow $O(t)$. A more schematic representation is shown in Figure 3.2.

The system shown in Figure 3.2 is assumed to be linear, time invariant and deterministic. The general form of such a multi-input linear model of a river reach is:

$$O(t) = \sum_{j=0}^{k-1} u_I(j) \cdot I(t-j) + \sum_{r=1}^{s} \sum_{j=0}^{k-1} u_{T_r}(j) \cdot T_r(t-j) + \sum_{i=1}^{n} \sum_{j=0}^{k-1} u_{P_i}(j) \cdot P_i(t-j) \qquad (3.1)$$

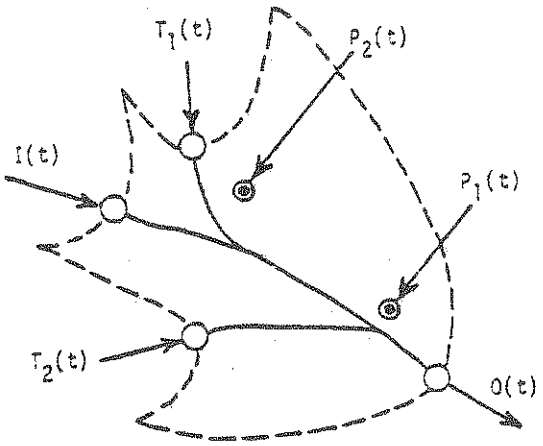

FIGURE 3.1 Channel Reach

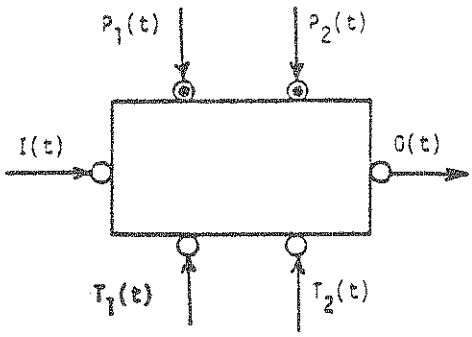

FIGURE 3.2 Representation of a Reach

where $u_I(j)$, $u_{T_r}(j)$ and $u_{P_i}(j)$ are the impulse response functions corresponding to the different inputs; s is the number of gaged tributary inflows; n is the number of gaged rainfall inputs; and j is a time lag.

The MIL model of Equation (3.1) can be written more compactly using the following vector notation:

$$\underset{\sim}{q} = \underset{\sim}{H}\underset{\sim}{u} \qquad (3.2)$$

where $\underset{\sim}{q} = [O(0), O(1), \ldots, O(T-1)]^t$ is a T-vector of outflow; $\underset{\sim}{u} = [\underset{\sim}{u}_1, \underset{\sim}{u}_{1+r}, \cdots, \underset{\sim}{u}_{1+s}, \underset{\sim}{u}_{1+s+i}, \cdots, \underset{\sim}{u}_N]^t$ is an (Nk) vector of impulse responses (N is the total number of inputs, i.e., N = 1+s+n and k is the number of impulse response ordinates); and $\underset{\sim}{H} = [\underset{\sim}{H}_1, \underset{\sim}{H}_{1+r}, \cdots, \underset{\sim}{H}_{1+s}, \underset{\sim}{H}_{1+s+i}, \ldots, \underset{\sim}{H}_N]$ is a (T, Nk) matrix of inputs in which r = 1, 2, ... s and i = 1, 2, ... n. The individual elements of $\underset{\sim}{u}$ are defined as: $\underset{\sim}{u}_1 = [u_I(o), u_I(1), \ldots u_I(k-1)]^t$, $u_{1+r} = [u_{T_r}(o), u_{T_r}(1), \ldots u_{T_r}(k-1)]^t$ and $\underset{\sim}{u}_{1+s+i} = [u_{P_i}(o), u_{P_i}(1), \ldots, u_{P_i}(k-1)]^t$. The individual elements of the matrix $\underset{\sim}{H}$, say for $\underset{\sim}{H}_1$, are defined as:

$$\underset{\sim}{H}_1 = \begin{bmatrix} I(o) & & & 0 \\ I(1) & I(o) & & \\ \cdot & \cdot & & \\ \cdot & \cdot & & \\ \cdot & \cdot & & \\ \cdot & \cdot & & \\ \cdot & \cdot & & \\ I(T-2) & I(T-3) & \cdots & I(T-k+1) \\ I(T-1) & I(T-2) & \cdots & I(T-k) \end{bmatrix}$$

Similarly the matrices $\underset{\sim}{H}_{1+r}$ and $\underset{\sim}{H}_{1+s+i}$ are formulated by using the symbols T_r and P_i instead of I.

Equation (3.2) represents an approximation of the physical system. The behavior of the system change because of factors unaccounted for in the

model (e.g., the effects of vegetation, temperature, cloud cover, moisture content, etc.). Such "behavior changes" make the system "non-stationary" and hence not representable by a fixed model. Moreover, the discharge and rainfall measurements at the gaging stations are affected by errors. Therefore, instead of Equation (3.2), the following expression for the multi-input linear model will represent the system better:

$$\underset{\sim}{q} = \underset{\sim\sim}{H}\underset{\sim}{u} + \underset{\sim}{\varepsilon} \tag{3.3}$$

where $\underset{\sim}{\varepsilon} = [\varepsilon(o), \varepsilon(1), \ldots, \varepsilon(T-1)]^t$ is a T-vector which includes both modeling and data errors.

3.2 PARAMETER ESTIMATION

The components of vector $\underset{\sim}{u}$ are related to the impulse response of the system. These components are also called "model parameters" or "parameters" which must be estimated. In this section we will discuss (a) the ordinary least squares and (b) a constrained linear systems estimation of $\underset{\sim}{u}$. A general discussion of parameter estimation techniques is found elsewhere (Bard, 1974; Natale and Todini, 1974, 1976).

3.2.1 Ordinary Least Square Estimation (OLS)

The length of each impulse response vector, k, must be selected before the parameters are estimated. Suppose for the moment that k is known and that all the vectors are of the same length k. The vector $\underset{\sim}{u}$ can be estimated by the method of least squares in which the following quadratic form is minimized:

$$\text{Min } J(\underset{\sim}{\varepsilon}) = \frac{1}{2}\,\underset{\sim}{\varepsilon}^t\,\underset{\sim}{R}^{-1}\,\underset{\sim}{\varepsilon} \tag{3.4}$$

where $\underset{\sim}{R}^{-1}$ must be a symmetric, positive definite matrix to ensure the existence of a minimum. Equation (3.4) can be written in terms of $\underset{\sim}{u}$ as follows:

$$\text{Min } [J(\underset{\sim}{u}) = \frac{1}{2}\,(\underset{\sim}{q} - \underset{\sim\sim}{H}\underset{\sim}{u})^t\,\underset{\sim}{R}^{-1}\,(\underset{\sim}{q} - \underset{\sim\sim}{H}\underset{\sim}{u})] \tag{3.5}$$

The necessary condition for the existance of an extreme is then obtained by taking the partial derivatives of (3.5) with respect to $\underset{\sim}{u}$ and equating those to zero, giving:

$$\frac{\partial J(\underset{\sim}{u})}{\partial \underset{\sim}{u}} = (\underset{\sim}{H}^t \underset{\sim}{R}^{-1} \underset{\sim}{H})\underset{\sim}{u} - \underset{\sim}{H}^t \underset{\sim}{R}^{-1} \underset{\sim}{q} = 0 \qquad (3.6)$$

The sufficient condition for a minimum is that:

$$\frac{\partial^2 J(\underset{\sim}{u})}{\partial \underset{\sim}{u}^2} = \underset{\sim}{H}^t \underset{\sim}{R}^{-1} \underset{\sim}{H} \qquad (3.7)$$

is positive definite. The least-square estimate of parameters $\underset{\sim}{u}$ can be obtained from (3.6).

$$\underset{\sim}{u} = (\underset{\sim}{H}^t \underset{\sim}{R}^{-1} \underset{\sim}{H})^{-1} \underset{\sim}{H}^t \underset{\sim}{R}^{-1} \underset{\sim}{q} \qquad (3.8)$$

If the varience V_ε of the error $\underset{\sim}{\varepsilon}$ is not known, one usually sets $\underset{\sim}{R} = \underset{\sim}{I}$ ($\underset{\sim}{I}$ = identity matrix). Inserting this into Equation 3.8 gives the following ordinary least square estimate of $\underset{\sim}{u}$:

$$\underset{\sim}{u}_{OLS} = (\underset{\sim}{H}^t \underset{\sim}{H})^{-1} \underset{\sim}{H}^t \underset{\sim}{q} \qquad (3.9)$$

where $\underset{\sim}{H}^t \underset{\sim}{H}$ is the autocorrelation matrix of the input and $\underset{\sim}{H}^t \underset{\sim}{q}$ is the cross-correlation vector of the input and the output (Eagleson et al., 1965).

3.2.2 Constrained Linear Systems Estimation (CLS)

The matrix $(\underset{\sim}{H}^t \underset{\sim}{H})$ in (3.9) is frequently ill-conditioned (Abadie, 1970). In addition Todini and Wallis (1977) have found that when N > 1 the error magnitudes due to the inversion become comparable to the values of the parameters that are to be estimated. Natale and Todini (1974) have shown that better estimators of $\underset{\sim}{u}$ are obtained by introducing equality and inequality constraints. The possible constraints that may be imposed in estimating $\underset{\sim}{u}$ are as follows:

i) The members in the $\underset{\sim}{u}$ vector cannot be negative, i.e., $\underset{\sim}{u} \geq 0$. Contrary to this concept, Boneh and Golan (1979) have proposed that unit-impulse response functions with negative ordinates are also capable of representing a real-world system. In the following discussion, it is assumed that all members of $\underset{\sim}{u}$ should be greater than or equal to zero.

ii) In many hydrologic applications it is also desirable to impose a set of linear constraints upon the response vector $\underset{\sim}{u}$ as follows:

$$\underset{\sim}{\underset{\sim}{G}}\underset{\sim}{u} = 1 \tag{3.10}$$

These constraints represent the condition of mass conservation. If the system under consideration is regarded as stationary or "time-invariant," then:

$$\sum_{j=0}^{k-1} u_{P_i}(j) = \Phi_i \qquad i = 1, 2, \ldots, n \tag{3.11}$$

with Φ_i a constant runoff coefficient which takes into account the water losses between the inputs associated with precipitation at i and the resulting output.

When reach inflow and tributary inflows are present, the conservation of mass relations read:

$$\sum_{j=0}^{k-1} u_I(j) = 1 \tag{3.12}$$

$$\sum_{j=0}^{k-1} u_{T_r}(j) = 1 \qquad r = 1, 2, \ldots, s \tag{3.13}$$

Under these constraints, the CLS estimates of the paramter $\underset{\sim}{u}$ are given by the following estimator (Todini and Wallis, 1977):

$$\text{Min } J(\underset{\sim}{u}) = \frac{1}{2}\,\underset{\sim}{u}^t\underset{\sim}{\underset{\sim}{H}}^t\underset{\sim}{\underset{\sim}{H}}\underset{\sim}{u} - \underset{\sim}{u}^t\underset{\sim}{\underset{\sim}{H}}^t\underset{\sim}{q} \tag{3.14}$$

subject to: $\underset{\sim}{u} \geq \underset{\sim}{0}$

$\underset{\sim}{\underset{\sim}{G}}\,\underset{\sim}{u} = \underset{\sim}{1}$

which can be solved by quadratic programming, provided that $J(\underset{\sim}{u})$ is convex.

The $\underset{\sim}{\underset{\sim}{G}}$-matrix in (3.14) is defined below. When there are no system inflows (i.e., only precipitation inputs $P_i(t)$ are present), $\underset{\sim}{\underset{\sim}{G}}$ is a (1,nk)-matrix for which the elements are:

$$g_{1,\,(i-1)k+j+1} = \frac{\sum_{\tau=0}^{T-j-1} P_i(\tau)}{\sum_{\tau=0}^{T-1} O(\tau)} \qquad (3.15)$$

$$i = 1, 2, \ldots, n \qquad j = 0, 1, 2, \ldots, k-1$$

The Equation (3.15) represents the following constraint:

$$\sum_{i=1}^{n} \sum_{j=0}^{k=1} u_{P_i}(j) \sum_{\tau=0}^{T-j-1} P_i(\tau) = \sum_{\tau=0}^{T-1} O(\tau) \qquad (3.16)$$

This constraint takes into account the water losses between the n precipitation inputs, P_i, and the output, O, if $P_i(\tau) = 0$ for $-k \leq \tau < 0$. Thus, the elements of $\underset{\sim}{\underset{\sim}{G}}$ are essentially the reciprocals of the runoff coefficients.

When, on the other hand, reach inflow and tributary flows are present, $\underset{\sim}{\underset{\sim}{G}}$ is an (s + 2, Nk)-matrix for which all elements are zero except for the following ones:

$$g_{1,\,j+1} = 1 \qquad j = 0, 1, 2, \ldots, k-1$$

$$g_{r+1,\,r(k)+j+1} = 1 \qquad r = 1, 2, \ldots, s$$

$$i = 1, 2, \ldots, n$$

$$g_{s+2,\,(i+s)k+j+1} = \frac{\sum_{\tau=0}^{T-j-1} P_i(\tau)}{\sum_{\tau=0}^{T-1} [O(\tau) - I(\tau) - \sum_{r=1}^{s} T_r(\tau)]} \qquad (3.17)$$

Equation (3.17) represents a worked-out version of the Equation (3.12) and (3.13) and the following water balance equation:

$$\sum_{i=1}^{n} \sum_{j=0}^{k-1} u_{P_i}(j) \sum_{\tau=0}^{T-j-1} P_i(\tau) = \sum_{\tau=0}^{T-1} [O(\tau) - I(\tau) - \sum_{r=1}^{s} T_r(\tau)] \qquad (3.18)$$

Equation (3.18) is a systems equation relating the reach inflow, a total of s tributary inflows, and a total of n precipitation inputs to the outflow discharge vector, provided $T \geq k$. For convenience, all the above equations have been written with k equal for all N inputs. The CLS program does permit one to vary k, however. Note that the first value of each impulse response vector (i.e., j=0) signifies an instantaneous effect of inputs on the output.

In the following it will be useful to employ a compact notation of the specific models obtained for individual river reaches. The representation below was devised by Rukvichai (1977). By way of example consider a river reach as shown in Figure 3.1; let the dependence of model output on the inflow I(t) be given by two terms in Equation (3.1), namely I(t-1) and I(t-2). Similarly, let the dependence of O(t) on tributary inflow $T_1(t)$ be given by three terms, namely $T_1(t)$, $T_1(t-1)$ and $T_1(t-2)$. Suppose that the second tributary inflow is represented by two terms, namely $T_2(t-1)$ and $T_2(t-2)$. Finally assume that the dependence on the precipitation at raingage 1 inputs is given by a single term $P_1(t)$, whereas the raingage 2 input dependency is represented by two terms, namely $P_2(t-1)$ and $P_2(t-2)$. In other words the system is considered representable by:

$$\begin{aligned} O(t) = {} & u_I(1)\ I(t-1) + u_I(2) \cdot I(t-2) + u_{T_1}(0) \cdot T_1(t) \\ & + u_{T_1}(1) \cdot T_1(t-1) + u_{T_1}(2) \cdot T_1(t-2) + u_{T_2}(1) \cdot T_2(t-1) \end{aligned} \qquad (3.19)$$

Equation (3.19) cont'd

$$+ u_{T_2}(2) \cdot T_2(t-2) + u_{P_1}(0) \cdot P_1(t) + u_{P_2}(1) \cdot P_2(t-1)$$

$$+ u_{P_2}(2) \cdot P_2(t-2)$$

More compactly one may denote the system responses by:

$$\begin{bmatrix} u_I(1) & u_{T_1}(0) & u_{T_2}(1) & u_{P_1}(0) & u_{P_2}(1) \\ u_I(2) & u_{T_1}(2) & u_{T_2}(2) & & u_{P_2}(2) \end{bmatrix}$$

and yet more compactly this can be represented by:

$$M \left\{ \begin{matrix} 1 & 0 & 1 & 0 & 1 \\ 2 & 2 & 2 & 0 & 2 \end{matrix} \right\} \qquad (3.20)$$

This notation is employed in Table 3.1.

3.3 MIL-MODEL APPLICATION TO GRB STREAMFLOW SYSTEM

The 9229 mi^2 Green River Basin (GRB) is roughly rectangular in shape. A systems graph of the GRB corresponding to the MIL model representation, is shown in Figure 3.3. As shown by solid hatchings, the GRB river system downstream of the four reservoirs has been decomposed into nine model components. These components represent the stream reaches between the gaging stations and their contributing watersheds. The gaging stations are used as system's control stations in operating the GRB reservoir system. There are four tributary watersheds which were not included in the MIL model representation. Their runoffs represent separate external inputs to one or another of the nine component models. These tributary watersheds are those of the local control stations at Gresham, Alvaton, Glen Dean and Horse Branch. Recently, Staab and Rao (1979) have developed unit hydrograph models for several of these gaged watersheds.

Table 3.1 Parameter Estimates and Statistics of Residuals of Models Whose Parameters are Estimated by OLS and CLS Methods

Reach No.	MIL-Model Representation	Pre. Stations for Avg. Local Rainfall Series	Final Models	Terms	Parameters by OLS Method	Parameters by CLS Method	Statistics of Residuals	Residuals Estimated by OLS Method	Residuals Estimated by CLS Method
							Mean	-10.7369	-0.6374
1	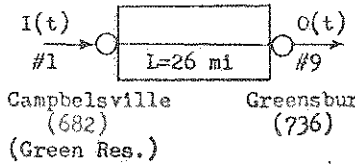	Green R. Dam Campbelsville Greensburg	$M\begin{pmatrix}0&0\\2&1\end{pmatrix}$	$U_I(0)$	0.5392	0.5182	Standard Dev.	286.8767	291.8191
				$U_I(1)$	0.5178	0.4818	Det.Coef.R^2	0.9630	0.9617
				$U_I(2)$	-0.0386	0.0000	Max.Pos.Err.	1459.7195	1556.3269
				$U_P(0)$	0.2888	0.3485	Max.Neg.Err.	-4191.5963	-4037.7574
				$U_P(1)$	0.1530	0.2325	% Err. Bet. Peaks	5.4851	3.1816
							Max.Obs.Flow	8340.00	8340.00
2	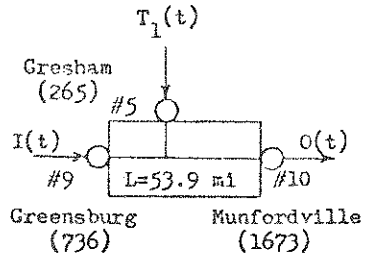	Greensburg Munfordville Edmonton Hodgenville Campbelsville Glasglow	$M\begin{pmatrix}1&0&1\\2&1&2\end{pmatrix}$	$U_I(1)$	0.9984	0.9301	Mean	-56.8876	-0.2788
				$U_I(2)$	0.1952	0.0699	Standard Dev.	905.0068	1550.9385
				$U_{T_1}(0)$	0.9341	0.3931	Det.Coef.R^2	0.9323	0.8011
				$U_{T_1}(1)$	1.8578	0.6069	Max.Pos.Err.	8397.9440	7313.6043
				$U_P(1)$	0.0255	0.2135	Max.Neg.Err.	-14214.5355	-15533.4985
				$U_P(2)$	0.0237	0.2016	% Err. Bet. Peaks	-21.2553	-28.8422
							Max.Obs.Flow	36400.0	36400.0

Table 3.1 (continued)

Reach No.	MIL-Model Representation	Pre. Stations for Avg. Local Rainfall Series	Final Models	Terms	Parameters by OLS Method	Parameters by CLS Method	Statistics of Residuals	Residuals Estimated by OLS Method	Residuals Estimated by CLS Method
3	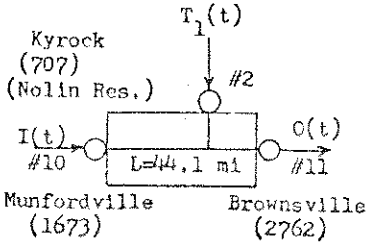	Munfordville Nolin R. Dam Mammoth Cave Brownsville	$M\{\begin{smallmatrix}0&0&0\\1&1&1\end{smallmatrix}\}$	$U_I(0)$ $U_I(1)$ $U_{T_1}(0)$ $U_{T_1}(1)$ $U_p(0)$ $U_p(1)$	0.6364 0.6410 0.7499 0.1858 0.0707 0.0189	0.1118 0.8882 0.7271 0.2729 0.2108 0.2735	Mean Standard Dev. Det.Coef.R^2 Max.Pos.Err. Max.Neg.Err. % Err. Bet. Peaks Max.Obs.Flow	31.1166 550.5322 0.9868 6604.1297 -5007.1291 9.2885 38500.000	-2.1655 1135.7979 0.9437 5794.8927 -7033.6232 -6.8005 38500.000
4	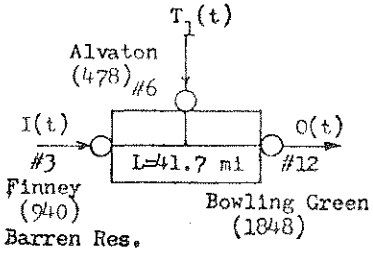	Barren R. Dam Bowling Green	$M\{\begin{smallmatrix}1&0&1\\2&2&2\end{smallmatrix}\}$	$U_I(1)$ $U_I(2)$ $U_{T_1}(0)$ $U_{T_1}(1)$ $U_{T_1}(2)$ $U_p(1)$ $U_p(2)$	1.1250 -0.1175 0.5316 0.9672 -0.0717 0.0071 0.0028	1.000 0.0000 0.3186 0.6814 0.0000 0.1309 0.1237	Mean Standard Dev. Det.Coef.R^2 Max.Pos.Err. Max.Neg.Err. % Err. Bet. Peaks Max.Obs.Flow	-13.7391 629.5068 0.9535 9149.3318 -9025.6845 0.0862 52000.000	-0.0541 1229.2476 0.8226 8291.327 -16710.030 -32.1347 52000.000

Table 3.1 (continued)

Reach No.	MIL-Model Representation	Pre. Stations for Avg. Local Rainfall Series	Final Models	Parameters Terms	Parameters OLS Method	Parameters CLS Method	Statistics of Residuals	Residuals Estimated by OLS Method	Residuals Estimated by CLS Method
5	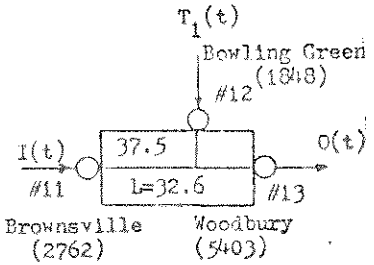	Brownsville	$M\begin{pmatrix}0&0&0\\1&1&1\end{pmatrix}$	$U_I(0)$	0.7028	0.0351	Mean	260.1107	-4.3255
		Bowling Green		$U_I(1)$	0.6624	0.9649	Standard Dev.	1633.4150	2662.3750
		Woodbury		$U_{T_1}(0)$	0.6254	0.0269	Det.Coef.R^2	0.9680	0.9151
		Russelville		$U_{T_1}(1)$	0.4222	0.9731	Max.Pos.Err.	10687.2493	14442.9296
		Leitchfield		$U_P(0)$	0.1011	0.2624	Max.Neg.Err.	-16590.0529	-17463.8610
		Nolin Res. Dam		$U_P(1)$	0.0401	0.3235	% Err. Bet. Peaks	16.5886	5.9155
							Max.Obs.Flow	59000.000	59000.000
6	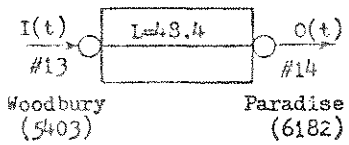	Woodbury	$M\begin{pmatrix}0&1\\1&2\end{pmatrix}$	$U_I(0)$	0.3381	0.0787	Mean	-132.9244	-4.9009
		Rochester		$U_I(1)$	0.7482	0.9213	Standard Dev.	2127.0708	2555.1536
		Dunmor		$U_P(1)$	0.0443	0.2114	Det.Coef.R^2	0.9538	0.9333
		Beaver Dam		$U_P(2)$	-0.0502	0.0921	Max.Pos.Err.	11279.0788	17873.4671
		Russelville					Max.Neg.Err.	-21353.3590	-21593.3256
		Paradise St.					% Err. Bet. Peaks	12.4417	5.5433
		Plant					Max.Obs.Flow	56000.000	56000.000

Table 3.1 (continued)

Reach No.	MIL-Model Representation	Pre. Stations for Avg. Local Rainfall Series	Final Models	Terms	Parameters by OLS Method	Parameters by CLS Method	Statistics of Residuals	Residuals Estimated by OLS Method	Residuals Estimated by CLS Method
7	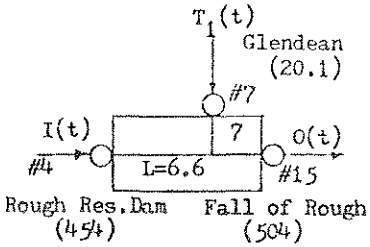	Rough Res. Dam	$M\{\begin{smallmatrix}0&0&0\\1&1&1\end{smallmatrix}\}$	$U_I(0)$	0.8184	0.7632	Mean	3.0978	-0.0361
				$U_I(1)$	0.1377	0.2368	Standard Dev.	91.3850	155.6596
				$U_{T_1}(0)$	2.3972	1.0000	Det.Coef.R^2	0.9792	0.9397
				$U_{T_1}(1)$	1.0537	0.0000	Max.Pos.Err.	1072.9718	594.6687
				$U_P(0)$	0.1583	0.3788	Max.Neg.Err.	-666.6895	-1615.9559
				$U_P(1)$	-0.0012	0.1097	% Err. Bet. Peaks	-17.7638	-51.3002
							Max.Obs.Flow	3150.000	3150.000
8	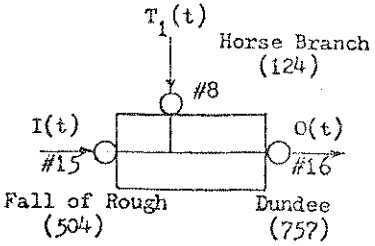	Rough Res. Dam Dundee	$M\{\begin{smallmatrix}0&0&0\\2&1&1\end{smallmatrix}\}$	$U_I(0)$	0.5544	0.2993	Mean	6.4527	-0.1387
				$U_I(1)$	0.6829	0.5840	Standard Dev.	229.8061	381.2446
				$U_I(2)$	-0.1404	0.1166	Det.Coef.R^2	0.9556	0.8779
				$U_{T_1}(0)$	0.8910	0.1693	Max.Pos.Err.	1232.3363	2108.1903
				$U_{T_1}(1)$	0.8688	0.8307	Max.Neg.Err.	-2284.0482	-1910.0828
				$U_P(0)$	0.0924	0.2621	% Err. Bet. Peaks	8.6806	-14.5834
				$U_P(1)$	0.0247	0.2277	Max.Obs.Flow	8270.000	8270.000

Table 3.1 (continued)

Reach No.	MIL-Model Representation	Pre. Stations for Avg. Local Rainfall Series	Final Models	Terms	Parameters by OLS Method	Parameters by CLS Method	Statistics of Residuals	Residuals Estimated by OLS Method	Residuals Estimated by CLS Method
9	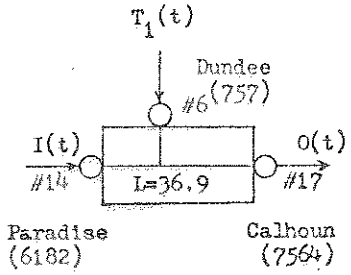	Dundee	$M\{\begin{smallmatrix}0&0&0\\1&1&1\end{smallmatrix}\}$	$U_I(0)$	0.3464	0.2882	Mean	-58.8318	-3.4145
		Rochester		$U_I(1)$	0.6458	0.7118	Standard Dev.	1528.0053	1590.8642
		Hartford		$U_{T_1}(0)$	1.2347	0.6766	Det.Coef.R^2	0.9799	0.9782
		Beaver Dam		$U_{T_1}(1)$	0.0356	0.3234	Max.Pos.Err.	8315.9941	8443.8271
		Calhoun		$U_P(0)$	0.0624	0.1275	Max.Neg.Err.	-9513.6622	-9973.0924
		Greenville		$U_P(1)$	0.0651	0.1341	% Err. Bet. Peaks	13.1140	13.4730
		Paradise St.					Max. Obs.Flow	49900.000	49900.000
		Plant							

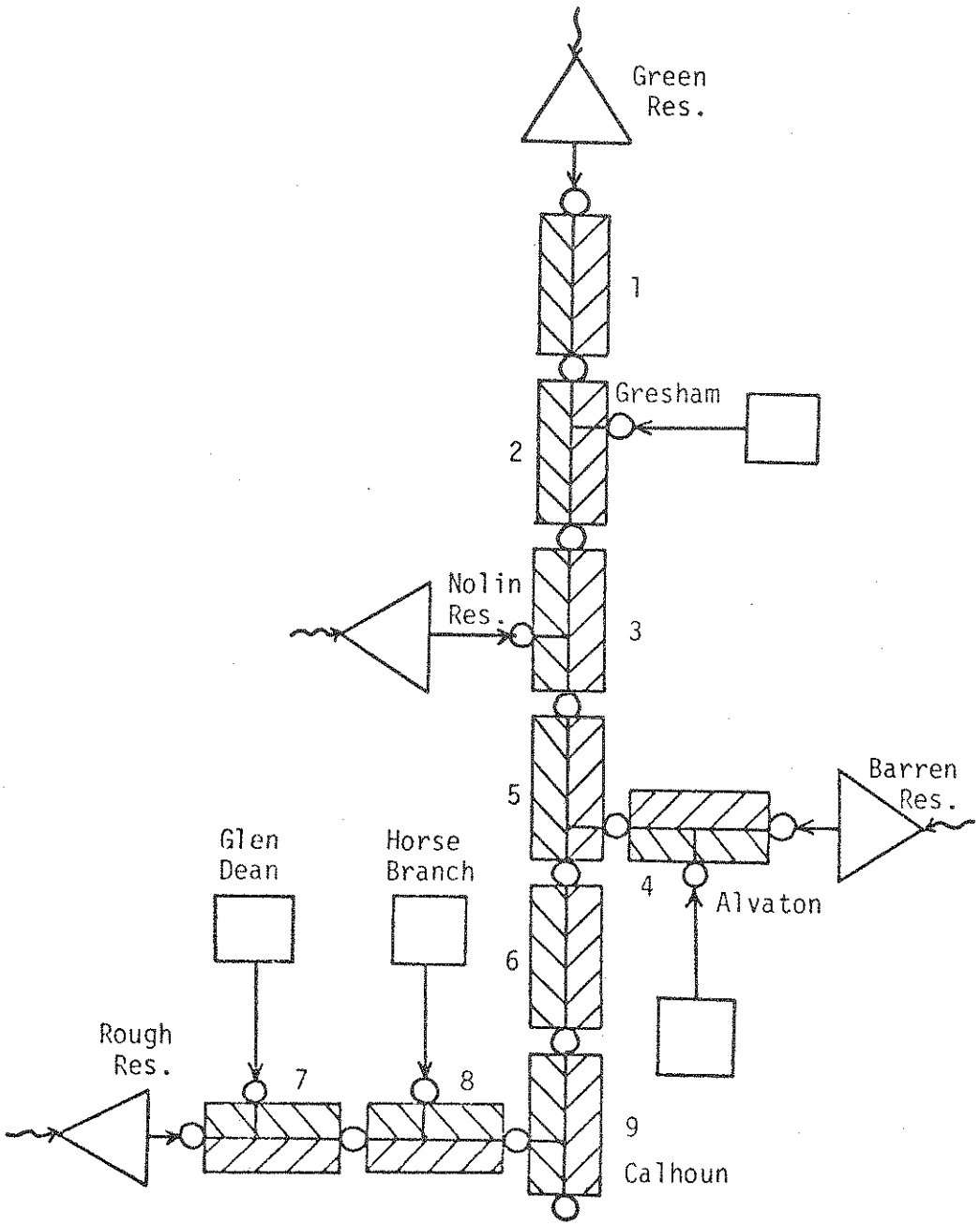

Figure 3.3 Systems Graph for the GRB System as Represented by MIL Models

3.3.1 Estimation of Model Parameters for GRB

Parameters of several preliminary models were estimated using both the OLS and CLS parameter estimation methods. Table 3.1 shows the black box model for each of the streamflow reaches along with the gaging stations that serve as input and output points. The symbols for inputs and outputs are as defined in Section 3.1. The drainage area for each gaging station or control station is shown in brackets just below its name. As there are no orographic or other reasons for weighing one nearby rain gage more heavily than another one, the average rainfall in the reach was considered as a single lumped input. The rainfalls measured at stations shown in Table 3.1 were averaged to obtain the precipitation input for different reaches.

The orders of terms corresponding to the inputs $I(\cdot)$, $T_r(\cdot)$, and $P_i(\cdot)$ in Eq. (3.1) must be selected prior to the estimation of parameters. Rukvichai (1977) adopted a trial and error scheme that involved use of the determination coefficient of the residual series, i.e. the R^2-criterion. The residual determination coefficient, R^2, is estimated by means of the vector of residual errors, $\hat{\underset{\sim}{\varepsilon}} = \underset{\sim}{q} - \hat{\underset{\sim}{q}}$, where $\hat{\underset{\sim}{q}}$ = the vector of predicted outflows, and $\underset{\sim}{q}$ = the vector of actual outflows, as follows:

$$\text{standard dev. of residuals} = v = \sqrt{\frac{\sum_{t=1}^{T} \hat{\varepsilon}_t^2 - \frac{\left(\sum_{t=1}^{T} \hat{\varepsilon}_t\right)^2}{T}}{T-1}} \tag{3.22}$$

$$\text{total variance} = T_v = \sum_{t=1}^{T} O_t^2 - \frac{\left(\sum_{t=1}^{T} O_t\right)^2}{T} \tag{3.23}$$

$$\text{Explained variance} = E_v = \left[\sum_{t=1}^{T} O_t^2 - \frac{\left(\sum_{t=1}^{T} O_t\right)^2}{T}\right] - \left[\sum_{t=1}^{T} \hat{\varepsilon}_t^2 - \frac{\left(\sum_{t=1}^{T} \hat{\varepsilon}_t\right)^2}{T}\right] \tag{3.24}$$

$$\text{Determination coefficient} = R^2 = \frac{E_v}{T_v} \tag{3.25}$$

The R^2-criterion simply involves increasing the model orders until the gain in R^2-value is less than a specified minimum value. The final model orders, the parameter estimates, and the R^2-values along with the statistics of the residuals for each of these reaches obtained by using the above mentioned criterion are shown in Table 3.1. The parameter estimates shown in Table 3.1 were obtained by using the 1968, 1969, and 1970 data. In addition to the statistics given by Eq. (3.22) through (3.25), the following statistics are also provided in Table 3.1.

$$\text{Maximum positive error } (\hat{\varepsilon}_{max}) = \text{maximum of } \underset{\sim}{\hat{\varepsilon}} \tag{3.26}$$

$$\text{Maximum negative error } (\hat{\varepsilon}_{min}) = \text{minimum of } \underset{\sim}{\hat{\varepsilon}} \tag{3.27}$$

$$\text{Maximum observed flow } (O_{max}) = \text{maximum of } \underset{\sim}{q} \tag{3.28}$$

$$\text{Maximum predicted flow } (\hat{O}_{max}) = \text{maximum of } \underset{\sim}{\hat{q}} \tag{3.29}$$

$$\text{Percentage error between peaks } (\%) = \left(\frac{\hat{O}_{max} - O_{max}}{O_{max}} \right) \times 100 \tag{3.30}$$

In order to simulate the preservation of mass balance, the constraints in the CLS method are such that the sum of the impulse response weights related to reach's inflow is unity. Similarly, the sum of the impulse response weights related to each tributary inflow, will equal unity. By constrast, the sum of impulse response weights related by precipitation equals the runoff coefficient. Results shown in Table 4.1 indicate that the model parameter estimates, i.e. the impulse response weights, obtained by the CLS method do indeed sum to unity or sum to the runoff coefficient as the case may be.

The impulse response weights estimated by the OLS method, on the other hand, generally violate the mass balance condition. Consequently, the outflow estimates obtained by using OLS models exhibit considerable bias. This is particularly true for the impulse response functions that model the tributary inflows at Gresham, Alvaton, Glen Dean and Horse Branch. The reason is that tributary inflows and the corresponding reach outflow exhibit a greater degree of correlation than the precipitation and reach outflow.

Table 3.1 shows that some of the impulse response weights estimated by the CLS method are zero. This indicates that the model order is longer than necessary.

The coefficient of determination, R^2, is slightly less for models whose parameters are estimated by the CLS method than for those estimated by the OLS method. For example, the R^2-values exceed 0.9 for six of the CLS-models and are between 0.8 and 0.9 for the remaining three models. By constrast the R^2-values are greater than 0.9 for all OLS models. This illustrates a drawback of using only the R^2-statistics to select models.

3.3.2. Development and Use of Models in Flow Forecasting (GRBSYS1-OLS and GRBSYS1-CLS)

The nine MIL models developed with the OLS and CLS approaches (see Section 3.3.1) were placed in series or "in succession", so as to obtain a basin-wide segmented model down to the Calhoun gaging station. These models, called GRBSYS1-OLS and GRBSYS1-CLS, can be used to estimate the flows or the state of the system at the control stations for a given set of anticipated or forecasted reservoir releases, tributary inflows, and precipitation during the operating horizon of L days. Note that the reservoir releases are to be generated by an operating policy model via an optimization algorithm which will be described in Chapter IV. Before proceeding with the development of that component, it is necessary to study the forecasting performances of the segmented models in order to select suitable MIL model parameters to be used within the operating policy algorithm. Details of the development and use of the segmented models in flow forecasting can be found in an earlier work (Yazicigil, Rao, and Toebes, 1979). Only a few results from that study are summarized herein.

The flow at Calhoun, the output node of the most downstream submodel, is considered the outflow from the Green River Basin. The flows at Calhoun were used to check the cumulative errors of the segmented models. Figures 3.4 and 3.5 display for the 1971 water year the one-day ahead forecasted flows as obtained

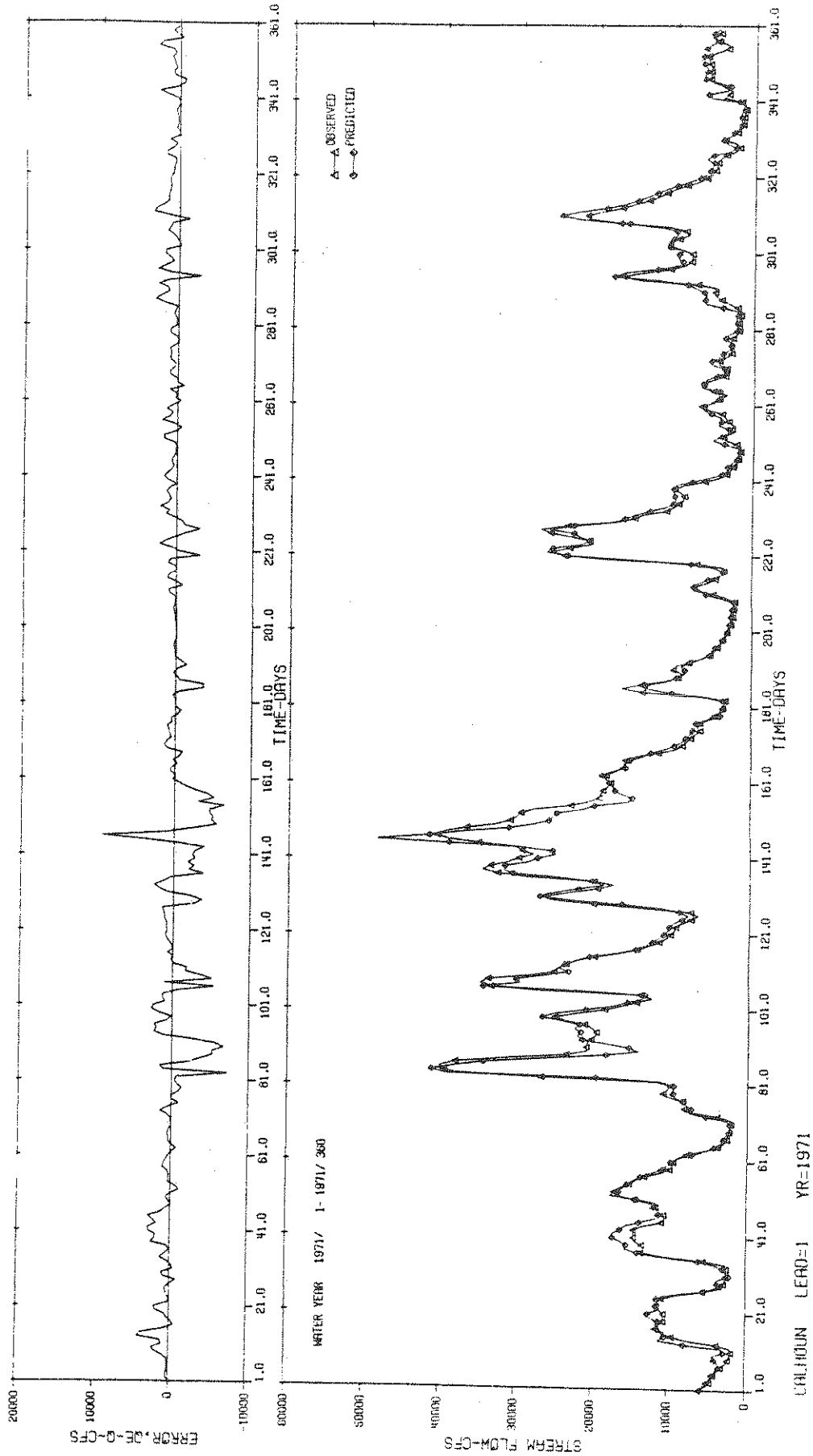

Figure 3.4 Observed and One-Day Ahead Forecast Flows and Forecast Errors at Calhoun Obtained from GRBSYS1-OLS for 1971 Water Year

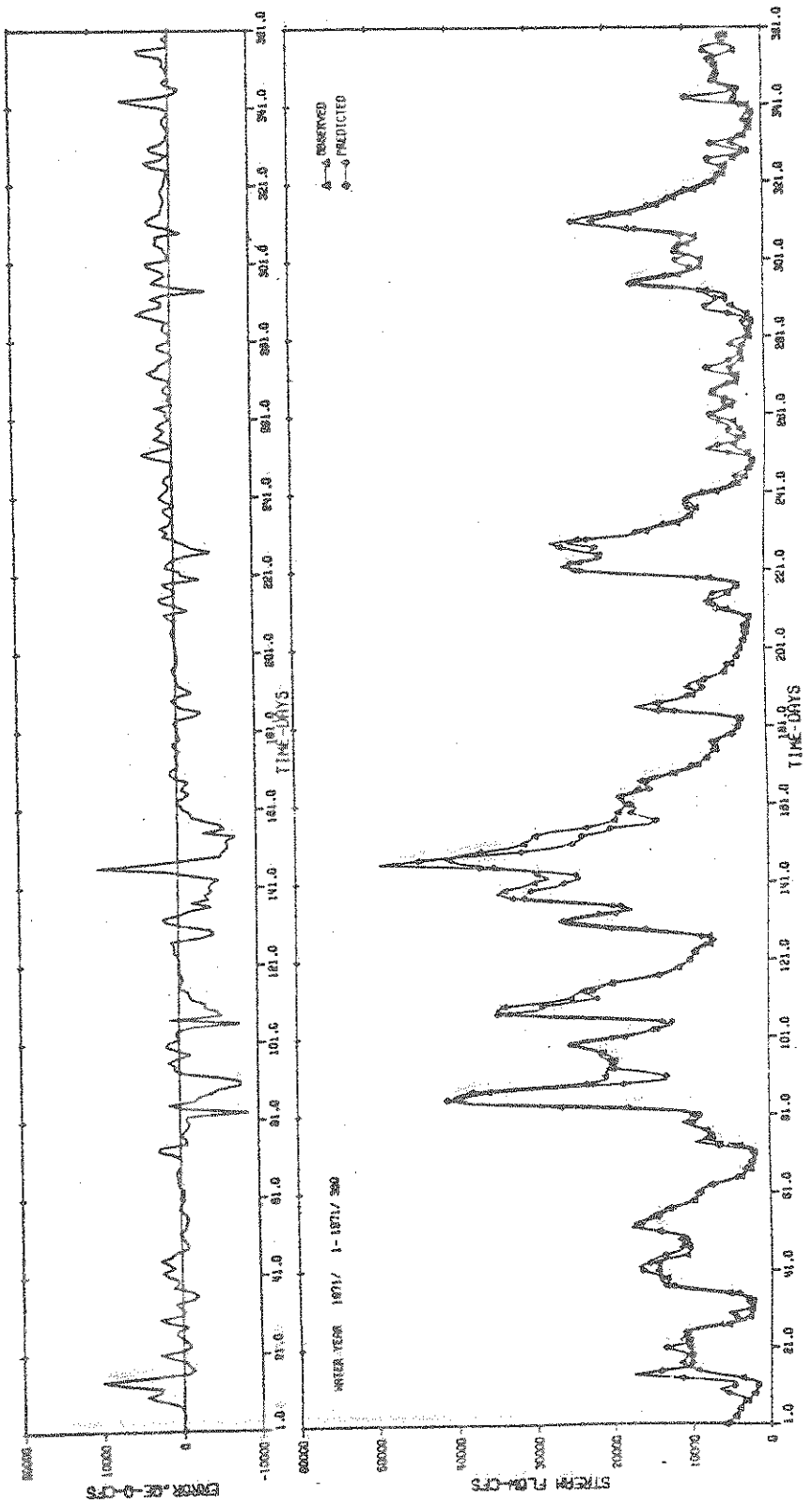

Figure 3.5 Observed and One-Day Ahead Forecast Flows and Forecast Errors at Calhoun Obtained from GRBSYS1-OLS for 1971 Water Year

from GRBSYS1-OLS and GRBSYS1-CLS models, respectively. These results were obtained by inputting "forecast" reservoir releases, tributary inflows and precipitation data (actually these "forecast" data were historic record values). Figure 3.4 and 3.5 also show the one-day ahead flow forecast errors (again at Calhoun). In general, the flow at Calhoun was overpredicted by both the GRBSYS1-OLS and GRBSYSL-CLS models during the dry season and was underpredicted during the wet season.

The ratios of the mean error to mean signal (ME/MS) and the mean square error to mean square signal (MSE/MSS) were calculated for all model nodes for one to five days ahead (Yazicigil, Rao, and Toebes, 1979).

The variation of the (ME/MS) and (MSE/MSS) ratios for different lead days for Calhoun are shown in Figure 3.6 for the 1971 water year. Also shown are the results for a flood event (Aug. 1 - Sept. 25, 1978) made available by the Corps of Engineers. From the results shown in Figure 3.6, it is clear that in both GRBSYS1-OLS and GRBSYS1-CLS models the one-day ahead forecast error is small but that the errors increase with increasing lead times.

The forecast errors of the 1978 data are higher than those for 1971 data. This may be due to non-stationarity of the system such as river bed changes during the 1971-78 period.

From the results presented in Figure 3.6 the measure of bias (ME/MS) is seen to be small in the GRBSYS1-CLS model as compared to the GRBSYS1-OLS model. This is, of course, a consequence of satisfying the continuity constraint. On the other hand, the (MSE/MSS) is smallest for the GRBSYS1-OLS model, at least for 1971. This is not true for the 1978 data: the GRBSYS1-CLS model yields more accurate forecasts for this event.

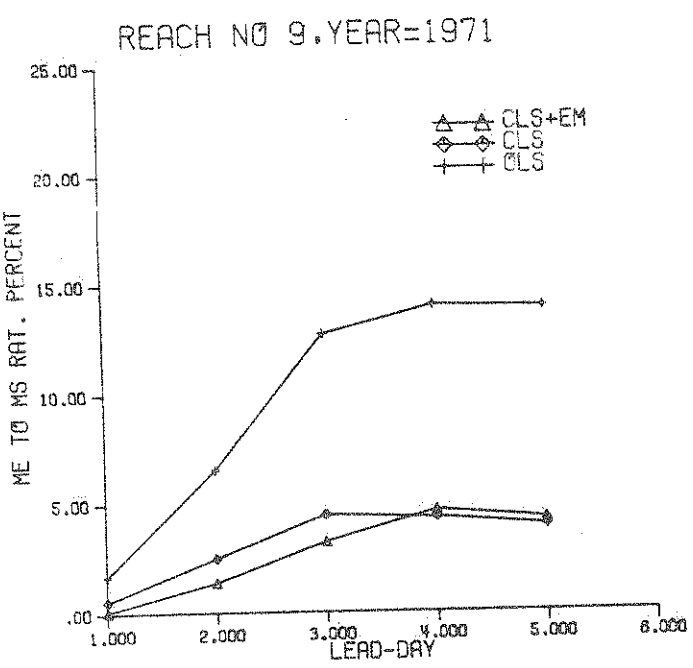

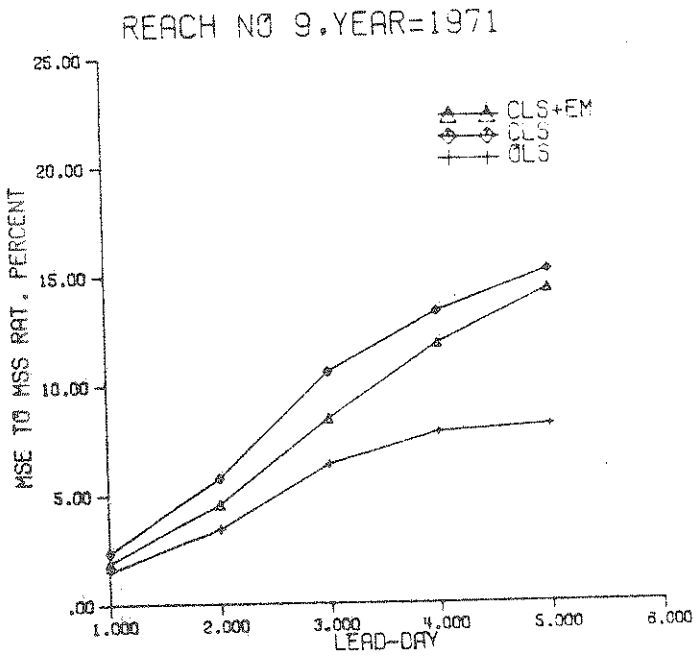

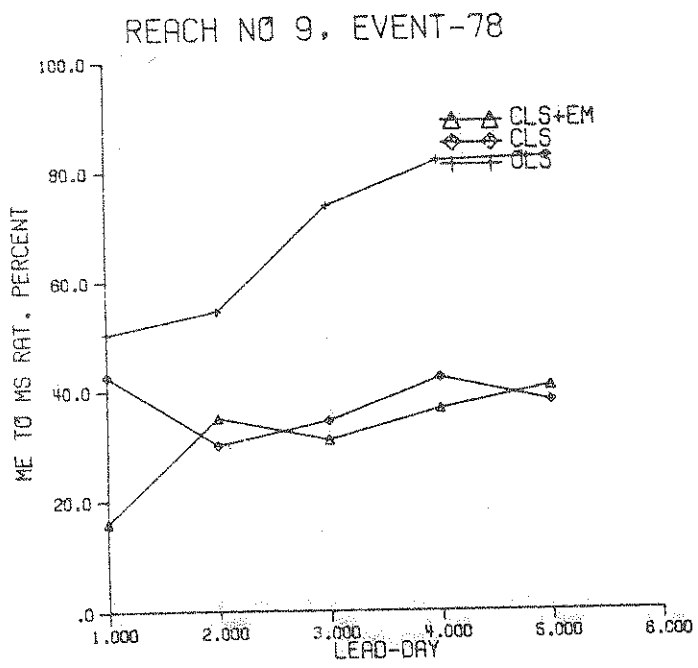

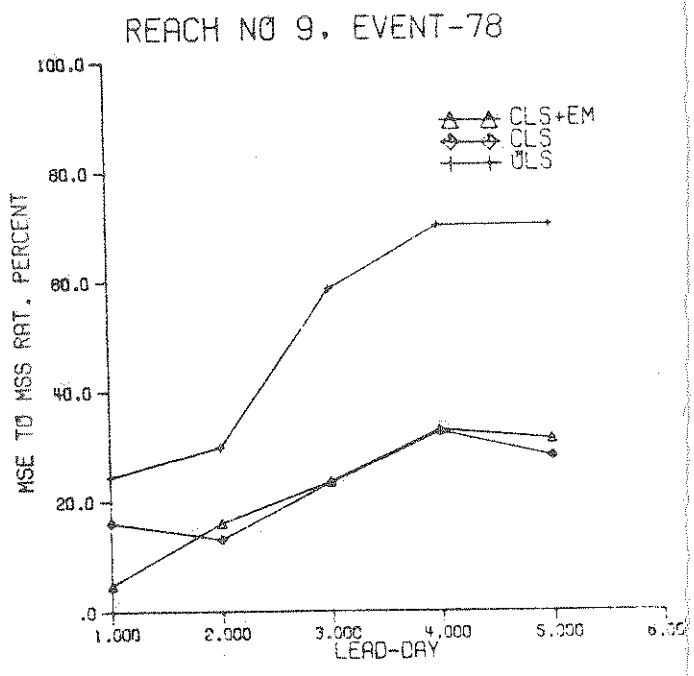

Figure 3.6 Comparison of (ME/MS) and (MSE/MSS) as a Function of Lead-Day at Calhoun (Reach 9) for 1971 and 1978 Data, Obtained from OLS-, CLS-, and CLS + EM-Based Models

3.3.3 Test on Residuals from MIL Models

The parameters of the above MIL models were estimated on the assumption that the residual sequence, $\hat{\varepsilon}(t)$, would be an uncorrelated sequence. It is necessary, therefore, to test the residuals of the fitted models, $\hat{\varepsilon}(t)$, to see whether this assumption is satisfied. Furthermore, the residual sequence $\hat{\varepsilon}(t)$ should exhibit no periodicities.

The correlogram and the cumulative periodogram of the residuals for reach 9 (i.e. Calhoun), whose parameters were estimated by the CLS method, are given in Figure 3.7. The Anderson's test based on the serial correlation coefficients and the *Portmanteau* lack-of-fit test (Box and Jenkins, 1970) were used to test the residual sequences for whiteness. The results of these two tests showed that the residuals of all MIL models, irrespective of whether the parameters were estimated by the OLS or CLS method, were correlated. Also, the residuals of the models were not free from periodicities at the 1% level (Figure 3.7). In order to extract the information present in the residuals, models were fitted to them.

The correlogram of the $\hat{\varepsilon}(t)$ series (Figure 3.7) indicates that autoregressive (AR) models are likely to fit the residual time series. Consequently, AR models of different orders p were fitted to the residual series $\hat{\varepsilon}(t)$ of the MIL models whose parameters were estimated by the CLS method. Here an AR(p) model is represented by:

$$\hat{\varepsilon}(t) = \sum_{j=1}^{p} \phi(j)\, \hat{\varepsilon}(t-j) + \eta(t) \qquad (3.31)$$

The AR parameters, $\phi(j)$, of these models were estimated by the maximum likelihood method (Box and Jenkins, 1970). In order to validate the $\hat{\varepsilon}(t)$-series models the residual sequences $\hat{\eta}(t)$ were tested for whiteness by using the Anderson's and *Portmanteau* tests. The presence of periodicities in $\hat{\eta}(t)$ was tested by the cumulative periodogram test. Among those error models which passed the validation tests, models with the smallest number of parameters were selected.

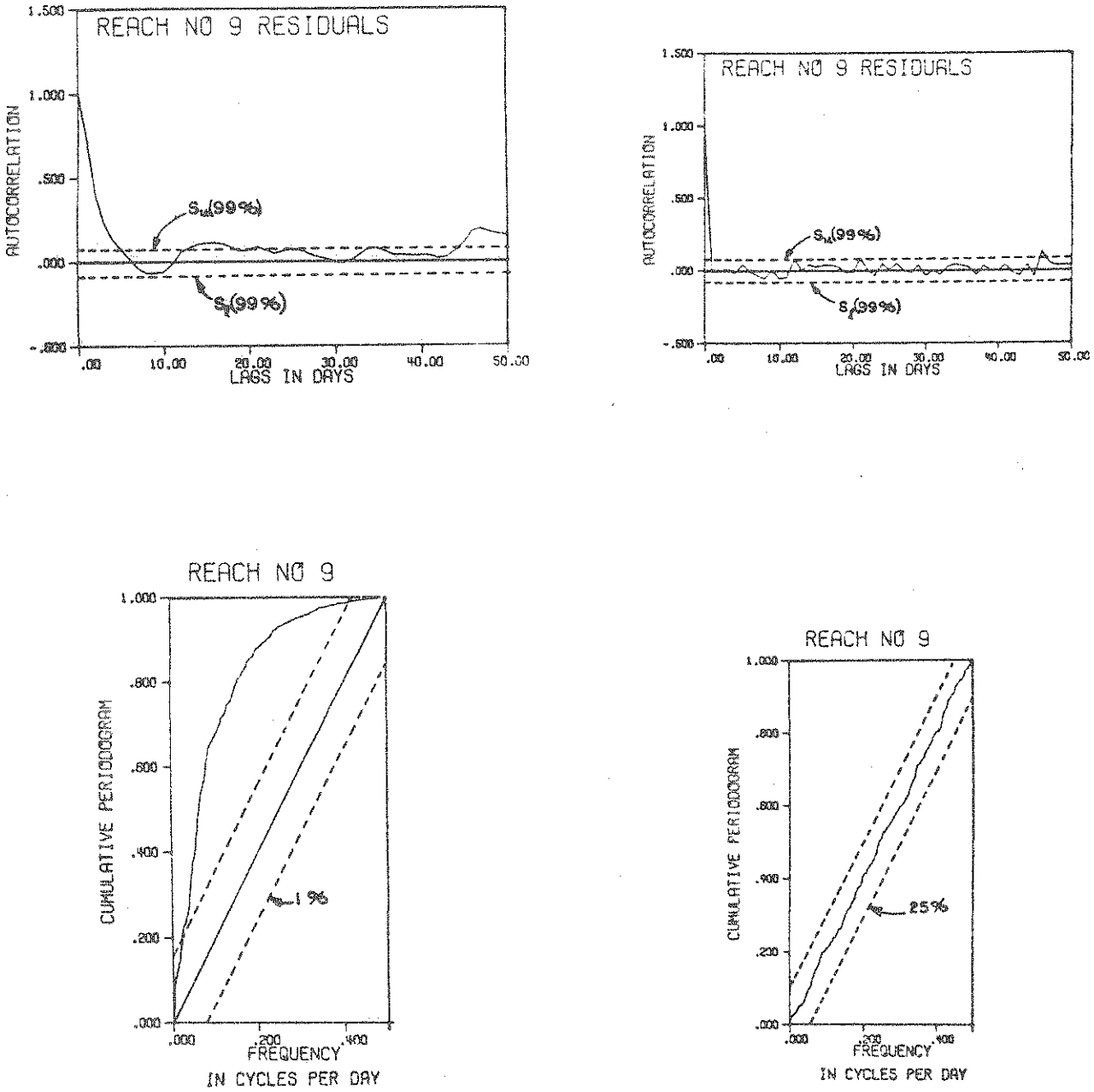

Figure 3.7 Correlogram and Cumulative Penodogram of Residual Sequences at Calhoun (Reach 9): (a) $\hat{\varepsilon}(t)$ series (b) $\hat{\eta}(t)$

In general, the AR models of order 4 and 5 were adequate to represent the $\hat{\varepsilon}(t)$ series. Parameter estimates of the selected error models are listed in Table 3.2. They indicate that the parameters $\phi(1)$ and $\phi(2)$ are large compared to other parameters in all the error models. This indicates that the $\hat{\varepsilon}(t)$ series is highly correlated at small lags.

The correlogram and cumulative periodogram for the residuals $\hat{\eta}(t)$ for reach 9 are shown also in Figure 3.7. This correlogram indicates that the error model residuals, $\hat{\eta}(t)$, are uncorrelated. The cumulative periodograms indicate the absence of periodicities at the 25% level.

3.3.4 Development and Use of an Error Model in Flow Forecasting (GRBSYS2)

The error models fitted to the residual sequences, $\hat{\varepsilon}(t)$, were combined with the MIL models whose parameters were estimated by the CLS method to derive another segmented model called GRBSYS2. (See Yazicigil, Rao, and Toebes, 1979). The GRBSYS2 model is similar to the GRBSYS1-CLS model. The one-day ahead forecasts with GRBSYS2 will, of course, differ from those obtained by means of GRBSYS1-CLS model. The results obtained by using GRBSYS2 are illustrated in Figures 3.6 and 3.8.

The one-day ahead forecast errors with GRBSYS2 are smaller than those obtained from GRBSYS1-CLS (see Figures 3.5 and 3.8). Also the bias in forecasts is smaller. The effect of the error model addition in reducing one-day ahead forecast errors is clearly brought out by the error statistics for the GRBSYS1-CLS and GRBSYS2 models which are listed in Table 3.3. The mean values of the one-day ahead forecast errors of the GRBSYS2 forecasts are about 50% of those obtained from the GRBSYS1-CLS model. This holds for the 1971 forecasts (Table 3.3) as well as for the 1978 event mentioned earlier (Yazicigil, Rao, and Toebes, 1979).

The ratios of (MSE/MSS) for the GRBSYS2 are smaller than the corresponding ratios for the GRBSYS1-CLS model by about 20-30% (Table 3.3). Thus the

Table 3.2 Parameter Estimates of the Best Models for the $\hat{\varepsilon}(t)$ Sequence

Reach No.	Best Model	Autoregressive Coefficients				
		$\phi(1)$	$\phi(2)$	$\phi(3)$	$\phi(4)$	$\phi(5)$
1	AR(5)	0.4110	0.0426	0.0327	0.0922	-0.0536
2	AR(5)	0.8799	-0.4912	0.4183	-0.1867	0.0960
3	AR(5)	0.7894	-0.2739	0.1655	-0.0191	0.0852
4	AR(4)	0.6313	-0.1851	0.0504	0.0598	
5	AR(4)	0.7462	-0.2012	0.1133	0.0439	
6	AR(2)	0.6406	-0.1300			
7	AR(4)	0.4372	-0.0111	0.0433	0.0999	
8	AR(5)	0.6929	-0.2247	0.2161	-0.0188	0.0534
9	AR(5)	0.9779	-0.4266	0.2083	-0.0971	0.0322

Table 3.3 Statistics of One-Day Ahead Forecast Errors Obtained from GRBSYS1-CLS and GRBSYS2 for 1971 Water Year

Reach No.	Statistics							
	Mean		Standard Deviation		ME/MS (%)		MSE/MSS (%)	
	GRBSYS1	GRBSYS2	GRBSYS1	GRBSYS2	GRBSYS1	GRBSYS2	GRBSYS1	GRBSYS2
1	-81.6	-38.6	329.3	350.8	5.13	2.43	2.05	2.22
2	-57.9	-19.7	1353.6	1236.4	1.83	0.62	10.33	8.61
3	-92.7	-19.6	1081.2	884.8	1.87	0.40	2.77	1.85
4	65.8	30.2	740.7	620.8	2.96	1.36	6.03	4.21
5	351.4	109.2	2462.3	1964.5	4.06	1.26	4.89	3.06
6	192.1	90.3	2068.1	1953.3	2.05	0.96	2.99	2.65
7	-49.4	-21.1	190.4	160.6	5.81	2.48	2.83	1.92
8	6.6	4.5	542.7	403.9	0.52	0.35	8.33	4.61
9	62.1	9.7	2240.9	2009.0	0.55	0.09	2.37	1.91

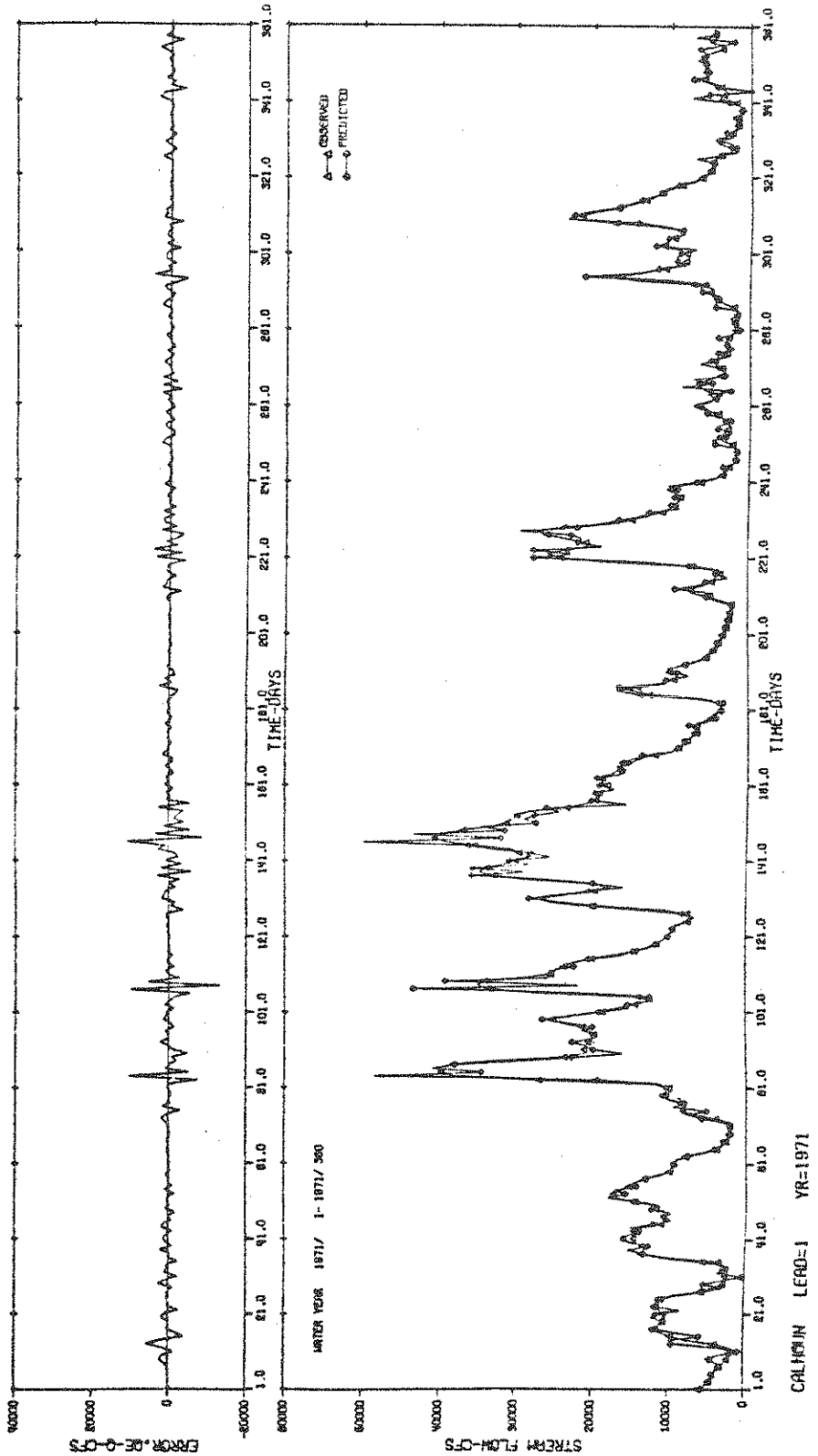

Figure 3.8 Observed and One-Day Ahead Forecast Flows, and Forecast Errors at Calhoun for 1971 Water Year Obtained from GRBSYS2 Model

forecasting performance of the GRBSYS2 model is better than that of the GRBSYS1-CLS model. The (ME/MS) and (MSE/MSS) ratios at Calhoun, as a function of lead time for 1971 and the 1978 event data, are shown in Figure 3.6. The improved performance of the GRBSYS2 model is brought out by a comparison of the CLS (i.e. GRBSYS1-CLS) and CLS + EM (i.e. GRBSYS2) curves.

It should be noted that the above comparative discussion of the GRBSYS1-CLS and GRBSYS2 model performances was limited to one-day ahead forecasts. This is because GRBSYS2 cannot be used for forecasting flows more than one-day ahead. The error model that is an integral part of GRBSYS2 operates on the differences between actual and predicted data. Because tomorrow's actual flow is not available, GRBSYS2 cannot be used for a two- or more days ahead forecasts. Of course one could try to use the error model as such to generate two- or more day ahead error forecasts. This was not attempted because it was expected that the two- or more days ahead error estimates could not be sufficiently accurate. Furthermore, the inaccuracy in the precipitation forecasts probably exceeds the correction afforded by such use of the error model. Therefore, two- or more days ahead forecasts were made with the GRBSYS1-CLS model except that the inflow from any upstream reach for day t+1 was forecast by using the GRBSYS2 model.

Note that the above discussed one-day ahead flow forecast at a control station c is given by:

$$\hat{\hat{Q}}_c(t+1) = \hat{Q}_c(t+1) - \left\{ \sum_{j=1}^{p} \phi(j)[\hat{Q}_c(t-j+1) - Q_c(t-j+1)] \right\} \qquad (3.32)$$

where $\hat{\hat{Q}}_c(t+1)$ and $\hat{Q}_c(t+1)$ are the modified (GRBSYS2) and unmodified (GRBSYS1-CLS) one-day ahead flow forecasts at a control station c and $Q_c(\cdot)$ is the historic flow.

3.3.5 Final Selection of the Model Parameters to be Used With the Operating Policy Algorithm

The operating policy model, which yields optimal daily reservoir releases, uses a linear programming algorithm (see Chapter IV). This model incorporates the multi-input linear models discussed in the preceeding sections in order to estimate the effects of reservoir releases on the flows at the downstream control stations. It is more appealing to use CLS estimates of model coefficients, rather than the OLS estimates in the operating policy model. This is because the CLS estimated model coefficients are stable and preserve the mass balance and non-negativity restrictions. Furthermore, the bias in forecasts obtained by using the GRBSYS1-CLS model is small as compared to the GRBSYS1-OLS model. In the long run, the CLS model parameters cause the volume of water under the predicted and actual hydrographs, to be equal.

Although the addition of an error model to GRBSYS1-CLS (i.e. GRBSYS2) further reduced the bias in forecasts and improved the forecasting accuracy of the model, it cannot be used with the long-run studies of the operating policy algorithm (Chapter V) because the error model that is an integral part of the GRBSYS2 needs actual flow data and these would not be available. Furthermore, the iterative nature of the GRBSYS2 model makes it difficult to include it in a real-time operating policy model involving linear programming. Therefore, it is recommended that the GRBSYS2 model be used only for studying the system's response for a specified set of reservoir releases not specified via linear programming algorithm; an example would be trial releases by the reservoir operators.

Based on these considerations, the CLS model parameters (i.e. GRBSYS1-CLS) will be used with the operating policy algorithm to be described in the next chapters. Recently, Katz and Toebes (1980) have develop-d several additional flow forecasting models for the GRB system. It was shown that a flow differencing

model which, furthermore, incorporates monthly runoff coefficients gives better forecasts. It is recommended that eventually that model be incorporated with the operating policy algorithm.

IV. GREEN RIVER BASIN OPTIMIZATION SIMULATION MODEL FOR RESERVOIR OPERATION (GRBOPM2)

The development of the policy component of the Green River Basin Optimization Simulation Model, GRBOPM2, is discussed in this chapter. Specific requirements and the need for this model were presented in Chapter I. The conceptual framework and the mathematical model are discussed presently.

4.1 GENERAL OVERVIEW OF RESERVOIR REGULATION PRACTICES

The Green River Basin reservoirs are operated in accordance with reservoir regulation schedules. These schedules constitute operations guides rather than algorithmic rules. They are derived from the reservoir regulation plan drawn up from detailed studies made during the reservoir planning and design stages and incorporate additions and revisions made during later operations. Toebes and Rukvichai (1978) discussed several examples of such regulation schedules for the GRB reservoirs.

The regulation plan for the GRB reservoirs was completed in 1967 (COE, 1967). It was developed on the basis of mass curve studies as well as the study of representative historical hydrologic events. They involve the use of rainfall-runoff and routing models. Much of the methodology is rooted in pre-computer days, however.

The regulation of the GRB reservoir system has been decomposed into four regulation schedules, one for each of the GRB reservoirs. They are shown in Appendix A. Each regulation schedule contains the following information (see e.g. Figure 4.1):

(a) The rule curve. Sometimes certain operating zones are indicated in the rule curve diagram, such as water quality pool, minimum pool, etc.;

(b) Several release schedules; and

(c) A set of constraints.

Schedule	Ohio River Evansville	Green River Lock 2, Upper Gage	Green River Lock 4, Upper Gage	Range in Pool Elevation	Time of Year	Regulation
A	(All stages must exist)			Minimum Pool, 480 (ft)	12/1-3/14	Release inflow necessary to maintain pool, provided release indicated in Maximum Release table is not exceeded.
	Below 37 or Below 46F	Below 19 or Below 29F	Below 17 or Below 22F			
B	← Same as Schedule A →			Spillway Crest (560)	12/1-3/14 3/15-11/30	Release at rate indicated in Maximum Release table. Maintain pool as near Rule Curve as possible while meeting minimum flow and flood control requirements.
C	(Any one condition to exist for application of Schedule C)			480-550	12/1-3/14 3/15-11/30	Release at a constant rate of 300 c.f.s. Release at a constant rate of 300 c.f.s. when pool is at or above elevations prescribed by Rule Curve. When below elevation prescribed by Rule Curve, release only the minimum requirement of 50 c.f.s.
	At or above 37R or 5 days before 42	At or above 19R or 4 days before 23	At or above 17R			
D	← Same as Schedule C →			550-560	All year	Release all inflow provided release indicated in Maximum Release table is not exceeded and outflows are never reduced to less than 300 c.f.s.
E	Control stations no longer considered			At 560 and above	All year	Release inflow up to capacity of conduit. If pool exceeds elevation 560 keep conduit open until pool returns to elevation 560. Maintain pool at elevation 560 by passing inflow until downstream conditions permit return to Schedule B. (At such times, the Reservoir Regulation Section will evaluate weather and river conditions to determine feasibility of releasing on recession of downstream stages to regain storage capacity for possible storm recurrence.)

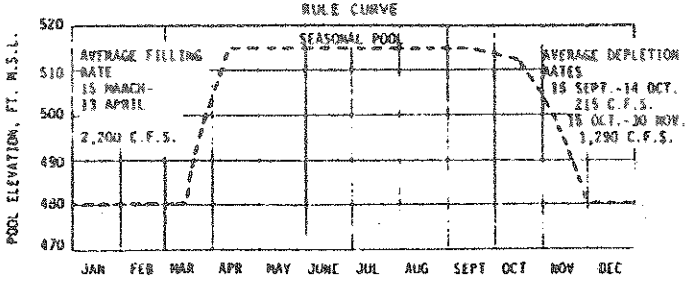

MAXIMUM RELEASE

Munfordville Stage (feet)	Release (c.f.s.)
Below 20.0	10,000
20.0 - 22.0	8,000
22.0 - 24.0	6,100
24.0 - 26.0	4,200
26.0 - 28.0	2,100
Above 28.0	300

MINIMUM LOW FLOW RELEASE

50 c.f.s.

Figure 4.1 Sample Regulation Schedule Showing Rule Curve, Several Release Schedules, and Constraints

The rule curve is a statement that specifies how, on the average, reservoir storage is to be used at any one time of the year. In essence, it represents the *long-run* operating policy for a reservoir. A graphical representation of the rule curve is shown in Figure 4.1. There is a specific curve for each reservoir. System dynamics are usually not reflected in the rule curves.

Due to the randomness of hydrologic inputs and short-run operations' objectives, the reservoir levels will necessarily deviate from the rule curves, especially during flood or drought events. The reservoir regulation procedures that are designed to return the reservoir elevation to the rule curve level may be called *short-run* regulation procedures. They are divided into a number of release schedules such as the schedules A, B, C, D, and E in Figure 4.1. These short-run regulation procedures are specified as a set of conditions involving the stages at control stations, the reservoir elevation, and the time of the year.

Finally, the overall regulation schedule shows various constraints on the release decisions. These constraints include the minimum required release, the maximum allowable release and others. The minimum release is made mainly for the purpose of water quality and low flow requirements. The maximum allowable release often becomes a function of downstream channel capacity, of the stages or flows at one or two local control stations, and of the time of the year.

In the regulation schedules, there is no explicit reference to the use of precipitation and runoff forecasts. In actual operation, however, forecast information is available and is being used in making release decisions.

Although the regulation schedules of each reservoir seem to be independent of each other, they are integrated via the control stations that they have in common such as Woodbury, Calhoun, and Evansville (Toebes and Rukvichai, 1978). In addition, joint operation of the reservoirs occurs during major flood

conditions when they are regulated, in part, as a subsystem of the Ohio River System. Finally, the concept of reservoir zoning or storage balancing rules may be used especially during critical flood periods. Each reservoir is divided into zones of storage and rules for filling and emptying the various zones of the system reservoirs are employed (Chang and Toebes, 1972, 1973). Typically, these rules may specify that the system be operated to maintain all reservoirs in the same zone, if possible.

Sometimes circumstances arise that require special regulation procedures. Such procedures vary from case to case. Toebes et al. (1976) and Toebes and Rukvichai (1978) attempted to document some of the more systematic informal procedures that are currently used in the operation of GRB reservoirs.

4.2 CONCEPT OF REAL-TIME OPERATION

As in earlier work (Chang and Toebes, 1972, 1973) that underlies the current efforts, the incorporation of current field level operations features into algorithmic form was the guiding principle in developing a real-time operations algorithm. Sigvaldason (1976) also suggests that a practical reservoir simulation-optimization model should emulate the mode of operation of a skilled reservoir operator. This implies the following:

(a) The model's logic should reflect the operator's decision and monitoring processes. The operator makes decisions at specific points in time on how a system of reservoirs should be operated over a specified operating horizon. He then monitors the system's inputs and the system's response and may enter another decision round at time that do not necessarily coincide with the end of the usual time step (which for the GRB models is $\Delta t = 1$[day]) and for which the (simulation) model (component) has been developed.

(b) The model should yield recommended operations decisions on the basis of limited information comparable to that available to the operator. That information is the current state of the system (i.e., a listing of current reservoir levels and channel flows) and a prediction of future reservoir inflows, precipitation and tributary inflows over some (operating) horizon.

(c) The model should permit ready adjustment to the balance among operating objectives and hence an adjustment of the corresponding operating rules.

The GRBOPM2 model presented herein captures the above aspects of real system operations. A run to obtain a recommended set of regulation decision requires only a definition of the current state of the system and a forecast of future inflows, precipitation and tributary inflows. It permits reasonable flexibility in specifying balances of operating objectives for the operating horizon.

4.3 GOALS AND PRIORITIES OF OPERATION

Before proceeding with the development of the policy or normative component of the GRBOPM2 model, it is necessary to establish a framework within which the goals of and priorities of reservoir operation can be represented systematically. To that end the state of the system (and the corresponding operations decisions) is divided into a target or *ideal* state (and corresponding *ideal* operating decisions) and non-ideal states. Deviations from the ideal state (and other than the ideal operating decisions to achieve the ideal state) are then associated with *penalties*. By assigning different weights to different deviations from the ideal component values of the state vector and by aggregating these penalties over an operating horizon, we have a consistent, yet flexible framework for judging the relative merit of different operating policies.

The components of the ideal systems state vector used in model construction are:

1. Four target elevations of reservoir levels;
2. Nine target flows at control stations in the system;
3. Four sets of target values which the rate of change in reservoir releases should not exceed.

Completing the operations model component are a number of relationships which one strives to maintain. These include the:

4. Desired order of filling and emptying of the system reservoirs;
5. Relationships between violation of ideal reservoir storage conditions; and violation of ideal flow conditions at stream control points.

In the model, the model penalties for deviations from ideal states are functions of the degree of deviation, of the particular system state component in question, of the time of year, and possibly of the operations event on hand.

The four target (reservoir) elevations are those specified by the rule curves. Rule curves implicitely reflect the established trade-offs among various project objectives in the long-run. For short-run and some longer-term operations, the rule curve represent a guide. Deviations are accepted especially during abnormally wet or dry conditions. For model purposes, however, all deviations of reservoir levels above and below their rule curves are penalized. In general, such deviations are indeed damaging. For example, excessive drawdowns and large fluctuations of water levels from the rule curve will disturb the recreational facilities, create an unattractive appearance and at certain times harm fish species. Note that the target elevations (rule curves) are time dependent.

Similarly all deviations from target flow zones at the various stream control points in the system are penalized and would in reality be damaging in terms of

decreasing water quality and estethics, or increasing damages due to high flows. Like the target reservoir elevations the target flow zones are time dependent.

The restrictions on the rates of change of reservoir releases are penalized because rapid decreases can lead to bank sloughing and sediment problems whereas rapid increases can endanger life and property. In the model, restrictions on the rate of change of flow are specified in terms of the allowable rates-of-change of release from the system reservoirs as proposed by Ford (1978).

The concept of reservoir zoning is frequently used to specify priorities of reservoir filling and emptying (Beard, 1967; Chang and Toebes, 1972, 1973). Following this concept, the model provides for dividing each reservoir into zones of storage, and sets specific rules for filling and emptying the various zones. A typical rule is to operate the reservoirs such that they are all maintained in corresponding zones. The number of zones and their magnitudes may vary as a function of time of the year and of the priority relationships among the system's reservoirs. The concept of reservoir zoning has also been incorporated in the Green River Basin Optimization-Simulation Model. Because of the spatial and temporal distribution of inflows and precipitation, it is not always possible to maintain the flows at their target zones at all control points in the system. Reservoir operators do have preferences as to which flows will be allowed to deviate (first) from their target levels. Typically this preference is a function of the state of the system reservoirs upstream of the control points. In the GRBOPM2, such relationships between storage in the system reservoirs and flow at control points are defined by differing penalty function values that are provided by the GRB Reservoir Regulation Section of the Louisville Distric of the Corps of Engineers. Penalty coefficients are specified for all reservoir storage zones and for all levels of flow at control stations. Their relative magnitudes govern the release decisions recommended by the model.

In keeping with a systems focus, the operations component of the GRBOPM2 model seeks to implement an operations objective, namely the minimization of the sum of all (daily) penalties over the operating horizon (typically 1 to 5 days) and over a study period (typically several seasons or years of operation). This implementation is pursued by means of one or another optimization or mathematical programming model.

4.4 SELECTION OF A SUITABLE OPTIMIZATION ROUTINE

The model used in this study may be called a simulation model with an imbedded mathematical programming model. For the latter, a Linear Programming (LP) model was selected.

Among several well-known optimization techniques, Linear Programming was selected because it is computationally efficient, flexible, and a well-understood technique. In anticipation of its use, the pertinent hydrologic processes and the components of reservoir-river system were already represented by linear functions such as the multi-input linear routing models discussed in Chapter III.

Dynamic Programming, another optimization approach, was not the primary choice because for systems with more than 2 to 3 reservoirs and control stations, and many analysis period, it becomes computationally less efficient than linear programming.

Expressed in matrix form, the Linear Programming problem is:

$$\text{minimize } Z = \underset{\sim}{C}\ \underset{\sim}{X} \tag{4.1a}$$

$$\text{subject to: } \underset{\sim}{A}\ \underset{\sim}{X} \gtreqless \underset{\sim}{B} \tag{4.1b}$$

$$\underset{\sim}{X} \geq 0 \tag{4.1c}$$

where $\underset{\sim}{X}$ is an (n x 1) column vector of decision variables which (because penalties associated with each of them) include: storages, releases, and stream-flows at control stations; $\underset{\sim}{A}$ is an (m x n) matrix of coefficients of the linear constraint equations used to describe the dynamic interrelationships of the

reservoir-river system; B is an (m x 1) column vector of right-hand-sides of the constraint equations. This vector represents the input information for the reservoir-river system model; the input includes forecasted inflows, precipitation, and tributary flows as well as the target levels; C is an (1 x n) row vector of penalty coefficients associated with each of the decision variables; and Z is the objective function or overall systems measure of effectiveness. This aggregate of penalties is what the optimization model solution is designed to minimize. The elements of these matrices are described in detail in the following sections IV-5, 6, and 7.

4.5 CONSTRAINTS OF THE LP MODEL

The constraints of the above LP model which derive from the simulation model (in which it is imbedded) define solutions that represent feasible system responses to specific hydrologic conditions and reservoir release decisions. This constraint set includes: (1) reservoir mass balance constraints, (2) storage zone constraints, (3) control station mass balance constraints, (4) flow zone constraints, and (5) release rate constraints. Also included in the constraint set are inequalities that limit the range of certain variables used in the formulation of the LP model.

In order to clarify this, first consider a single reservoir-river system shown in Figure 4.2. The inputs to the reservoir during the next operating horizon are the net reservoir inflow (gross inflows minus losses due to evaporation and seepage), $RI(t + \ell)$, where ℓ denotes the ℓ-day ahead forecast, ℓ = 1, 2, ..., L. Typically, the operating horizon is five days (L = 5). The daily reservoir releases, $RO(t + \ell)$, during the L-day operating horizon are the decision variables which one seeks to define optimally by means of the model. The resulting pool elevations, $E(t + \ell)$, or equivalently, the resulting storages, $S(t + \ell)$, are the state variables that define the state of the system's reservoir.

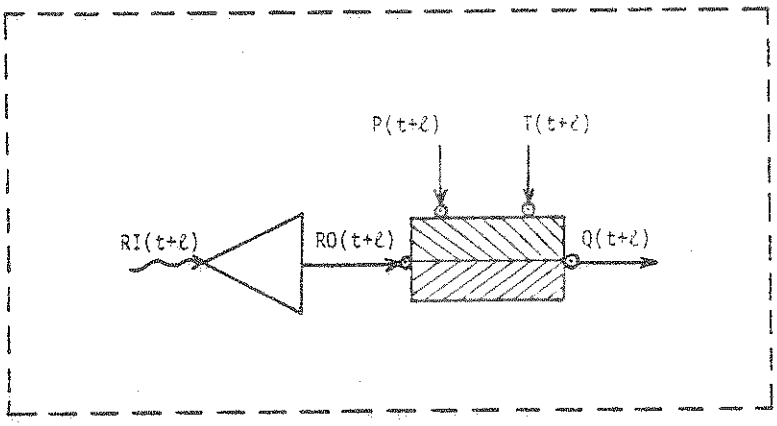

Figure 4.2 Single Reservoir-River System

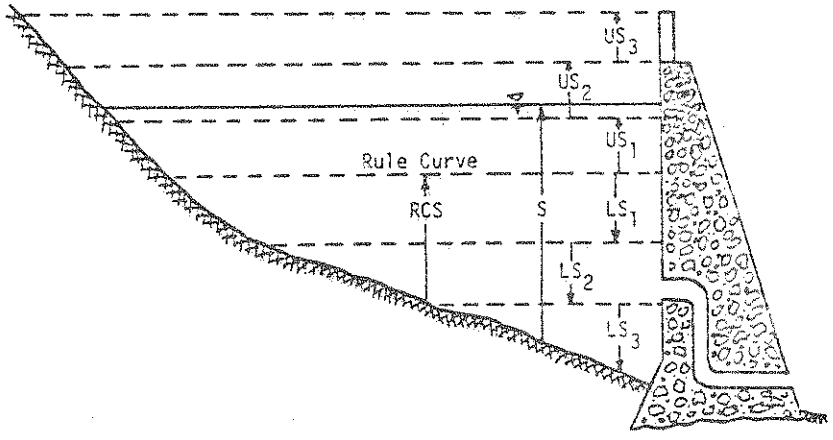

Figure 4.3 Reservoir Storage Representation

4.5.1 Reservoir Mass Balance Constraints

The reservoir mass balance equation is based on the principle of continuity and states that: during any period, the net average inflow volume to the reservoir minus the average volume of release must equal the change in storage. Thus;

$$\left[RI(t+\ell) - RO(t+\ell)\right] \Delta\ell = S(t+\ell) - S(t+\ell-1) \qquad (4.2)$$

where $\Delta\ell$ is the time step selected for analysis of system's structure as well as its operation. In this study $\Delta\ell = 1$[day]. For each day ℓ, the net reservoir inflow, $RI(t+\ell)$, is a forecasted quantity. As these are among the model inputs, they will form the right-hand-sides of the reservoir mass balance constraints, (see Eq. 4-1b). Thus Eq. (4.2), when written in the standard LP format, reads as follows:

$$RO(t+\ell)\ \Delta\ell + S(t+\ell) - S(t+\ell-1) = RI(t+\ell)\ \Delta\ell \qquad (4.3)$$

Because the quantity $S(t+\ell-1)$ is known for $\ell=1$, it too will be made part of the equation's right-hand side:

$$RO(t+\ell)\ \Delta\ell + S(t+\ell) = RI(t+\ell)\ \Delta\ell + S(t+\ell-1) \qquad (4.4)$$

Selection of the optimal releases $RO^*(t+\ell)$ for each day ℓ requires the estimation of the future impact of these releases. This is accomplished by solving for each day ℓ a limited multi-period problem that reflects estimated future conditions over an "operating horizon". The operation and interaction of system components in these future periods, i.e., $\ell \geq 2$ and generally $\ell \leq 5$ must be modeled also. Consequently one has for each day ℓ, the reservoir mass balance equation and the associated constraints must be included in the constraint set.

4.5.2 Storage Zone Constraints

The day ℓ storage in a reservoir can be represented as the sum of the prescribed rule curve storage, $RCS(t+\ell)$, plus the deviation $DS(t+\ell)$, from the rule curve storage, thus;

$$S(t+\ell) = RCS(t+\ell) + DS(t+\ell) \qquad (4.5)$$

In turn the storage deviation variable, $DS(t+\ell)$ is represented as a sum of the six variables US_i and LS_i shown in Figure 4.3. Thus;

$$DS(t+\ell) = \sum_{i=1}^{3} US_i(t+\ell) - \sum_{i=1}^{3} LS_i(t+\ell) \tag{4.6}$$

or in general

$$DS(t+\ell) = \sum_{i=1}^{NSA(\ell)} US_i(t+\ell) - \sum_{i=1}^{NSB(\ell)} LS_i(t+\ell) \tag{4.7}$$

where $NSA(\ell)$ = number of storage zones above the rule curve for period ℓ; $NSB(\ell)$ = number of storage zones below the rule curve for period ℓ. Note that for any value of $DS(t+\ell)$, either all of the US_i will equal zero or all of the LS_i will equal zero. Furthermore, the value of US_i is restricted to zero unless the value of US_{i-1} is equal to its upper bond. A similar restriction exists for the values of LS_i.

The number of zones, $NSA(\cdot)$ and $NSB(\cdot)$, are not fixed; they can vary from reservoir to reservoir and also from time period to time period.

By substituting Eq. (4.7) into Eq. (4.5) the basic constraint equation that represents the state of the reservoir becomes;

$$S(t+\ell) - \sum_{i=1}^{NSA(\ell)} US_i(t+\ell) + \sum_{i=1}^{NSB(\ell)} LS_i(t+\ell) = RCS(t+\ell) \tag{4.8}$$

Once again note that if $S(t+\ell)$ exceeds $RCS(t+\ell)$, then $\sum US_i$ will equal the excess storage and $\sum LS_i$ will equal zero; whereas if $S(t+\ell)$ is less than $RCS(t+\ell)$, $\sum LS_i(t+\ell)$ will equal the deficit storage and $\sum US_i(t+\ell)$ will equal zero.

4.5.3 Control Station Mass Balance Constraints

The inputs to the river reach shown in Figure 4.2 are the reservoir outflows, $RO(t+\ell)$; the precipitation, $P(t+\ell)$; and the tributary inflow(s), $T(t+\ell)$. The resulting streamflow at the downstream end of river reach, $Q(t+\ell)$, is the state variable for that reach. Its locale is identified with the control

stations of the model. By means of the multi-input linear (MIL) routing models discussed in Chapter III, the $Q(t+\ell)$ can be expressed as follows:

$$Q(t+\ell) = \sum_{j=0}^{k-1} u_{RO}(j) \cdot RO(t+\ell-j) + \sum_{j=0}^{k-1} u_P(j) \cdot P(t+\ell-j) + \sum_{j=0}^{k-1} u_T(j) \cdot T(t+\ell-j) \tag{4.9}$$

Because $T(\cdot)$ and $P(\cdot)$ are externally generated forecasted values, they will form the right-hand-sides when casting Eq. 4.9 in the form of Eq. 4-1b:

$$Q(t+\ell) - \sum_{j=0}^{k-1} u_{RO}(j) \cdot RO(t+\ell-j) = \sum_{j=0}^{k-1} u_P(j) \cdot P(t+\ell-j) + \sum_{j=0}^{k-1} u_T(j) \cdot T(t+\ell-j) \tag{4.10}$$

4.5.4 Flow Zone Constraints

As was the case with reservoir storages, channel flows can also be represented as the sum of the prescribed target flow level, $TFL(t+\ell)$ and the deviation, $DQ(t+\ell)$, from the target flow level:

$$Q(t+\ell) = TFL(t+\ell) + DQ(t+\ell) \tag{4.11}$$

As was done in formulating Eq. 4.7, the flow deviation, $DQ(t+\ell)$ at control stations can be similarly represented:

$$DQ(t+\ell) = \sum_{i=1}^{NQA(\ell)} UQ_i(t+\ell) - \sum_{i=1}^{NQB(\ell)} LQ_i(t+\ell) \tag{4.12}$$

where $NQA(\ell)$ = number of flow zones above the target flow range for period ℓ; $NQB(\ell)$ = number of flow zones below the target flow range for period ℓ (see Figure 4.4).

By substituting Eq. (4.12) into Eq. (4.11) the equation that represents the state of the channel flow at the control station can be obtained:

$$Q(t+\ell) - \sum_{i=1}^{NQA(\ell)} UQ_i(t+\ell) + \sum_{i=1}^{NQB(\ell)} LQ_i(t+\ell) = TFL(t+\ell) \tag{4.13}$$

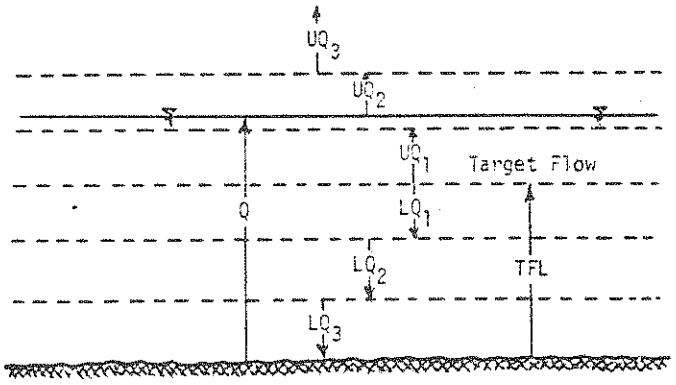

Figure 4.4 Channel Flow Representation

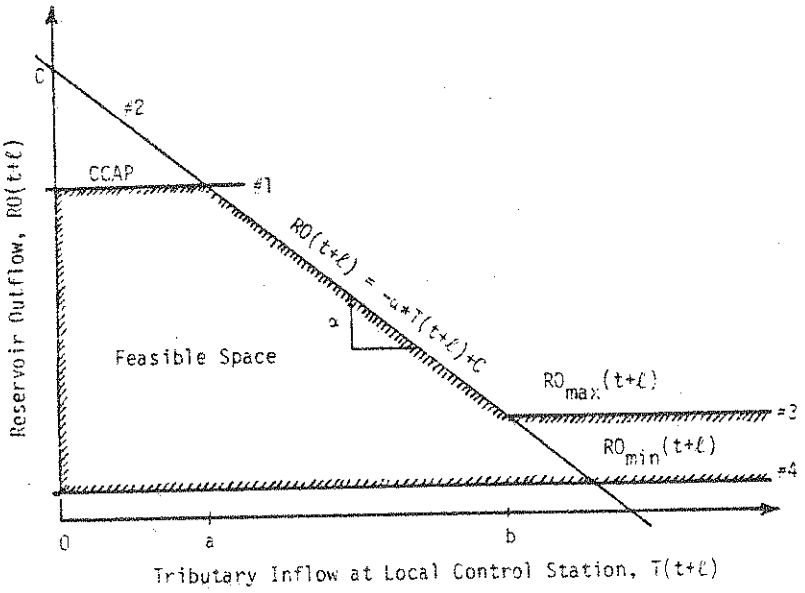

Figure 4.5 Maximum Allowable Reservoir Release Schedule Constraints

4.5.5 Release Rate Constraints

The constraints imposed upon selection of release decisions, $RO(t+\ell)$, are the rate-of-change of release constraints, the minimum release requirement and the maximum allowable release schedules.

a) Rate-of-Change of Release

The average reservoir release for a period is related to the release in the previous period by:

$$RO(t+\ell) = RO(t+\ell-1) + \dot{RO}(t+\ell) \cdot \Delta\ell \qquad (4.14)$$

where $RO(t+\ell)$ is the net rate-of-change of release for period ℓ, i.e., $\frac{dR}{d\ell}$. The net rate-of-change of release can be divided into two components, as follows:

$$\dot{RO}(t+\ell) = \dot{ROI}(t+\ell) - \dot{ROD}(t+\ell) \qquad (4.15)$$

where $\dot{ROI}(t+\ell)$ = net rate-of-increase of release for period ℓ; $\dot{ROD}(t+\ell)$ = net rate-of-decrease of release for period ℓ. In order to impose restrictions on the rate-of-change of release, each of these components is divided into two components: an allowable rate-of-change and an excessive rate-of-change. Thus

$$\dot{ROI}(t+\ell) = \dot{ROAI}(t+\ell) + \dot{ROEI}(t+\ell) \qquad (4.16)$$

and

$$\dot{ROD}(t+\ell) = \dot{ROAD}(t+\ell) + \dot{ROED}(t+\ell) \qquad (4.17)$$

where $\dot{ROAI}(t+\ell)$ = actual rate-of-increase of release within allowable limit for period ℓ; $\dot{ROEI}(t+\ell)$ = actual rate-of-increase of release in excess of allowable limit for period ℓ; $\dot{ROAD}(t+\ell)$ = actual rate-of-decrease of release within allowable limit for period ℓ; $\dot{ROED}(t+\ell)$ = actual rate-of-decrease of release in excess of allowable limit for period ℓ.

Substitution of Eqs. (4.15), (4.16), and (4.17) into (4.14) gives the basic rate-of-change of release equation:

$$RO(t+\ell) = RO(t+\ell-1) + [\dot{ROAI}(t+\ell) + \dot{ROEI}(t+\ell)] \cdot \Delta\ell - [\dot{ROAD}(t+\ell) + \dot{ROED}(t+\ell)] \cdot \Delta\ell \qquad (4.18)$$

For ℓ=1, RO(t+ℓ-1) is known, and it will be made the right-hand-side of Eq. (4.18):

$$RO(t+\ell) - [\dot{RO}AI(t+\ell) + \dot{RO}EI(t+\ell)]\,\Delta\ell + [\dot{RO}AD(t+\ell) + \dot{RO}ED(t+\ell)]\,\Delta\ell = RO(t+\ell-1) \tag{4.19}$$

For all other periods, i.e., $\ell \geq 2$, the Eq. (4.19) becomes:

$$RO(t+\ell) - RO(t+\ell-1) - [\dot{RO}AI(t+\ell) + \dot{RO}EI(t+\ell)]\,\Delta\ell + [\dot{RO}AD(t+\ell) + \dot{RO}ED(t+\ell)]\,\Delta\ell = 0 \tag{4.20}$$

b) Minimum Release Requirement

The low flow requirements on reservoir outflows (see Appendix A) is accommodated by imposing a lower bound on the release rate:

$$RO(t+\ell) \geq RO_{min}(t+\ell) \tag{4.21}$$

where $RO_{min}(t+\ell)$ is the required minimum release from the reservoir during period ℓ.

As shown in Appendix A constant minimum releases of 50 cfs are prescribed for the Rough, Nolin, and Barren Reservoirs. Because of water quality concerns, a minimum release of 150 cfs has been adopted for Green Reservoir.

c) Maximum Allowable Release Schedules

Local control stations have been selected for each GRB reservoir in order to achieve flood protection in the reaches immediately downstream of the reservoirs during flood control operations (Appendix A). These stations are Gresham for Green Reservoir, Munfordville for Nolin Reservoir, Alvaton for Barren Reservoir, and Glen Dean and Horse Branch for Rough Reservoir. The flows at these local controls as well as downstream channel capacities constrain the maximum releases from each reservoir.

By way of example, let us assume that the maximum allowable release from the reservoir is a function of downstream channel capacity and of the flows at the local control station at which the tributary inflow joins the river reach. Graphically this can be represented as shown in Figure 4.5.

Unfortunately, the feasible space represented by the maximum allowable release schedules is not a convex region which is required for the solution of LP problem (see Figure 4.5). However, the tributaory inflows, $T(t+\ell)$, are not the decision variables; rather, they are externally generated forecast values. Therefore, the non-convexity problem can be eliminated by using the following set of upper bounds and constraints:

1) if $T(t+\ell) \leq a$ then $RO(t+\ell) \leq CCAP$ where CCAP is the downstream channel capacity; (4.22)

2) if $a < T(t+\ell) \leq b$ then $RO(t+\ell) \leq c - \alpha * T(t+\ell)$, where c = intercept of line #2 in Figure 4.5; α = slope of line #2 in Figure 4.5; (4.23)

3) if $b < T(t+\ell)$ then $RO(t+\ell) \leq RO_{max}$ where RO_{max} is the maximum allowable release during flood conditions. (4.24)

Eq. (4.22) is not included in the constrain set; instead, it is included as an upper bound on the release decisions for every period of operation. The releases are constrained such that they should be less than or equal to the right-hand-sides defined by Eqs. (4.23) or (4.24) depending on whether Eq. (4.23) or (4.24) is active, i.e., binding. If the tributary flows are greater than "a" but less than or equal to "b", then Eq. (4.23) becomes active. If the tributary inflows exceed "b" then Eq. (4.24) becomes binding. If both are inactive, i.e., $T(t+\ell) \leq a$, then the releases are bounded only by the downstream channel capacity.

4.6 BOUNDS

In order to assure realism within the model, it is necessary to specify that all variable values fall between a lower bound and an upper bound. The lower bounds for all variables are taken to be zero except for the reservoir releases for which they are set equal to the minimum required release, $RO_{min}(t+\ell)$, (see Eq. (4.21)).

The upper bound for reservoir storage, $S(t+\ell)$ is set equal to the reservoir capacity RCAP. The downstream channel capacity, CCAP, is the upper bound for the reservoir releases. The actual rates-of-change of release within allowable limits, $\dot{RO}AI(t+\ell)$ and $\dot{RO}AD(t+\ell)$, are bounded by the prescribed operational limits as

$$\dot{RO}AI(t+\ell) \leq \dot{RO}AI_{max}(t+\ell) \tag{4.25}$$

and

$$\dot{RO}AD(t+\ell) \leq \dot{RO}AD_{max}(t+\ell) \tag{4.26}$$

where $\dot{RO}AI_{max}(t+\ell)$ = allowable rate-of-increase of release for period ℓ; $\dot{RO}AD_{max}(t+\ell)$ = allowable rate-of-decrease of release for period ℓ.

These bounds do not limit the rate-of-change of release; they only segregate the actual rate-of-change of release into components.

The variables denoting components of channel flow and of reservoir storage are bounded by the prescribed operational limits (see Figure 4.3 and 4.4). The capacity of each storage and flow zone is specified with upper bounds on the appropriate terms,

$$US_i(t+\ell) \leq \overline{US}_i(t+\ell) \tag{4.27}$$

$$LS_i(t+\ell) \leq \overline{LS}_i(t+\ell) \tag{4.28}$$

$$UQ_i(t+\ell) \leq \overline{UQ}_i(t+\ell) \tag{4.29}$$

$$LQ_i(t+\ell) \leq \overline{LQ}_i(t+\ell) \tag{4.30}$$

where $\overline{US}_i(\cdot)$ and $\overline{LS}_i(\cdot)$ denote the storage zone capacities (upper bounds) for each storage component; and $\overline{UQ}_i(\cdot)$ and $\overline{LQ}_i(\cdot)$ denote the flow zone capacities for each flow component.

The upper bound for channel flow is specified as an arbitrarily large number (i.e. $\overline{UQ}_{NQA}(t+\ell) = \infty$) as no apparent physical constraints exist on the total channel flows.

4.7 OBJECTIVE FUNCTION

4.7.1 Component System

The objective function Z for the component system of Figure 4.2 aggregates all penalties associated with undesirable conditions, i.e. with deviations of storage from reservoir rule curves, with excessive rates-of-change of release, and with deviations of channel flows from target levels. The objective of minimizing Z then reads:

$$\text{Min } Z = \sum_{\ell=1}^{L} \left[\sum_{i=1}^{NSA(\ell)} P_{US_i}(t+\ell) * US_i(t+\ell) + \sum_{i=1}^{NSB(\ell)} P_{LS_i}(t+\ell) * LS_i(t+\ell) \right.$$
$$+ \sum_{i=1}^{NQA(\ell)} P_{UQ_i}(t+\ell) * UQ_i(t+\ell) + \sum_{i=1}^{NQB(\ell)} P_{LQ_i}(t+\ell) * LQ_i(t+\ell)$$
$$\left. + P_{\dot{ROEI}}(t+\ell) * \dot{ROEI}(t+\ell) + P_{\dot{ROED}}(t+\ell) * \dot{ROED}(t+\ell) \right] \qquad (4.31)$$

where $P_{US_i}(t+\ell)$ = per unit penalty for storage deviation above the rule curve storage in zone i for period ℓ; $P_{LS_i}(t+\ell)$ = per unit penalty for storage deviation below the rule curve storage in zone i for period ℓ; $P_{UQ_i}(t+\ell)$ = per unit penalty for flow deviation above the target flow level in zone i for period ℓ; $P_{LQ_i}(t+\ell)$ = per unit penalty for flow deviation below the target flow level in zone i for period ℓ; $P_{\dot{ROEI}}(t+\ell)$ = per unit penalty for rate-of-increase of release in excess of allowable limit for period ℓ; $P_{\dot{ROED}}(t+\ell)$ = per unit penalty for rate-of-decrease of release in excess of allowable limit for period ℓ; L = short-run operating horizon.

The sum of the first two terms of this objective function represents the total reservoir storage penalty; the sum of the next two terms represents the total penalty for flow at the control station, and the sum of the last two terms represents the total penalty for excess rates-of-change of release. The objective of operation of the system (as yet the system shown in Figure 4.2) is to

minimize the total penalty during the operating horizon L. Therefore, each term is to be summed over L.

The objective function allows penalties to be assessed, using selectable unit penalties, for any or all undesirable operations results and thereby provides the flexibility to represent most goals and priorities of operation. In selecting unit penalties there is one constraint, namely that the unit penalties for each successive zone farther away from the target levels must exceed the per unit penalty of the previous zone (see Figures 4.6 and 4.7). This will define a separable function of flow or of storage. This restriction does not significantly limit the application of the model because in practice each successive level of deviation of flow or storage from their target levels is indeed more objectionable than deviations in the previous zone. Also, concave penalty functions could be accommodated by using mixed integer linear programming techniques; however, this is not necessary in this study.

4.7.2 GRB System

The LP model for the single reservoir-river system discussed in the preceeding section can be extended to model many reservoir, many interconnecting river channels, many control stations and many periods of analysis. Any reservoir-river system configuration, i.e. parallel or serial, can be accommodated. Table 4.1 summarizes the constraints and the objective function that define the LP problem for several reservoirs and control stations.

The dimensions of the technological coefficient matrix, $\underset{\sim}{A}$, of the LP problem are as follows:

$$n = 6 * L * NRES + L * NST + \sum_{r=1}^{NRES} \sum_{\ell=1}^{L} [NSA^r(\ell) + NSB^r(\ell)]$$

$$+ \sum_{c=1}^{NST} \sum_{\ell=1}^{L} [NQA^c(\ell) + NQB^c(\ell)] \qquad (4.32)$$

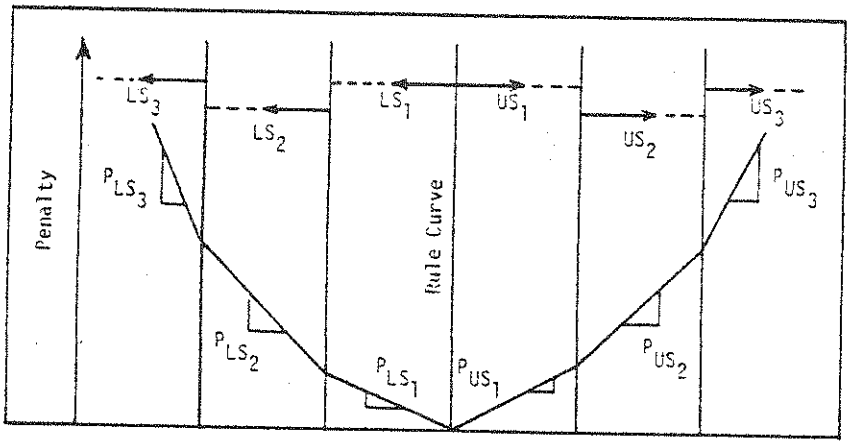

Figure 4.6 Penalty Representation for Reservoir Storage (Adapted from Sigvaldason, 1976)

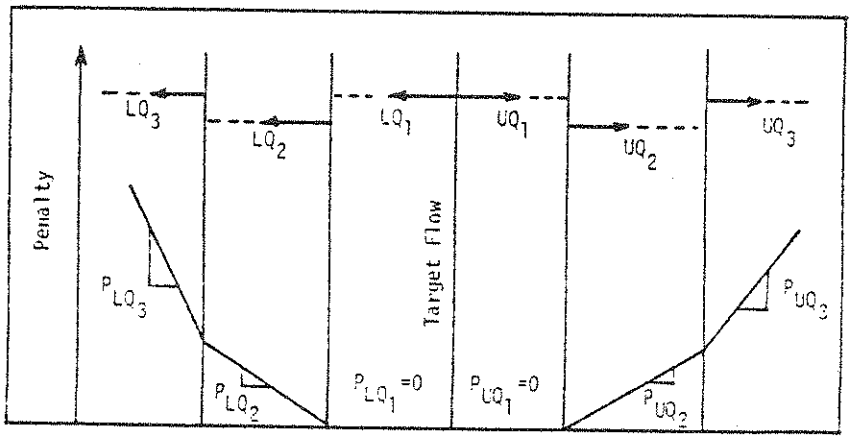

Figure 4.7 Penalty Representation for Channel Flow (Adapted from Sigvaldason, 1976)

Table 4.1 Objective Function and Constraints of Linear Programming Model

OBJECTIVE FUNCTION

$$\text{Min } Z = \sum_{\ell=1}^{L} \left\{ \sum_{r=1}^{NRES} \left[\sum_{i=1}^{NSA^r(\ell)} P^r_{US_i}(t+\ell) * US^r_i(t+\ell) + \sum_{i=1}^{NSB^r(\ell)} P^r_{LS_i}(t+\ell) * LS^r_i(t+\ell) \right] \right.$$

$$+ \sum_{c=1}^{NCT} \left[\sum_{i=1}^{NQA^c(\ell)} P^c_{UQ_i}(t+\ell) * UQ^c_i(t+\ell) + \sum_{i=1}^{NQB^c(\ell)} P^c_{LQ_i}(t+\ell) * LQ^c_i(t+\ell) \right]$$

$$\left. + \sum_{r=1}^{NRES} \left[P^r_{\dot{R}OEI}(t+\ell) * \dot{R}OEI^r(t+\ell) + P^r_{\dot{R}OED}(t+\ell) * \dot{R}OED^r(t+\ell) \right] \right\}$$

CONSTRAINTS

Reservoir Mass Balance Constraints:

$$RO^r(t+\ell) * \Delta\ell + S^r(t+\ell) = RI^r(t+\ell) * \Delta\ell + S^r(t+\ell-1) \qquad \forall r, \forall \ell = 1$$

$$RO^r(t+\ell) * \Delta\ell + S^r(t+\ell) - S^r(t+\ell-1) = RI^r(t+\ell) * \Delta\ell \qquad \forall r, \forall \ell \geq 2$$

Storage Zone Constraints:

$$S^r(t+\ell) - \sum_{i=1}^{NSA^r(\ell)} US^r_i(t+\ell) + \sum_{i=1}^{NSB^r(\ell)} LS^r_i(t+\ell) = RCS^r(t+\ell) \quad \forall r, \forall \ell$$

Control Station Mass Balance Constraints:

$$Q^c(t+\ell) - \sum_{j=0}^{k-1} u_I(j) * I(t+\ell-j) = \sum_{j=0}^{k-1} u_p(j) * P(t+\ell-j) + \sum_{j=0}^{k-1} u_T(j) * T(t+\ell-j) \quad \forall c, \forall \ell$$

Flow Zone Constraints:

$$Q^c(t+\ell) - \sum_{i=1}^{NQA^c(\ell)} UQ^c_i(t+\ell) + \sum_{i=1}^{NQB^c(\ell)} LQ^c_i(t+\ell) = TFL^c(t+\ell) \quad \forall c, \forall \ell$$

Rate-of-Change of Release Constraints:

$$RO^r(t+\ell) - [\dot{R}OAI^r(t+\ell) + \dot{R}OEI^r(t+\ell)]\Delta\ell + [\dot{R}OAD^r(t+\ell) + \dot{R}OED^r(t+\ell)]\Delta\ell = RO^r(t+\ell-1) \quad \forall r, \forall \ell = 1$$

$$RO^r(t+\ell) - RO^r(t+\ell-1) - [\dot{R}OAI^r(t+\ell) + \dot{R}OEI^r(t+\ell)]\Delta\ell + [\dot{R}OAD^r(t+\ell) + \dot{R}OED^r(t+\ell)]\Delta\ell = 0 \quad \forall r, \forall \ell \geq 2$$

Maximum Allowable Release Constraints:

$$RO^r(t+\ell) \leq c - \alpha * T(t+\ell) \quad \text{or} \quad RO^r(t+\ell) \leq RO^r_{max} \qquad \forall r, \forall \ell$$

Storage Zone Bounds:

$$0 \leq US^r_i(t+\ell) \leq \overline{US}^r_i(t+\ell) \quad \forall i, \forall r, \forall \ell$$

$$0 \leq LS^r_i(t+\ell) \leq \overline{LS}^r_i(t+\ell) \quad \forall i, \forall r, \forall \ell$$

$$0 \leq S^r(t+\ell) \leq RCAP^r \qquad \forall r, \forall \ell$$

Flow Zone Bounds:

$$0 \leq UQ^c_i(t+\ell) \leq \overline{UQ}^c_i(t+\ell) \quad \forall i, \forall c, \forall \ell$$

$$0 \leq LQ^c_i(t+\ell) \leq \overline{LQ}^c_i(t+\ell) \quad \forall i, \forall c, \forall \ell$$

$$0 \leq Q^c(t+\ell) \leq \infty \qquad \forall c, \forall \ell$$

Release Rate Bounds:

$$0 \leq \dot{R}OAI^r(t+\ell) \leq \dot{R}OAI^r_{max}(t+\ell) \quad \forall r, \forall \ell$$

$$0 \leq \dot{R}OAD^r(t+\ell) \leq \dot{R}OAD^r_{max}(t+\ell) \quad \forall r, \forall \ell$$

$$RO^r_{min}(t+\ell) \leq RO^r(t+\ell) \leq CCAP^r \quad \forall r, \forall \ell$$

$$m = L(4 * NRES + 2 * NST) \quad (4.33)$$

where n = number of columns of matrix (number of decision variables); m = number of rows of matrix (number of constraints); r = reservoir index; NRES = number of reservoirs; c = control station index; NST = number of control stations.

4.8 METHOD OF SOLUTION

Solution of the operation problems for multi-purpose multi-reservoir systems as modeled herein requires solution of successive linear programming problems. Use of digital computer for solution is mandatory because of the dimensions of the LP matrices and the number of times the solution process must be repeated.

Individual LP problems are solved by the "simplex" method. Among many available LP algorithms that implement the simplex method, XMP is selected for use in this study because of its efficiency, reliability, portability and extendability (Marsten, 1980). XMP was developed at the National Bureau of Economic Research, and at the University of Arizona, under a grant from the National Science Foundation.

The XMP library consists of 48 subroutines written in FORTRAN that perform the various functions involved in solving linear programs. In order to facilitate the use of XMP for solving the optimal operations' problem of GRB reservoirs, two additional packages of routines were developed by the author: one to manage the input data structure, called XMPINP, which itself consists of a main program and 13 subroutines, and one for the output data structure called XMPOUT which consists of five subroutines. Thus the total GRBOPM2 model is composed of a main program and 66 subroutines. The roles and the interaction of XMPINP, XMPOUT, and XMP routines are shown in Figure 4.8.

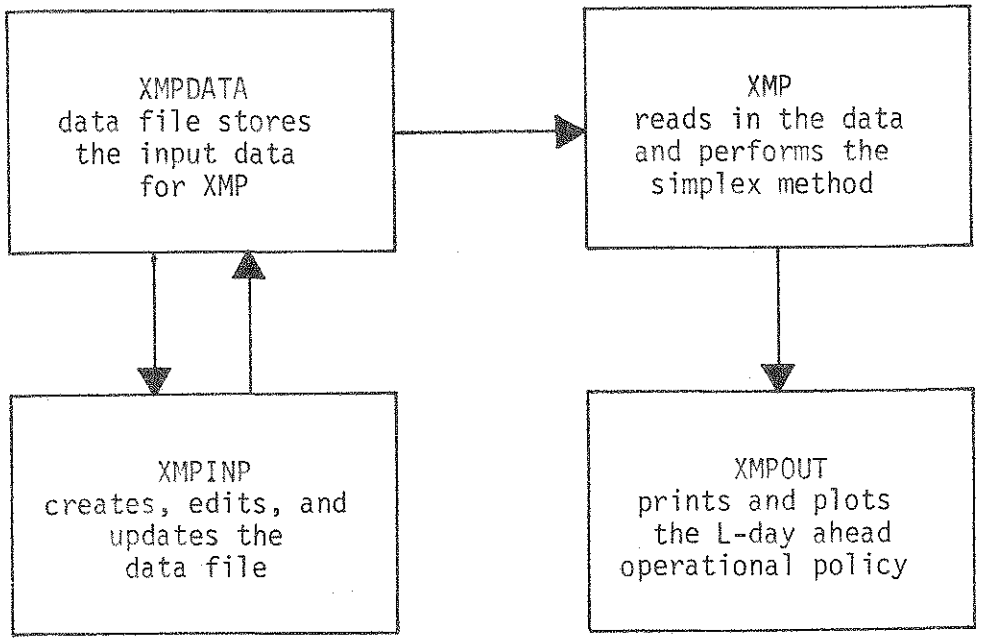

Figure 4.8 Roles and Interactions of XMPINP, XMPOUT, and XMP Routines

V. USE OF GRBOPM2 IN RESERVOIR OPERATION STUDIES

The GRBOPM2 model discussed in Chapter IV can be used in two modes. These two modes of use are: (1) special reservoir operations studies, or a "study mode," for short; (2) real-time operations. The use of the model in real-time operations will be discussed in Chapter VI. In this chapter, the use of the GRBOPM2 model in special reservoir operations studies is discussed.

5.1 SCOPE OF SPECIAL RESERVOIR OPERATIONS STUDIES

Special reservoir operations studies are typically made to study alternative operating policies over periods of time much longer than that normally used in real-time operations. Special operations studies are aimed at obtaining the long-run systems responses for a proposed plan, or project, or revision thereof.

The study mode is used by analysts as well as operators to improve the model structure as well as its daily use. In regard to the model structure, results obtained in the study mode permit making refinements to the long-run operating strategy, such as changes in rule curves, target flows, various zones, and the penalty coefficients.

The maintenance of optimal selections for rule curves, target flows, zones, and penalty coefficients depends, of course, on the project purposes, i.e. system's objectives. There are two main project objectives, namely flood control and recreation. In the absence of fixed market values thereof, the study mode results must be presented in the form of trade-off curves (see Section 5.8). Since the relative significance of these objectives depends on the season, study mode results have been generated for the summer as well as the winter seasons. The above study results were obtained for both historical hydrologic data as well as synthetic model input data.

By generating trade-off curves using operating policies that had different operating horizons, it was possible to study the selection of that horizon for short-run operations.

5.2 STEPS IN USING GRBOPM2 MODEL IN A STUDY MODE

The model's use in the study mode generally requires the following steps:

(1) Define long-run target conditions by specifying the rule curve, and the target flow levels at the control stations.

(2) Specify zones of deviation for the reservoir storages, S, and the control station flows, Q, (LS_i^r, US_i^r, LQ_i^c, and UQ_i^c where i = zone index; r = reservoir index; c = control station index).

(3) Specify penalty coefficients for each zone of deviation ($P^r_{LS_i}$, $P^r_{US_i}$, $P^c_{LQ_i}$, and $P^c_{UQ_i}$; $\forall r$, $\forall c$) from long-run targets.

A minimum of two zones must be specified for each reservoir and for each control station: one above the rule curve or target flow level and one below (i.e. $NSA^r \geq 1$, $NSB^r \geq 1$, $NQA^c \geq 1$, and $NQB^c \geq 1$; $\forall r$, $\forall c$). The penalties for storage and flow deviations must describe a convex function: as the deviations increase, the corresponding penalty coefficients must similarly increase (i.e. $P^r_{LS_{i+1}} \geq P^r_{LS_i}$, $P^r_{US_{i+1}} \geq P^r_{US_i}$, $P^c_{LQ_{i+1}} \geq P^c_{LQ_i}$, and $P^c_{UQ_{i+1}} \geq P^c_{UQ_i}$; $\forall r$, $\forall c$, $\forall i$).

(4) Define maximum allowable rates of change of release ($\dot{ROAI}^r_{max}$ and $\dot{ROAD}^r_{max}$; $\forall r$) and penalties for exceeding these limits ($P^r_{\dot{ROEI}}$ and $P^r_{\dot{ROED}}$; $\forall r$); I ≡ increase; D ≡ decrease.

(5) Define the short-run operating horizon, L, over which constraints defined in Table 4.1 must be checked.

(6) At the beginning of the run, initialize all needed data time series namely reservoir outflows $RO^r(t)$, reservoir elevations $E^r(t)$, and reservoir inflows $RI^r(t)$, for r = 1, 2, 3, 4 and for $-5 \leq t \leq 0$. Other initial input data are the average rainfall $P^{rr}(t)$ at nine river

reaches, rr = 1, 2, ...9, tributary inflows $T^s(t)$ at four tributaries (Gresham, Alvaton, Glen Dean, and Horse Branch); and finally the flows at nine control stations $Q^c(t)$, c = 1, 2, ...9, and $-5 \leq t \leq 0$.

(7) In addition, the model input data for t = 1, 2, ...T, (where T = length of study period) are then defined, or assumed, or externally generated. Among the exogeneously generated input data one finds the reservoir inflow, average precipitation, and tributary inflows.

The model is then run in stages as illustrated in Figure 5.1 much like one would find in a dynamic programming approach. There is one stage per model time step (i.e. one day). For each stage the status of the system is summarized by a set of state variables which permit calculating a vector of optimal release decisions for the next L-day period.

The directed arcs in Figure 5.1 represent the direction of information flow, and the rectangles represent the decision process. In order to obtain day t+1 releases, the initial state of the system, (i.e. $E^r(t)$, $RO^r(t)$, $RI^r(t)$, $P^{rr}(t)$, $T^s(t)$, and $Q^c(t)$) as well as the generated inflows $RI^r(t+\ell)$; r = 1, 2, 3, 4, the precipitations $P^{rr}(t+\ell)$; rr = 1, 2, ... and the tributary inflows $T^s(t+\ell)$; s = 1, 2, 3, 4 for ℓ = 1, 2, ..., L are needed. With this information optimal releases $RO^r(t+1)$ for period t+1 are calculated[1].

Going from "stage" t+1 to stage t+2, the reservoir elevations, $E^r(t+1)$, and the flows at control stations, $Q^c(t+1)$, as well as the releases, $RO^r(t+1)$, resulting from day t+1 calculation, are automatically transferred and used to update the model for the day t+2 calculation. After also updating the forecasts for ℓ = 2, 3, ..., L+1 (see Figure 5.1), this process continues until t = T.

[1] *although optimal results for t+2, t+3, ... t+L, are computed also, they are not used in further calculations in the study mode.*

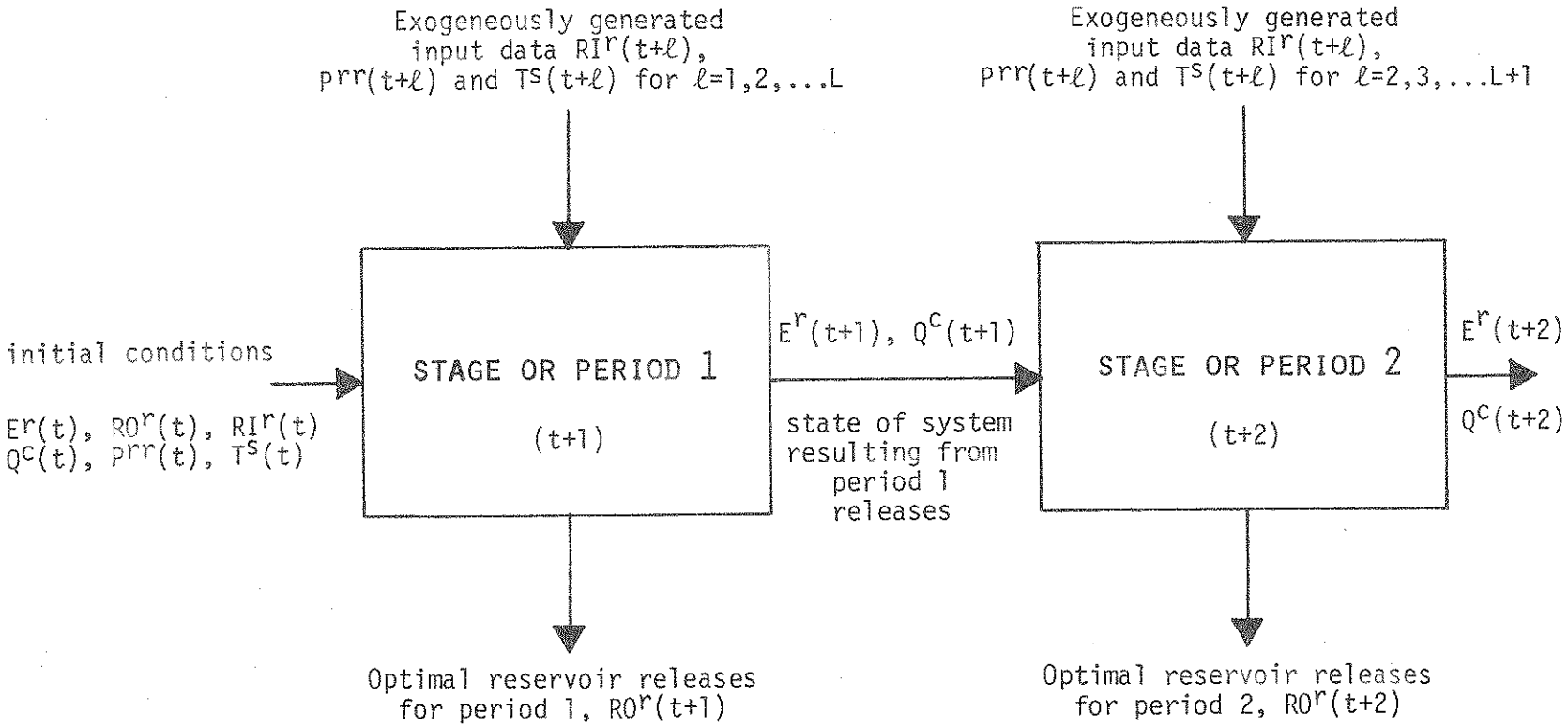

Figure 5.1 Diagram of GRBOPM2 Used in the Study Mode

5.3 USE OF DUAL SIMPLEX ALGORITHM

In running GRBOPM2 it is important to have at the start of each computation stage t an initial feasible solution that is "close to" the optimal solution for stage t. As the initial feasible solution, it was decided to use the optimal solution calculated for stage t-1. In some cases, that solution will be infeasible because the right-hand sides of the constraint equations shown in Table 4.1 have been changed as part of the updating process. In such cases one can use the dual simplex algorithm to clear the infeasibility associated with new right-hand sides and attain the primal feasibility criterion (i.e. optimality criterion for the dual simplex algorithm). Therefore, after obtaining the optimal solutions for the first period (i.e. t=1) by using the primal simplex algorithm, all subsequent solutions (i.e. t = 2, 3, ... T) were obtained by the dual simplex algorithm. The use of this approach provided approximately 90% reduction in the cost of program execution as compared to the use of primal simplex algorithm independently for each period ($0.15 versus $1.5).

5.4 USER SUPPLIED PENALTY COEFFICIENTS AND ZONES

As stated earlier in Chapter II, the four reservoirs in Green River Basin are regulated primarily for flood control. A secondary objective is recreation. In addition, all four reservoirs also contribute something to low flow augmentation in the basin; Green Reservoir has an allocation of storage specifically for water quality control in upper Green River.

Major floods have been caused by cyclonic storms which usually occur in the winter and early spring. Convective storms which generally occur in the summer months seldom cause important flooding because they are localized and transpiration and infiltration losses then are high. Damages resulting from winter floods, on the other hand, are not as high as those occurring when crops are on the fields. Only extreme floods in the winter cause serious damage when stages are sufficiently high to affect real property, stored crops, highways, etc. Thus flood damages

are heavily dependent on the season. In order to minimize flooding, reservoir levels are drawn down to winter holding levels, thereby providing storage for winter and early spring runoff.

Recreation includes boating, picnicking, fishing and other activities occurring either in the reservoirs or in and along the stream channels. Recreational values are also season dependent and occur mainly in the summer season.

Low flow augmentation purposes include water quality control (in upper reaches) as well as the maintenance of a minimum flow in all channels. In order to offset effects of oil industry operations in the upper Green, a total of 64,000 ac-ft of storage is allocated in Green Reservoir for low flow augmentatio

Thus most of the project purposes are seasonal. This is reflected in the rule curve which prescribes two distinct target states for the GRB reservoir namely a winter and a summer season. These two periods were simulated and studi and the results reported herein. Other seasons such as the spring and fall seasons (which correspond to reservoir filling and depletion periods) are not considered in this study.

No specific criteria are offered here for selection of the values for the various penalty coefficients. Such a selection is ultimately the reservoir operators' prerogative. Thus one of the modeling principles was to make penalty coefficients selectable by the reservoir operators who have the most experience in defining the goals and priorities of the GRB reservoir system operation. For effective model building purposes, however, it was essential to have reasonable initial values for the penalty coefficient and zone limits. Thus, during the course of the study, regular contact was maintained with the agency staff in or to "best" define the model's study parameters. The results of all these discussions were refined by Mr. R. A. Biel[1] in Tables 5.1 and 5.2 for the winter

[1] *Chief, Reservoir Regulation Section, Louisville District Office, Corps of Engineers*

Table 5.1 Storage Zone Levels and the Corresponding Penalty Coefficients for GRB Reservoirs in Winter Season

Storage Zone Levels and Corresponding Penalty Coefficients	Reservoirs			
	Green	Nolin	Barren	Rough
$US_3=f(UE_3)$	724-734	570-580	608-618	544-554
P_{US_3}	1000	1000	1000	1000
$US_2=f(UE_2)$	713-724	560-570	590-608	524-544
P_{US_2}	65	65	65	65
$US_1=f(UE_1)$	664-713	490-560	525-590	470-524
P_{US_1}	3	2	2	4
RCS=f(RCE)	664	490	525	470
$LS_1=f(LE_1)$	655-664	476-490	520-525	465-470
P_{LS_1}	1	2	2	2
$LS_2=f(LE_2)$	Datum-655	Datum-476	Datum-520	Datum-465
P_{LS_2}	200	150	200	200

Table 5.2 Flow Zone Levels and the Corresponding Penalty Coefficients for GRB Control Stations in Winter Season

Flow Zones and Penalty Coefficients	CONTROL STATIONS								
	Greensburg	Munfordville	Brownsville	Bowling Green	Woodbury	Paradise	Falls of Rough	Dundee	Calhoun
UQ_3	10000-∞	17000-∞	23000-∞	14000-∞	25000-∞	35000-∞	2000-∞	4000-∞	40000-∞
P_{UQ_3}	15	11	9	19	23	19	14	14	24
UQ_2	4000-10000	12000-17000	13000-23000	6800-14000	17000-25000	26000-35000	1200-2000	2000-4000	31000-40000
P_{UQ_2}	5	6	4	4	8	4	4	4	9
UQ_1	2000-4000	6000-12000	7000-13000	3400-6800	8500-17000	13000-26000	600-1200	1000-2000	15000-31000
P_{UQ_1}	1	1	1	1	1	1	1	1	1
TFL	2000	6000	7000	3400	8500	13000	600	1000	15000
LQ_1	25-2000	45-6000	95-7000	60-3400	260-8500	280-13000	5-600	10-1000	320-15000
P_{LQ_1}	0	0	0	0	0	0	0	0	0
LQ_2	0-25	0-45	0-95	0-60	0-260	0-280	0-5	0-10	0-320
P_{LQ_2}	100	100	100	250	250	250	100	100	250

season. The model parameters for summer season are shown in Tables 5.3 and 5.4. The storage zone levels in Tables 5.1 and 5.3 are presented in terms of elevation levels [ft] (i.e. UE_i and LE_i); in the model, however, these elevation levels are converted into corresponding storages by using the storage-elevation-curves for each reservoir.

The penalty coefficients are constants within their storage deviation zones. This means that with respect to reservoir elevation deviations the coefficients would be slightly non-linear.

5.4.1 Winter Season

In the winter season, a total of five storage zones were defined for each reservoir (see Table 5.1). The upper storage deviations are divided into three classes or zones; the lower storage deviations are divided into two zones. In order to maintain a balance of storage among the four reservoirs approximately equal penalty coefficients were assigned to corresponding storage zones. The storage penalty coefficients [penalty points/acre-ft] are approximately 2.0-4.0 for the first storage zone, 65 for the second storage zone and 1000 for the last storage zone above the rule curve. Thus, under flood conditions when water must be stored in the system reservoirs, the model will distribute the water, if possible, within the same zone of all reservoirs before the storage in any reservoir enters the next, more expensive (in terms of accumulating penalties) zone.

Similar considerations hold for storage violations below the rule curve. For example, the model insures that during extremely dry conditions when water must be released in order to meet downstream minimum flow requirements, all reservoirs will normally be emptied to their lower most storage zone (i.e. S_2^r; $\forall r$) before any reservoir enters the lowest zone.

It is not always possible to maintain an exact balance of storage in the system reservoirs. This may be due to irregular areal and temporal distribution of flood inflows, to the different target flow levels at control stations

Table 5.3 Storage Zone Levels and the Corresponding Penalty Coefficients for GRB Reservoirs in Summer Season

Storage Zone Levels and Corresponding Penalty Coefficients	Reservoirs			
	Green	Nolin	Barren	Rough
$US_4=f(UE_4)$	724-734	570-580	608-618	544-554
P_{US_4}	1000	1000	1000	1000
$US_3=f(UE_3)$	713-724	560-570	590-608	524-544
P_{US_3}	65	65	65	65
$US_2=f(UE_2)$	678-713	518-560	554-590	497-524
P_{US_2}	4	6	6	9
$US_1=f(UE_1)$	675-678	515-518	552-554	495-497
P_{US_1}	3	2	2	4
RCS=f(RCE)	675	515	552	495
$LS_1=f(LE_1)$	661-675	486-515	547-552	492-495
P_{LS_1}	1	2	2	3
$LS_2=f(LE_2)$	655-661	476-486	520-547	465-492
P_{LS_2}	2	4	4	5
$LS_3=f(LE_3)$	Datum-655	Datum-476	Datum-520	Datum-465
P_{LS_3}	200	150	200	200

Table 5.4 Flow Zone Levels and the Corresponding Penalty Coefficients for GRB Control Stations in Summer Season

Flow Zones and Penalty Coefficients	CONTROL STATIONS								
	Greensburg	Munfordville	Brownsville	Bowling Green	Woodbury	Paradise .	Falls of Rough	Dundee	Calhoun
UQ_3	10000-∞	17000-∞	23000-∞	14000-∞	25000-∞	35000-∞	2000-∞	4000-∞	40000-∞
P_{UQ_3}	60	65	40	40	90	50	90	90	105
UQ_2	4000-10000	12000-17000	13000-23000	6800-14000	17000-25000	26000-35000	1200-2000	2000-4000	31000-40000
P_{UQ_2}	50	60	35	35	75	35	35	35	90
UQ_1	700-4000	1700-12000	2800-13000	1850-6800	5400-17000	6200-26000	500-1200	750-2000	7600-31000
P_{UQ_1}	1	1	1	1	1	1	2	2	2
TFL	700	1700	2800	1850	5400	6200	500	750	7600
LQ_1	150-700	180-1700	270-2800	100-1850	360-5400	400-6200	50-500	100-750	400-7600
P_{LQ_1}	0	0	0	0	0	0	0	0	0
LQ_2	50-150	90-180	190-270	60-100	260-360	280-400	10-50	20-100	320-400
P_{LQ_2}	1	5	10	20	20	20	5	15	20
LQ_3	0-50	0-90	0-190	0-60	0-260	0-280	0-10	0-20	0-320
P_{LQ_3}	100	100	100	250	250	250	100	100	250

throughout the system, and to limits on release capacity of a particular reservoir. In such situations the order in which the reservoirs should deviate from their rule curve levels is specified by assigning slightly different coefficient values in corresponding zones. For example, Rough Reservoir has the least allowable release capacity. Therefore, a slightly larger penalty coefficient was assigned for storage violations in the first zone above the rule curve as compared to the other reservoirs (a value of [4 points/ac-ft] as compared to [2-3 points/ac-ft]). On the other hand, the storage violations in the first zone (LS_1) below the rule curve in Green Reservoir are not as objectionable as those of other reservoirs. This is because that zone was allocated for water quality purposes. Thus, a penalty coefficient of 1[penalty points/ac-ft] was assigned for this zone as compared to penalty coefficient of [2 points/ac-ft] for the other three reservoirs (see Table 5.1). Thus, the model tends to promote releases from Green Reservoir.

Deviations from target flow levels at the nine control stations were each represented by a total of five flow zones (Table 5.2). Three are above and two are below the target levels.

The lower boundaries of the uppermost flow zones represent the maximum flow rates for which no flood damages occur (COE, 1967). The penalty coefficients [penalty points/cfs] for flows exceeding these levels are assigned relatively large values [9-24 penalty points/cfs]. Because of the daily time step of the model, each acre-foot of water released from a reservoir produces a proximately a 2 [cfs] flow downstream. Therefore, each unit of penalty assesse against flows at a control station [penalty points/cfs] is equivalent to two units of penalty assessed against storage at a reservoir [penalty points/ac-ft] Thus, because the penalty coefficients for the uppermost flow zones (i.e. P_{UQ_3}) are more than twice as large as the penalty coefficients for reservoir storage

(i.e. P_{US_1}), water will be retained in the reservoir, if possible, rather than released. This, of course, reflects the system's purpose of flood control.

The first flow zone (UQ_1^c; ¥c) below the target flow level carries no real penalty because it corresponds to normal flow conditions. Therefore, a penalty coefficient of zero was assigned (Table 5.2). On the other hand, penalty coefficients in the order of 100-250 [penalty points/cfs] were assigned for the lowermost flow zone (i.e. LQ_2) because it corresponds to the required minimum flow conditions.

5.4.2. Summer Season

In the summer season, the target elevations of the reservoirs are well above those of winter season (see Tables 5.1 and 5.3) in order to provide surface area for reservoir recreation. On the other hand, the target flow levels at the control stations are held lower than those of winter season because of in-stream recreation as well as high potential of flood damages due to the crop season (see Tables 5.2 and 5.4). Deviations from the ideal state of the reservoirs in this season were represented therefore by a total of seven zones, four above and three below the target storages (Table 5.3). Again the interreservoir priority relationships that reflect the relative recreational potential of each reservoir in terms of visitor-days were represented by assigning slightly larger penalty coefficients for those reservoirs in which the recreation potential is higher (see Table 5.3). That ranking derived from the relative number of visitor-days is: Rough (most), Barren, Nolin, and Green (least).

Deviations from target flow levels at the control stations were represented by a total of six zones, three above and three below the target flows. The uppermost two zones (i.e. UQ_2 and UQ_3) correspond to winter flow zones (see Tables 5.2 and 5.4); however, the penalties assigned for these two zones are considerably higher than corresponding penalties in the winter season. This

may be due to the fact that floods which occur during crop season (April to October) cause the most serious damage.

In the summer season, low-flow requirements may be critical. The lowermost flow zones (i.e. LQ_3) correspond to "acceptable" minimum flow levels; these are equivalent to 7-day, 10-year pre-project flows. Penalties for these zones were assigned such that the model tends to provide releases which assure maintenance of low-flow criteria. In addition to this zone, a second zone (i.e. LQ_2) which corresponds to the "desired" levels of low flow was establishe in order to maintain in-stream recreation and in part of the system to offset the evaporation losses due to the withdrawal of cooling water by the TVA steam plant at Paradise. Note that this zone is absent in the winter season (see Tables 5.2 and 5.4).

5.5 RATE-OF-CHANGE OF RELEASE PENALTY COEFFICIENTS AND ZONES

From past release records it had been deduced that the reservoir operators gave weight to not changing release rates. Consequently, a penalty structure was introduced for rate of change of releases as shown in Section IV 5.5.a. The selection of "zone" limits and the coefficients [penalty points/cfs/day] was based on a statistical analysis of historical rates of change of releases.

Thus, cumulative distribution functions (CDFs) of the historical rates-of-change of releases were developed for each reservoir and for each of the two seasons. Only three years of data (water years 1970-1972) were used becaus Green Reservoir was not completed until 1969. The CDFs for the winter and summer periods are shown in Figure 5.2. For this study, the maximum allowable rates-of-change of release are defined as the 0.95 percentile levels of each CDF. These and other statistical characteristics of the rates-of-change of release data are tabulated in Tables 5.5 and 5.6. From an examination of the Tables 5.5 and 5.6, it is apparent that the rates-of-change of releases are smaller in the summer season than in the winter season. Furthermore, it can

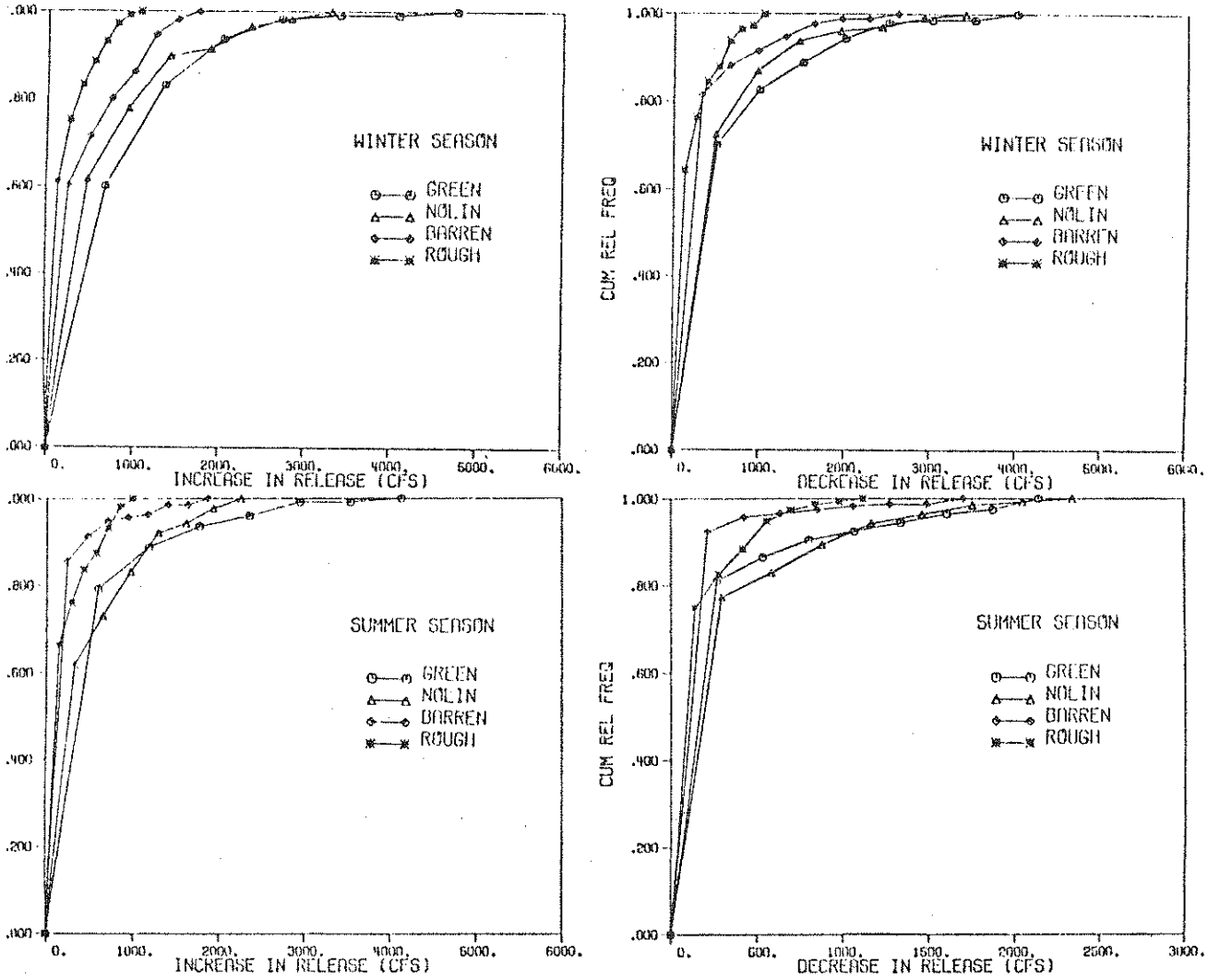

Figure 5.2 Cumulative Distribution Functions of the Historical Rates-of-Change of Releases for the GRB Reservoirs in Winter and Summer Seasons

Table 5.5 Statistics of Rates-of-Change of Release for GRB Reservoirs in Winter Season

Rates-of-Change of Release in Winter Season	Reservoirs			
	Green	Nolin	Barren	Rough
Increase-of-Release				
• Mean (cfs)	718.0	570.0	382.0	188.0
• Standard Deviation (cfs)	777.0	689.0	435.0	235.0
• Minimum (cfs)	1.0	1.0	1.0	0.1
• Maximum (cfs)	4770.0	3310.0	1760.0	1082.0
• 0.95 percentile level	2250.0	2210.0	1270.0	735.0
Decrease-of-Release				
• Mean (cfs)	536.0	449.0	236.0	173.0
• Standard Deviation (cfs)	728.0	612.0	451.0	246.0
• Minimum (cfs)	1.0	6.0	2.0	0.1
• Maximum (cfs)	3997.0	3390.0	2604.0	1047.0
• 0.95 percentile level	2100.0	1700.0	1310.0	710.0

Table 5.6 Statistics of Rates-of-Change of Release for GRB Reservoirs in Summer Season

Rates-of-Change of Release in Summer Season	Reservoirs			
	Green	Nolin	Barren	Rough
Increase-of-Release				
• Mean (cfs)	371.0	438.0	129.0	181.0
• Standard Deviation (cfs)	688.0	530.0	318.0	245.0
• Minimum (cfs)	1.0	1.0	1.0	0.1
• Maximum (cfs)	4130.0	2262.0	1870.0	992.0
• 0.95 percentile level	2100.0	1680.0	750.0	760.0
Decrease-of-Release				
• Mean (cfs)	214.0	279.0	72.0	120.0
• Standard Deviation (cfs)	450.0	428.0	240.0	203.0
• Minimum (cfs)	1.0	4.0	1.0	0.1
• Maximum (cfs)	2140.0	2340.0	1700.0	1122.0
• 0.95 percentile level	1400.0	1280.0	390.0	580.0

be seen from Figure 5.2 that the rates-of-change of releases are relatively small for Rough and Barren Reservoirs because of their limited release capacities and probably their high recreation potential in terms of visitor-days. Penalties assessed for exceeding the maximum allowable rates-of-change of releases will be discussed further in Section 5.8.

5.6 MAXIMUM ALLOWABLE RELEASE SCHEDULE CONSTRAINTS

The maximum allowable release schedule constraints (see Section 4.5.5.c) that are included for each reservoir were derived from the regulation schedules shown in Appendix A. After converting the stages at the local control stations into flows using the stage-discharge relationships given in Table 2.5, these constraints are represented as shown in Figure 5.3. These constraints are the same for both winter and summer seasons for each reservoir except Barren (Figure 5.3). Maximum allowable releases for Barren Reservoir are smaller in the summer season than those of the winter season. This may be due to increased agricultural activity in the summer season.

5.7 NUMBER OF CONSTRAINTS AND DECISION VARIABLES OF THE MODEL

The use of GRBOPM2 model in special reservoir operations studies as described in Section 5.2 requires solving a succession of linear programming problems. The number of decision variables and the constraint equations (see Equations 4.32 and 4.33) that define the LP problem to be solved at each stage is a function of: (1) the number of reservoirs, NRES; (2) the number of control stations, NST; (3) the number of storage zones for each reservoir, NSA and NSB; (4) the number of flow zones for each control station, NQA and NQB; and (5) the operating horizon, L[days]. The number of reservoirs and control stations included in the operations study of the GRB system is fixed, namely four reservoirs (i.e., NRES=4) and nine control stations (i.e., NST=9). Furthermore, the number of storage and flow zones is dependent on the season. Also

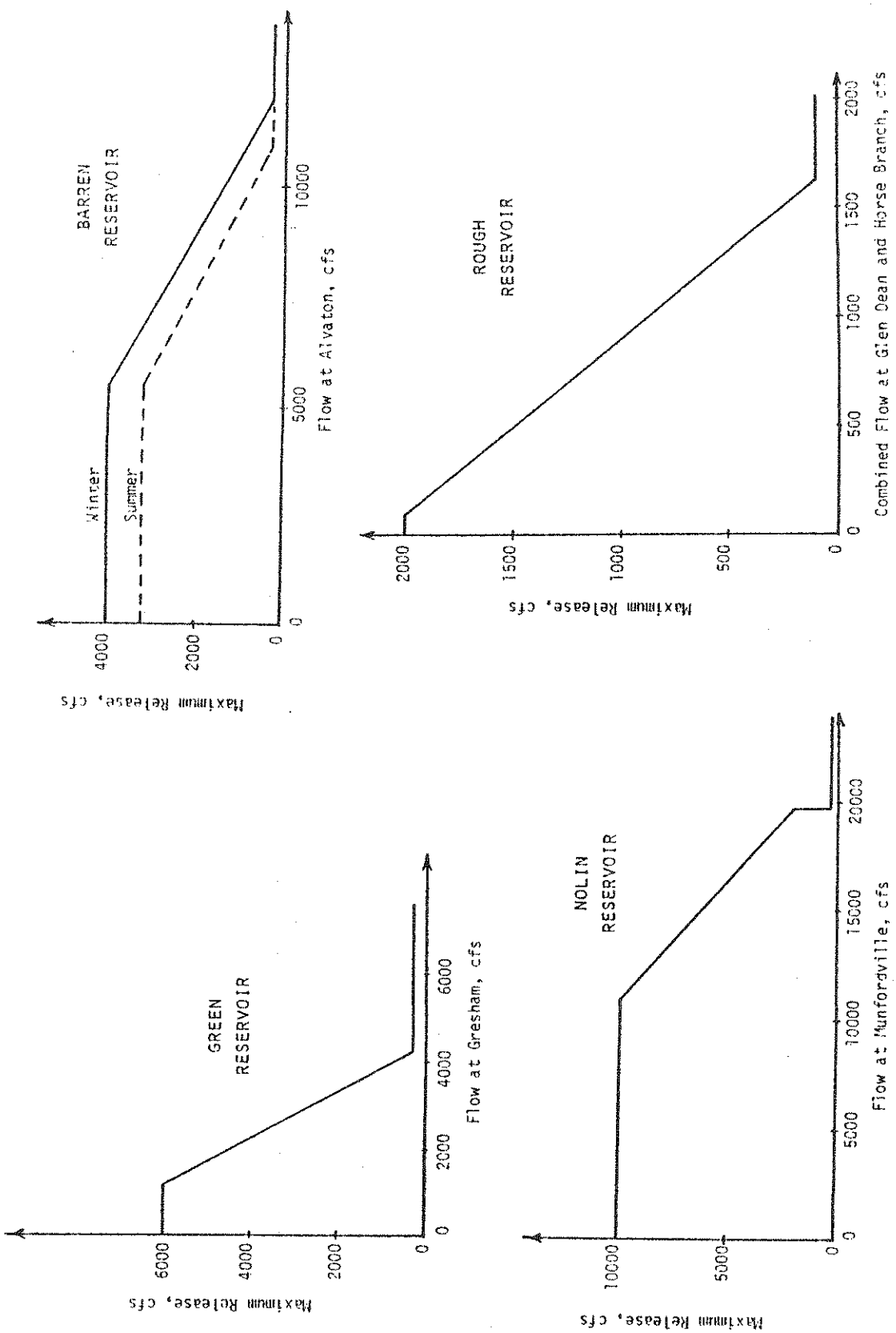

Figure 5.3 Maximum Allowable Release Schedule Constraints for the GRB Reservoirs

the operating horizon, L, over which the constraint equations of Table 4.1 must be checked is a function of the availability of forecasted and/or generated input information.

5.7.1 Winter Season

As described in Section 5.4.1 the total number of storage zones in the wint season for each of the reservoirs equals five (see Table 5.1). Similarly, the total number of flow zones for each of the control stations equals five (see Table 5.2). Thus, the number of decision variables and the constraints of the LP problem depend only on the operating horizon, L. For different values of L, the Equations 4.32 and 4.33 give the dimensions of the technological coefficient matrix $\underset{\sim}{A}$ (see Eq. 4.1.b) for the winter season. They are tabulated in Table 5.7. The slack and artificial variables that are required for finding the starting feasible solution for the LP problem, however, are not included in Table 5.7. The model automatically adds a slack variable for each less-than-or-equal-to constraint and an artificial variable for each equality constraint. Thus, in addition to the decision variables shown in Table 5.7, a total of m slack and artificial variables must also be considered (m = number of constraints) when setting the dimensions of the model's arrays.

The computational efficiency and hence the cost of using the simplex algorithms is more sensitive to the number of constraints than to the number of decision variables (Phillips, Ravindran, and Solberg, 1976). Eq. 4.33 shows that the number of constraints of the LP problem for the Green River Basin is directly related with the operating horizon L (see Table 5.7). Therefore, the marginal improvements in the system's measure of effectiveness (i.e. decrements in total penalty) obtainable by increasing L must be studied in the light of the rapidly increasing computational burden. This aspect will be discussed further in Section 5.10.

Table 5.7 Dimensions of the Technological Coefficient Matrix $\underset{\sim}{A}$ of the LP Problem as a Function of Operation Horizon, L for Winter Season

Dimensions of the Technological Coefficient Matrix $\underset{\sim}{A}$ in Winter	Operating Horizon, L			
	1-day	3-day	5-day	10-day
number of decision variables, n	98	294	490	980
number of constraints, m	34	102	170	340

Table 5.8 Dimensions of the Technological Coefficient Matrix $\underset{\sim}{A}$ of the LP Problem as a Function of Operation Horizon, L for Summer Season

Dimensions of the Technological Coefficient Matrix $\underset{\sim}{A}$ in Summer	Operating Horizon, L			
	1-day	3-day	5-day	10-day
number of decision variables, n	115	345	575	1150
number of constraints, m	34	102	170	340

Fortunately, the number of decision variables which are mainly determined by the number of storage and flow zones for GRB does not greatly affect the computational burden. Therefore, if need be the state of the system in the reservoirs and at the control stations could be represented by even more zones. Hence, the continuous penalty functions could be approximated yet more closely; the number of parameters to be determined would increase further, however.

The size of the LP model proposed herein grows as the number of systems components increases (i.e., reservoirs and stream channels). Consider a river system containing as many as 50 reservoirs and 100 control stations. Assuming five zones for storage and flow for each component and an operating horizon of five days, the LP model would consist of 2000 constraints and 7750 variables (including slack and artifical variables). A model of this size can still be handled by an LP algorithm. It could not possibly be handled via the DP approach.

5.7.2 Summer Season

The number of constraints of the LP model in the summer season is the same as in the winter season. The only difference is the increased number of decision variables due to the increased number of storage and flow zones. The decision variables and constraints are tabulated as a function of the operating horizon L in Table 5.8.

5.8 USE OF MODEL WITH HISTORICAL INPUTS TO DEVELOP TRADE-OFF CURVES

The use of the GRBOPM2 model in so called special reservoir operations studies was discussed in Section 5.2. A set of reservoir releases are selected for each day by minimizing the user-defined penalty functions (see Section 5.4) during two well-defined seasons of the year, namely winter and summer.

The objective function (Eq. 4.31) can be divided into three components as follows:

$$\text{Min } Z = f(\text{storage, flow, release})$$
$$\text{Min } Z = Z_1 + Z_2 + Z_3 \qquad (5.1)$$

The first objective Z_1 is a measure of deviations of storage from target levels (i.e. rule curve) at the reservoirs. The second objective Z_2 is a measure of deviations of flow from target levels at the control stations downstream of the reservoirs. The third objective Z_3 is a measure of deviations of excessive rate-of-change of release values from allowable limits. All three objectives conflict physically; because of this, minima of Z_1, Z_2, and Z_3 cannot be achieved simultaneously (see Figure 5.4). Thus, there exists a trade-off surface between the three objectives. The model permits one to generate and present such a trade-off surface to decision makers (here the Corps of Engineers staff directly responsible for the operation of the GRB system).

The trade-off surface between the three sub-objectives (i.e. MIN[Z_1], MIN[Z_2], and MIN[Z_3]) may be generated by a variable weighting of two of the sub-objectives and holding Z = constant for the third one. This amounts to "decomposing" or slicing the trade-off surface or "non-inferior set" and projecting it onto a plane. The procedure may be repeated for different levels of third objective until the entire trade-off surface is generated.

In this study, the entire trade-off surface has not been generated; rather, the trade-off curve between the first two sub-objectives (i.e. Z_1 and Z_2) was generated by holding the third sub-objective parameter value, Z_3, constant. This was achieved by adopting penalty coefficients for "excessive" rate-of-change of release at each reservoir that were very large, namely 3000[penalty points/cfs/day], as compared to the maximum penalty coefficient for storage at that reservoir. Therefore, the model will always choose to store a unit of water rather than to release it if that would make for a release in excess of the previous release plus the allowable increase. Consequently Z_3 = 0 and the original problem reduces to:

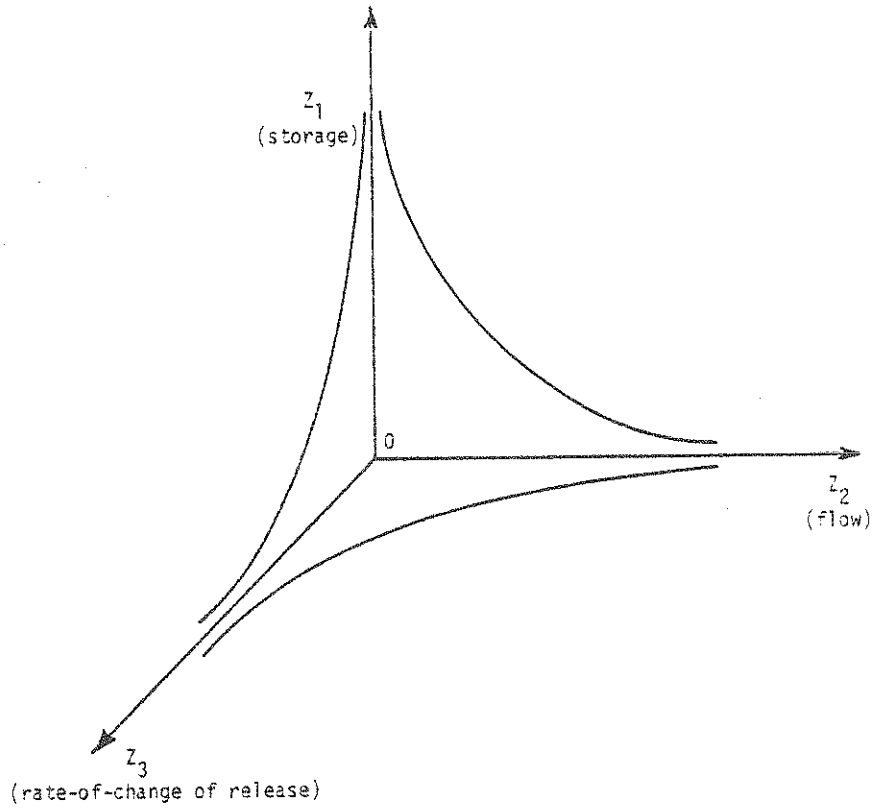

Figure 5.4 Trade-off Surface Between Three Objectives

$$\text{Min} \quad Z = Z_1 + Z_2 \tag{5.2}$$

subject to the constraints defined in Table 4.1. The generation of the trade-off curve between Z_1 and Z_2 is achieved by varying the ratio of the weights that contribute to the Z_1 and Z_2-values. The ratios are such that at one extreme the (weighted, aggregate) deviation of storages from target levels (Z_1) becomes minimized while at the other end only the (weighted, aggregate) deviation of flows from target levels (Z_2) becomes minimized. The final weighted objective function for intermediate situations reads:

$$\text{Min } Z = (1-\lambda)Z_1 + \lambda Z_2 \tag{5.3}$$

The term λ is a weighting factor between the two objectives. The values of λ range between zero and one. Both objectives are equally weighted or important when value of λ equals 0.5.

The above procedure was used to generate the trade-off curves between storage and flow penalties for the winter and summer seasons of the 1970 water year. The initializing data as well as all subsequent data inputs defined in Section 5.2 were historical data. The operating horizon L over which the constraint equations of Table 4.1 must be checked was set equal to 3.

5.8.1 Winter Season

The GRBOPM2 model was run in study mode between days 87 through 161 (Dec. 26, 1969 - March 10, 1970) of the 1970 water year. The model was not run for the entire winter season which corresponds to a period between December 1 and March 14 because there was a change in the rule curve levels on December 23, 1969, for Nolin, Barren, and Rough Reservoirs. The historical and model determined reservoir elevations, releases, and control station flows are shown in Figures 5.5 through 5.21. These figures show the case of $\lambda = 0.5$ (i.e. the original winter penalty coefficients as provided by the COE and shown in Tables 5.1 and 5.2).

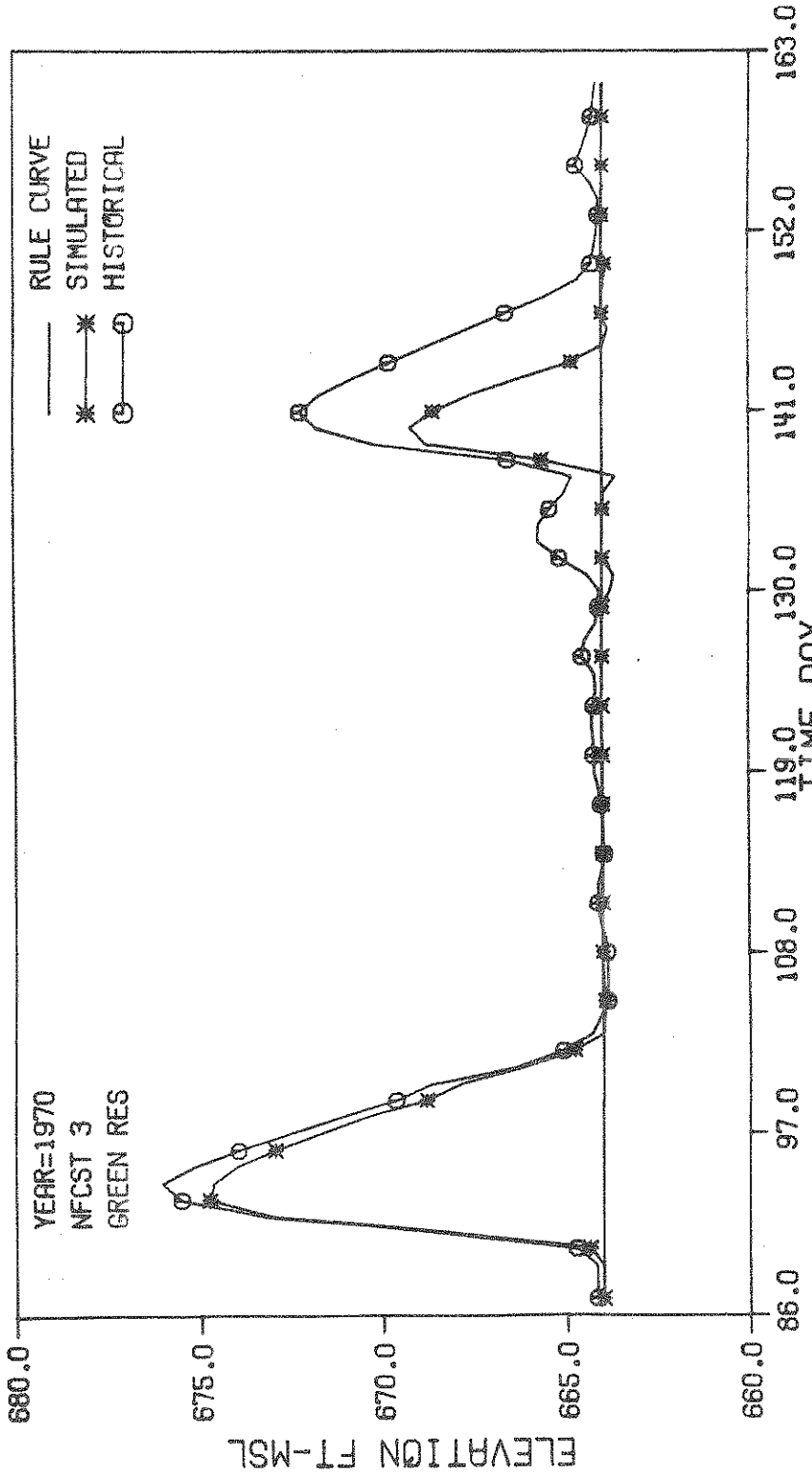

Figure 5.5 Simulated and Historical Elevations for Green Reservoir in the Winter Season of the 1970 Water Year

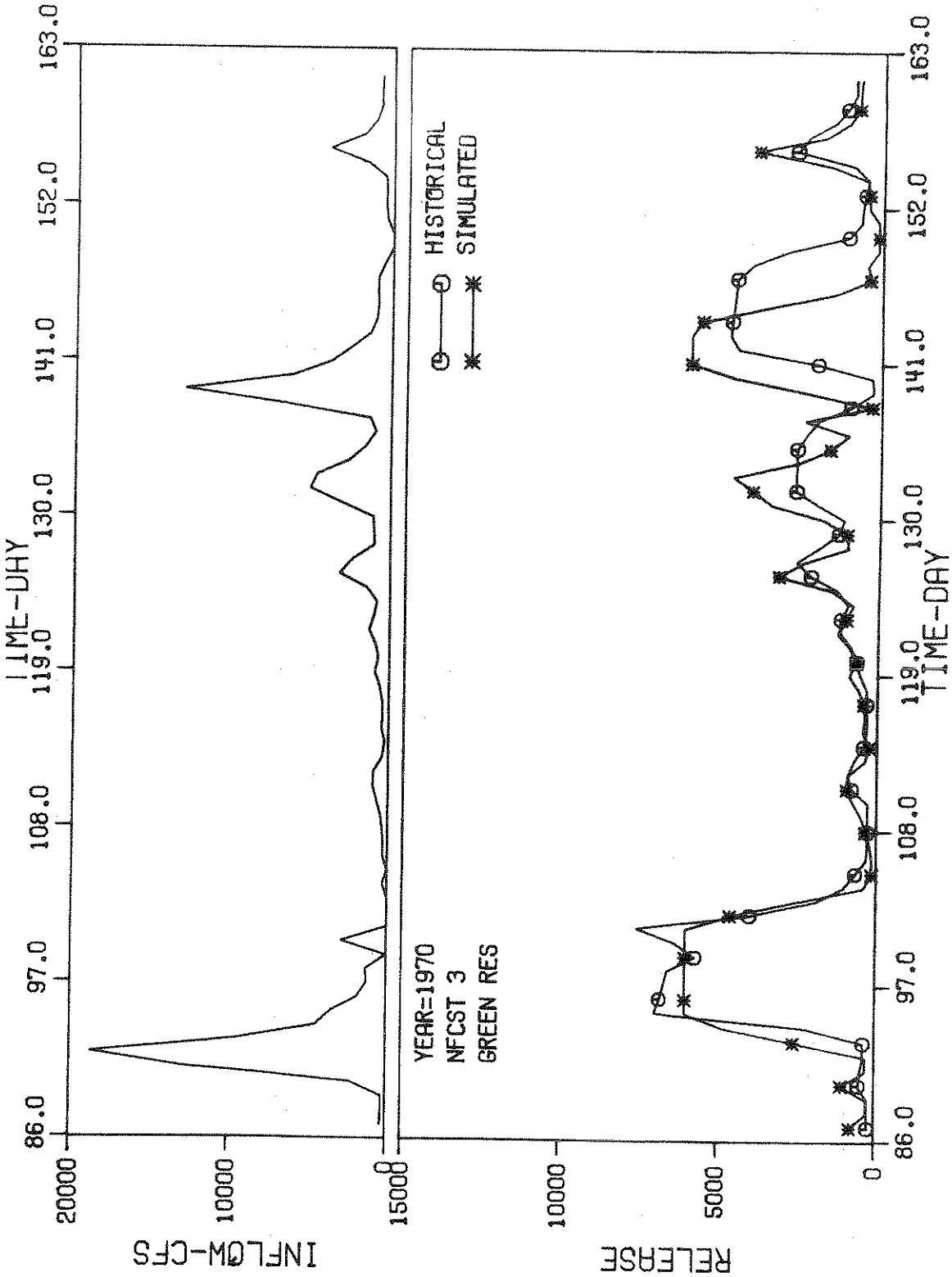

Figure 5.6 Simulated and Historical Releases for Green Reservoir in the Winter Season of the 1970 Water Year

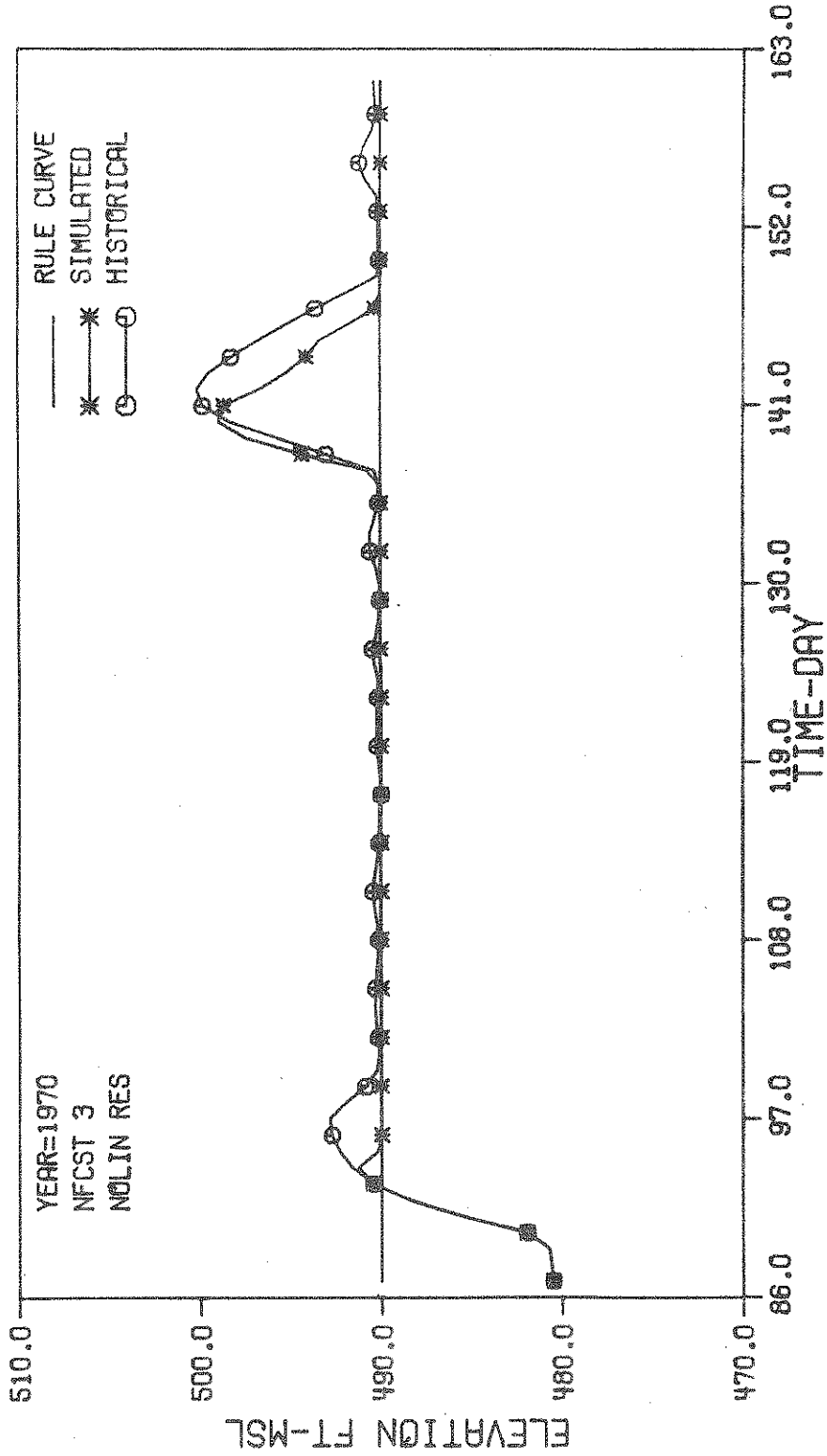

Figure 5.7 Simulated and Historical Elevations for Nolin Reservoir in the Winter Season of the 1970 Water Year

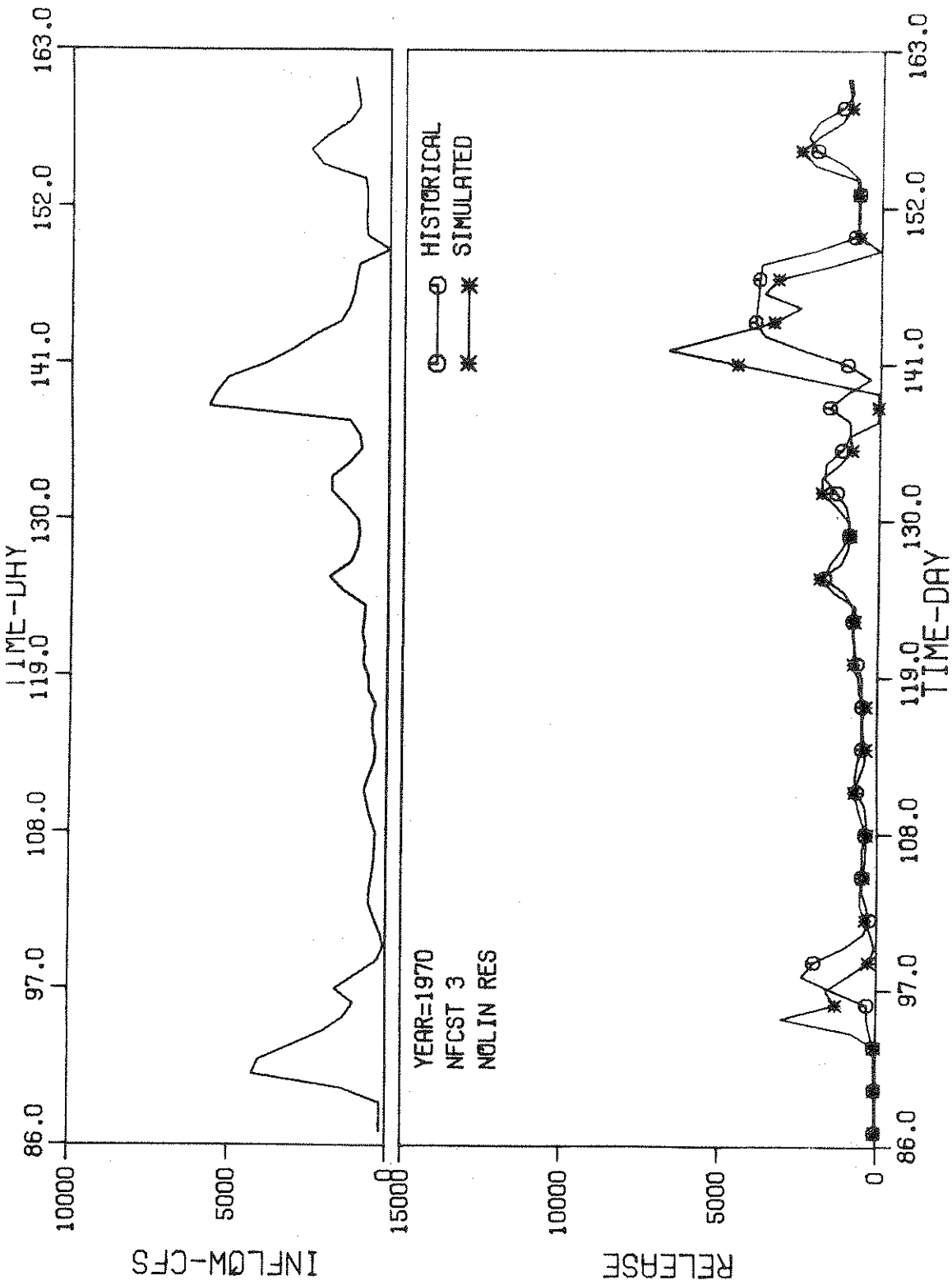

Figure 5.8 Simulated and Historical Releases for the Nolin Reservoir in the Winter Season of the 1970 Water Year

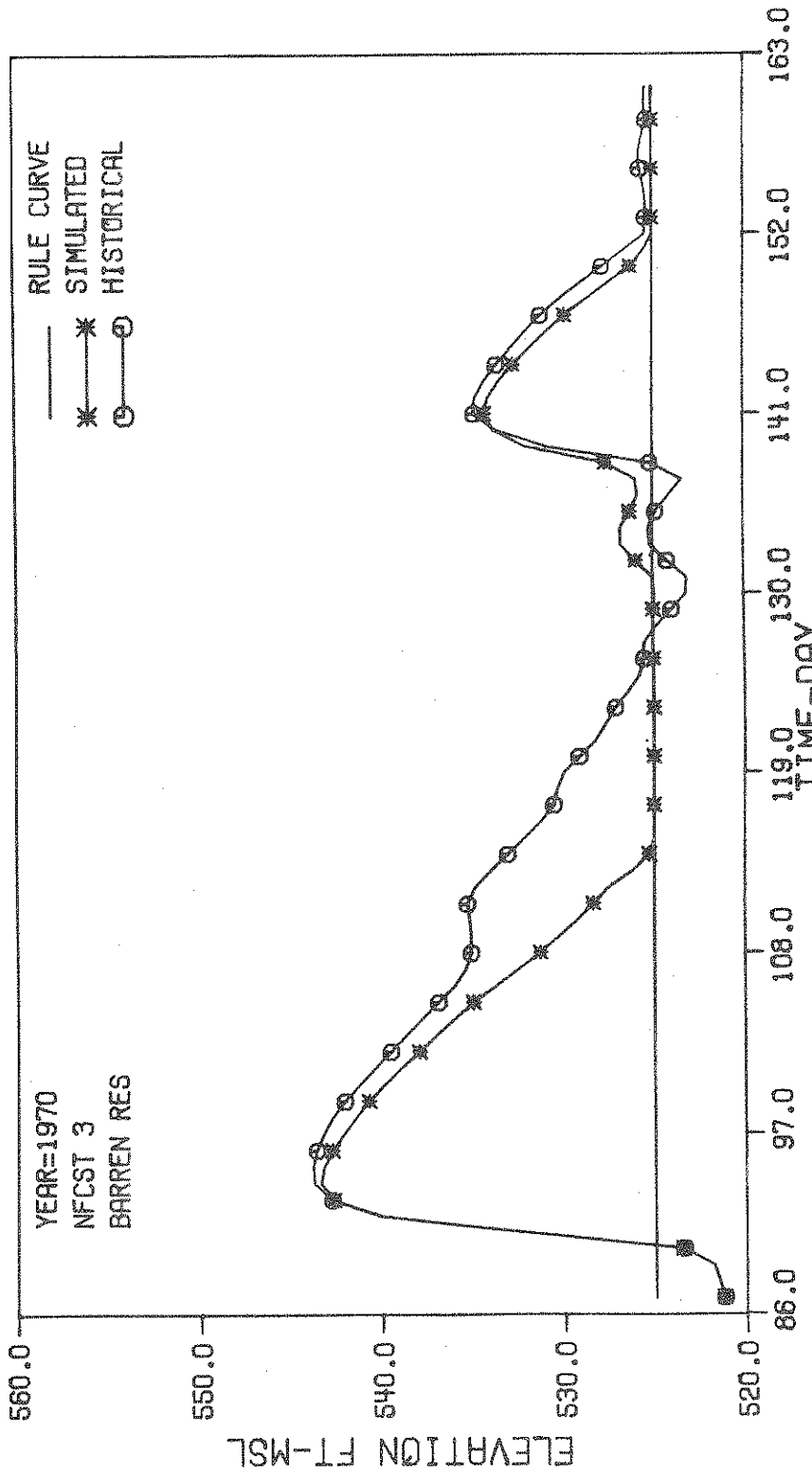

Figure 5.9 Simulated and Historical Elevations for the Barren Reservoir in the Winter Season of 1970 Water Year

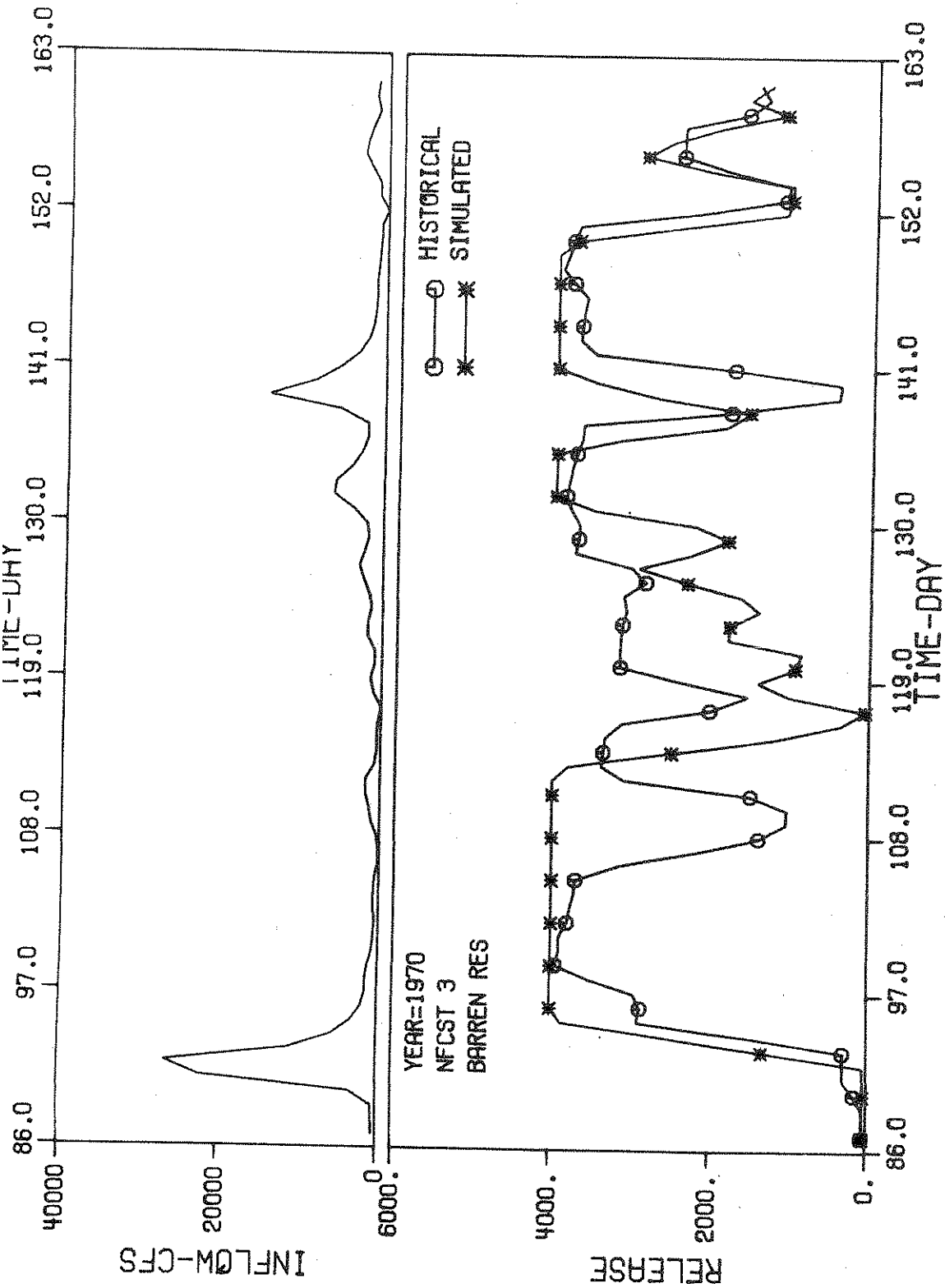

Figure 5.10 Simulated and Historical Releases for Barren Reservoir in the Winter Season of the 1970 Water Year

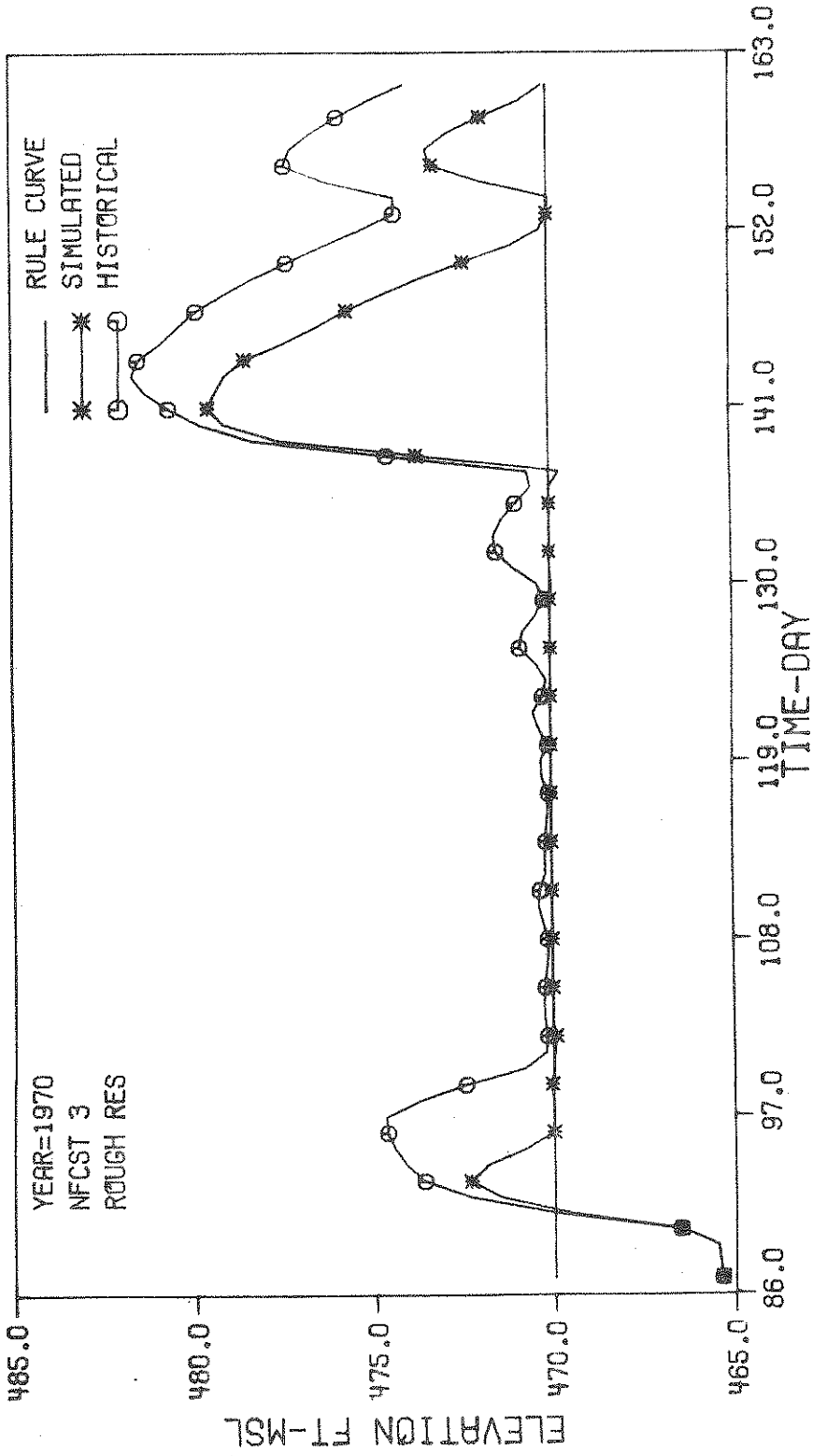

Figure 5.11 Simulated and Historical Elevations for Rough Reservoir in the Winter Season of the 1970 Water Year

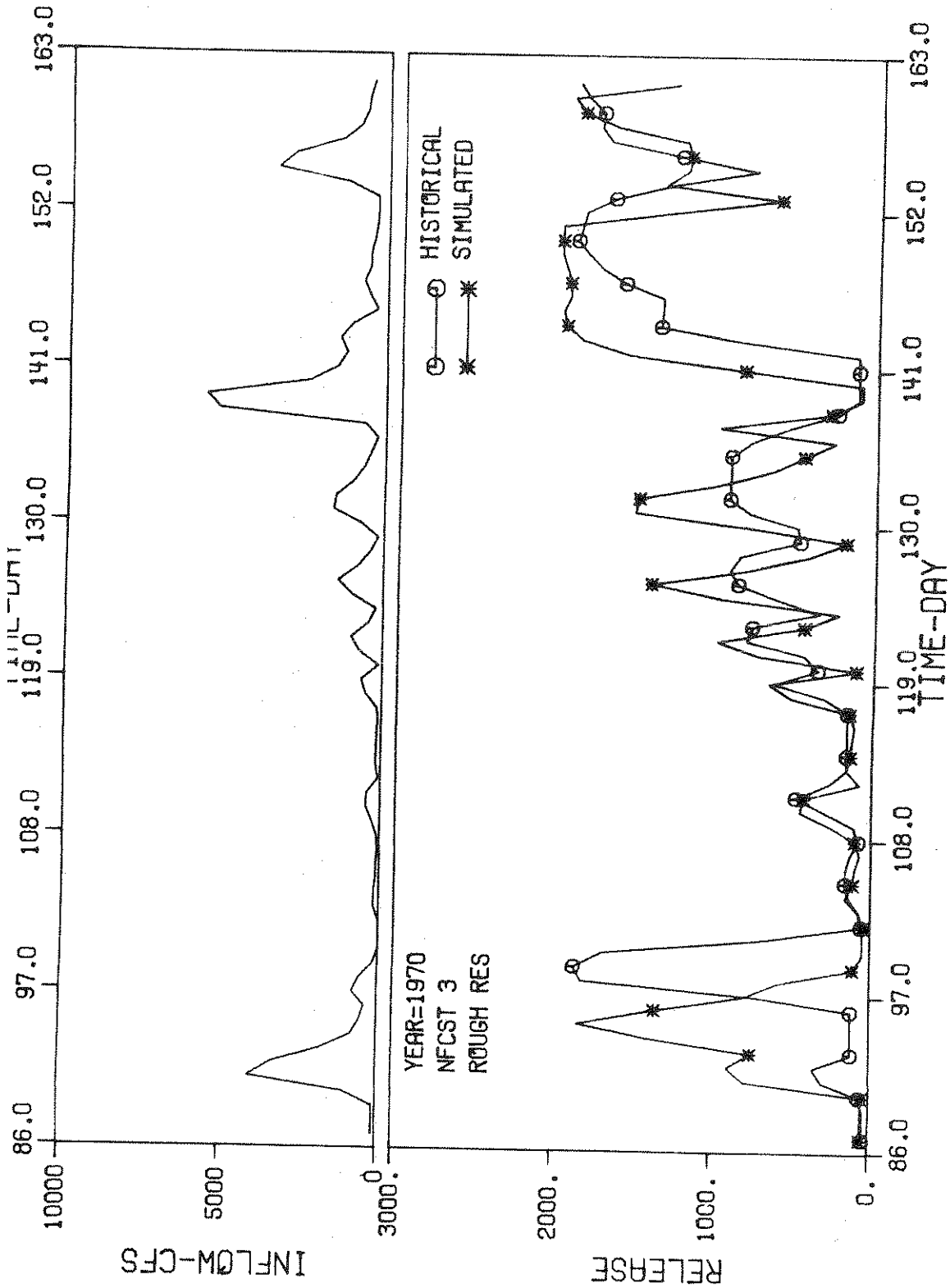

Figure 5.12 Simulated and Historical Releases for Rough Reservoir in the Winter Season of the 1970 Water Year

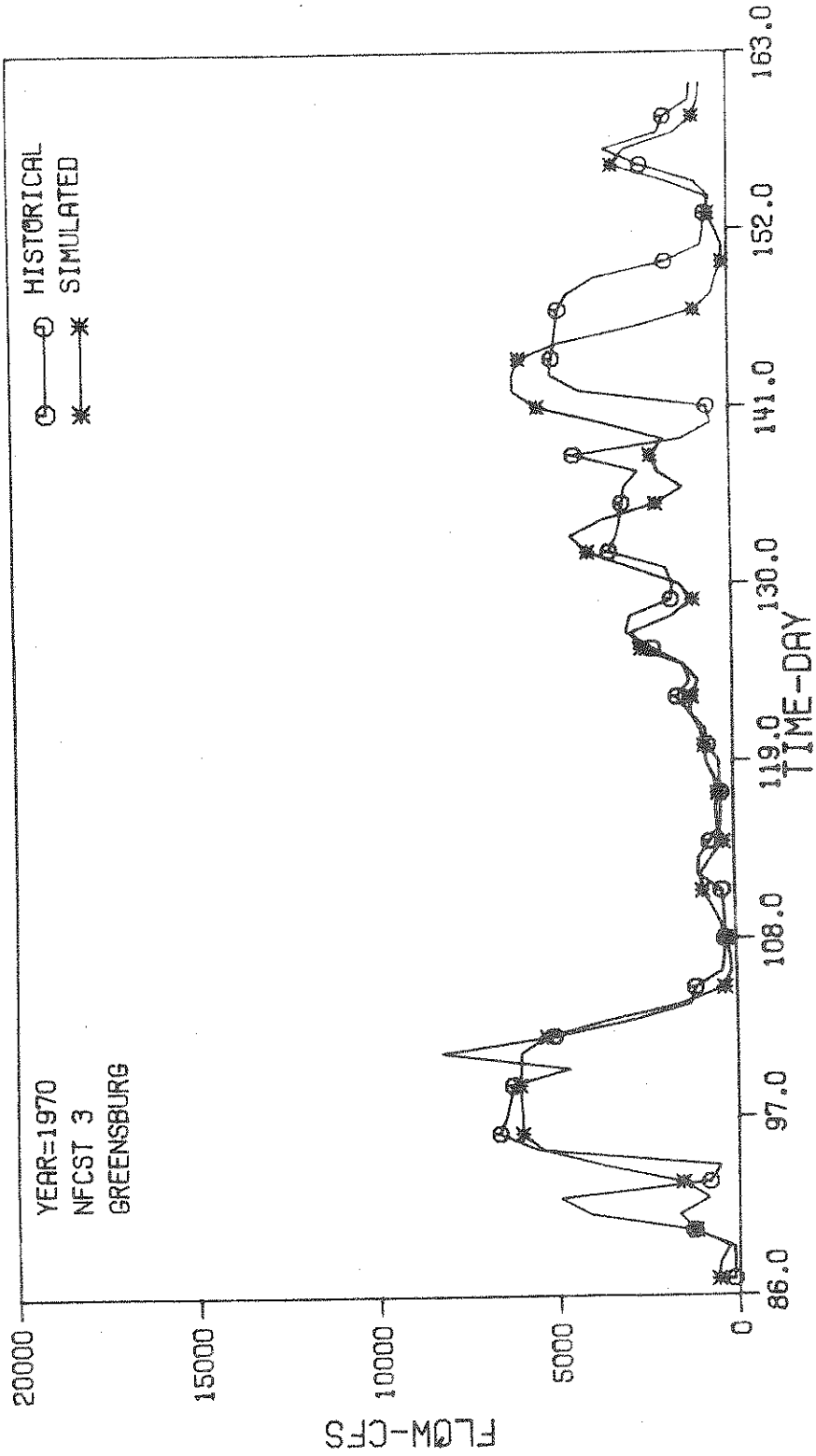

Figure 5.13 Simulated and Historical Flows at Greensburg in the Winter Season of the 1970 Water Year

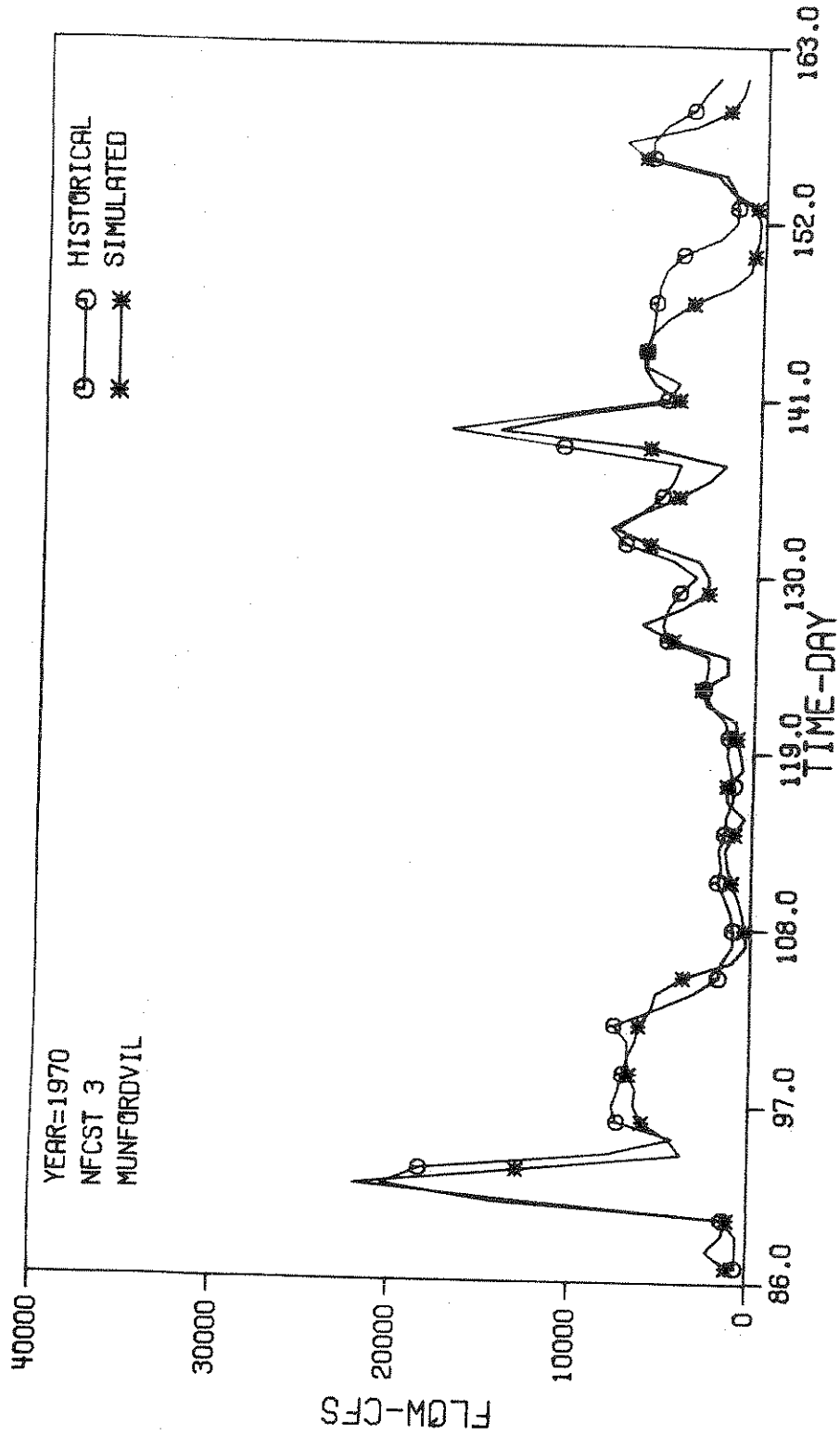

Figure 5.14 Simulated and Historical Flows at Munfordville in the Winter Season of the 1970 Water Year

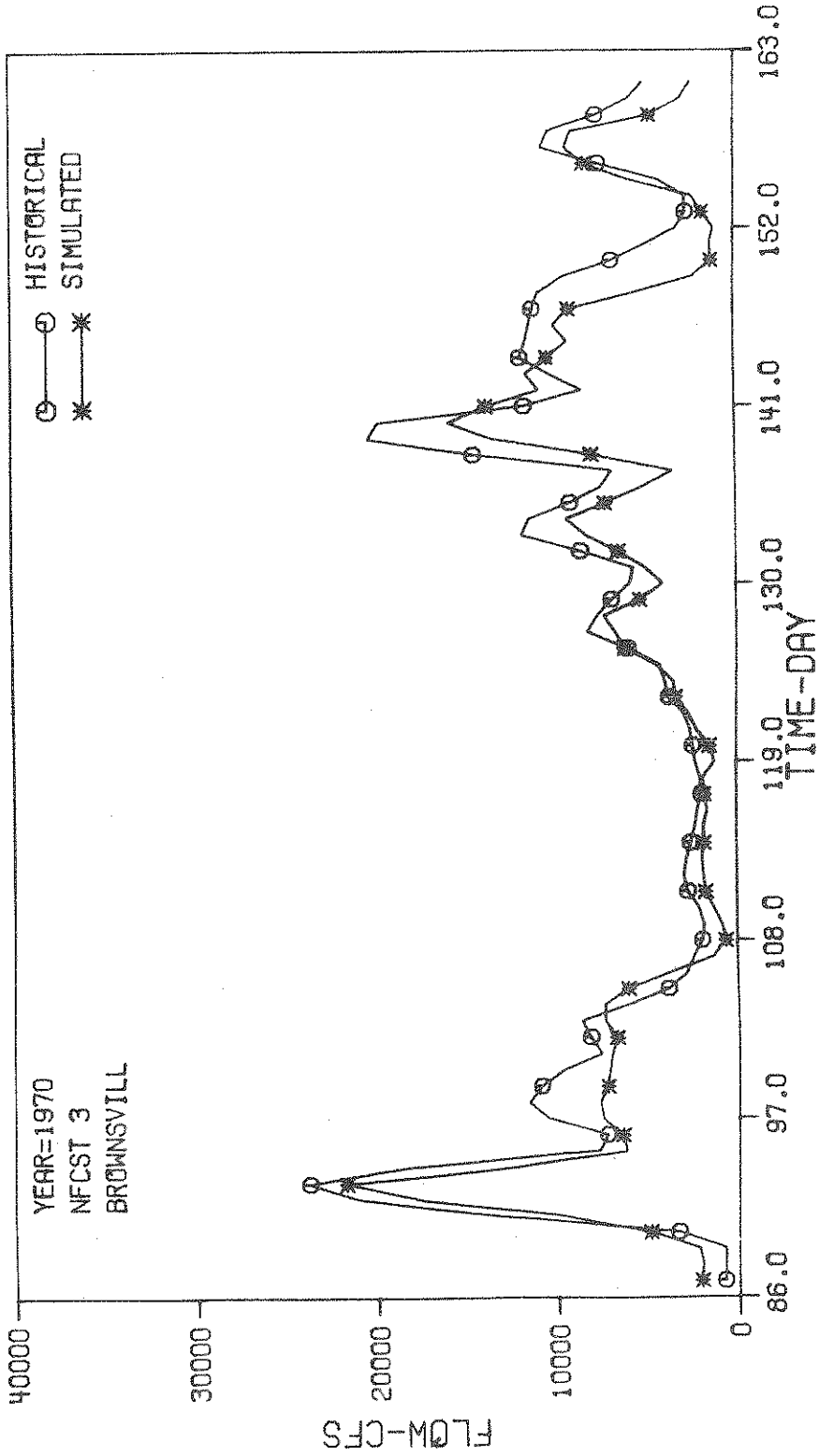

Figure 5.15 Simulated and Historical Flows at Brownsville in the Winter Season of the 1970 Water Year

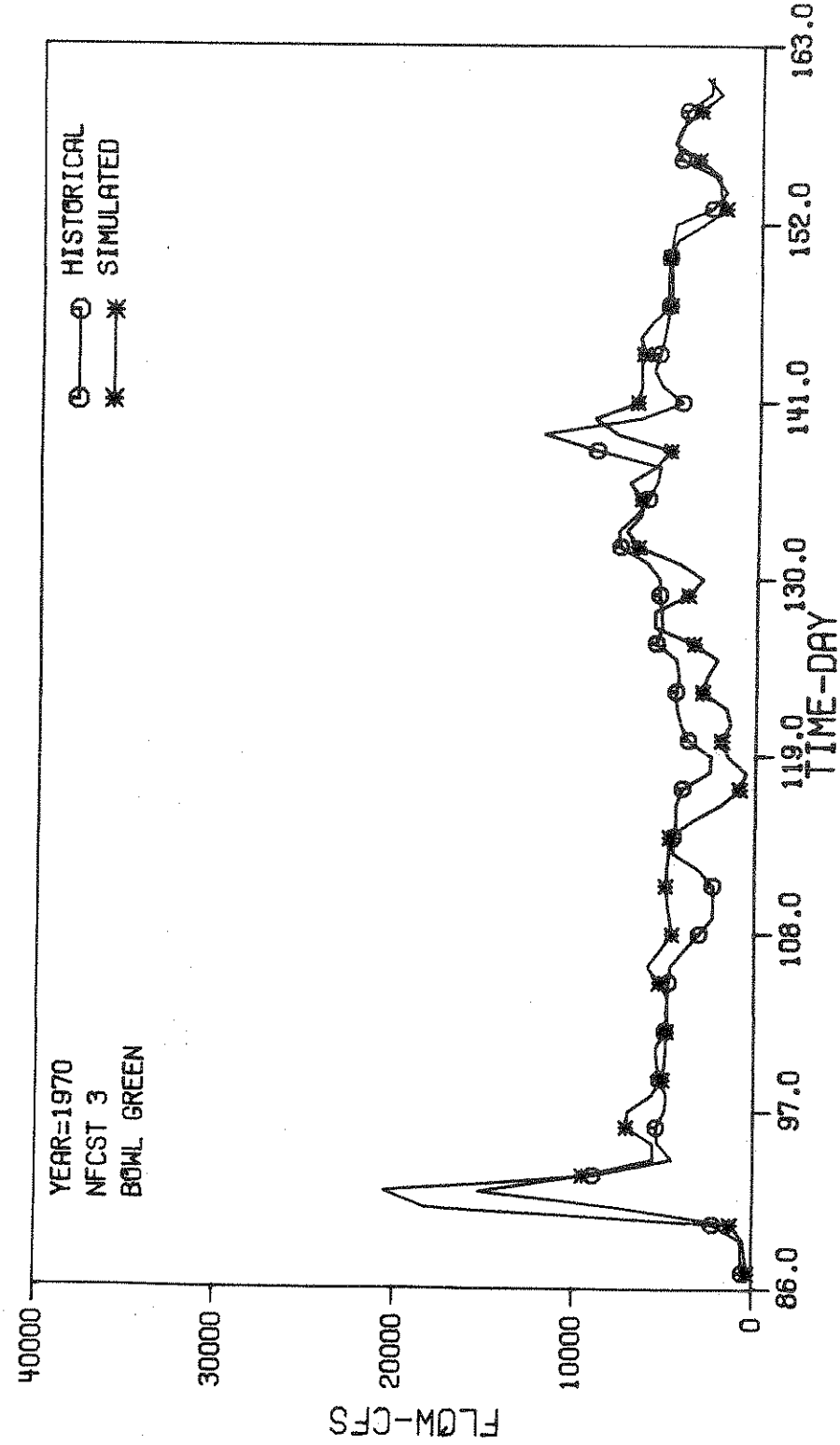

Figure 5.16 Simulated and Historical Flows at Bowling Green in the Winter Season of the 1970 Water Year

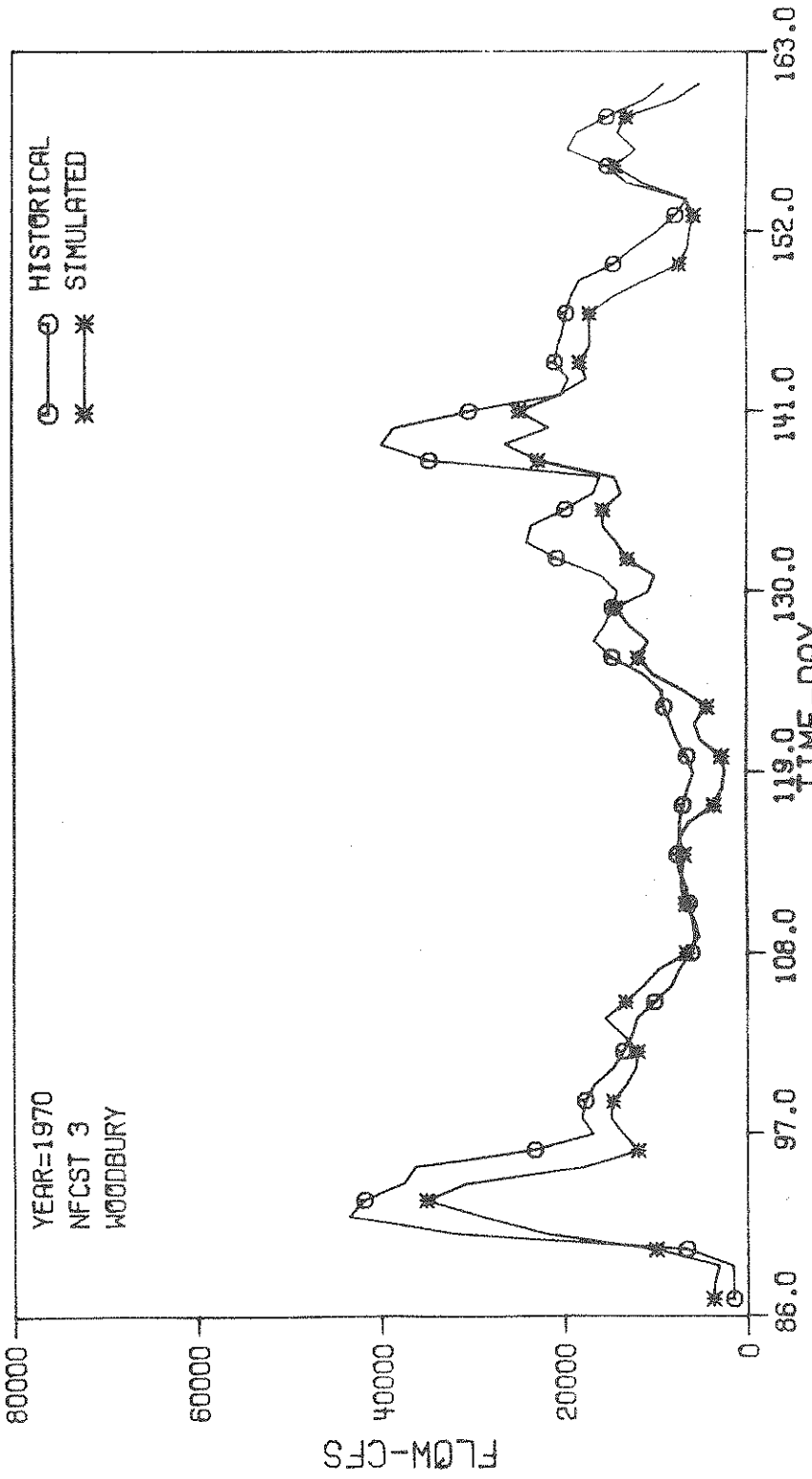

Figure 5.17 Simulated and Historical Flows at Woodbury in the Winter Season of the 1970 Water Year

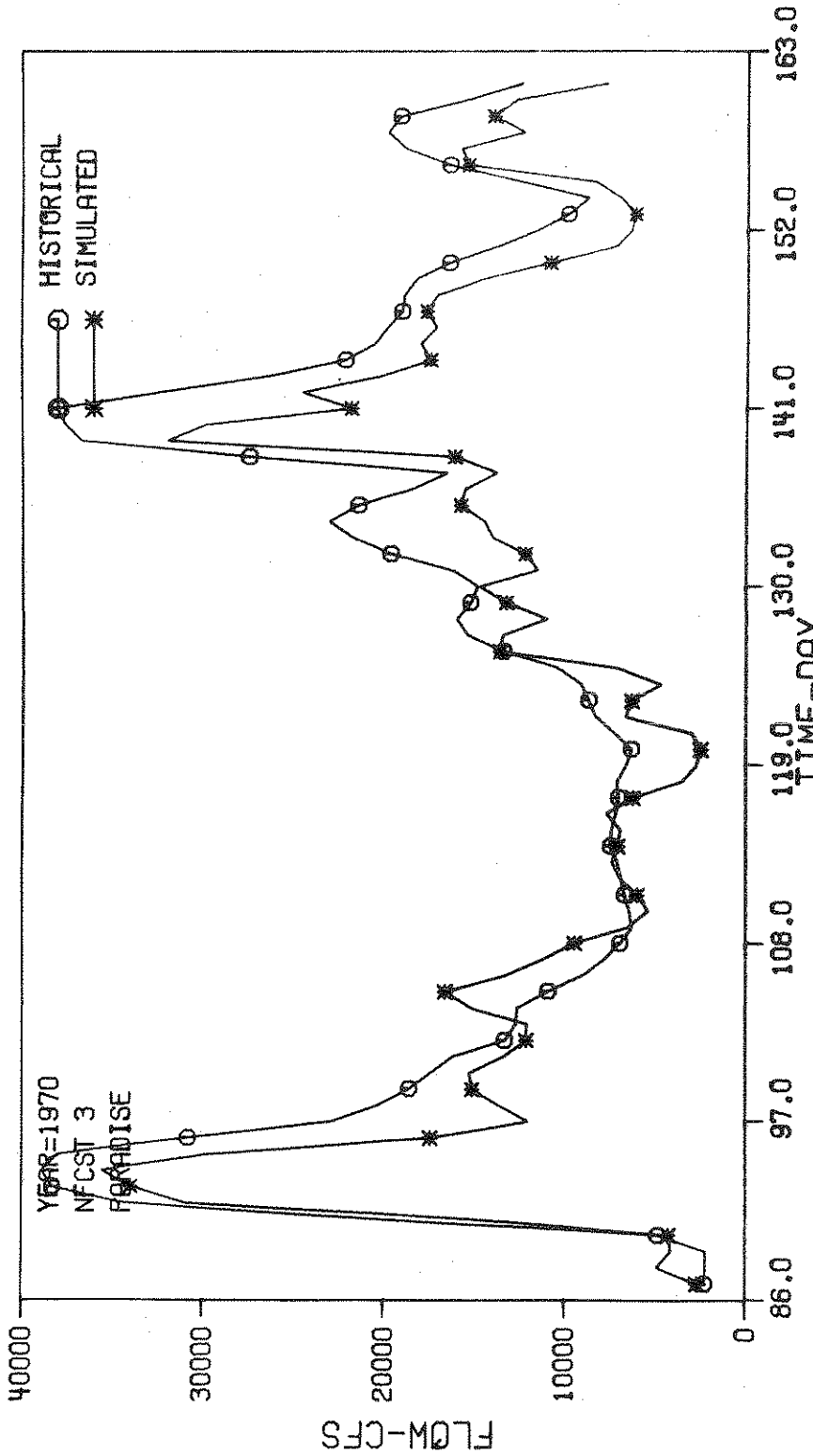

Figure 5.18 Simulated and Historical Flows at Paradise in the Winter Season of the 1970 Water Year

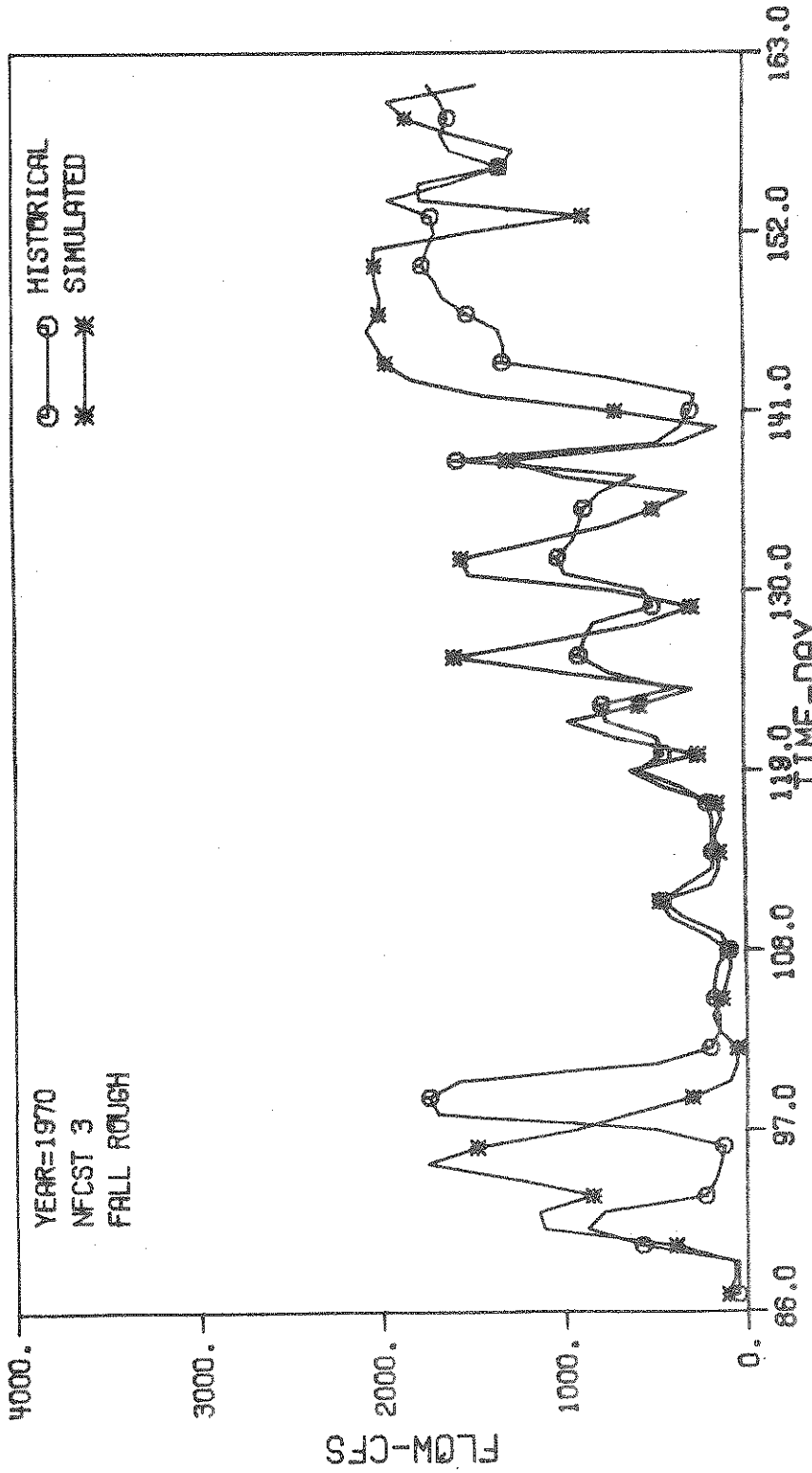

Figure 5.19 Simulated and Historical Flows at Falls of Rough in the Winter Season of the 1970 Water Year

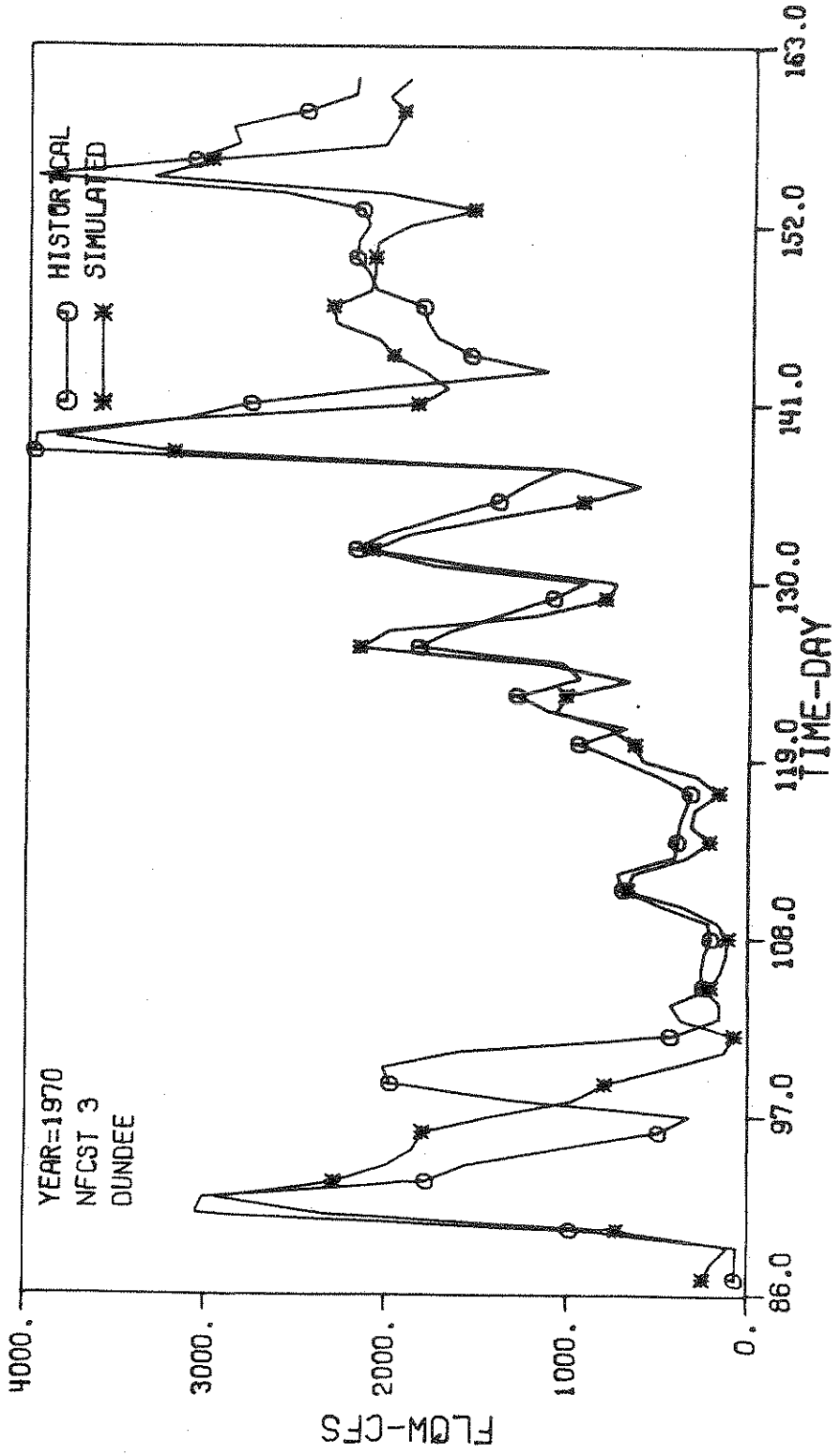

Figure 5.20 Simulated and Historical Flows at Dundee in the Winter Season of the 1970 Water Year

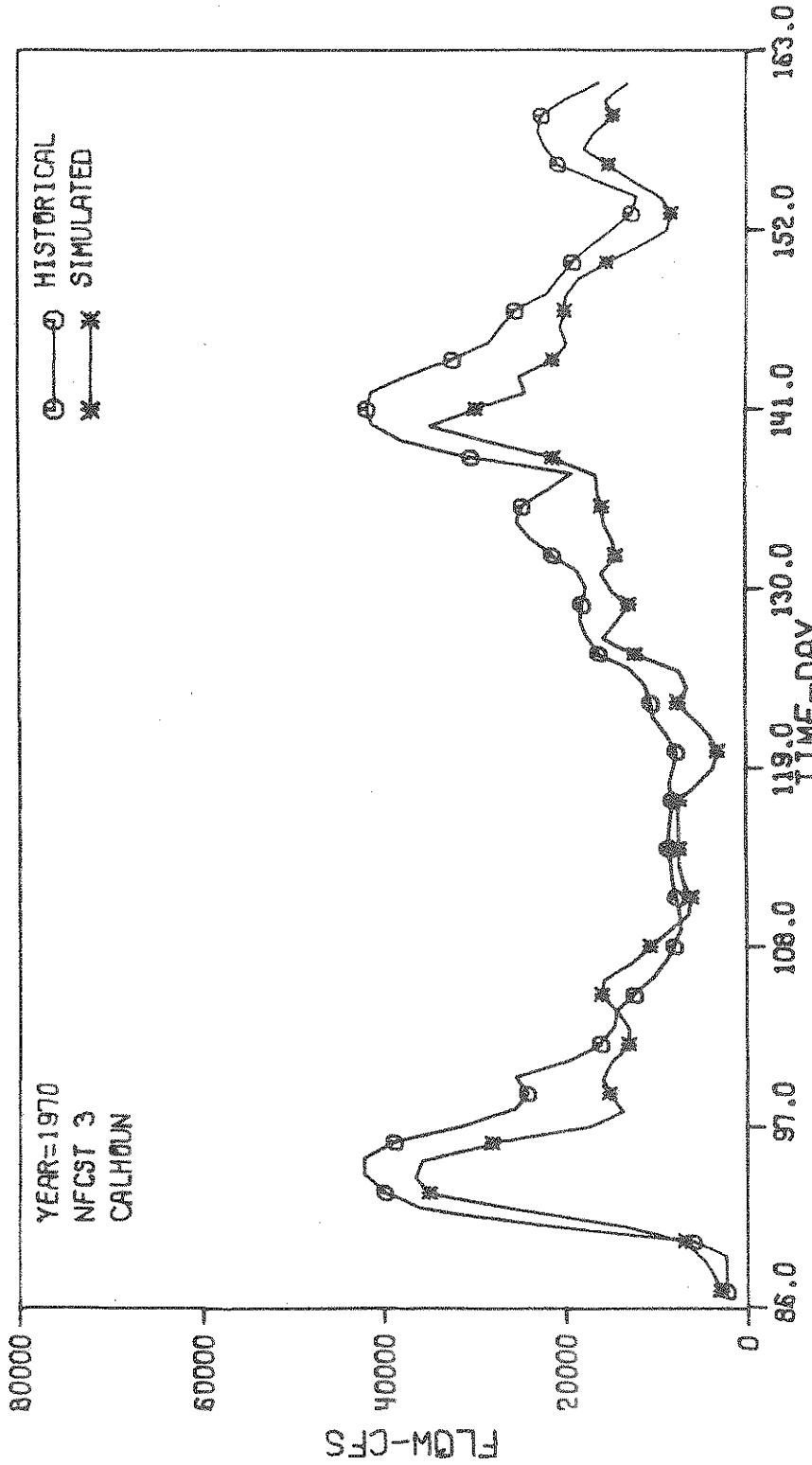

Figure 5.21 Simulated and Historical Flows at Calhoun in the Winter Season of the 1970 Water Year

Figures 5.5, 5.7, 5.9, and 5.11 show the simulated and historical reservoir elevations together with the rule curve levels (i.e. target levels) for Green, Nolin, Barren and Rough Reservoirs, respectively. The simulated and historical reservoir releases together with the reservoir inflow data are shown in Figures 5.6, 5.8, 5.10, and 5.12 for Green, Nolin, Barren, and Rough Reservoirs, respectively.

The model-derived simulated elevations for all four reservoirs deviate from the rule curve less than the historical data resulting from actual operation. There were several periods during which the simulated elevations did not deviate from the rule curve at all except during floods (see Figures 5.5, 5.7, 5.9, and 5.11). The simulated releases, on the other hand, follow the same pattern as the historical releases except that they occur earlier (see Figures 5.6, 5.8, 5.10, and 5.12). This is mainly due to the use of historical input data in the model (i.e. assuming perfect forecast information during the next 3 days). This does indicate that accurate forecasts of reservoir inflows as well as of precipitation data are important to effective reservoir operations.

During the analysis period, there were several occasions where the maximum capacity of the Barren Reservoir outlet (i.e. 4000 cfs) was reached (see Figure 5.10). This shows that the Barren Reservoir has relatively small downstream channel capacity as compared to its relatively large watershed (i.e. largest among all the reservoirs).

The simulated and historical flows at nine control stations are shown in Figures 5.13 through 5.21. From an examination of these figures, it is seen that the shape of the simulated hydrographs at the control stations are similar to the historical ones. However, the flood peaks are appreciably reduced in the simulated hydrographs as compared to the historical hydrographs for all control stations except for Falls of Rough. During the simulation period, the flood stages (i.e. the lower boundary of the uppermost flow zone given in

Table 5.2) were exceeded once or twice for all control stations except Greensburg which is the most upstream control station (Figures 5.13 through 5.21). System low flow requirements were satisfied both by the historical and simulated flows.

5.8.2 Model Performance in Winter Season

In order to summarize model performance, to compare it with historical operations, and to compare different policies, L-values, etc., the objective function parameter values Z were used. The Z-values associated with historical operations shown in Table 5.9 were used as reference values (for a given λ-value).

Thus the percent reduction in simulated storage penalties, PRSP, due to use of the GRBOPM2 model are defined as follows:

$$PRSP = 100\left(\frac{Z_1^h - Z_1^*}{Z_1^h}\right) [\%] \qquad (5.4)$$

where Z_1^h equals the total storage penalty that resulted from the historical operations; Z_1^* equals the total storage penalty that resulted from model simulated operations. These results are also shown in Table 5.9.

Table 5.9 shows the Z_1^*-values for the GRBOPM2 simulated storage deviations to be less than the historical deviations. This is true for all reservoirs. The total reduction in storage penalty for all reservoirs was about 35%.

Similar results were obtained for flow penalties at each of the nine control stations as shown in Table 5.10. The percent reduction in simulated flow penalties, PRFP, are defined similarly to the percent reduction in storage penalties:

$$PRFP = 100\left(\frac{Z_2^h - Z_2^*}{Z_2^h}\right) [\%] \qquad (5.5)$$

Table 5.9 Comparison of Storage Penalties between Historical and Simulated Results in Winter Season of 1970 Water Year

Reservoirs	Historical Storage Penalties	Simulated Storage Penalties	Percent Reduction in Storage Penalties, PRSP
Green	$3.37613*10^6$	$2.13146*10^6$	36.9
Nolin	$8.49985*10^5$	$5.58057*10^5$	34.3
Barren	$5.32095*10^6$	$3.95202*10^6$	25.7
Rough	$2.54619*10^6$	$1.21532*10^6$	52.3
Total Z_1^h & Z_1^*	$1.20933*10^7$	$7.85685*10^6$	35.0

Table 5.10 Comparison of Flow Penalties between Historical and Simulated Results in Winter Season of 1970 Water Year

Control Stations	Historical Flow Penalties	Simulated Flow Penalties	Percent Reduction in Flow Penalties, PRFP
Greensburg	$1.65939*10^5$	$1.56761*10^5$	5.5
Munfordville	$2.09850*10^5$	$1.45158*10^5$	30.8
Brownsville	$2.79830*10^5$	$1.37886*10^5$	50.7
Bowling Green	$4.16719*10^5$	$1.95166*10^5$	53.2
Woodbury	$3.87714*10^6$	$1.24898*10^6$	67.8
Paradise	$9.40000*10^5$	$3.20064*10^5$	66.0
Falls of Rough	$5.27210*10^4$	$7.29669*10^4$	-38.4
Dundee	$9.57300*10^4$	$7.19463*10^4$	24.8
Calhoun	$1.33920*10^6$	$3.52473*10^5$	73.7
Total Z_2^h & Z_2^*	$7.37713*10^6$	$2.70140*10^6$	63.4

where Z_2^h equals total flow penalty that resulted from historical operations, and Z_2^* equals total flow penalty that resulted from model simulated operations. The percent reductions in flow penalties exceeded the percent reductions in storage penalties. This may be due to relatively larger penalty coefficients assigned to flow deviations as compared to the storage deviations (Tables 5.1 and 5.2). Such relatively higher penalty coefficients are to be expected because flood control at downstream control stations is the primary project purpose.

Earlier it was seen (Figure 5.19) that at Falls of Rough the simulated flows were higher than the historical flows. The seemingly anomolous result can be observed also in Table 5.10. The percent reduction in simulated flow penalty, PRFP, for Falls of Rough is negative, namely 38.4%. This is because Falls of Rough, located immediately below Rough Reservoir, has a smaller relative penalty coefficient as compared to the storage penalty coefficients for Rough Reservoir (Tables 5.1 and 5.2). Thus, the model "forced" release decisions that made storage to remain close to the Rough Reservoir rule curve rather than to keep flows close to the target flows at Falls of Rough. The reduction of historical Z_1-values was 52.3% for Rough Reservoir as compared to 36.9%, 34.3%, and 25.7% for the Green, Nolin, and Barren Reservoirs, respectively. This is so despite the fact that Rough Reservoir has the smallest release capacity of all four reservoirs.

The total reduction in the overall systems measure of effectiveness Z^* (i.e. $Z^* = Z_1^* + Z_2^*$) from that of historical operations Z^h (i.e. $Z^h = Z_1^h + Z_2^h$) was about 45.8%. This result, once again, shows that the GRBOPM2 model produced better simulated operation of the GRB reservoir system than the historical operations. The better performance of the GRBOPM2 model may be attributed to: (1) the use of an explicit optimization technique in finding the values for decision variables, and (2) the use of three-day ahead perfect forecast inputs

(i.e. historical inputs). With current methods reservoir regulators have neither the time nor the tools to arrive at optimal operating decisions because the number of decision determinants is so large. The use of optimization techniques makes the solution of problems with that many variables, practicable. In addition, their use makes it worthwhile to spend resources on obtaining more reliable forecasts. Systematic work to fully substantiate this proposition does not seem to have been undertaken as yet. Therefore, the use of the GRBOPM2 model in judging the extent and the value of more accurate and extended forecast information will be considered briefly in Section 5.10.

Returning to the trade-off curve between the two objectives, Z_1^* and Z_2^*, it was generated by varying the value of λ in Eq. 5.3 between 0.0 and 1.0 at selected intervals as shown along the middle curve in Figure 5.22. The point corresponding to the historical operations is also shown in Figure 5.22 (note that the Z_2-axis is interrupted). For all values of λ, the GRBOPM2-generated trade-off curve lies considerably closer to the "ideal" operations result (i.e. the point at which all storage and flow penalties would equal zero) than the historical operation. The ideal operations point is generally unattainable due to randomness of the hydrologic inputs, uncontrolled inflows downstream of the reservoirs, lack of information, etc. However, it is important to stay as close to the ideal operation as possible. This may be achieved by having accurate estimates of the forecast inputs and by using an optimization routine to select the optimal release decisions within the confines of the many constraints of the system.

5.8.3 Summer Season

The GRBOPM2 model was run also for the summer season (between days 197 and 346) of the 1970 water year by using the summer season penalty coefficients given in Tables 5.3 and 5.4. Again the value of λ was set equal to 0.5 and three-day

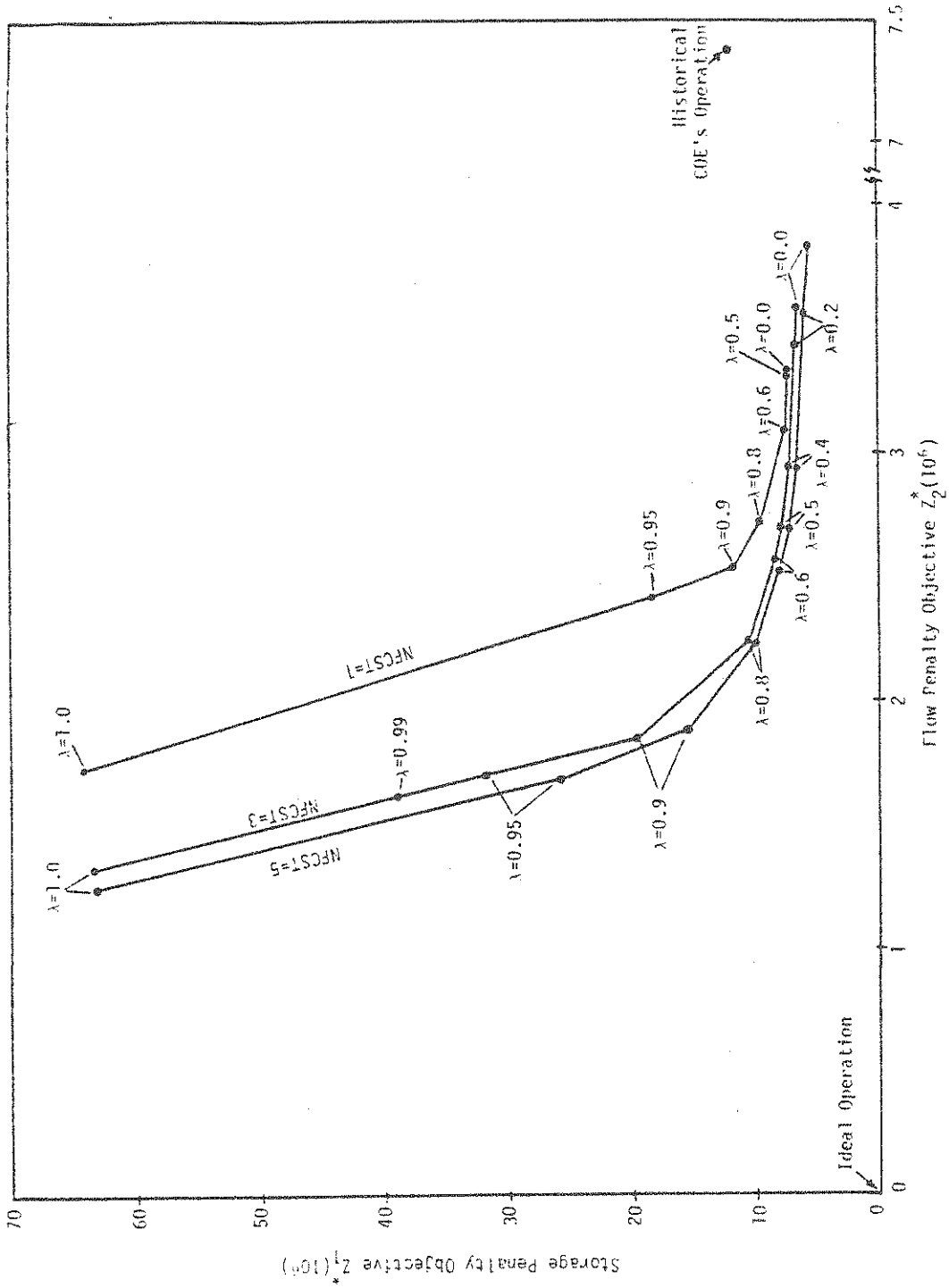

Figure 5.22 Trade-off Curves Between Minimum Storage and Minimum Flow Penalty Objectives for the 1970 Winter Season Using 1, 3, and 5 Day-Ahead Forecast Information

ahead forecast inputs were used (i.e. NFCST = 3). The results are shown in Figures 5.23 through 5.39. The total storage penalties corresponding to the historical and the simulated operations as well as the percent reductions for the latter are given in Table 5.11. Corresponding results for flow penalties are given in Table 5.12.

From examination of Figures 5.23, 5.25, 5.27, and 5.29, and Table 5.11, it is seen that the simulated elevation or storage deviations were less than the historical ones for Barren and Rough Reservoirs. The slightly larger simulated elevation deviations in Green Reservoir occurred between days 250 and 346. These were caused mainly by the minimum release requirement of 150 [cfs]. Although the regulation schedules given in Appendix A show that a minimum release of 150 [cfs] was required from Green Reservoir, the historical operations did not meet this requirement. Rather, the historical releases from Green Reservoir were about 75 [cfs]. No reason for this is apparent. However, the resulting differences between historical and simulated storage penalties are minor; Table 5.11 shows the percent increase in storage penalty, PRSP, to be only 2%.

The relatively larger differences between simulated and historical elevations for the Nolin Reservoir, on the other hand, are attributed to the large penalty coefficient associated with flows at the control station (Brownsville) immediately below the reservoir. The penalty for exceeding 13,000 [cfs] at Brownsville is 35 [penalty units/cfs] whereas the storage penalty for exceeding the elevation 518 feet at Nolin Reservoir is only 6 [penalty units/ac-ft] (Tables 5.3 and 5.4). Converting units of flow into units of storage shows that for corresponding zones the flow penalty is about three times larger than the storage penalty. Thus, the model did not yield releases from Nolin Reservoir that made for flows in excess of 13,000 [cfs] (Figures 5.26 and 5.33). This feature may also be recognized in the significant reduction in simulated flow penalties (76%) as compared to historical flow penalties at Brownsville (see Table 5.12).

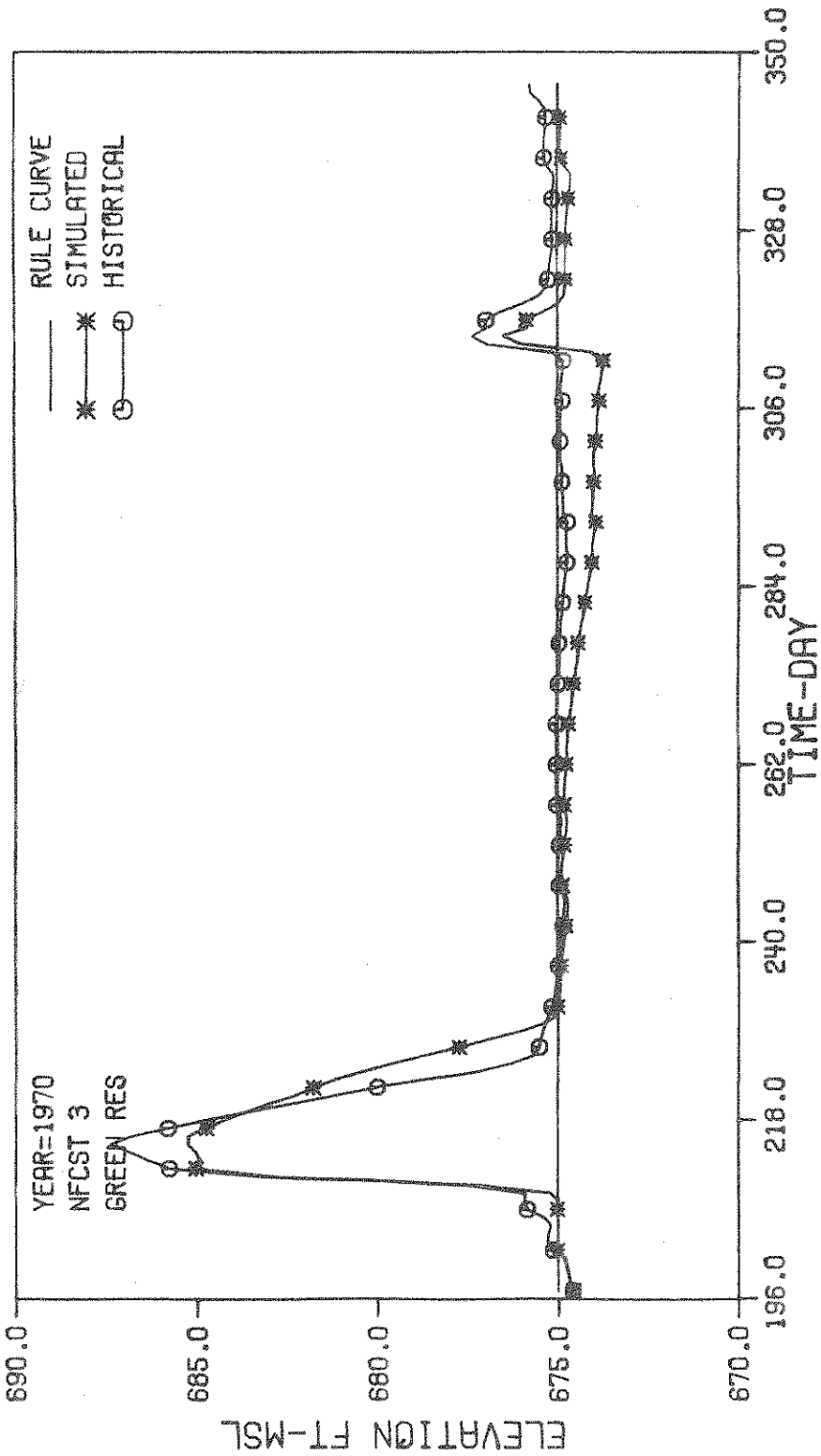

Figure 5.23 Simulated and Historical Elevations for Green Reservoir in the Summer Season of the 1970 Water Year

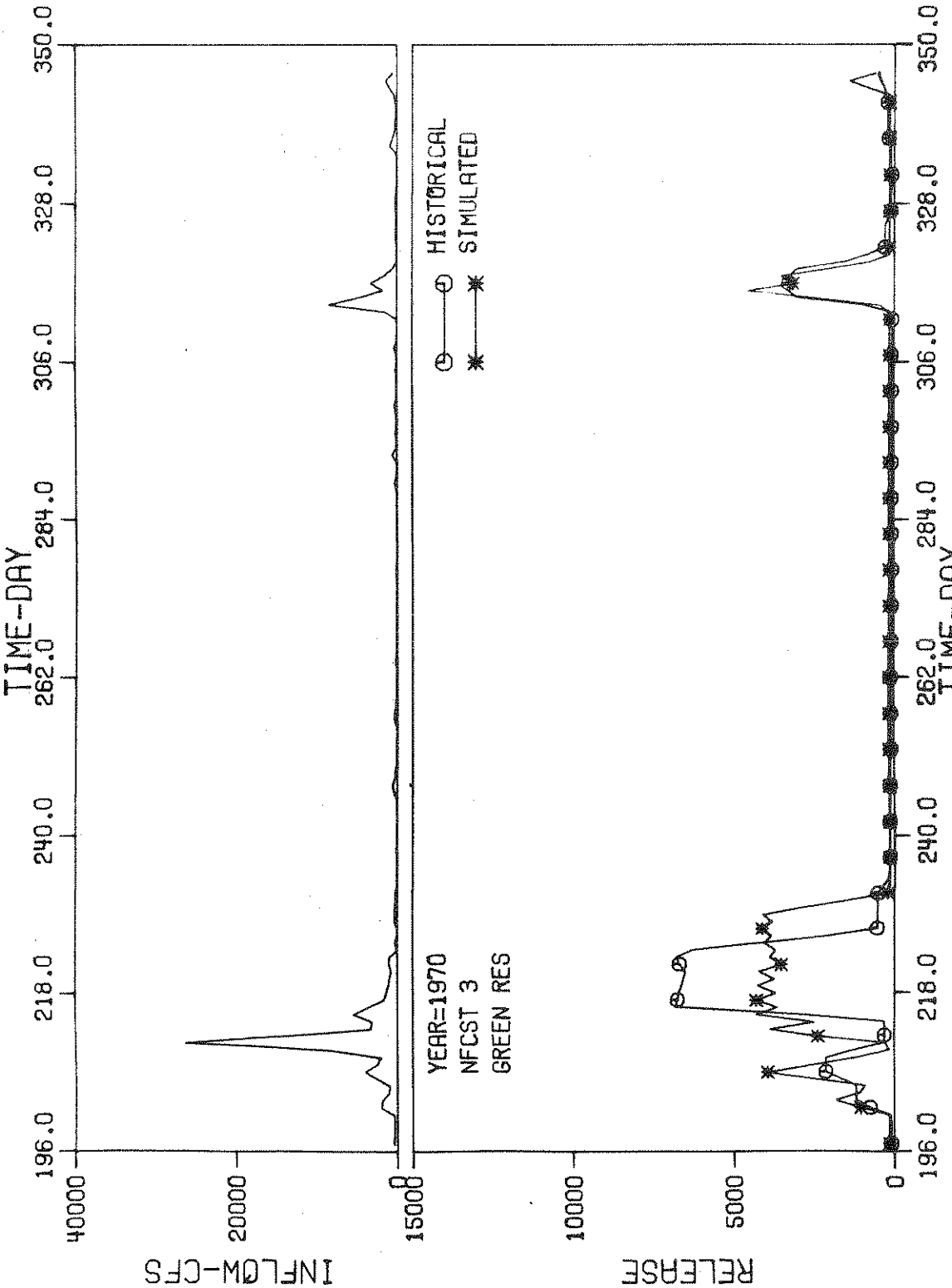

Figure 5.24 Simulated and Historical Releases for Green Reservoir in the Summer Season of the 1970 Water Year

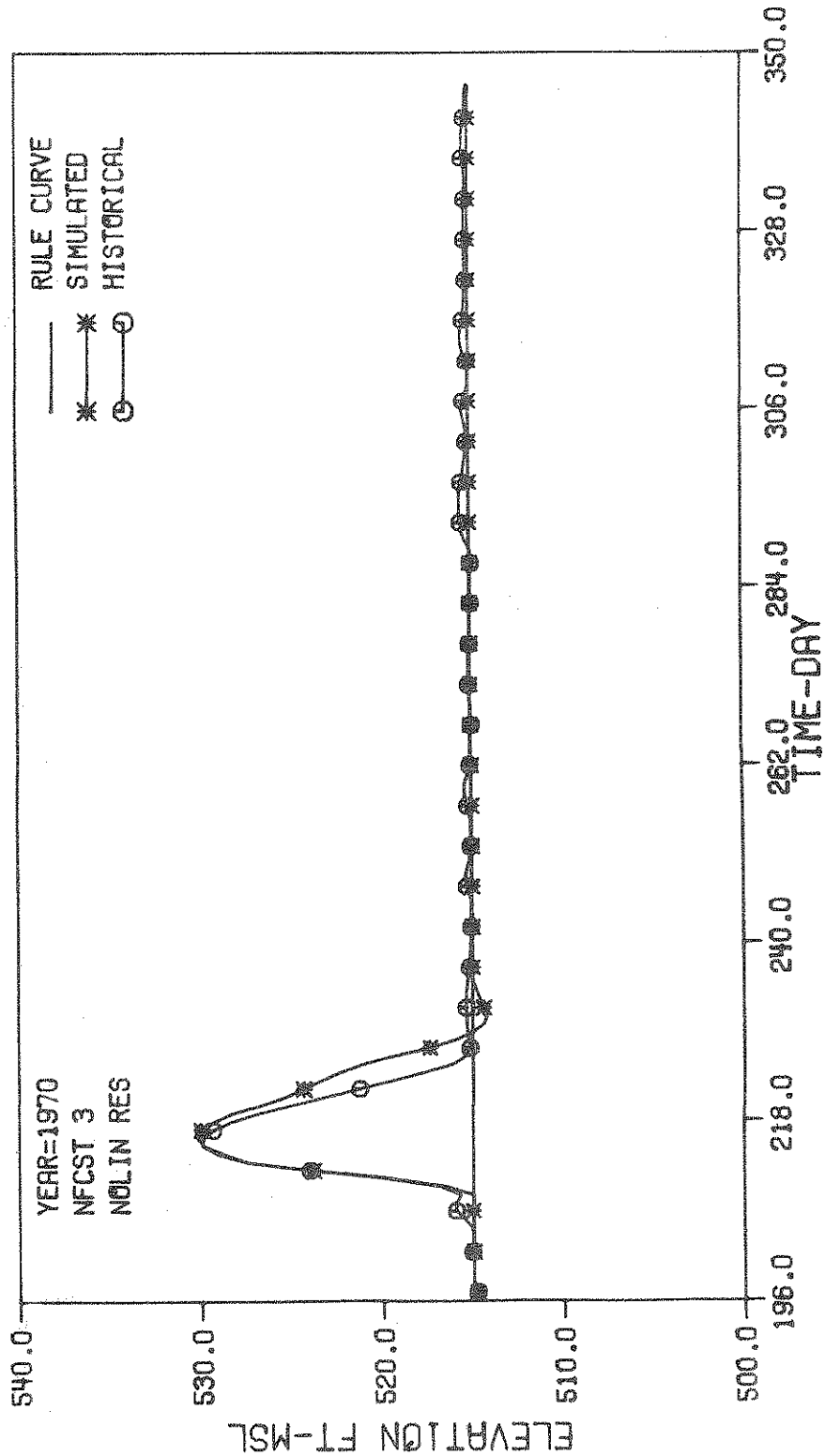

Figure 5.25 Simulated and Historical Elevations for Nolin Reservoir in the Summer Season of the 1970 Water Year

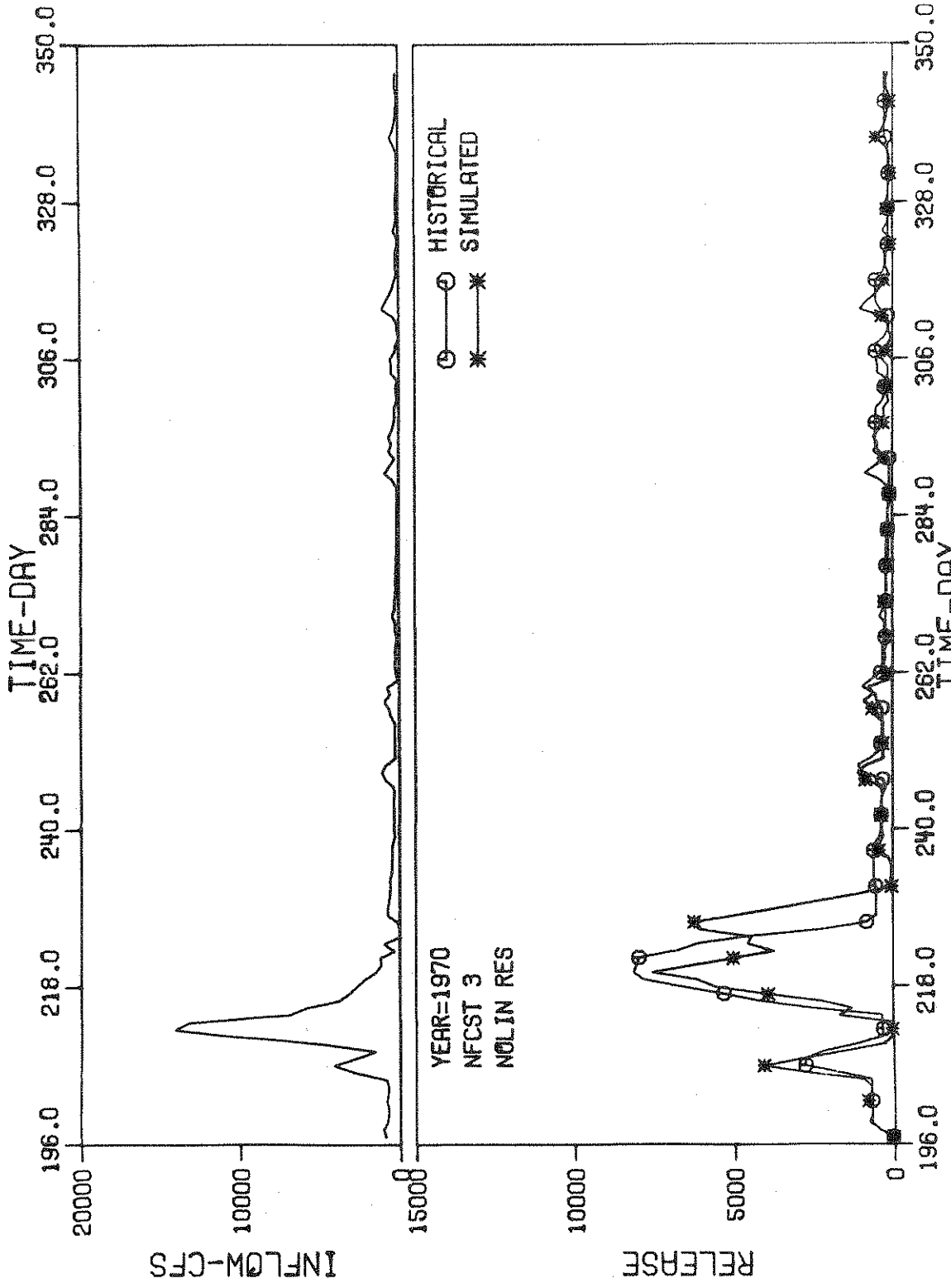

Figure 5.26 Simulated and Historical Releases for the Nolin Reservoir
In the Summer Season of the 1970 Water Year

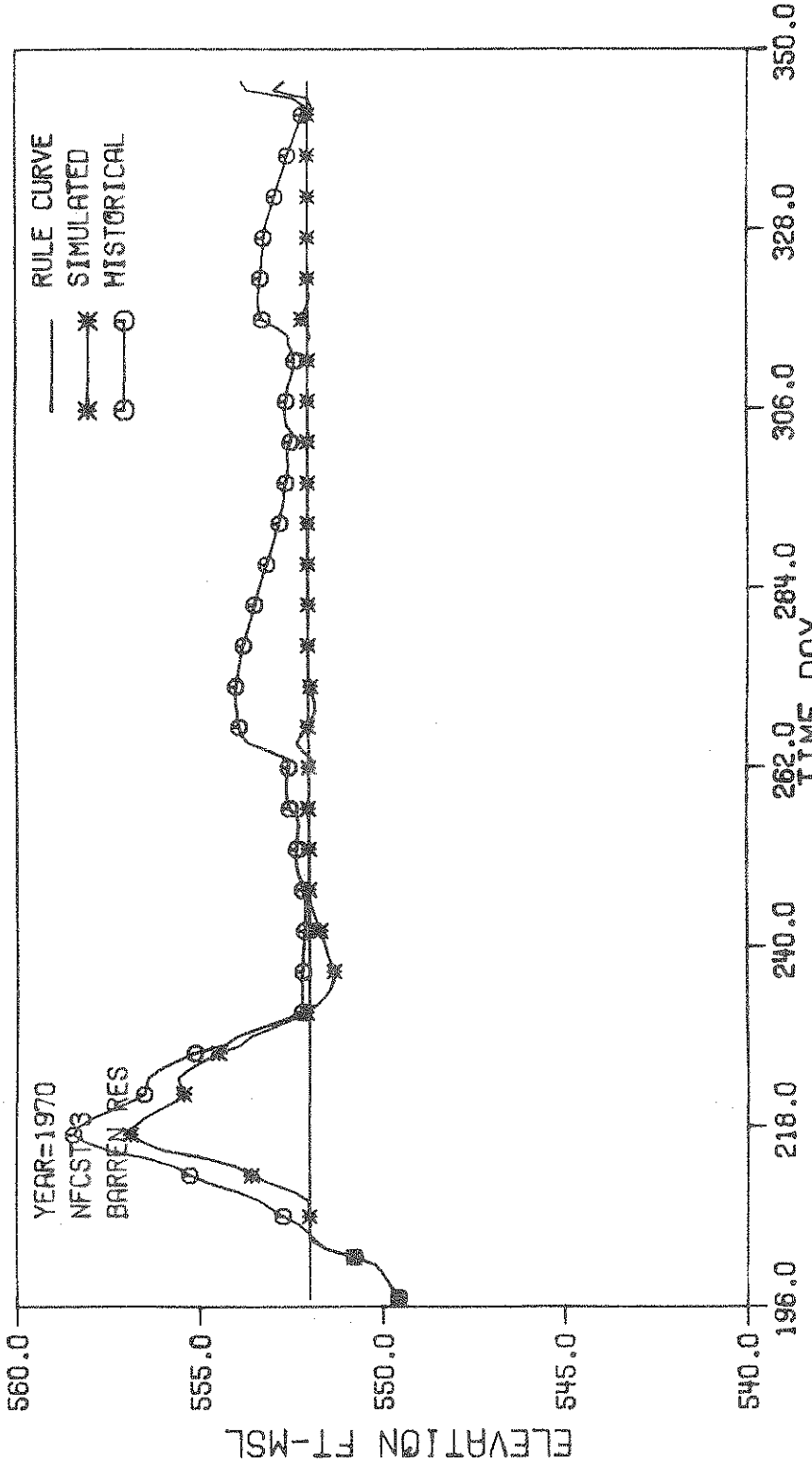

Figure 5.27 Simulated and Historical Elevations for the Barren Reservoir in the Summer Season of the 1970 Water Year

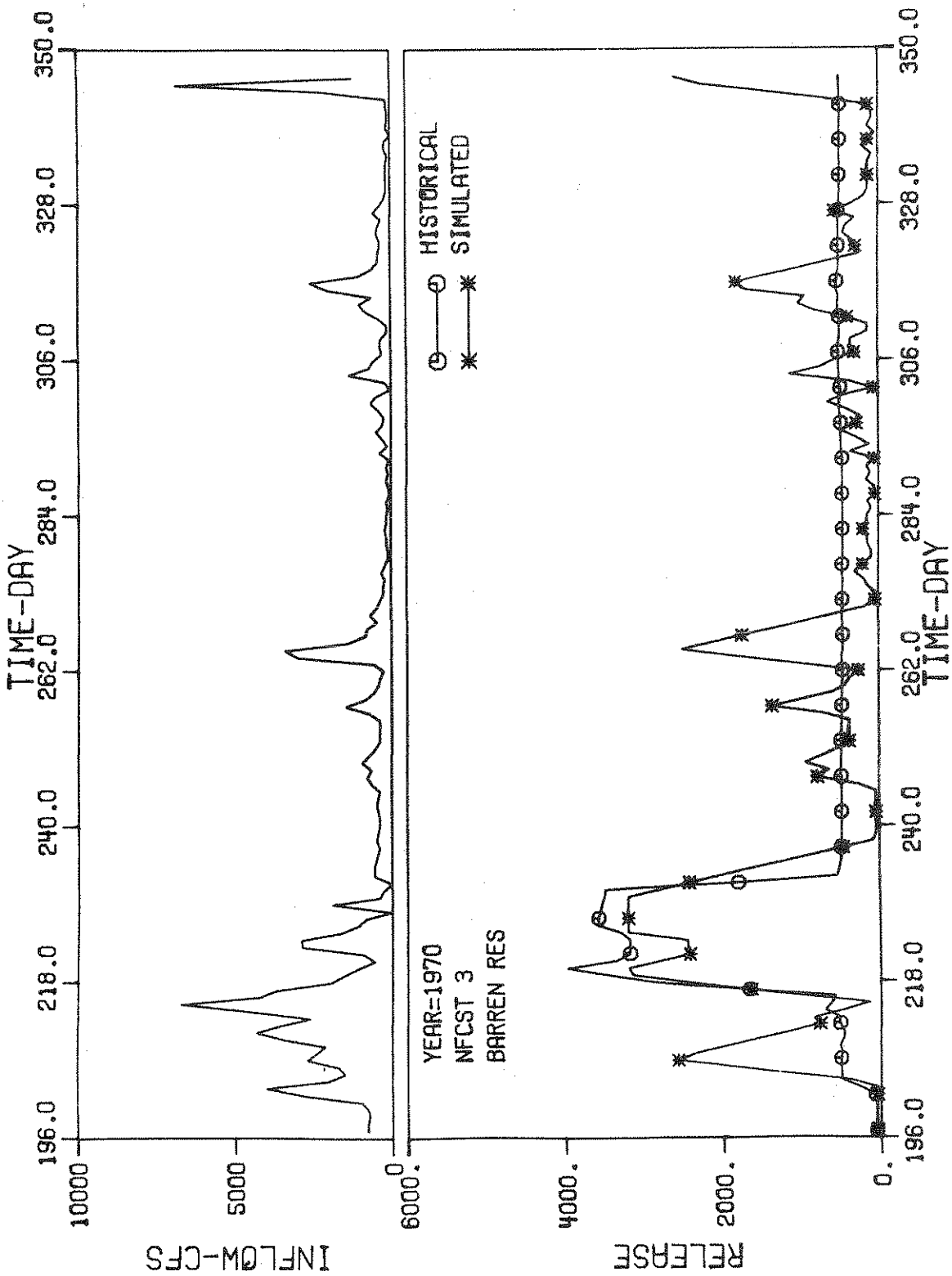

Figure 5.28 Simulated and Historical Releases for Barren Reservoir in the Summer Season of the 1970 Water Year

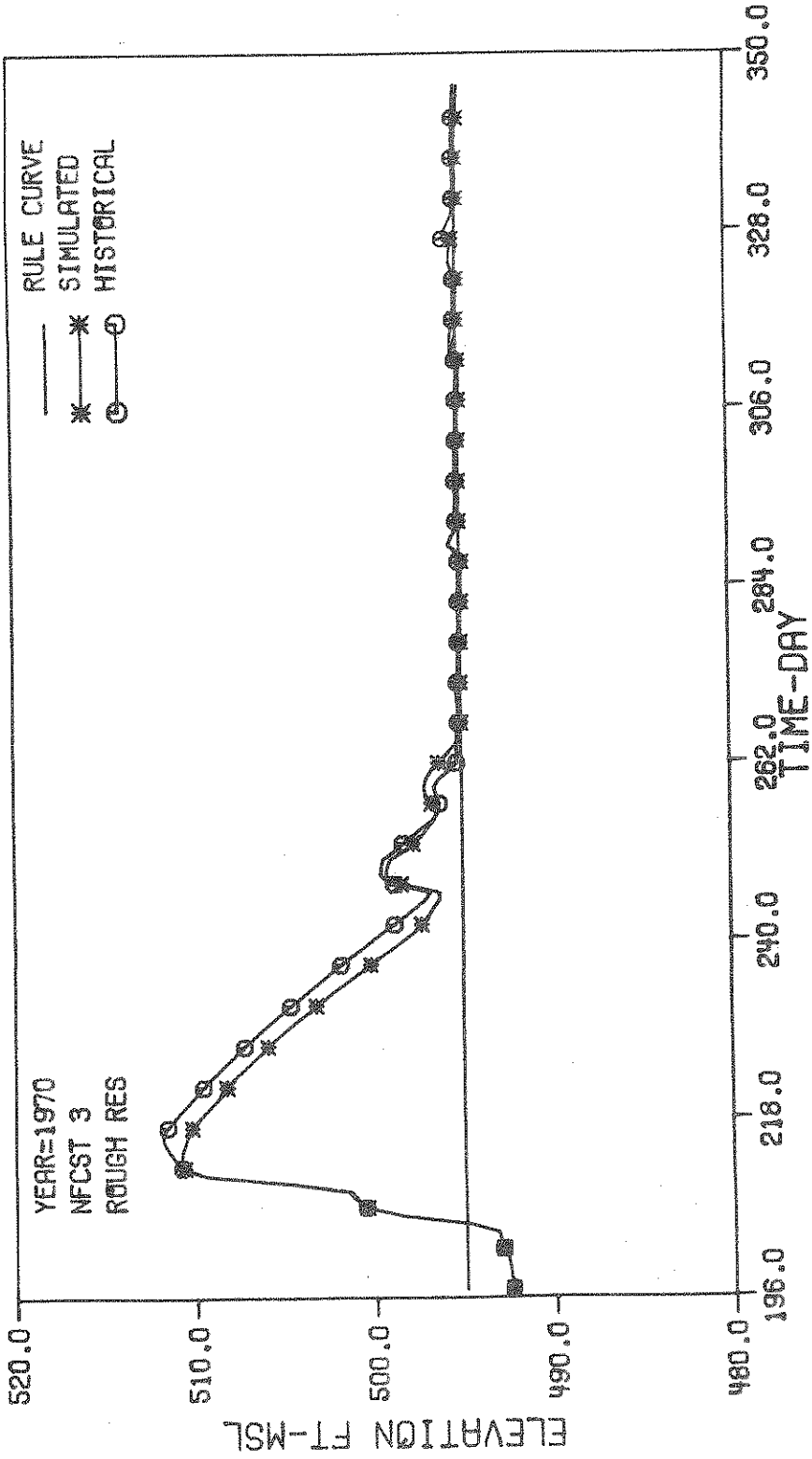

Figure 5.29 Simulated and Historical Elevations for Rough Reservoir in the Summer Season of the 1970 Water Year

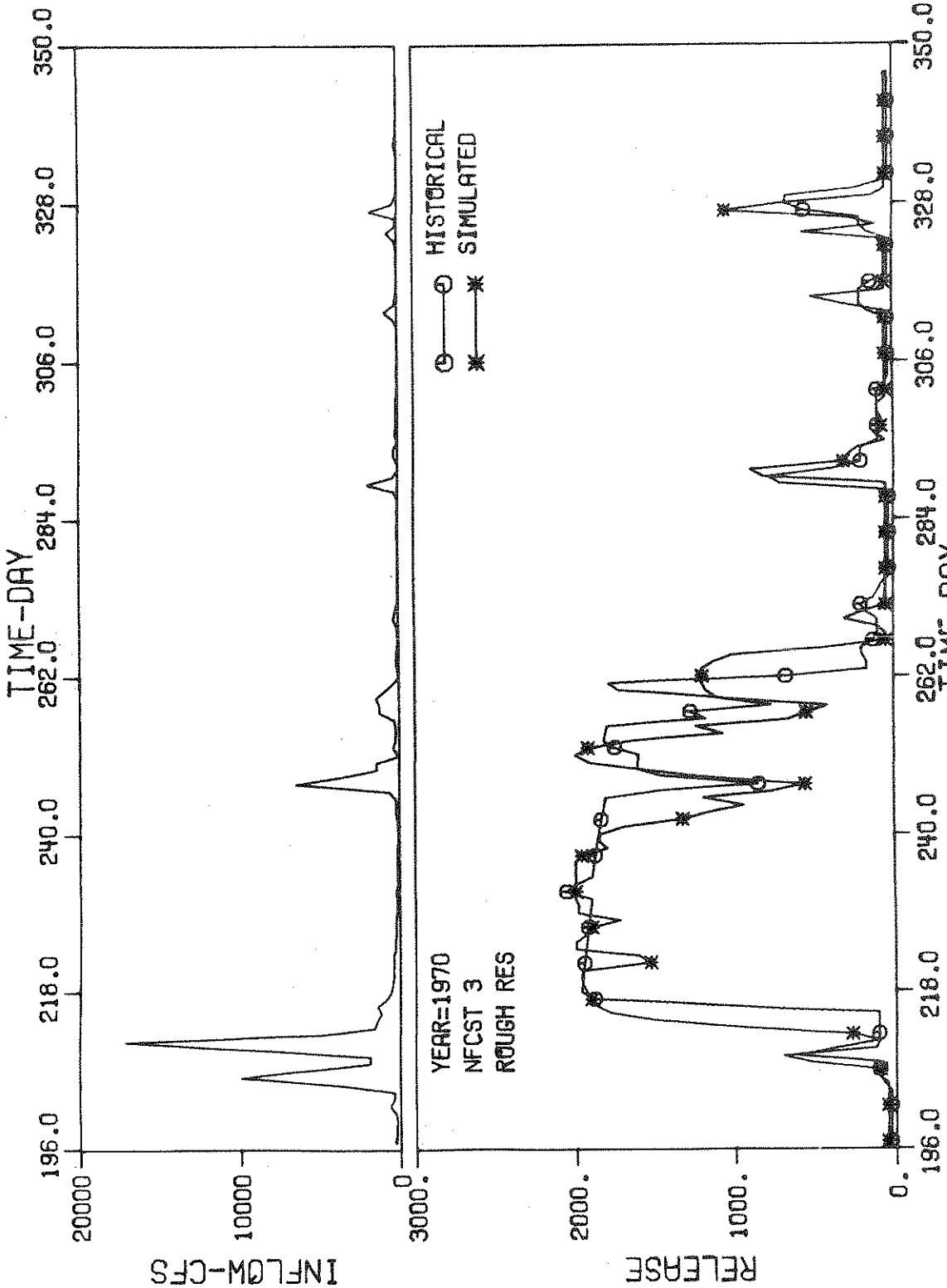

Figure 5.30 Simulated and Historical Releases for Rough Reservoir in the Summer Season of the 1970 Water Year

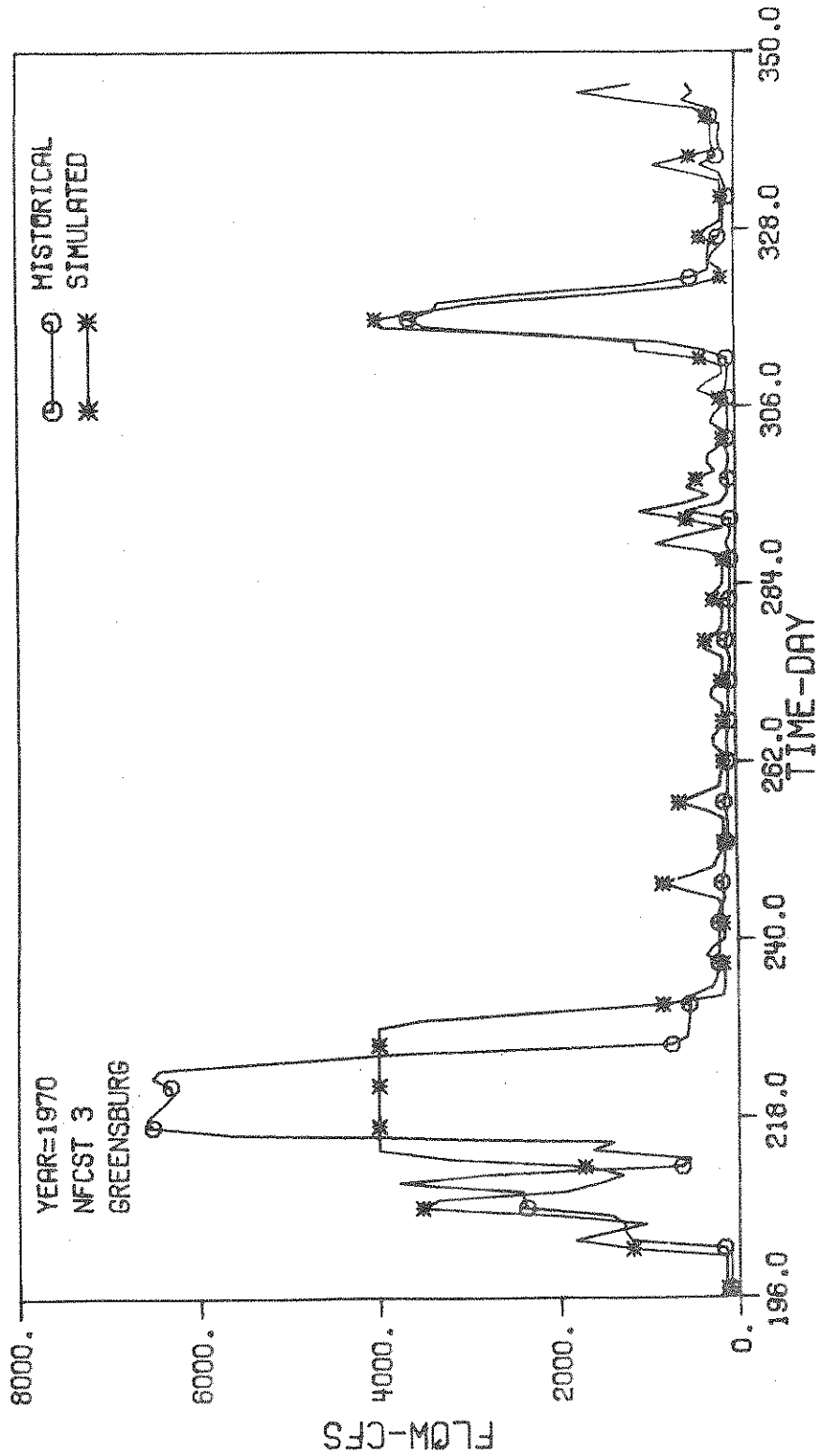

Figure 5.31 Simulated and Historical Flows at Greensburg in the Summer Season of the 1970 Water Year

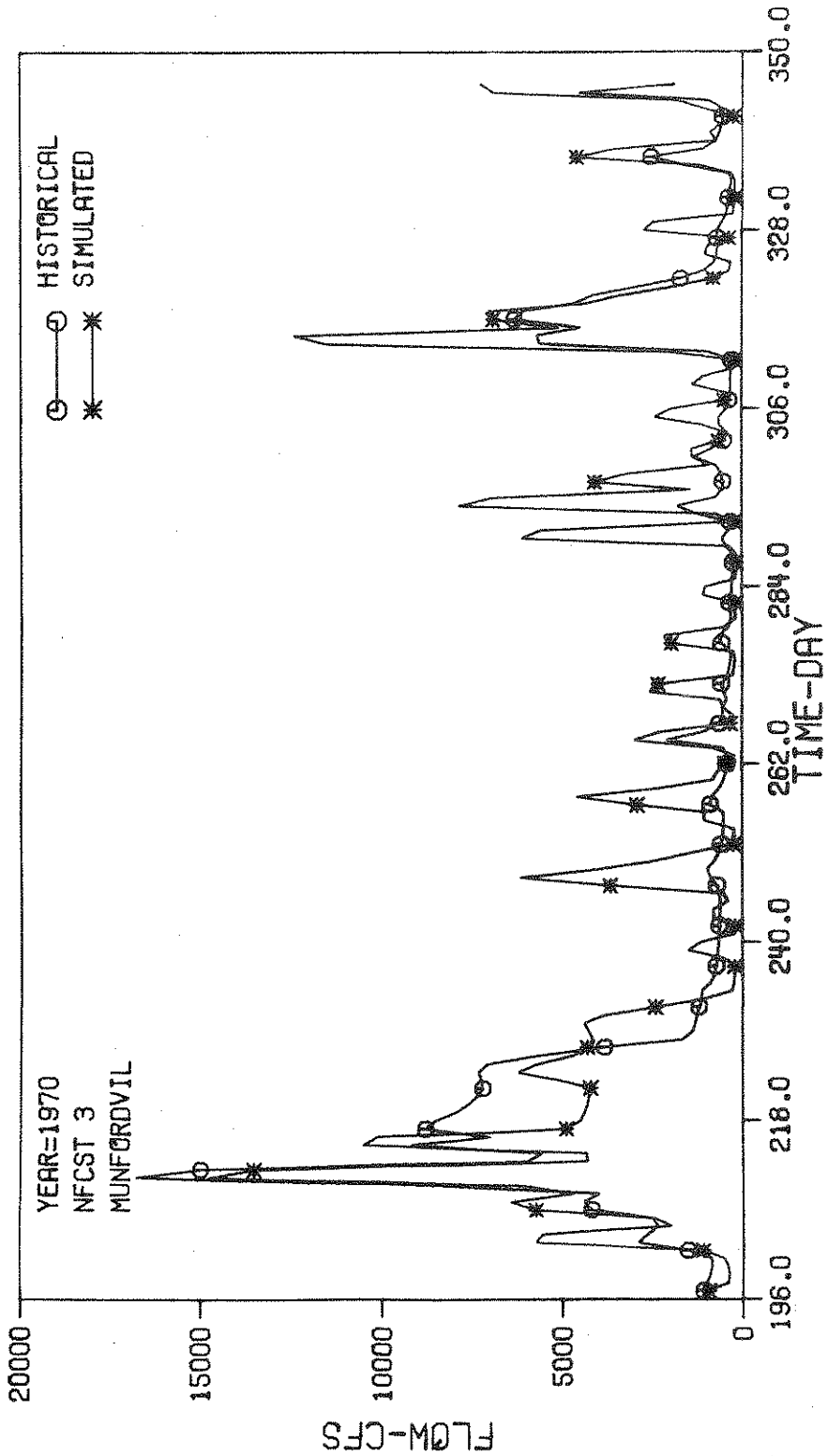

Figure 5.32 Simulated and Historical Flows at Munfordville in the Summer Season of the 1970 Water Year

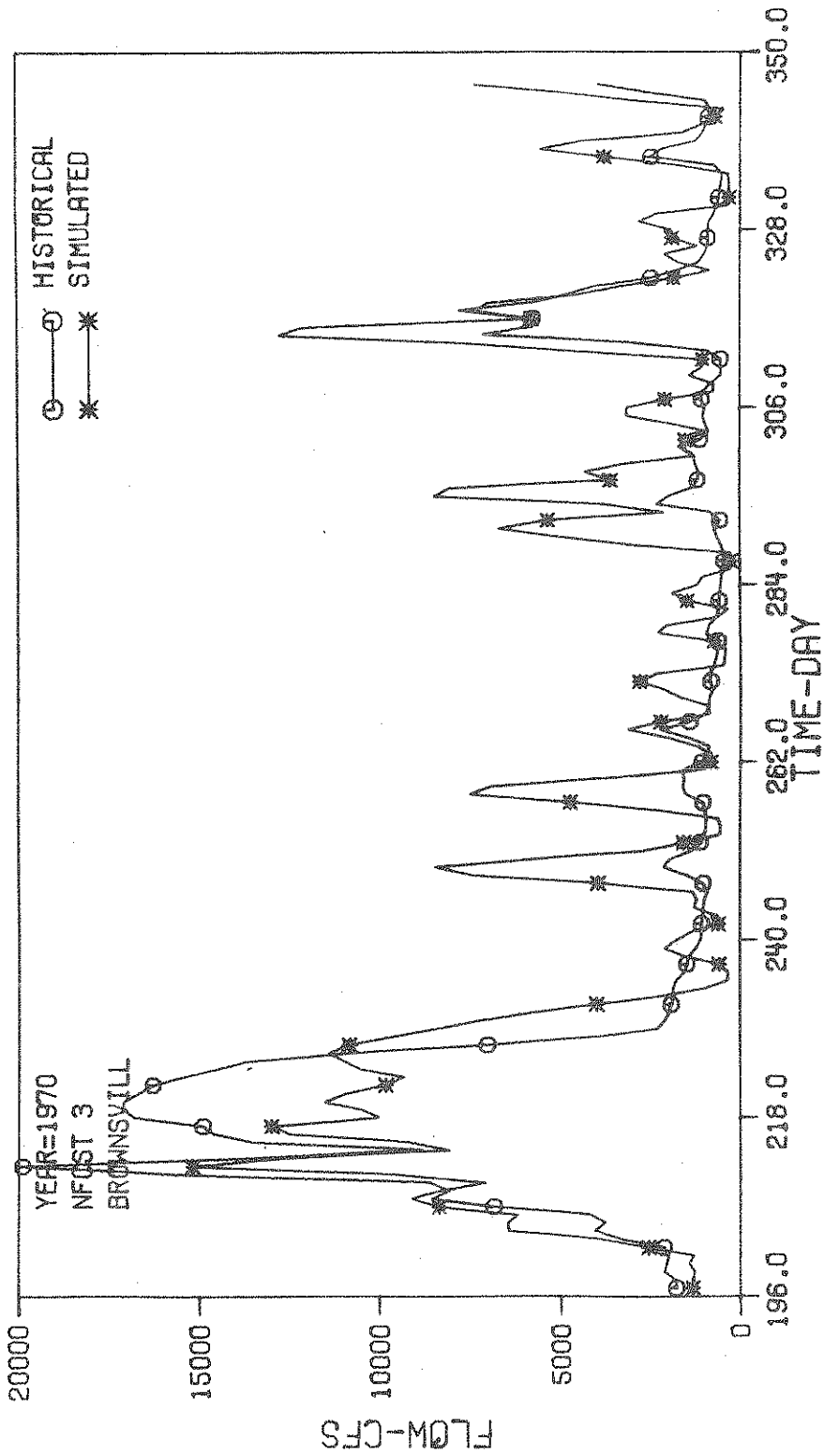

Figure 5.33 Simulated and Historical Flows at Brownsville in the Summer Season of the 1970 Water Year

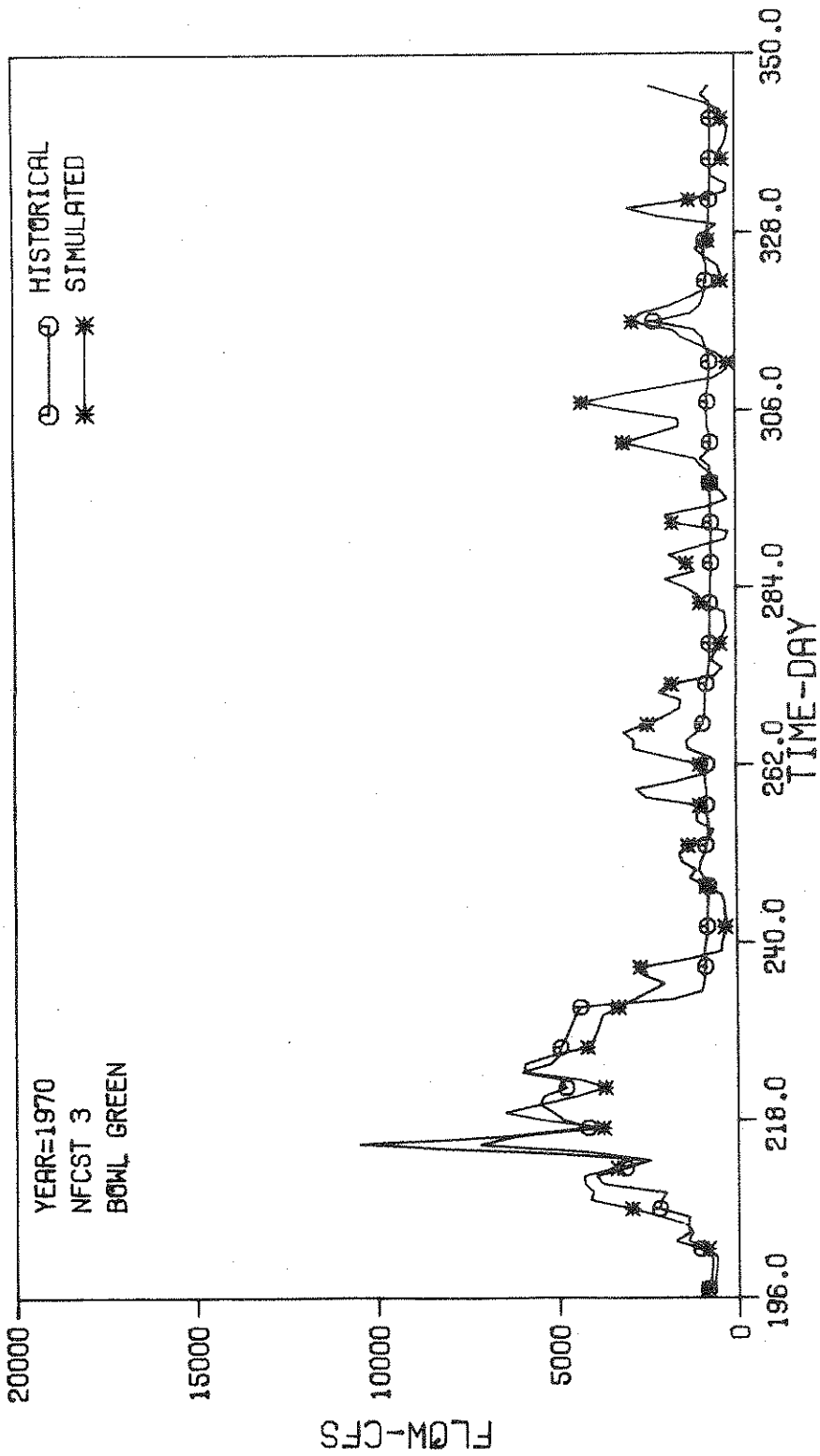

Figure 5.34 Simulated and Historical Flows at Bowling Green in the Summer Season of the 1970 Water Year

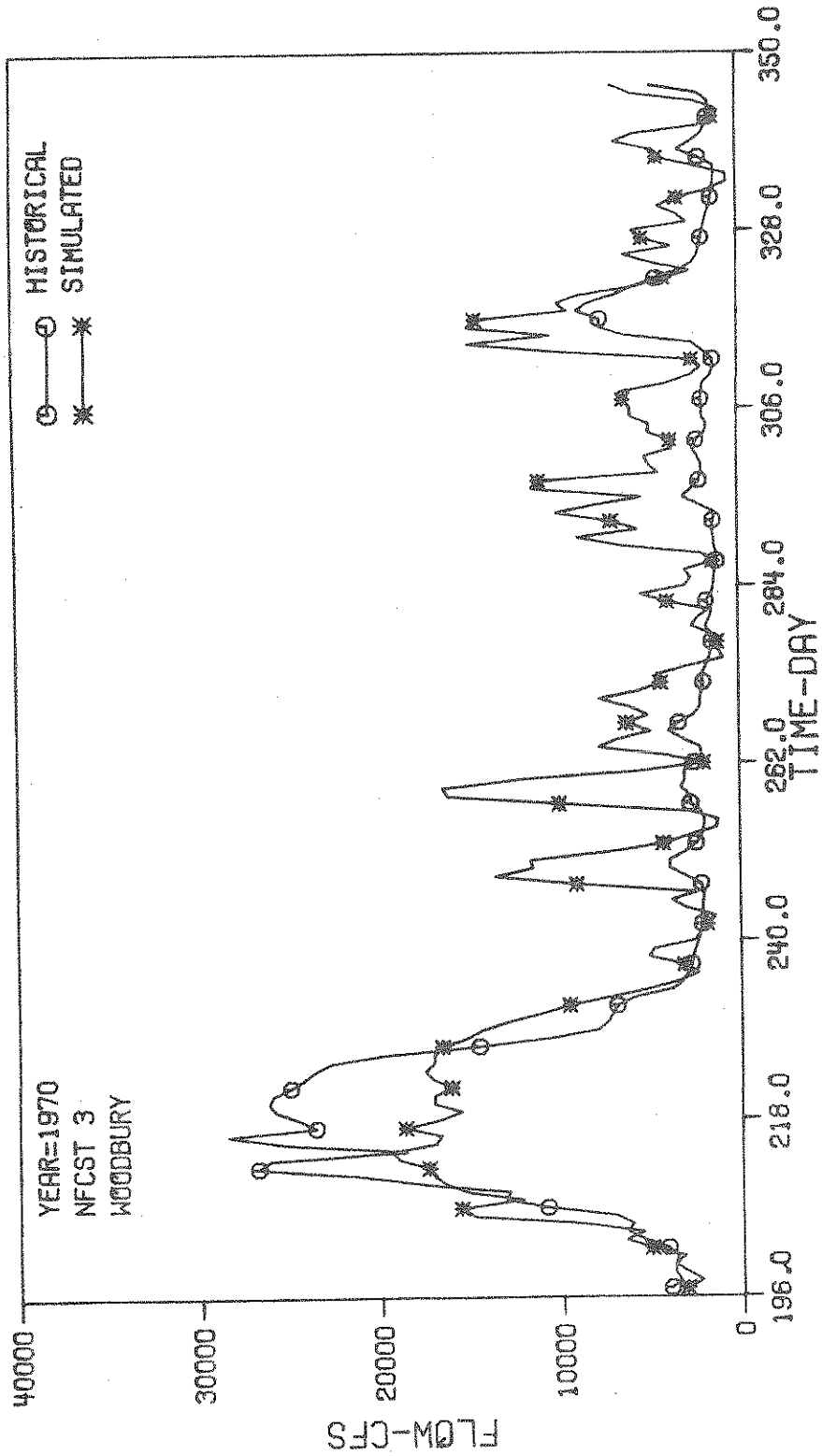

Figure 5.35 Simulated and Historical Flows at Woodbury in the Summer Season of the 1970 Water Year

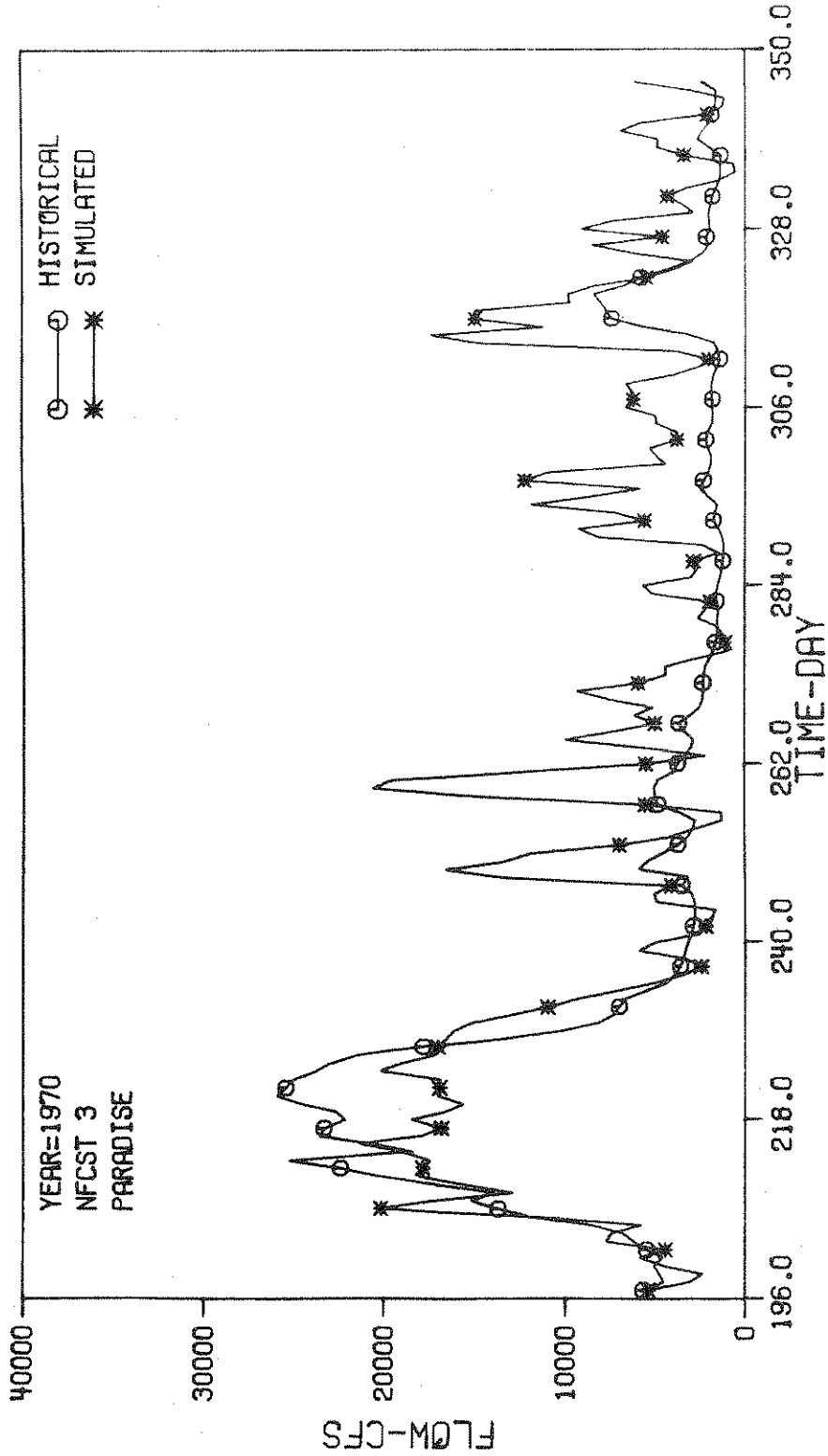

Figure 5.36 Simulated and Historical Flows at Paradise in the Summer Season of the 1970 Water Year

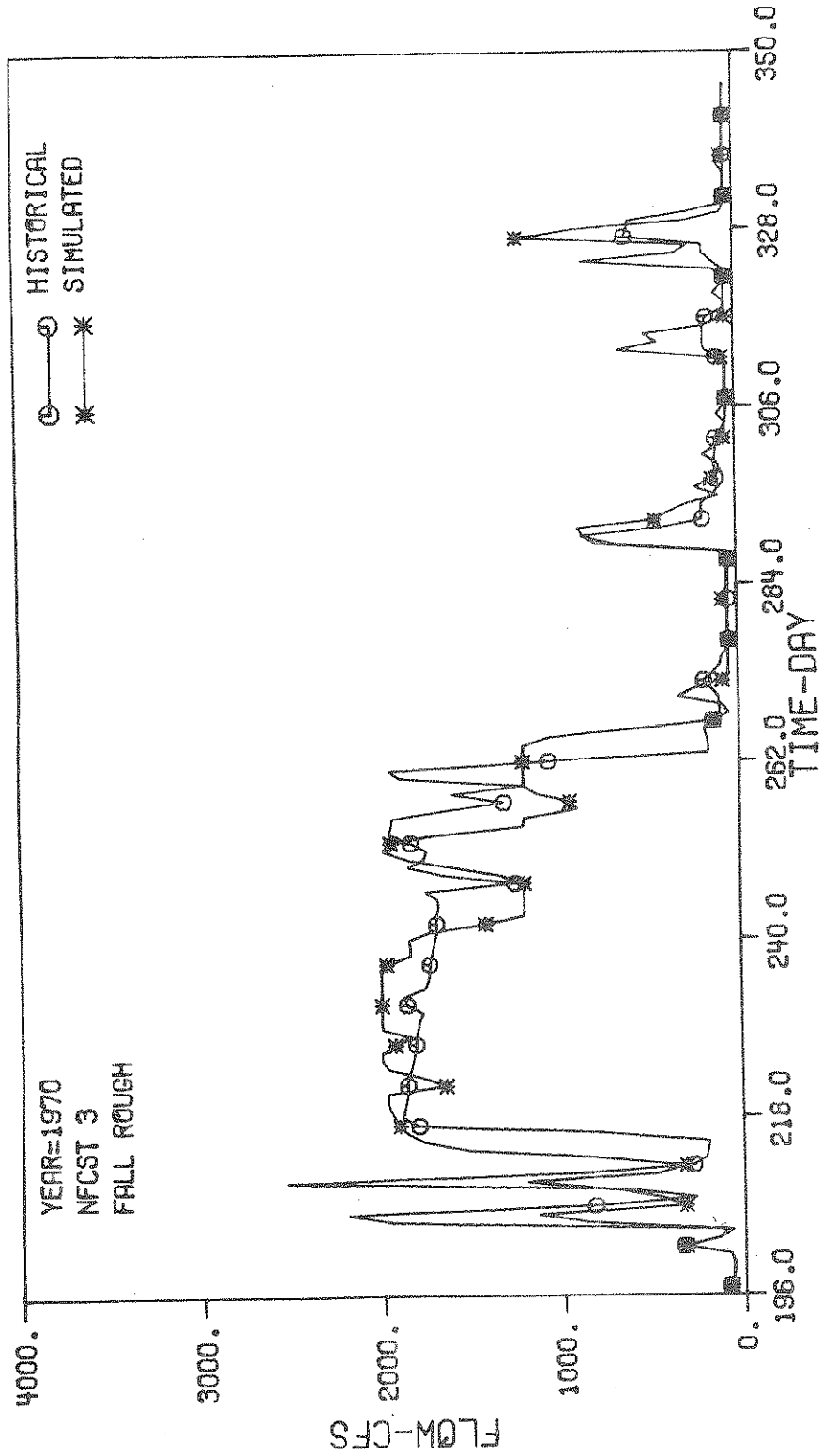

Figure 5.37 Simulated and Historical Flows at Falls of Rough in the Summer Season of the 1970 Water Year

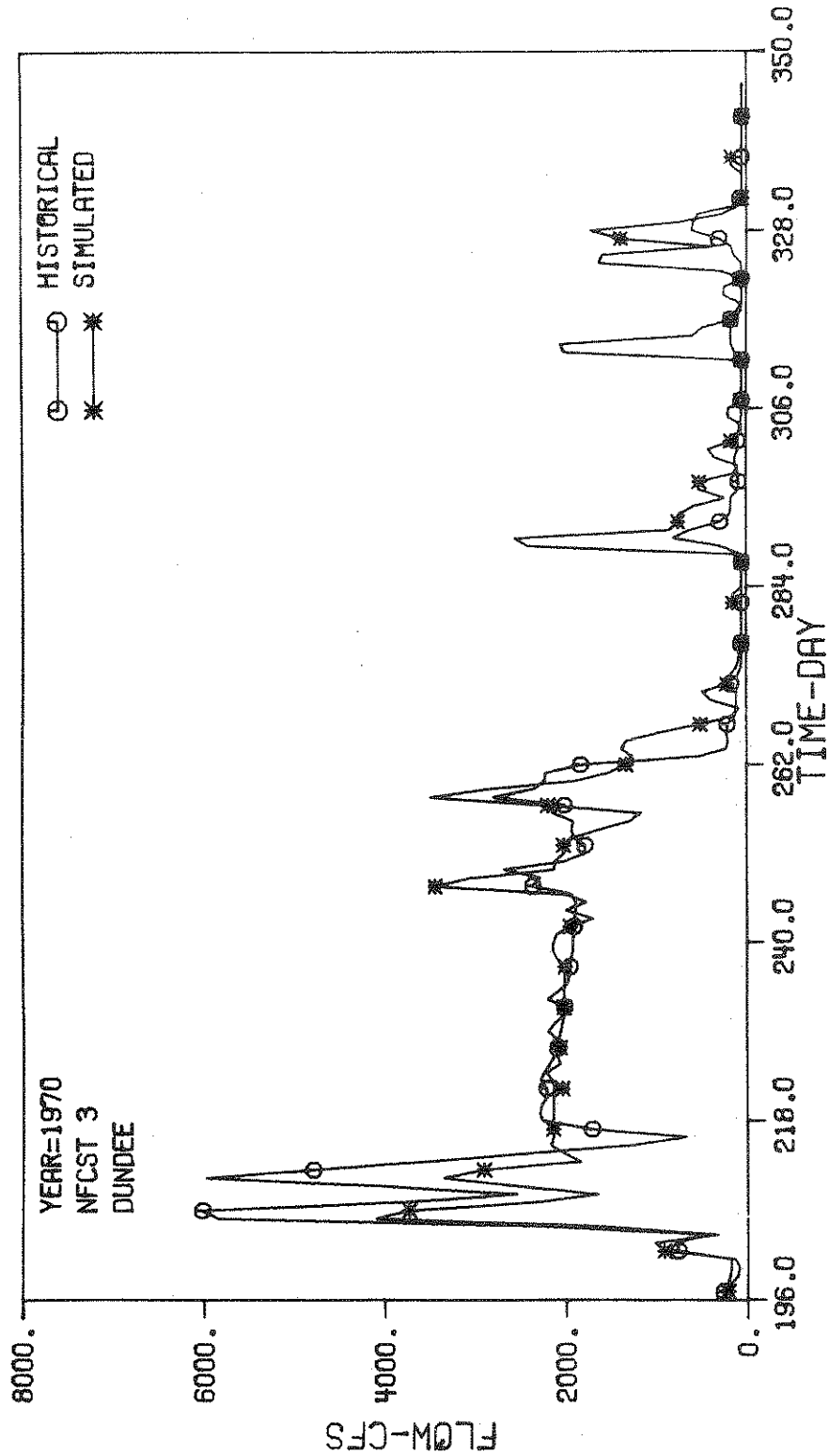

Figure 5.38 Simulated and Historical Flows at Dundee in the Summer Season of the 1970 Water Year

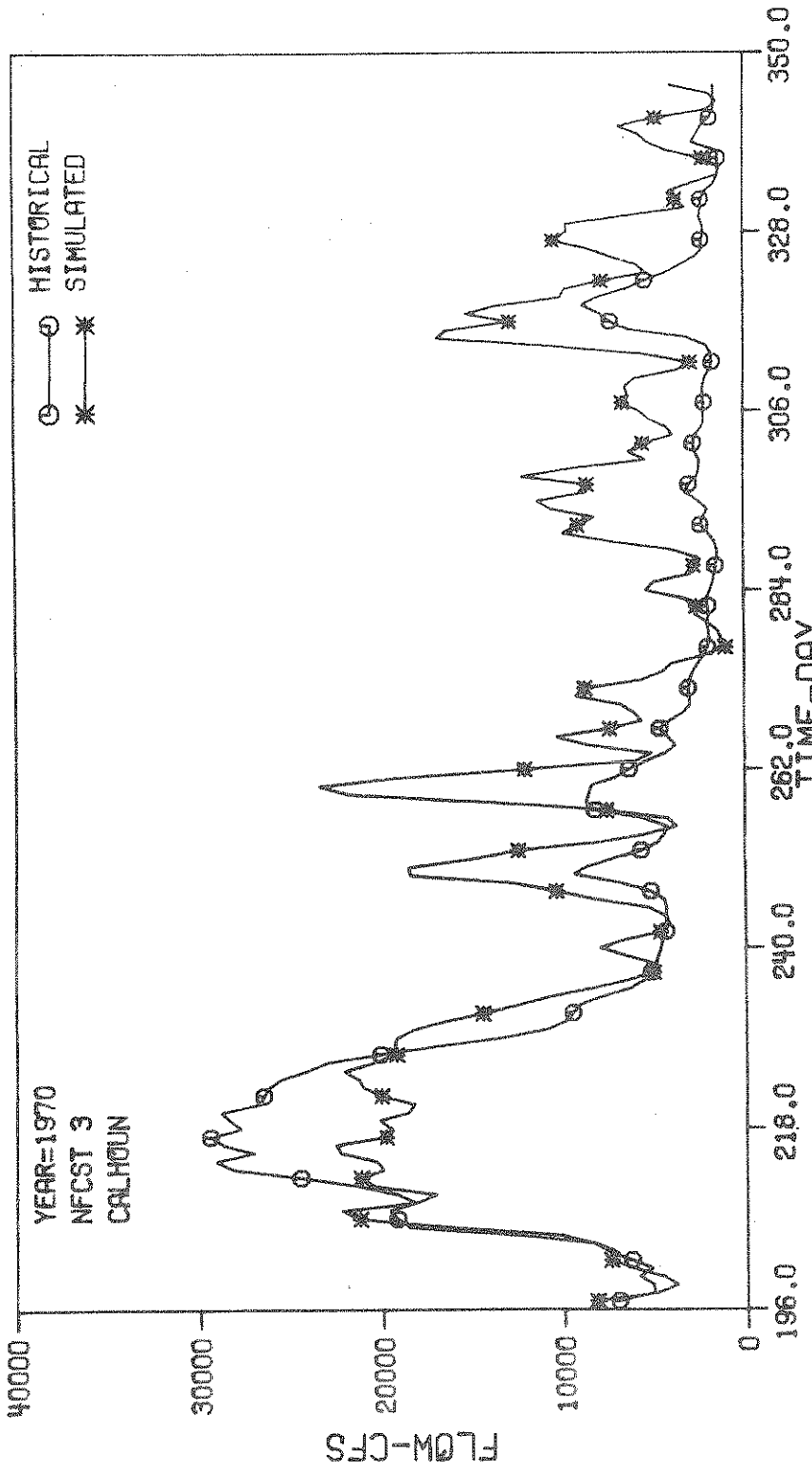

Figure 5.39 Simulated and Historical Flows at Calhoun in the Summer Season of the 1970 Water Year

Table 5.11 Comparison of Storage Penalties Between Historical and Simulated Results in Summer Season of 1970 Water Year

Reservoirs	Historical Storage Penalties	Simulated Storage Penalties	Percent Reduction in Storage Penalties, PRSP
Green	$4.80037*10^6$	$4.89724*10^6$	-2.0
Nolin	$5.03577*10^6$	$5.76889*10^6$	-14.6
Barren	$5.96031*10^6$	$2.73665*10^6$	54.1
Rough	$2.20206*10^7$	$1.91466*10^7$	13.1
Total Z_1^h & Z_1^*	$3.78171*10^7$	$3.25493*10^7$	13.9

Table 5.12 Comparison of Flow Penalties between Historical and Simulated Results in Summer Season of 1970 Water Year

Control Stations	Historical Storage Penalties	Simulated Storage Penalties	Percent Reduction in Flow Penalties, PRFP
Greensburg	$1.18228*10^6$	$9.02045*10^4$	92.4
Munfordville	$6.17000*10^5$	$4.93076*10^5$	20.1
Brownsville	$1.54298*10^6$	$3.70347*10^5$	76.0
Bowling Green	$1.99490*10^5$	$1.03062*10^5$	48.3
Woodbury	$9.14088*10^6$	$9.52512*10^5$	89.6
Paradise	$3.47170*10^5$	$4.58909*10^5$	-32.2
Falls of Rough	$1.09513*10^6$	$8.88939*10^5$	18.8
Dundee	$1.47633*10^6$	$7.44312*10^5$	49.6
Calhoun	$8.20840*10^5$	$1.01964*10^6$	-24.2
Total Z_2^h & Z_2^*	$1.64221*10^7$	$5.12100*10^6$	68.8

The sum of storage penalties for all reservoirs, Z_1^*, was reduced by 13.9% as compared to the historical operations value, Z_1^h.

By and large, simulated reservoir releases follow the historical releases. There are differences, especially for Green and Barren Reservoirs (Figures 5.24 and 5.28). For Green Reservoir the simulated high-flow releases were less than the historical releases. This is mainly due to the fact that the relative penalty coefficient for exceeding 4,000 [cfs] at Greensburg just downstream of the Green Reservoir is about six times larger than the penalty coefficient for exceeding the rule curve level at Green Reservoir (Tables 5.3 and 5.4). Therefore, GRBOPM2 did not yield recommended release decisions from Green Reservoir that resulted in flows in excess of 4,000 [cfs] at Greensburg. This can be seen by comparing Figure 5.24 and 5.31. The historical flows were in the range of 6,500 [cfs], however (see Figure 5.31). This did, in fact, exceed the 6,000 [cfs] release constraint specified in Appendix A.

In regard to Barren Reservoir, the differences between simulated and historical releases were due to the making of constant historical releases of about 480 [cfs] between days 233 and 346. This indicates that there may be an unwritten rule in the historical operations to change gate settings and hence release rates as little as possible even when there are substantial deviations from the rule curve (Figures 5.27 and 5.28).

Figures 5.31 through 5.39 show that the simulated flow flood peaks at most control stations were appreciably smaller than the historical flows with the exception of Paradise and Calhoun (Table 5.12). This is probably due to the high flood stage elevations of the latter (Table 5.4).

The overall systems measure of effectiveness for flow penalties (i.e. Z_2^*) was reduced significantly as compared to the historical one (i.e. Z_2^h); the percent reduction in flow penalties (PRFP) amounted to 68.8%. The acceptable

minimum flow requirements were met by both the historical and simulated operations during the entire summer season.

The reduction in the overall systems measure of effectiveness Z^*, i.e. $Z^h - Z^*$, where $Z^* = Z_1^* + Z_2^*$, $Z^h = Z_1^h + Z_2^h$, was about 30.5%. In summary, the GRBOPM2 model yielded recommended GRB reservoir system operations decisions that were better as compared to the historical operations in both the summer and winter seasons.

A summer trade-off curve similar to that generated for the winter season was again obtained by varying the value of λ between 0.0 and 1.0 at selected intervals as shown by the middle curve in Figure 5.40. The trade-off points for $\lambda = 1.0$ were not plotted in Figure 5.40 (for $\lambda = 1$ the values of Z_1^* and Z_2^* were equal to $5.11715*10^8$ and $1.98420*10^6$, respectively). As was the case for the winter season, the trade-off curve lies closer to the ideal operations condition than the historical operation (Figure 5.40).

5.9 USE OF MODEL WITH SYNTHETIC INPUTS TO DEVELOP TRADE-OFF CURVES

Using only the historic flow records as input to GRBOPM2 makes for a bias in the obtained trade-off curves. There is no guarantee that the historical flow record will repeat itself or will even be typical for the basin. By testing the model against a range of flow sequences which could occur, the variability of possible future performance may be understood better. In turn this promotes a fuller study of alternative operating policies, of penalty functions, and of the desired trade-offs between objectives.

5.9.1 Development of Balanced Hydrographs

Various techniques have been proposed for the generation of synthetic inputs; the balanced inflow hydrograph generation technique proposed by Beard (1975) was used in this study. A balanced flood is one that is of equal severity for all possible critical durations of floods. Here severity is expressed in

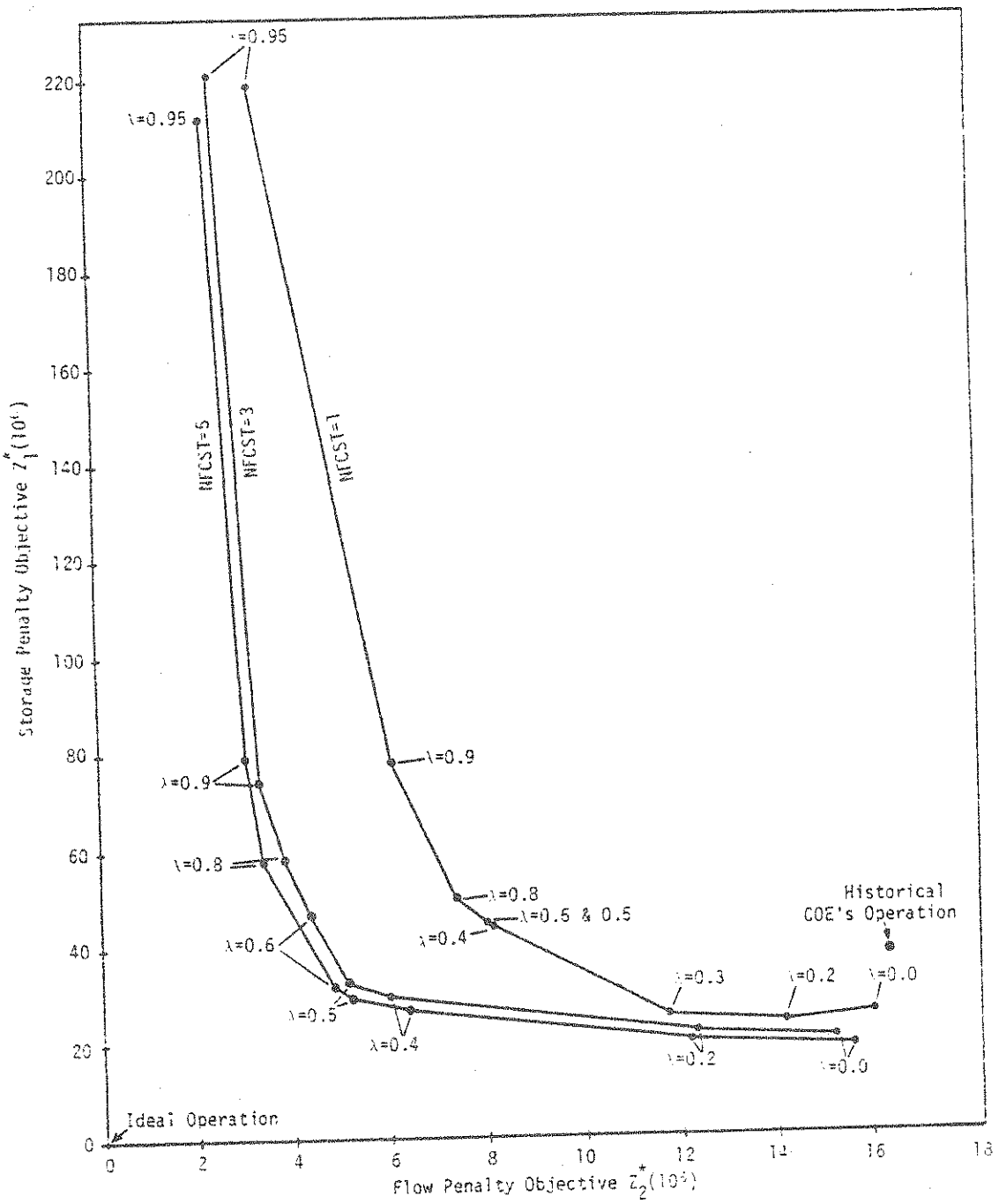

Figure 5.40 Trade-Off Curves Between Minimum Storage and Minimum Flow Penalty Objectives for the 1970 Summer Season Using 1, 3, and 5 Day-Ahead Forecast Information

terms of an exceedence probability or exceedence frequency for flood volume for various durations or hydrograph time basis, T_b. The relevant duration of floods in the Green River Basin varies between two to three days in the upper reaches and two to three weeks in the lower reaches (COE, 1967).

The steps for the generation of balanced inflow hydrographs as suggested by Beard (1975) and their application to the GRB are summarized below.

Step 1. Develop maximum average flow-frequency-duration curves for each watershed whose runoff is counted as an external input to the model by using historical data which are available or have been generated for between 10 and 20 years. To this end the available GRB daily flow data were scanned to determine the annual maximum average flows, $\overline{Q}$, for T_b = 1, 3, 5, 10, and 30 day durations for the four reservoir watersheds (Green, Nolin, Barren, and Rough), the four gaged tributary watersheds (Gresham, Alvaton, Glen Dean, and Horse Branch) and the nine river reach side inflow series (the latter series were generated using MIL models). Figure 5.41 shows the average flow-frequency-duration curves, i.e. $\overline{Q} = \overline{Q}(T_b, p)$, developed for Horse Branch (here p = probability of exceedence). Similar curves for other watersheds were also developed.

Step 2. Select a representative hydrograph. This can be of any shape. For the GRB system, triangular hydrographs whose peak discharges occur at one-third of the time base of the hydrograph were selected as the representative hydrograph for all watersheds (see Figure 5.42a).

Step 3. Select an exceedence frequency suited to the needs of a particular problem. Exceedence frequencies of p = 0.43, 0.1, and 0.05 [yr^{-1}] which correspond to return periods of 2.33, 10 and 20 years, respectively, were selected for the GRB system.

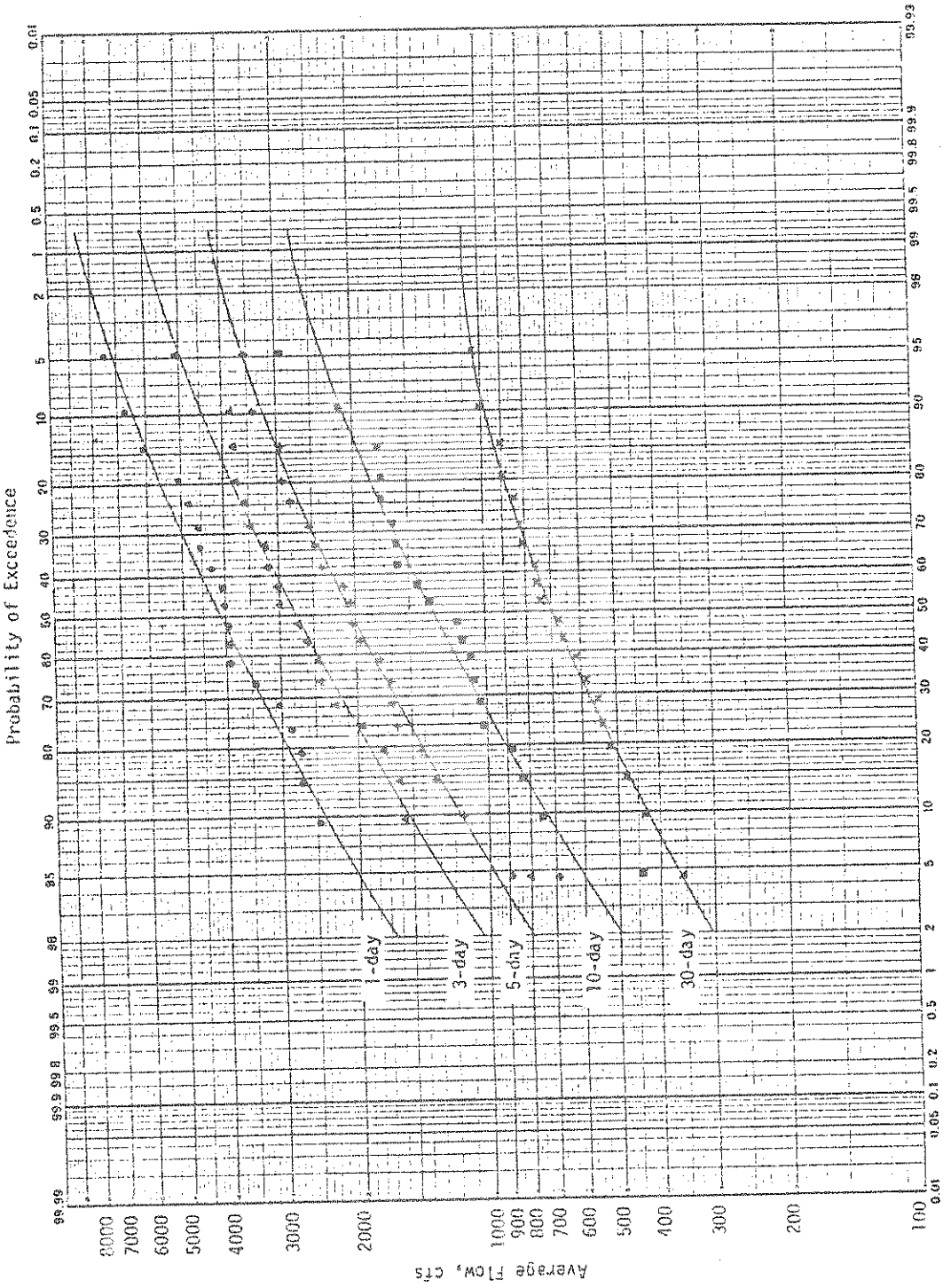

Figure 5.41 Maximum Average Flow-Frequency-Duration Curves for Horse Branch

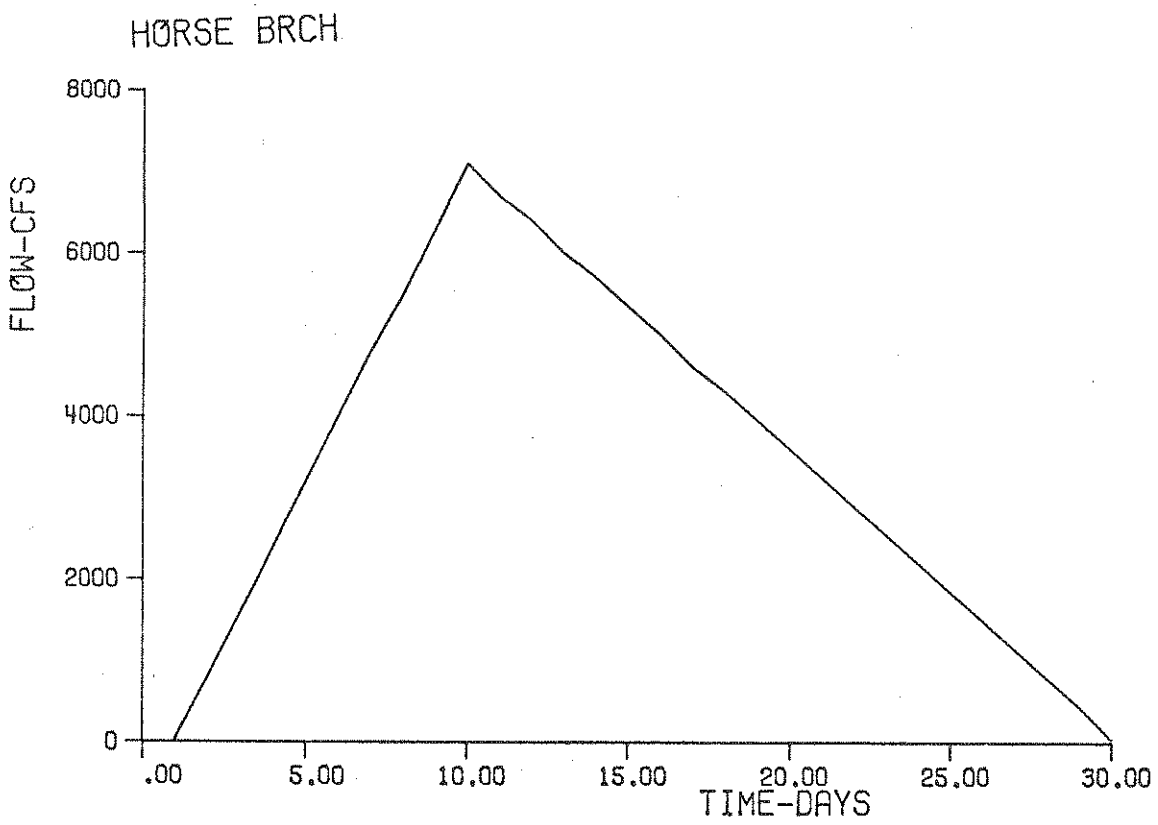

Figure 5.42a Representative Hydrograph

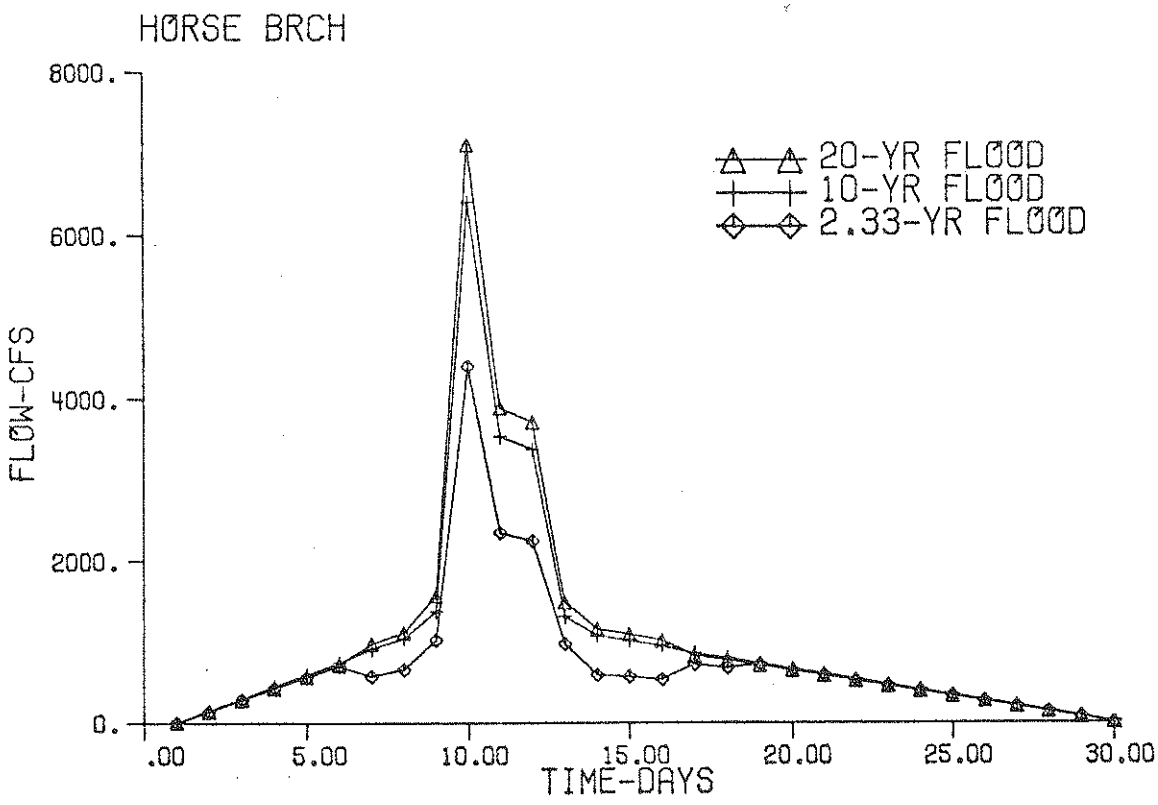

Figure 5.42b Balanced Hydrographs for Horse Branch

Step 4. Obtain the flow $\bar{Q} = \bar{Q}(T_b, p)$ for the selected T_b and p values. The results are tabulated in Table 5.13.

Step 5. These $\bar{Q}$-flows shown in Table 5.13 are then used in the balanced hydrograph composition scheme outlined in Appendix B. Typical results for Horse Branch are shown in Figure 5.42b.

5.9.2 Use of Balanced Hydrographs

The balanced hydrographs were used as input to GRBOPM2 to develop trade-off curves. For this study, it was assumed that these balanced inflow hydrographs all occur at the same time throughout the basin. This is an overly conservative assumption for most basins; although the COE (1967) manual does indicate that basin-wide flooding is common in the GRB. More refined studies would require the use of spatially as well as temporally varied balanced inflow hydrographs. To that end one would have to study the temporal and spatial distribution characteristics of runoff in the basin.

The process of generating trade-off curves using balanced hydrograph inputs is illustrated in Figure 5.43. The scheme applies to both the summer and the winter seasons.

5.9.3 Winter Season Trade-Off Curves

The balanced hydrograph inputs were imposed onto the GRB system following a period in which constant inflows were applied while the reservoir elevations were held constant (at winter rule curve levels). An operating horison of $L = 3$[day] was used.

Trade-off curves between storage and flow penalty objectives were developed for 2.33 and for 20 year return period as was done for the historical records. These are shown in Figures 5.44 and 5.45. The shapes of the trade-off curves for both return periods are similar to the trade-off curve developed from historical

Table 5.13 Calculated Average Flow Rates for Various Return Periods and Durations

Watershed	AVERAGE FLOW RATES (CFS)														
	2.33 Year Return Period					10 Year Return Period					20 Year Return Period				
	1-Day	3-Day	5-Day	10-Day	30-Day	1-Day	3-Day	5-Day	10-Day	30-Day	1-Day	3-Day	5-Day	10-Day	30-Day
Green	15,500	12,200	9,600	7,100	3,700	24,500	19,000	14,500	10,600	5,600	27,000	21,000	15,600	11,600	6,100
Nolin	11,800	10,000	8,900	6,350	3,400	16,500	14,300	12,800	9,400	4,850	17,000	15,100	13,500	10,000	5,400
Barren	23,500	16,800	12,800	8,900	5,000	55,000	38,000	26,500	15,900	7,900	73,000	50,000	34,000	19,000	9,000
Rough	15,700	9,500	6,900	4,500	2,550	27,000	18,200	13,000	8,200	3,750	35,000	23,000	16,500	10,000	4,400
Gresham	8,800	5,850	4,200	2,800	1,475	18,500	12,500	9,000	5,200	2,550	24,000	16,000	11,500	6,400	3,050
Alvaton	15,500	10,200	7,900	5,000	2,470	39,500	24,000	17,800	9,600	3,750	53,000	32,000	23,000	12,000	4,300
Glen Dean	1,080	570	370	220	112	2,100	1,100	680	370	190	2,750	1,400	880	560	270
Horse Br.	4,400	3,000	2,200	1,410	730	6,400	4,440	3,200	2,100	980	7,100	4,900	3,550	2,310	1,040
Reach 1	3,800	1,970	1,280	820	460	5,900	2,800	1,800	1,250	780	6,800	3,100	2,050	1,500	980
Reach 2	47,500	22,700	15,700	9,600	5,750	58,000	30,000	19,000	13,500	8,800	62,000	33,000	20,500	16,000	10,800
Reach 3	27,000	13,400	8,500	5,500	3,290	32,500	18,000	12,500	8,200	4,400	34,500	20,000	15,000	10,800	4,800
Reach 4	31,000	16,000	11,500	6,900	3,850	51,000	24,000	16,000	8,600	4,500	61,000	27,000	17,700	9,200	4,700
Reach 5	50,500	26,000	18,900	11,500	6,700	76,000	42,000	32,000	19,500	8,900	94,000	52,000	41,000	25,000	9,800
Reach 6	58,000	32,000	20,500	13,700	6,700	105,000	52,000	33,000	22,500	9,200	165,000	61,000	38,000	26,500	10,300
Reach 7	2,300	1,000	690	440	255	2,700	1,550	1,000	625	330	2,800	2,000	1,300	800	355
Reach 8	8,000	4,100	2,850	1,890	1,040	11,600	7,000	4,500	3,200	1,450	14,500	10,000	6,500	5,000	1,800
Reach 9	46,000	22,500	15,000	9,900	5,300	68,000	40,000	25,000	17,000	7,400	82,000	53,000	36,000	24,000	8,850

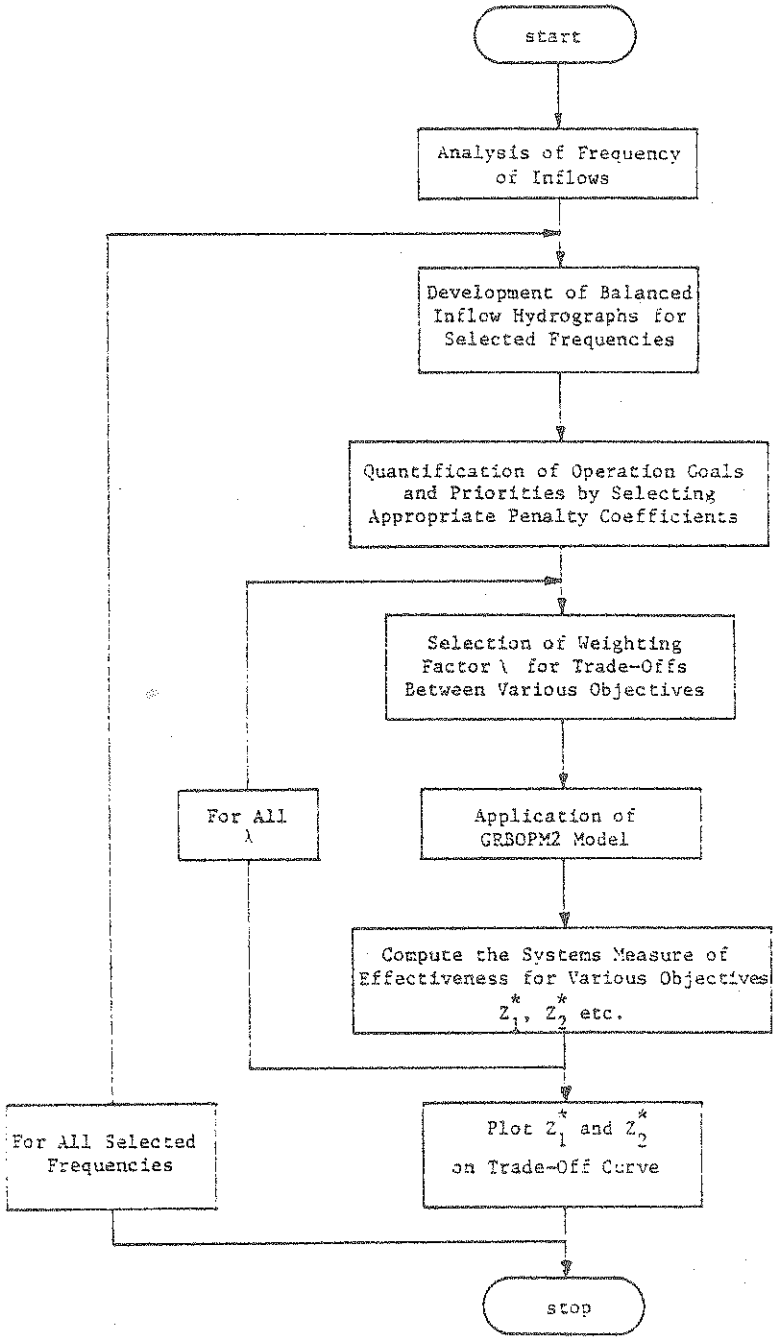

Figure 5.43 Use of GRBOPM2 Model With Synthetic Inputs to Develop Trade-Off Curves

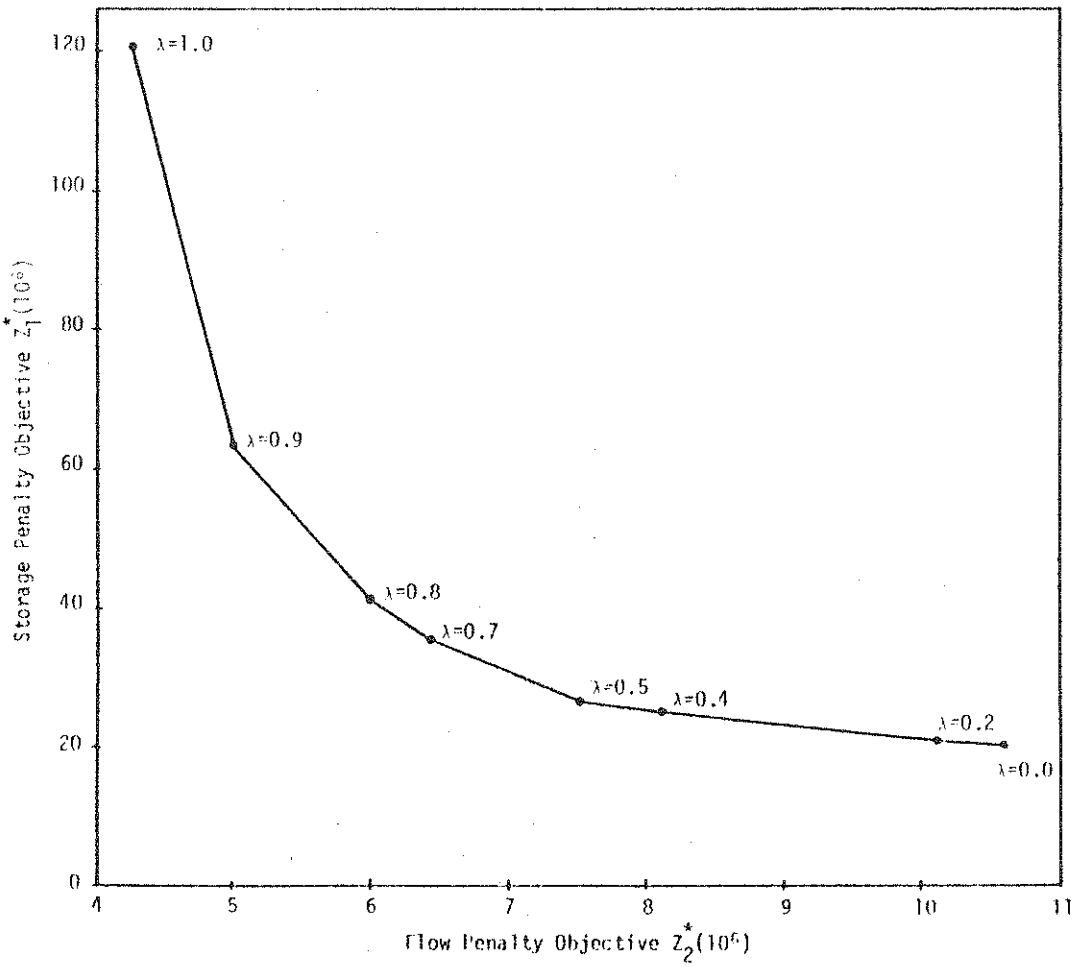

Figure 5.44 Trade-Off Curve Between Minimum Storage and Minimum Flow Penalty Objectives for Synthetic Inputs With a Return Period of 2.33 Years in Winter Season

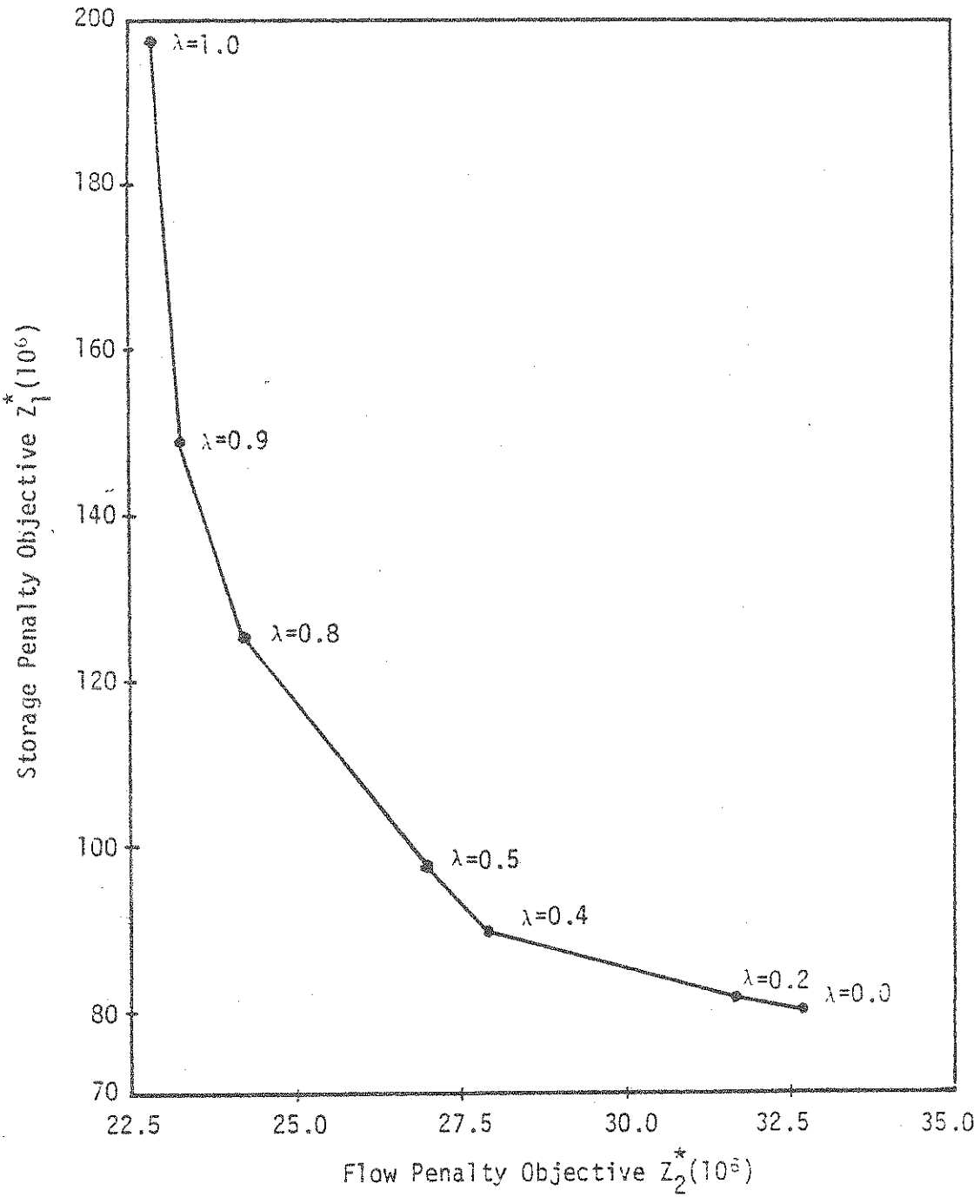

Figure 5.45 Trade-Off Curve Between Minimum Storage and Minimum Flow Penalty Objectives for Synthetic Inputs With a Return Period of 20 Years in Winter Season

data (Figures 5.22, 5.44, and 5.45). However, the total storage and flow penalties for the balance hydrograph inputs are much larger. This is due to the extreme input combination (i.e. uniform basin-wide flooding).

The trade-off curves may be used to answer a variety of questions. For example, if general flooding conditions occur throughout the basin, the question of what percentages of the flood storage space would be filled if one wants to minimize only the flow penalties (i.e. $\lambda = 1.0$) is readily answered. In that case, all reservoir inflows will be stored completely and only uncontrolled tributary and side inflows contribute to the flooding at the control stations. Typical results from such an operation are shown in Tables 5.14 and 5.15. As seen from Table 5.14, the occupied flood control storage zones (i.e. US_1 in Table 5.1) vary between 26% to 49% when the return period equals 2.33 years, and between 48% and 85% when the return period equals 20 years. The flood control storage zone for the Rough Reservoir was occupied more than any other reservoir (49% and 85% for return periods of 2.33 and 20 years, respectively). This is due to the relatively small flood control capacity of this reservoir as compared to the others (Table 5.14). As seen in Table 5.15, the flood levels, which correspond to the lower boundary of the uppermost flow zones in Table 5.2 at all control stations, except Greensburg, were exceeded for both return periods.

It is noted that among the historical flood peaks the magnitudes shown in Table 5.15 for T = 20[yr] were exceeded by a factor of two on several occasions.

5.9.4 Summer Season Trade-Off Curves

Trade-off curves between storage and flow penalty objectives were developed by using the synthetic balanced inflow hydrographs with return periods of 2.33 and 10 years. These are shown in Figures 5.46 and 5.47. The values of the storage and flow penalty objective (i.e. Z_1^* and Z_2^*) in the summer season were larger than those of the winter season because of the relatively large magnitude of the

Table 5.14 Simulated Peak Elevation and Percent Occupied Flood Control Capacities for 2.33 and 20 Year Return Periods at Reservoirs in Winter Season (λ = 1.0)

Reservoirs	Winter Flood Control Storage Capacity in ac-ft (US_1)	2.33 Year Return Period		20 Year Return Period	
		Peak Elevation in ft	Occupied Flood Control Storage Capacity in %	Peak Elevation in ft	Occupied Flood Control Storage Capacity in %
Green	561,438	688.14	37.0	700.10	62.4
Nolin	545,408	521.11	26.5	536.07	48.3
Barren	750,848	561.17	39.0	577.99	70.7
Rough	303,610	505.17	49.0	519.30	85.3

Table 5.15 Flood Levels and Simulated Flood Peaks for 2.33 and 20 Year Return Periods at Control Stations in Winter Season (λ = 1.0)

Control Stations	Flood Levels i.e. UQ_3 in Table 5.2 (cfs)	Flood Peaks for 2.33 Year Return Period (cfs)	Flood Peaks for 20 Year Return Period (cfs)
Greensburg	10,000	1,713	2,593
Munfordville	17,000	20,894	35,178
Brownsville	23,000	23,790	39,930
Bowling Green	14,000	17,740	51,647
Woodbury	25,000	42,707	97,786
Paradise	35,000	48,742	105,295
Falls of Rough	2,000	2,026	4,031
Dundee	4,000	7,892	14,900
Calhoun	40,000	51,369	116,536

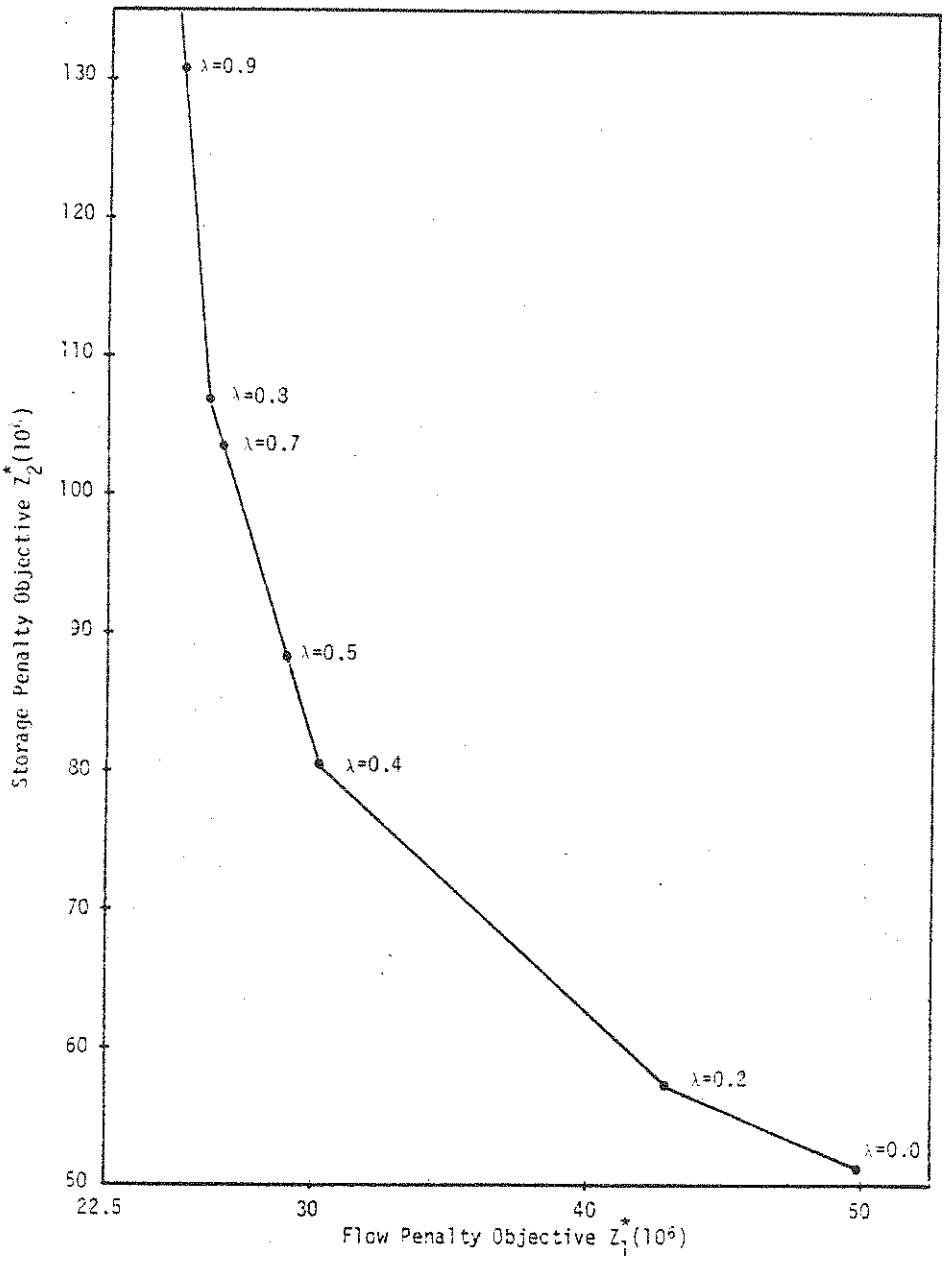

Figure 5.46 Trade-Off Curve Between Minimum Storage and Minimum Flow Penalty Objectives for Synthetic Inputs With a Return Period of 2.33 Years in Summer Season

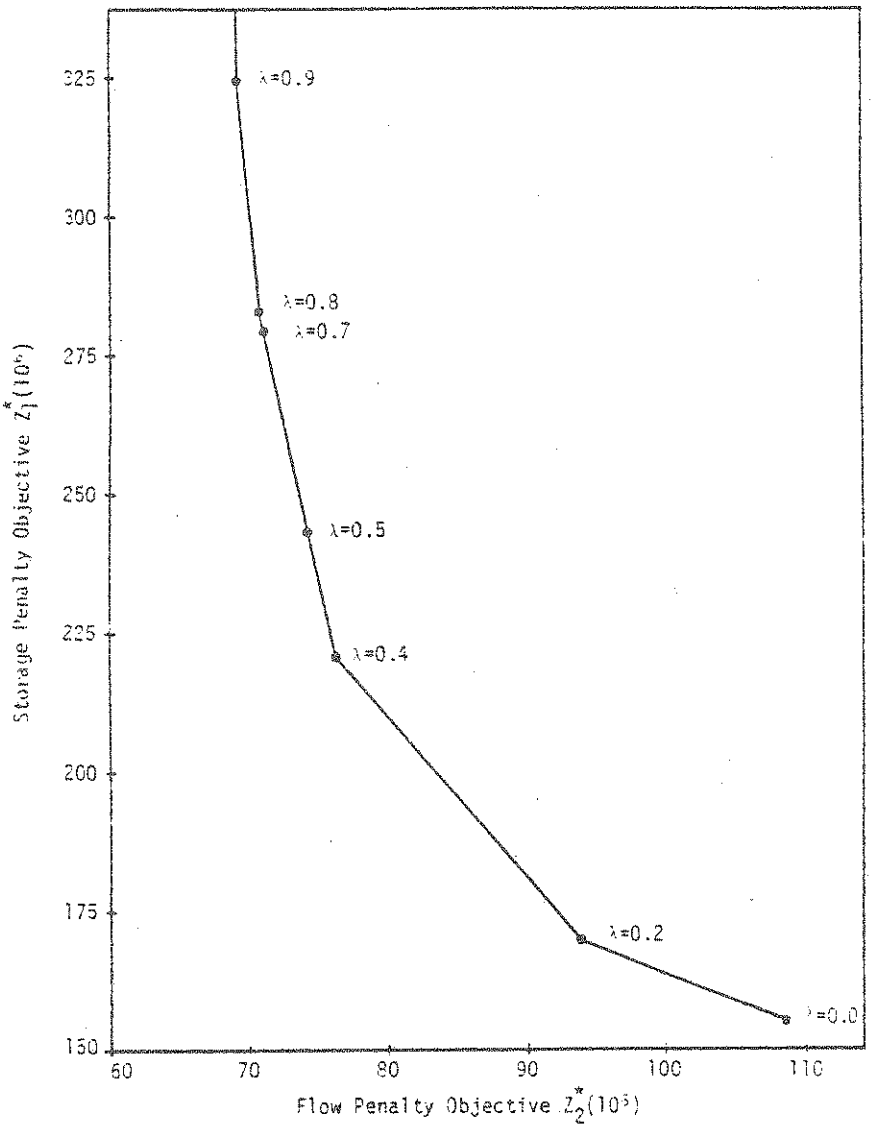

Figure 5.47 Trade-Off Curve Between Minimum Storage and Minimum Flow Penalty Objectives for Synthetic Inputs With a Return Period of 10 Years in Summer Season

penalty coefficients assigned for storage and flow zone deviations in the summer season (Tables 5.1 through 5.4). The shapes of the summer season's trade-off curves were similar to those of the winter season's.

The same analysis that was made in the winter season for λ = 1.0 (Section 5.8.1) was repeated for the summer season with return periods of 2.33 and 10 years. These results are presented in Tables 5.16 and 5.17. When all the reservoir inflows are completely retained in the reservoirs, the occupied flood control storage capacities vary from 43% to 70% for the return period of 2.33 years, and from 63% to 100% for the return period of 10 years. The relative order of magnitude of the occupied flood control storage capacities among the reservoirs was the same as for the winter season (Tables 5.14 and 5.16) but the percentages of occupied flood control capacities were larger. This is because of the relatively small flood control capacity in the summer season due to high rule curve levels. An interesting aspect is that for a λ = 1.0 condition a 10-year, 30-day duration flood will occupy all of the flood control storage capacity of the Rough Reservoir up to the spillway level (524 ft). Again, the results from Table 5.17 show that flood levels were exceeded at all the control stations except for Greensburg. Because Greensburg is the most upstream station. In the absence of accumulated side-inflows, flood conditions were not reached. The flooding of the other control stations was due to the uncontrolled tributary and side inflows as all the reservoir inflows were completely stored in the reservoirs. Similar analyses could be carried out for other values of λ and various return periods.

5.10 USE OF THE MODEL TO JUDGE THE VALUE OF FORECAST INFORMATION

The forecasted state of the system within the operating horizon is affected by the projected optimal release decisions as well as the inevitable differences between forecasted and actual system inputs (i.e. reservoir inflows, tributary inflows and precipitation). The longer the operating horizon and the more

Table 5.16 Simulated Peak Elevation and Percent Occupied Flood Control Capacities for 2.33 and 10 Year Return Periods at Reservoirs in Summer Season (λ = 1.0)

Reservoirs	Summer Flood Control Storage Capacity in ac-ft (US_1)	2.33 Year Return Period		10 Year Return Period	
		Peak Elevation in ft	Occupied Flood Control Storage Capacity in %	Peak Elevation in ft	Occupied Flood Control Storage Capacity in %
Green	482,323	695.61	43.8	703.68	67.2
Nolin	439,092	539.58	43.5	547.58	63.1
Barren	558,130	574.82	51.6	584.94	82.5
Rough	324,011	516.98	69.5	524.00	100.0

Table 5.17 Flood Levels and Simulated Flood Peaks for 2.33 and 10 Year Return Periods at Control Stations in Summer Season (λ = 1.0)

Control Stations	Flood Levels i.e. UQ_3 in Table 5.2 (cfs)	Flood Peaks for 2.33 Year Return Period (cfs)	Flood Peaks for 10 Year Return Period (cfs)
Greensburg	10,000	1,713	2,252
Munfordville	17,000	20,894	29,630
Brownsville	23,000	23,790	33,265
Bowling Green	14,000	17,740	39,455
Woodbury	25,000	42,707	77,852
Paradise	35,000	48,742	81,755
Falls of Rough	2,000	2,026	3,277
Dundee	4,000	7,892	12,191
Calhoun	40,000	51,369	89,979

accurate the forecasts, the more optimal the decisions will be. However, in real-time reservoir operations, the availability and accuracy of the forecast information decreases as the operating horizon, L, increases. Furthermore, as discussed in Section 5.5, the computational effort and hence the cost of the solution increases nearly linearly with L. Therefore, there is a need to assess the extent and utility of forecast information.

In Sections 5.8 and 5.9, three-day ahead forecast or generated input data were used in running the model for L = 3. The GRBOPM2 model was run for the winter and the summer seasons with different operating horizons, namely L = 1 and 5, to generate the trade-off curves shown in Figure 5.22 and 5.40. These figures show that as the number of periods of forecast information increases, the trade-off curves lie closer to the ideal operating point. However, going from a three-day to a five-day ahead forecast period, the objective function values for both objective (i.e. Z_1^* and Z_2^*) do not decrease as much as they do when going from one-day to three-day ahead forecast period or operating horizon. Since computing cost increases linearly whereas the penalty decrease diminishes with L, there must be an optimal forecast period to be used with GRBOPM2.

It is interesting to note that as the forecast period increases, the relative improvement in Z_2^* is larger than the relative improvement in Z_1^* (Figure 5.22 and 5.40). (Z_2^* = flow objective parameter values, Z_1^* = storage objective parameter value.) This emphasizes that better forecasts for uncontrolled tributary and precipitation inputs is important.

Another result of changing L showed up. In spite of the fact that very large penalty coefficients were assigned for the excessive rates-of-change of releases from the reservoirs (see Section 5.6), the Barren and Rough Reservoir releases exceeded their allowable rates-of-change of release limits in the summer season when one-day ahead forecasts were used in the model. During the entire summer simulation period, the total rates-of-change of release in excess of

those allowable were small. They occur because the allowable rates-of-change of release limits for Barren and Rough reservoirs are quite small in the summer season (see Tables 5.5 and 5.6).

Furthermore, one-day ahead operation cannot adjust for sudden events that occur just beyond that one-day period. For example, an increase in local control station flow at t = 2 will dictate a sudden decrease in the release for day t = 2.

5.11 OTHER RECOMMENDED USES OF GRBOPM2 MODEL

The results presented in the preceeding sections represent only a few examples of model use. Extended use is facilitated by the fact that individual reservoir rule curves and zone definitions as well as channel flow limits can be altered from one run to the next since these parameters are among the model's daily input data.

The GRBOPM2 model may also be used as an aid in design and planning. For example, effect on operating results of the addition or deletion of the Mining City Reservoir could be studied readily. This reservoir has been authorized but is not built and is subject of controversy.

VI. USE OF GRBOPM2 IN REAL-TIME RESERVOIR OPERATIONS

In the preceeding chapter, the use of the GRBOPM2 model in so called special reservoir operations studies was discussed. The ultimate aim of this study, however, is to generate and adapt a systems model to aid in real-time operation of the GRB reservoir system. In this chapter, the use of the GRBOPM2 model in real-time operation of the GRB system is considered.

6.1 CHARACTERISTICS OF REAL-TIME OPERATIONS

Special reservoir operations studies as described in the preceeding chapter are typically long-run operations studies. Time of computation and analysis are not among the critical factors. In real-time operations of a reservoir system whose main purpose is flood control, the time needed for computation and analysis can be critical. The GRBOPM2 model described herein has been designed keeping these model use factors in mind. In other words, special attention was given to computational efficiency, to input requirements, and to output selection and formating.

In real-time operations, release decisions are necessarily made without perfect knowledge of future events. Hence, the GRBOPM2 model is built to accept forecasted data over an L-day period. With this model, a set of recommended reservoir releases are computed that are optimal for an operating horizon of L days. Only optimal releases for the one-day ahead period (i.e. $RO^*(t+1)$) would be implemented. The releases selected for two and more days ahead (i.e. ℓ = 2, 3, ... L) will be revised during the next model run (at times t+1) as updated forecast information is obtained.

It is noted that the "degree of optimality" of the model results obtained at time t depends on the accuracy of the forecasted inputs during the operating horizon.

6.2 STEPS IN USING GRBOPM2 MODEL IN REAL-TIME OPERATION

The steps followed in using the GRBOPM2 model in real-time operations are similar to those given for the special reservoir operations studies (Section 5.2). The essential steps are as follows:

(1) update all data time series using observed data up to the present day, t;

(2) input the forecasted data for the days $t+\ell$, $\ell = 1, 2, \ldots, L$;

(3) define the goals and priorities for system operation by specifying target flows, rule curves, zones, and penalty coefficients;

(4) run the model to obtain the optimal releases for days t+L. Only the release policy for day t+1 would be implemented.

In real-time operation, a new set of forecasted data will be available on day t+1. The model would, therefore, be updated and rerun for the period $t+1+\ell$, $\ell = 1, 2, \ldots, L$.

A scheme for using GRBOPM2 model in real-time operation is portrayed in Figure 6.1. An interactive computer program would facilitate the input data set-up for GRBOPM2. This program provides to the GRBOPM2 model the updated data and forecasted input data for the operating horizon of L days. The forecast inputs are: net reservoir inflows for four reservoirs, $RI^r(t+\ell)$; tributary inflows from four four tributary watersheds, $T^s(t+\ell)$; and average rainfall over the local side-inflow areas of each of the nine river reaches, $P^{rr}(t+\ell)$. The GRBOPM2 model then returns the optimal release decisions, $RO^r(t+\ell)^*$, the optimal reservoir elevations $E^r(t+\ell)^*$, and the flows at control stations, $Q^c(t+\ell)^*$, over the L-day operating horizon. Also returned is the optimal value for the systems measure of effectiveness, Z^* (i.e. objective function values). The results are displayed by means of tables on the computer printouts and as well as in the form of plots.

Upon considering the displayed results, the reservoir operators may want to respecify some of the penalty coefficients, zones, target flows, etc. The model is then rerun with these new set of parameters.

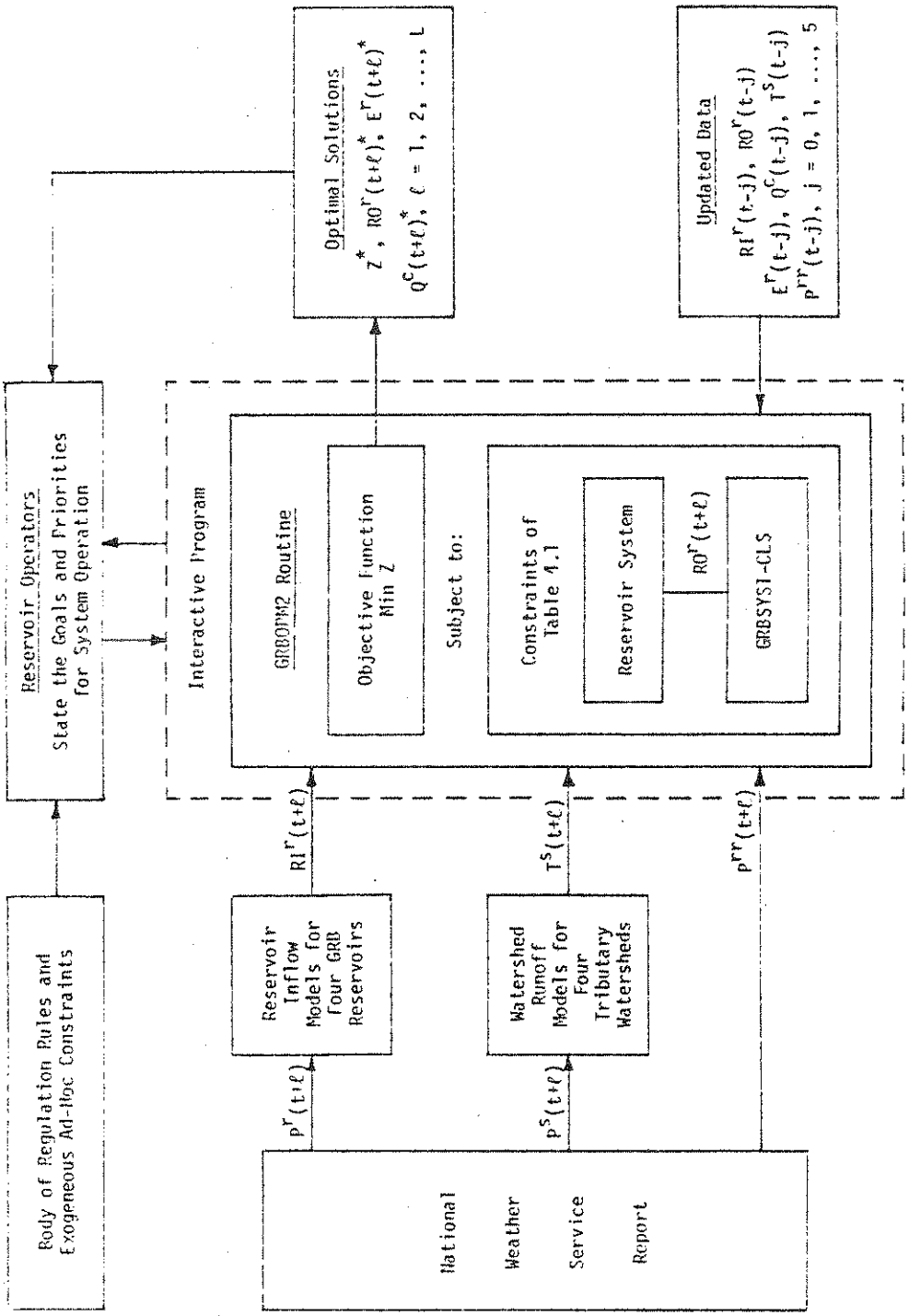

Figure 6.1 Real-Time Operation Use of GRBOPM2

Certain additions to the GRBOPM2 model could be made permitting more effective use in real-time operation. For example, the reservoir inflow forecast models for four GRB reservoirs have been developed already by Tao et al. (1975) and Rao et al. (1977). Recently, Staab and Rao (1979) have developed unit hydrograph models for the four tributary watersheds which may be used to forecast flows from those watersheds. These potential conditions are shown in Figure 6.1.

6.3 A SAMPLE RUN OF GRBOPM2 IN REAL-TIME OPERATIONS

A sample run of GRBOPM2 was made to illustrate its utility. The real-time use of the model requires inputs that are actual forecasts. Such data are not available for past years. In lieu of forecasted input data that would be available during field operations, the sample run was provided with historical data.

Table 6.1 shows the results of using GRBOPM2 with L=5 days for day t = 209 (April 29, 1970) of the 1970 water year. Since the period corresponds to the summer season, the penalty coefficients and zones for that season were used. The first set of output rows displays the water year and the days corresponding to the operating horizon, L, and the various units for flow, time, storage and elevation variables. The second set of rows displays the initialization data (for day 205 to day 209) for four reservoirs. These include reservoir inflows, reservoir elevations, and reservoir releases. The next set shows the one-day ahead (i.e. day 210) recommended release decisions as well as related systems state information. Similar information is shown in the next four sets pertaining to days 211, 212, 213, and 214.

These same outputs may also be displayed graphically as shown in Figures 6.2 through 6.4. These figures provide the reservoir operators with a good picture of what would happen in the basin during the operating horizon due to a given set of release decisions for a given set of forecasted inputs. This graphical representation facilitates the possible adjustments of the model parameters

Table 6.1 Sample Printed Output from GRBOPM2 in Real-Time Operations

```
**************
* G R B O S M *
**************
GREEN RIVER BASIN OPTIMIZATION - SIMULATION MODEL
WATER YEAR: 1970        DAYS: 210 THROUGH 214
FLOW UNIT: CFS    TIME UNIT: DAY    STORAGE UNIT: AC-FT    ELEV UNIT: FEET
```

UPDATED DATA DURING THE PREVIOUS 5 DAY PERIOD

		GREEN RESERVOIR			NOLIN RESERVOIR			BARREN RESERVOIR			ROUGH RESERVOIR		
DAY	IT	INFLOW	ELEV	REL	INFLOW	ELEV	REL	INFLOW	ELEV	REL	INFLOW	ELEV	REL
205	-4	893.	675.20	1180. *	867.	515.12	720. *	1500.	552.05	499. *	3808.	494.76	71. *
206	-3	2409.	675.39	1630. *	2782.	515.49	1690. *	1716.	552.29	509. *	9994.	498.46	101. *
207	-2	4040.	675.85	2140. *	4161.	515.95	2790. *	2687.	552.72	509. *	6100.	500.54	102. *
208	-1	2482.	675.93	2150. *	2760.	515.94	2790. *	2385.	553.09	495. *	1893.	501.14	102. *
209	0	1942.	675.88	2150. *	1493.	515.69	2240. *	2117.	553.40	522. *	1815.	501.54	607. *

1 - DAY AHEAD OPERATIONAL POLICY

DATE	RESERVOIR	INFLOW	RELEASE	STORAGE	ELEV	RULE CURVE STORAGE	RULE CURVE ELEV
210	GREEN	8152.0	750.0	263911.6	677.63	242046.9	675.0
210	NOLIN	4795.4	1723.3	180280.2	516.71	170145.2	515.0
210	BARREN	3433.4	132.0	278091.9	554.04	257419.7	552.0
210	ROUGH	9897.2	586.4	174199.5	504.49	119476.9	495.0

FLOW AT CONTROL AND TRIBUTARY STATIONS AT DAY 210

GRSBU	MUNF	BROWN	BOWL	WOOD	PARA	FALL	DUND	CALH	GRES	ALVA	GLEN	HORSE
2337.	6398.	7701.	2861.	14078.	13285.	1535.	2573.	17398.	3570.	2560.	578..	638.

2 - DAY AHEAD OPERATIONAL POLICY

DATE	RESERVOIR	INFLOW	RELEASE	STORAGE	ELEV	RULE CURVE STORAGE	RULE CURVE ELEV
211	GREEN	26408.5	150.0	315985.3	683.33	242046.9	675.0
211	NOLIN	10365.5	443.3	199961.0	519.84	170145.2	515.0
211	BARREN	4314.6	50.0	286550.7	554.84	257419.7	552.0
211	ROUGH	17165.1	100.0	208048.2	509.41	119476.9	495.0

FLOW AT CONTROL AND TRIBUTARY STATIONS AT DAY 211

GRSBU	MUNF	BROWN	BOWL	WOOD	PARA	FALL	DUND	CALH	GRES	ALVA	GLEN	HORSE
1504.	15529.	10705.	2898.	16274.	15911.	585.	3582.	18439.	5160.	2400.	51..	1920.

Table 6.1 (Continued)

3 - DAY AHEAD OPERATIONAL POLICY

DATE	RESERVOIR	INFLOW	RELEASE	STORAGE	ELEV	RULE CURVE STORAGE	RULE CURVE ELEV
212	GREEN	13223.5	2250.0	337761.2	685.52	242046.9	675.0
212	NOLIN	14145.6	50.0	227919.7	523.93	170145.2	515.0
212	BARREN	3516.6	50.0	280420.6	555.49	257419.7	552.0
212	ROUGH	5000.0	271.0	217428.1	510.68	119476.9	495.0

FLOW AT CONTROL AND TRIBUTARY STATIONS AT DAY 212

GRSBU	MUNF	BROWN	BOWL	WOOD	PARA	FALL	DUND	CALH	GRES	ALVA	GLEN	HORSE
1569.	13763.	16009.	2246.	17000.	17128.	317.	3007.	19554.	1520.	1760.	25..	1440.

4 - DAY AHEAD OPERATIONAL POLICY

DATE	RESERVOIR	INFLOW	RELEASE	STORAGE	ELEV	RULE CURVE STORAGE	RULE CURVE ELEV
213	GREEN	3275.6	3303.8	335515.0	685.40	242046.9	675.0
213	NOLIN	13247.0	50.0	254095.9	527.45	170145.2	515.0
213	BARREN	2585.4	800.0	296968.0	555.82	257419.7	552.0
213	ROUGH	1553.7	958.8	218608.1	510.84	119476.9	495.0

FLOW AT CONTROL AND TRIBUTARY STATIONS AT DAY 213

GRSBU	MUNF	BROWN	BOWL	WOOD	PARA	FALL	DUND	CALH	GRES	ALVA	GLEN	HORSE
3158.	4167.	13021.	1705.	18656.	17169.	813.	1846.	19374.	918.	1430.	17..	905.

5 - DAY AHEAD OPERATIONAL POLICY

DATE	RESERVOIR	INFLOW	RELEASE	STORAGE	ELEV	RULE CURVE STORAGE	RULE CURVE ELEV
214	GREEN	3052.5	2503.8	337603.3	685.51	242046.9	675.0
214	NOLIN	6874.1	1730.0	264299.4	528.75	170145.2	515.0
214	BARREN	4530.1	1550.0	302879.1	556.36	257419.7	552.0
214	ROUGH	1412.2	1108.9	219209.8	510.92	119476.9	495.0

FLOW AT CONTROL AND TRIBUTARY STATIONS AT DAY 214

GRSBU	MUNF	BROWN	BOWL	WOOD	PARA	FALL	DUND	CALH	GRES	ALVA	GLEN	HORSE
4000.	4239.	7940.	4130.	18908.	18876.	1200.	1921.	19966.	1470.	5730.	17..	420.

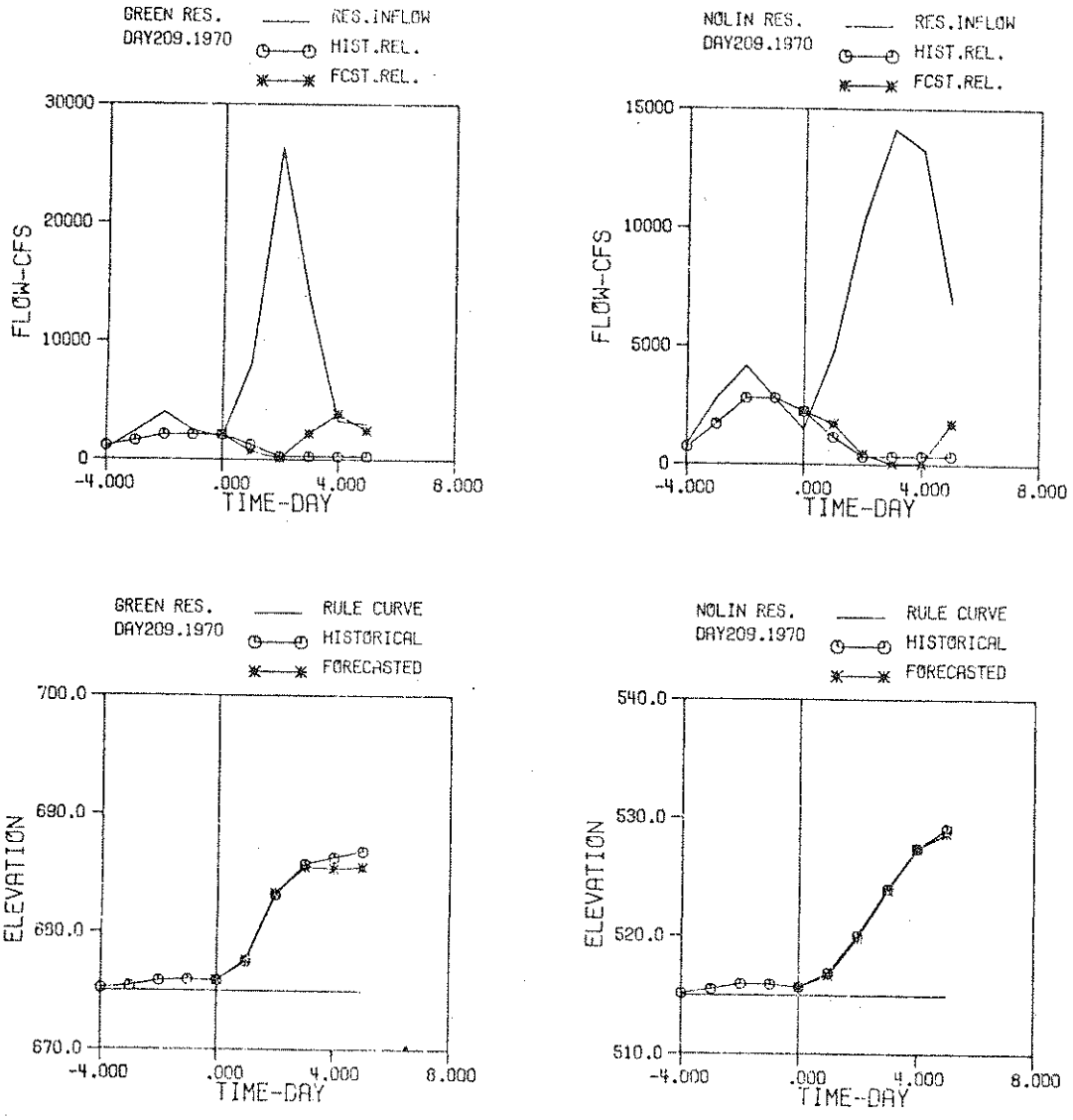

Figure 6.2 Comparison of Historical Data and Forecasted Results from the Use of GRBOPM2 in Real-Time Operations for Green and Nolin Reservoirs

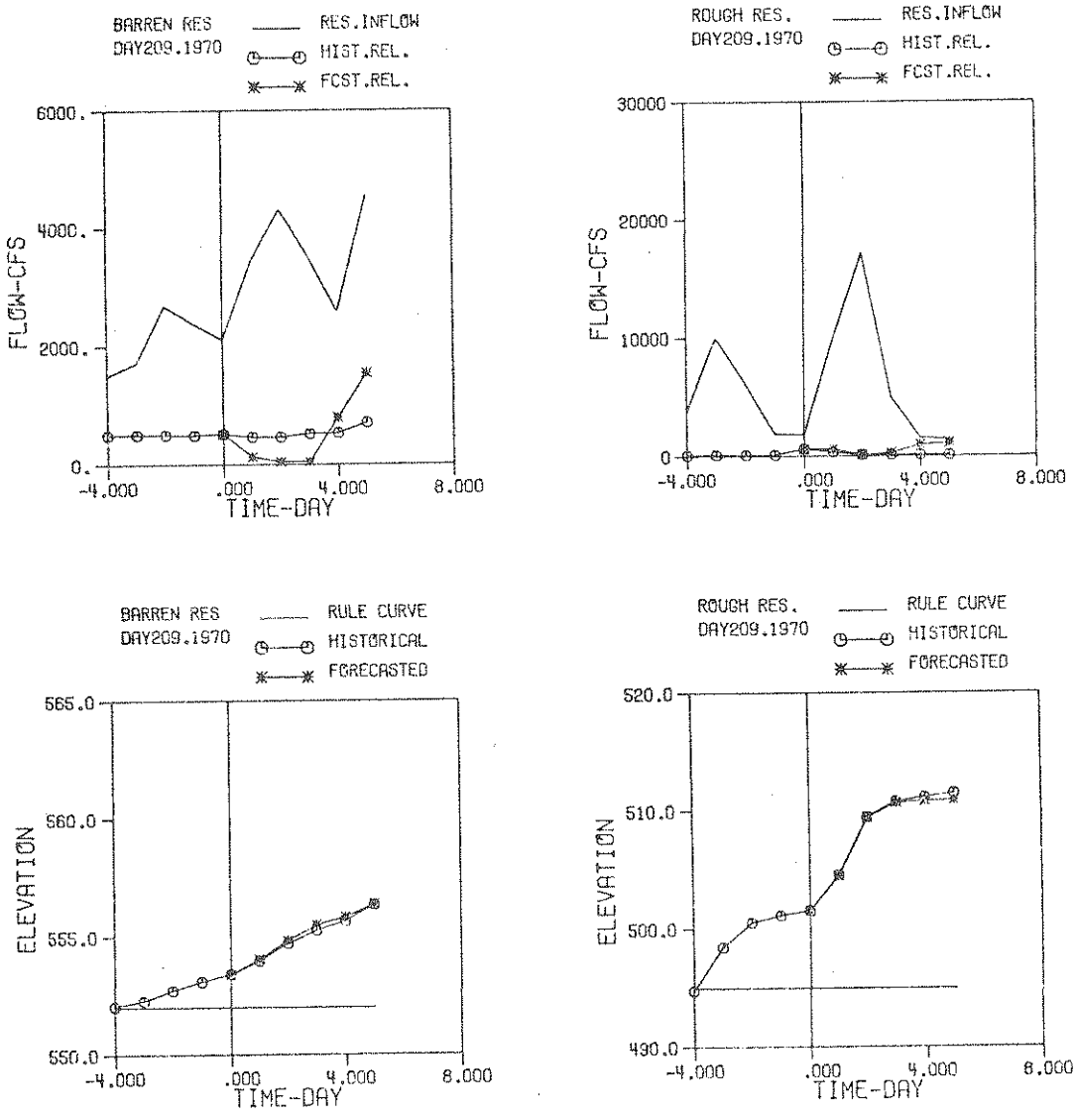

Figure 6.3 Comparison of Historical Data and Forecasted Results from the Use of GRBOPM2 in Real-Time Operations for Barren and Rough Reservoirs

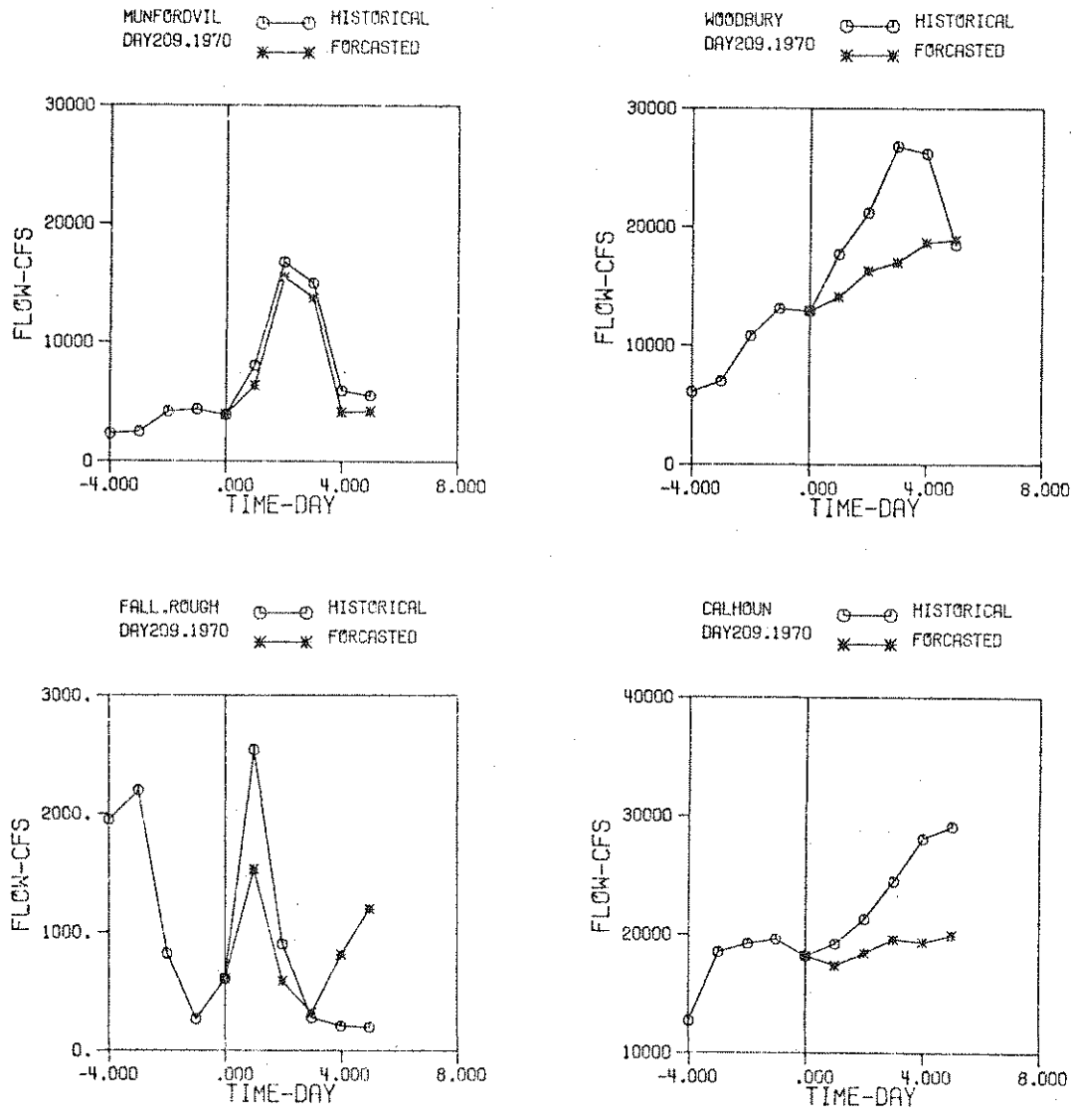

Figure 6.4. Comparison of Historical Data and Forecasted Results from the Use of GRBOPM2 in Real-Time Operations at Munfordville, Woodbury, Falls of Rough, and Calhoun

(i.e. penalty coefficients, zones, target levels, constraints, etc.). He can also vary some of the forecasted inputs to see how sensitive the release decisions are.

6.4 COMPARISON OF GRBOPM2 RESULTS WITH HISTORICAL OPERATION

The results from the sample run for t = 209 were compared with the historical operations. To that end the historical operations are also shown in Figures 6.2 through 6.4.

From the results for Green and Barren Reservoirs (Figures 6.2 and 6.3), it is evident that an unwritten rule was used in historical operations to minimize changes in gate settings and hence to keep release rates nearly constant. For Nolin and Rough Reservoirs, however, the forecasted releases agreed well with the historical data.

Figure 6.4 shows that the flood peaks were appreciably reduced at four of the control stations as compared to historical flood peaks. Similar results were found for the other control stations.

The aggregate penalty or the system's measure of effectiveness for the L-day operating horizon was estimated both for historical (Z^h) and model-recommended operations (Z^*). These were equal to $1.10050*10^7$ and $8.17865*10^6$ for historical and model-recommended operations, respectively. Thus, the use of GRBOPM2 provided a 25.7% reduction in the system's measure of effectiveness.

6.5 A SENSITIVITY ANALYSIS SAMPLE RUN

None of the forecasted hydrologic inputs is entirely certain. The sensitivity of model release recommendations to changes in one or more input-value for ℓ = 1, 2, 3, ..., L can be obtained by inputting a distribution of input values and computing recommended releases $RO^r(t+\ell)^*$ for each input set. For example, one might increase precipitation and/or reservoir inflows by say +10% and/or -10% and obtain the $\Delta RO^r(t+\ell)^*$s.

By way of example, consider the GRBOPM2 run for t = 209 of 1970 water year presented in Section 6.3. The precipitation inputs for the middle and lower reaches (3, 5, 6, and 9) and for ℓ = 1, 2, 3, ..., L are shown in Table 6.2. After changing each of the four precipitation inputs for t = 211 or ℓ = 2 to 2.0", the model was rerun (at t = 209). The results are shown in Table 6.3 and Figures 6.5 through 6.7.

Table 6.2 Precipitation (Inches Per Day) Over the Reaches 3, 5, 6, and 9 During Days 210 Through 214 of 1970 Water Year

Reach No.	Days				
	210	211	212	213	214
3	0.745	0.185	0.000	0.130	0.983
5	0.088	0.102	0.435	0.003	0.013
6	0.347	0.020	0.543	0.000	0.005
9	0.448	0.062	0.000	0.006	0.211

By comparing these results with those of the previous run (Table 6.1 and Figures 6.2 through 6.4), it is seen that the model-recommended releases from Green and Barren reservoirs remain unchanged. However, the recommended releases from Nolin reservoir were reduced for t = 210 and t = 211; the release from Rough reservoir was reduced for t = 212, 213, and 214. The degree of change in recommended reservoir release can be obtained conveniently from the Tables 6.1 and 6.3.

The two inches of rainfall over the reaches 3, 5, 6, and 9 increased the flood peaks at Brownsville, Woodbury, Paradise, and Calhoun. These control stations are located at the output nodes of the reaches 3, 5, 6, and 9 (Table 3.1). The increases in flood peaks as compared to those of the previous run (defined by Table 6.1) were approximately 5,000 [cfs] for Brownsville, 14,000 [cfs] for Woodbury and 17,000 [cfs] for Paradise as well as Calhoun. However, the lower boundaries of the uppermost flow zones (UQ_3 in Table 5.4) at which no flood

Table 6.3 Sample Printed Output from GRBOPM2 for Sensitivity Analysis Studies in Real-Time Operations

```
**************
* G R B O S M *
**************
GREEN RIVER BASIN OPTIMIZATION - SIMULATION MODEL
WATER YEAR: 1970        DAYS: 210 THROUGH 214
FLOW UNIT: CFS    TIME UNIT: DAY    STORAGE UNIT: AC-FT    ELEV UNIT: FEET
```

UPDATED DATA DURING THE PREVIOUS 5 DAY PERIOD

		GREEN RESERVOIR				NOLIN RESERVOIR				BARREN RESERVOIR				ROUGH RESERVOIR			
DAY	IT	INFLOW	ELEV	REL	*	INFLOW	ELEV	REL	*	INFLOW	ELEV	REL	*	INFLOW	ELEV	REL	*
205	-4	893.	675.20	1180.	*	867.	515.12	720.	*	1500.	552.05	499.	*	3808.	494.76	71.	*
206	-3	2409.	675.39	1630.	*	2782.	515.49	1690.	*	1716.	552.29	509.	*	9894.	498.46	101.	*
207	-2	4040.	675.65	2140.	*	4161.	515.95	2790.	*	2687.	552.72	509.	*	6100.	500.54	102.	*
208	-1	2482.	675.93	2150.	*	2760.	515.94	2790.	*	2385.	553.09	495.	*	1893.	501.14	102.	*
209	0	1942.	675.88	2150.	*	1493.	515.69	2240.	*	2117.	553.40	522.	*	1815.	501.54	607.	*

1 - DAY AHEAD OPERATIONAL POLICY

DATE	RESERVOIR	INFLOW	RELEASE	STORAGE	ELEV	RULE CURVE STORAGE	RULE CURVE ELEV
210	GREEN	8152.0	750.0	263811.6	677.63	242046.9	675.0
210	NOLIN	4735.4	930.0	181794.2	516.96	170145.2	515.0
210	BARREN	3423.4	132.0	278091.9	554.04	257419.7	552.0
210	ROUGH	8897.2	586.4	174199.5	504.49	113476.9	495.0

FLOW AT CONTROL AND TRIBUTARY STATIONS AT DAY 210

GRSBU	MUNF	BROWN	BOWL	WOOD	PARA	FALL	DUND	CALH	GRES	ALVA	GLEN	HORSE
2337.	6398.	7146.	2861.	14059.	13283.	1535.	2573.	17397.	3570.	2560.	578.	638.

2 - DAY AHEAD OPERATIONAL POLICY

DATE	RESERVOIR	INFLOW	RELEASE	STORAGE	ELEV	RULE CURVE STORAGE	RULE CURVE ELEV
211	GREEN	26408.5	150.0	315995.3	683.33	242046.9	675.0
211	NOLIN	10365.5	50.0	202255.0	520.19	170145.2	515.0
211	BARREN	4314.6	50.0	286550.7	554.84	257419.7	552.0
211	ROUGH	17165.1	100.0	208048.2	509.41	113476.9	495.0

FLOW AT CONTROL AND TRIBUTARY STATIONS AT DAY 211

GRSBU	MUNF	BROWN	BOWL	WOOD	PARA	FALL	DUND	CALH	GRES	ALVA	GLEN	HORSE
1504.	15529.	14140.	2898.	24431.	16535.	585.	3582.	22771.	5160.	2400.	51.	1920.

Table 6.3 (Continued)

3 - DAY AHEAD OPERATIONAL POLICY

DATE	RESERVOIR	INFLOW	RELEASE	STORAGE	ELEV	RULE CURVE STORAGE	RULE CURVE ELEV
212	GREEN	13223.5	2250.0	337761.2	685.52	242046.9	675.0
212	NOLIN	14145.6	50.0	230213.7	524.25	170145.2	515.0
212	BARREN	3516.6	50.0	293426.6	555.49	257419.7	552.0
212	ROUGH	5000.0	50.0	217866.5	510.74	119476.9	495.0

FLOW AT CONTROL AND TRIBUTARY STATIONS AT DAY 212

GRSBU	MUNF	BROWN	BOWL	WOOD	PARA	FALL	DUND	CALH	GRES	ALVA	GLEN	HORSE
1569.	13763.	21000.	2246.	31058.	34517.	149.	2957.	29383.	1520.	1760.	25..	1440.

4 - DAY AHEAD OPERATIONAL POLICY

DATE	RESERVOIR	INFLOW	RELEASE	STORAGE	ELEV	RULE CURVE STORAGE	RULE CURVE ELEV
213	GREEN	3275.6	3903.8	336515.0	685.40	242046.9	675.0
213	NOLIN	13247.0	50.0	256390.0	527.74	170145.2	515.0
213	BARREN	2585.4	800.0	296968.0	555.82	257419.7	552.0
213	ROUGH	1553.7	50.0	220849.1	511.13	119476.9	495.0

FLOW AT CONTROL AND TRIBUTARY STATIONS AT DAY 213

GRSBU	MUNF	BROWN	BOWL	WOOD	PARA	FALL	DUND	CALH	GRES	ALVA	GLEN	HORSE
3158.	4167.	13021.	1705.	23472.	34319.	67.	1524.	36460.	918.	1430.	17..	905.

5 - DAY AHEAD OPERATIONAL POLICY

DATE	RESERVOIR	INFLOW	RELEASE	STORAGE	ELEV	RULE CURVE STORAGE	RULE CURVE ELEV
214	GREEN	3052.5	2503.8	337603.3	685.51	242046.9	675.0
214	NOLIN	6874.1	1730.0	236593.4	529.04	170145.2	515.0
214	BARREN	4530.1	1550.0	302879.1	556.36	257419.7	552.0
214	ROUGH	1412.2	810.0	222043.6	511.29	119476.9	495.0

FLOW AT CONTROL AND TRIBUTARY STATIONS AT DAY 214

GRSBU	MUNF	BROWN	BOWL	WOOD	PARA	FALL	DUND	CALH	GRES	ALVA	GLEN	HORSE
4000.	4239.	7940.	4130.	18908.	23113.	757.	1333.	32950.	1470.	5730.	17..	420.

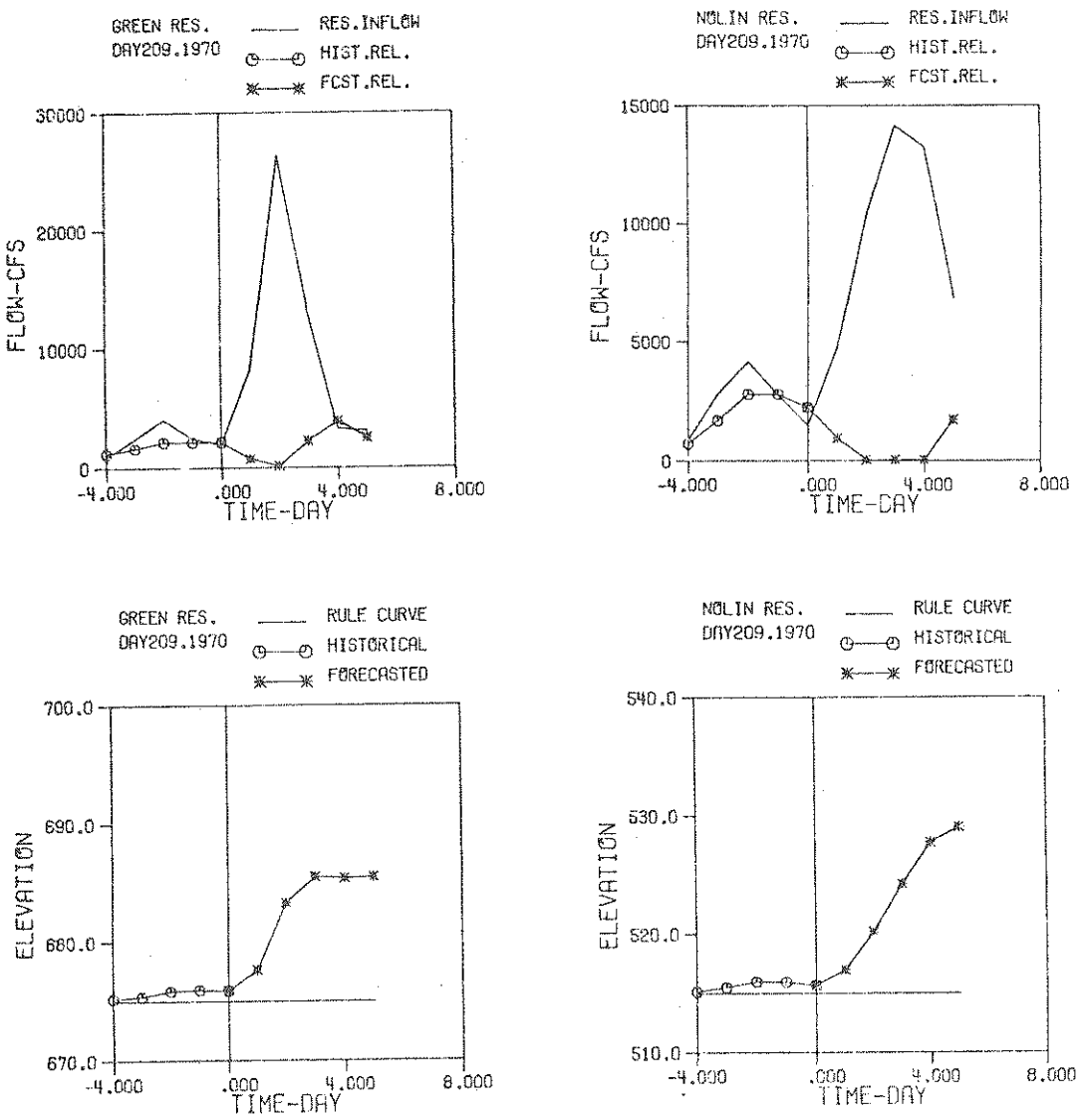

Figure 6.5 Results From the Use of GRBOPM2 for Sensitivity Analysis Studies in Real-Time Operations for Green and Nolin Reservoirs

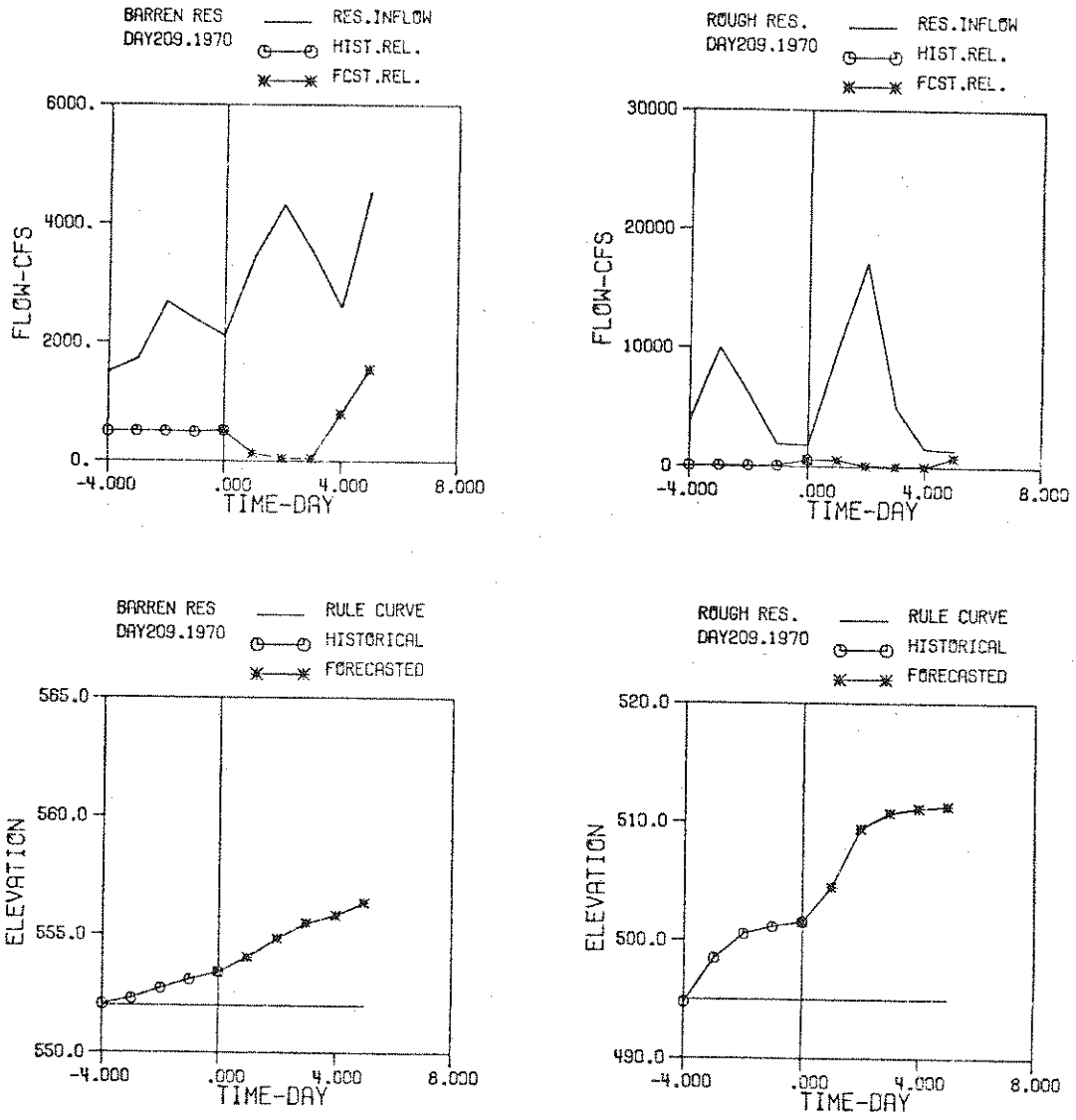

Figure 6.6 Results From the Use of GRBOPM2 for Sensitivity Analysis Studies in Real-Time Operations for Barren and Rough Reservoirs

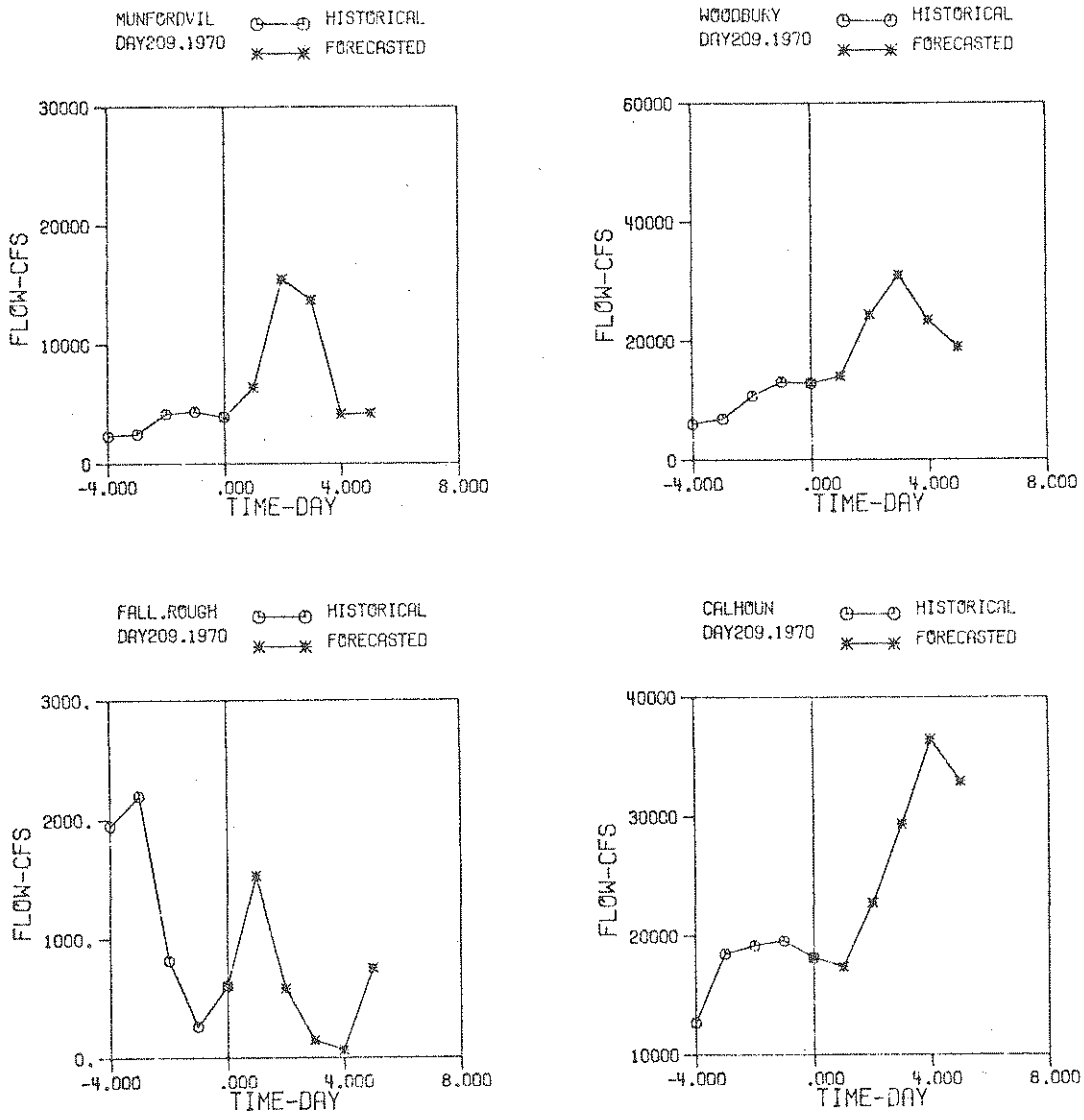

Figure 6.7 Results From the Use of GRBOPM2 for Sensitivity Analysis Studies in Real-Time Operations at Munfordville, Woodbury, Falls of Rough, and Calhoun

damages occur, were exceeded only at Woodbury (at t = 212). The two inches of rainfall over the reaches 3, 5, 6, and 9 increased the total penalty by 45.7% as compared to those of the previous run.

VII. SUMMARY, CONCLUSIONS, AND RECOMMENDATIONS

7.1 SUMMARY AND CONCLUSIONS

The study reported herein is concerned with the optimal operation of an existing multipurpose multireservoir system with a view toward making the best possible use of forecast data and operations research techniques. The system consists of four flood control reservoirs in the Green River Basin, Kentucky, having recreation and low-flow augmentation as secondary objectives. This reservoir system is operated by the U. S. Army Corps of Engineers via the Lousville District's Reservoir Regulation Section.

The operation of complex reservoir systems requires models which have descriptive as well as prescriptive or policy components. The descriptive component relates the state of the system to a given set of release decisions and a number of uncontrolled flows. The prescriptive component, on the other hand, specifies what decisions are to be made such that the system is operated optimally within a set of given constraints. To that end, an optimization-simulation model, herein called GRBOPM2, was developed. Its descriptive component consists of a segmented model comprising nine multi-input linear (MIL) models of the river system downstream of the reservoirs. The prescriptive component employs a mathematical programming model in the form of a Linear Program.

7.1.1 Descriptive Component

Each of the nine components of the segmented model represents a routing model for a reach between control stations. Each reach and the watershed producing side inflow to the reach were modeled as a multi-input linear (MIL) model having reach inflow, precipitation, and tributary inflows as model inputs and the reach's outflow as model output. The parameters of each MIL model were estimated by two different methods. The first was an ordinary least squares (OLS) method in which the parameters were not subject to any constraints. By

using the second method, namely constrained linear systems (CLS) method, the model parameters were estimated subject to nonnegativity and mass balance constraints. The resulting reach models when placed in series constitute the overall segmented models called GRBSYS1-OLS and GRBSYS1-CLS, respectively.

GRBSYS1-OLS and GRBSYS1-CLS models were used to estimate the flows or the state of the system at the control stations for a given set of reservoir releases, tributary inflows, and reach precipitation during a set operating horizon. The following results were obtained and conclusions are drawn:

(1) The GRBSYS1-OLS model produced biased forecasts. Dry season flows were overpredicted and wet season flows were underpredicted.

(2) The GRBSYS1-CLS model reduced the bias in forecasts and improved the accuracy of the forecasts.

(3) The residual time series for models whose parameters were estimated by both OLS and the CLS methods were correlated. Consequently, models of residuals obtained by the CLS method were developed to extract the information still present in the residuals. The error models fitted to the residual sequences were then combined with the MIL models whose parameters were estimated by the CLS method to derive another segmented model called GRBSYS2. The GRBSYS2 model further reduced the bias in forecasts and it predicted flows better than GRBSYS1-CLS.

7.1.2 Prescriptive Component

The development of the operation policy component involved an investigation of goals and priorities for reservoir operation. To that end the system's state variables at the reservoirs and at the control stations were divided into time-varying target or ideal values or ranges. The components of the ideal systems state vector included: (1) four target elevations of reservoir levels, (2) nine target flows at control stations in the system, and (3) four sets of target values which the rates-of-change of reservoir releases should not

exceed. Deviations from the ideal state vector were then divided into various magnitude classes, called "zones"; different penalties were associated with different zones. By aggregating these penalties over an operating horizon, most of the goals of and priorities for reservoir operation were commensurated into an overall systems effectiveness measure. This measure proved useful in the conduct of special reservoir operations studies as well as the study of real-time operations simulations.

The GRBOPM2 model was constructed such that penalty weights and zones could be changed readily, if need be at the beginning of each new time step.

In special reservoir operations studies, the GRBOPM2 model was used to study the system responses under various operating and hydrologic conditions. The trade-off curves between various systems objectives were generated for the winter as well as the summer seasons. These results were obtained for both historical hydrologic data as well as synthetic model input data. In these investigations the model has proved to be very effective in assessing the impact of alternative policies of operation during various seasons of the year.

Secondly, the use of GRBOPM2 in the (simulation of) real-time operations was studied. The availability of forecasted data and their importance in real-time operations were recognized early in the study. Hence the GRBOPM2 was constructed such that it accepts forecasted data available for an operating horizon. Using those data, GRBOPM2 yields recommended optimal release decisions, and associated optimal reservoir elevations, and flows at the control stations throughout the operating horizon. The sensitivity of model recommended release decisions to changes in various forecasted input values was illustrated by performing a sample run. The results indicate that the model has considerable promise as an operational tool to aid in real-time operation of the GRB reservoir system.

In terms of methodology, model use, and development, the following conclusions are drawn:

(1) The linear descriptive models that are part GRBOPM2 appear to be adequately accurate to make the use of a formal optimization model (the prescriptive component of GRBOPM2) meaningful. Their linearity permits the use of linear programming.

(2) The built-in model allows the examination of the operation of a complex reservoir-river system for a variety of operational policies.

(3) Model inputs were selected so as to be limited to readily available data. For example, only normally available forecast information is used.

(4) The model results have been represented in the form of trade-off curves that promote insight into obtained results. In addition the short-run results are represented in an integrated set of graphs that appear to be useful in eventual field application of GRBOPM2.

(5) The methodology presented herein appears readily extendable to any existing system of reservoirs and interconnecting river channels.

7.2 RECOMMENDATIONS

It is recommended that:

(1) The GRBOPM2 model be field-tested by the Corps of Engineers.

(2) The four reservoir inflow models and the four tributary watershed models be made part of GRBOPM2.

(3) That more general synthetic inflow studies be made after investigating the temporal and spatial distribution characteristics of those inflows.

(4) The procedures and methodology presented herein may be applied fruitfully to other reservoir systems.

VIII. LIST OF REFERENCES

1. Abadie, J., Integer and Nonlinear Programming, North-Holland, Amsterdam, 1970.

2. Bard, Y., Nonlinear Parameter Estimation, Academic Press, Inc., New York, 1974.

3. Beard, L. R., "Functional Evaluation of a Water Resources System," Conference on Water for Peace, Washington, DC, May 28-31, 1967.

4. Beard, L. R., "Hydrologic Engineering Methods for Water Resources Development, Vol. 5, Hypothetical Floods," Corps of Engineers, U. S. Army, The Hydrologic Engineering Center, Davis, California, March 1975.

5. Boneh, A., and Golan, A., "Instantaneous Unit Hydrograph with Negative Ordinates-Possible?", Water Resources Research, Vol. 15, No. 1, February 1979.

6. Box, G. E. P., and Jenkins, G. M., Time Series Analysis: Forecasting and Control, Holden-Day, San Francisco, 1970.

7. Chang, T. P., and Toebes, G. H., "Operating Policies for the Upper Wabash Surface Water System," Technical Report No. 31, Purdue University Water Resources Research Center, December 1972.

8. Chang, T. P., and Toebes, G. H., "Initial Results from the Upper Wabash Simulation Model," Technical Report No. 33, Purdue University Water Resources Research Center, March 1973.

9. COE, "Green River Basin Reservoir Regulation Plan: Master Manual and Four Appendicies (A for Rough, B for Nolin, C for Barren, D for Green River Reservoirs)," Corps of Engineers-Louisville District, U. S. Army, February 1967.

10. Eagleson, P. S., Mejia, R., and March, F., "The Computation of Optimum Realizable Unit Hydrographs from Rainfall and Runoff Data," Report No. 84, MIT Hydrodynamics Laboratory, 1965.

11. Ford, D. T., "Optimization Model for the Evaluation of Flood-Control Benefits of Multipurpose Multireservoir Systems," Technical Report CRWR-158, Center for Research in Water Resources, University of Texas, Austin, Texas, May 1978.

12. Katz, P. G., and Toebes, G. H., "Green River Basin Flow Forecasting Models," Technical Report No. 136, Purdue University Water Resources Research Center, October 1980.

13. Marsten, R. E., "The Design of the XMP Linear Programming Library," MIS Technical Report No. 80-2, Department of Management Information Systems, University of Arizona, Tucson, Arizona, 1980.

14. Natale, L., and Todini, E., "A Constrained Parameter Estimation Technique for Linear Models in Hydrology," Pub. No. 13, Institute of Hydraulics, University of Pavia, Pavia, Italy, 1974.

15. Natale, L., and Todini, E., "A Stable Estimator for Linear Models 1. Theoretical Development and Monte Carlo Experiments," Water Resources Research, Vol. 12, No. 4, August 1976.

16. Phillips, D. T., Ravindran, A., and Solberg, J. J., Operations Research: Principles and Practice, John Wiley & Sons, 1976.

17. Rao, A. R., Rukvichai, C., and Tao, P. C., "Stochastic Forecasting Models of Reservoir Inflows for Daily Operation III. Models for Nolin, Barren and Green Reservoir Inflows," Hydromechanics Report CE-HYD-77-1, School of Civil Engineering, Purdue University, April 1977.

18. Rukvichai, C., "Operating Model for the Green River Basin Reservoir System," Ph.D. Thesis, Purdue University, August 1977.

19. Sigvaldason, O. T., "A Simulation Model for Operating a Multipurpose Multireservoir System," Water Resources Research, Vol. 12, No. 2, April 1976.

20. Staab, G. E., and Rao, A. R., "Hydrograph Analysis and Testing A Runoff Simulation Model for Karst Watersheds," Hydraulic and Systems Engineering Report CE-HSE-79-2, School of Civil Engineering, Purdue University, 1979.

21. Stevens, S., Rao, A. R., Toebes, G. H., and Chassiakos, A., "Green River Data Base System," Hydraulic and Systems Engineering Report CE-HSE-78-2, School of Civil Engineering, Purdue University, 1978.

22. Tao, P. C., Rao, A. R., and Rukvichai, C., "Stochasting Forecasting Models of Reservoir Inflows for Daily Operation I. Model Development and Application to Rough River Reservoir Inflows," Hydromechanics Report CE-HYD-75-8, School of Civil Engineering, Purdue University, August 1975.

23. Todini, E., and Wallis, J. K., "Using CLS for Daily or Longer Period Rainfall-Runoff Modeling," In: Mathematical Models for Surface Hydrology. Wiley, New York, N.Y., pp. 149-168, 1977.

24. Toebes, G. H., and Rukvichai, C., and Lin, Y. S., "Operating Policy Simulation for a Reservoir System," Technical Report No. 80, Purdue University Water Resources Research Center, August 1976.

25. Toebes, G. H., and Rukvichai, C., "Reservoir System Operating Policy-Case Study," Journal of the Water Resources Planning and Management Division, ASCE, Vol. 104, No. WR1, Proc. Paper 14167, November 1978, pp. 175-191.

26. Yazicigil, H., Rao, A. R., and Toebes, G. H., "The Green River Basin Routing Model," Hydraulic and Systems Engineering Report CE-HSE-79-1, School of Civil Engineering, Purdue University, 1979.

APPENDIX A

REGULATION SCHEDULES FOR GREEN RIVER BASIN RESERVOIRS

GREEN RIVER RESERVOIR

SCHEDULE OF REGULATION

FLOOD CONTROL AND LOW FLOW REGULATION

Schedule	Controlling Stages (feet) Ohio River Evansville	Green River Lock 2, Upper Gage	Green River Lock 4, Upper Gage	Range in Pool Elevation (feet)	Time of Year	Regulation
	(All stages must exist)					
A	Below 37 or Below 46F	Below 19 or Below 29 F	Below 17 or Below 22 F	Water Quality Pool (664) - Minimum Pool (653)	1 December - 14 March	Maintain Water Quality Pool as near as possible provided release indicated in Maximum Release table is not exceeded; and outflows are never less than 150 c.f.s.
B	Same as Schedule A			664 - Spillway Crest (713) 653 - 713	1 December - 14 March 15 March - 30 November	Release at rate indicated in Maximum Release table. Maintain pool as near Rule Curve as possible while meeting minimum flow and flood control requirements.
	(Any one condition to exist for application of Schedule C)					
C	At or above 37R or 7 days before 42	At or above 19R or 6 days before 23	At or above 17R	653 - 664 664 - 713	All year 1 December - 14 March 15 March - 30 November	Release at constant rate of 150 c.f.s. Release at constant rate of 300 c.f.s. When below Rule Curve release 150 c.f.s. When at or above Rule Curve release 300 c.f.s.
D	Control stations no longer considered			At 713 and above	All year	Release inflow up to capacity of conduit. If pool exceeds elevation 713 keep conduit open until pool returns to elevation 713. Maintain pool at elevation 713 by passing inflow until downstream conditions permit return to Schedule B. (At such a time the Reservoir Regulation Section will evaluate weather and river conditions to determine feasibility of releasing on recession of downstream stages to regain storage capacity for possible storm recurrence.)

MAXIMUM RELEASE

Gresham (Stage in feet)	Allowable Release (c.f.s.)
Below 10.0	~~8,000~~ 6000
10.0 - 11.0	~~7,000~~ 5000
11.0 - 12.0	~~5,500~~ 4000
12.0 - 13.0	~~4,000~~
13.0 - 14.0	~~2,500~~ 3000
14.0 - 15.0	~~1,000~~ 2000
Above 15.0	~~300~~ 1000
	300

MINIMUM LOW FLOW RELEASE

150 c.f.s.

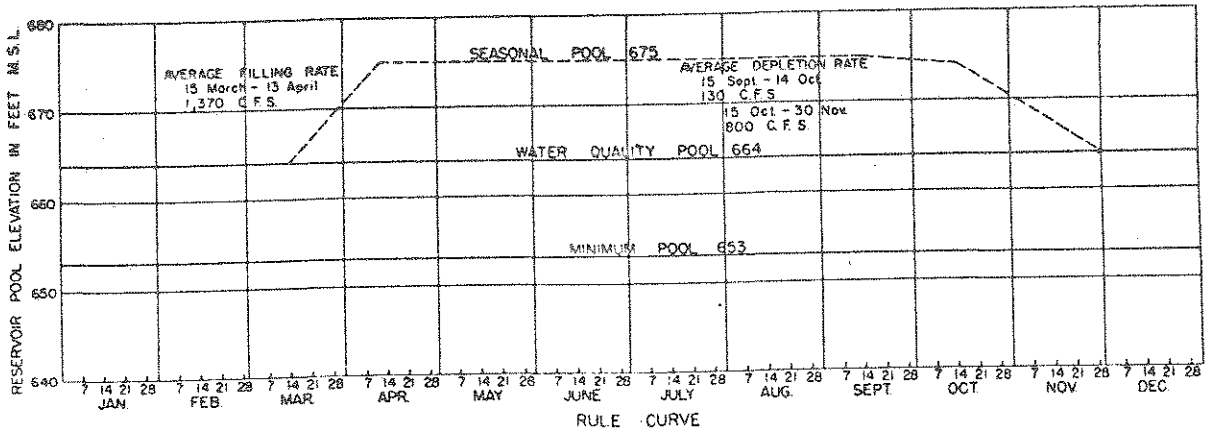

NOLIN RIVER RESERVOIR

SCHEDULE OF REGULATION

FLOOD CONTROL AND LOW FLOW REGULATION

Schedule	Controlling Stages (feet) Ohio River Evansville	Green River Lock 2, Upper Gage	Green River Lock 4, Upper Gage	Range in Pool Elevation (feet)	Time of Year	Regulation
	(All stages must exist)			490		
A	Below 37 or Below 46F	Below 19 or Below 29F	Below 17 or Below 22F	Minimum Pool, ~~480~~	1 December - 14 March	Release inflow necessary to maintain pool, provided release indicated in Maximum Release table is not exceeded.
B	——— Same as Schedule A ———			490 ~~480~~ - Spillway Crest (560)	1 December - 14 March	Release at rate indicated in Maximum Release table.
					15 March - 30 November	Maintain pool as near Rule Curve as possible while meeting minimum flow and flood control requirements.
	(Any one condition to exist for application of Schedule C)			490		
C	At or above 37R or 5 days before 42	At or above 19R or 4 days before 23	At or above 17R	~~480~~ - 550	1 December - 14 March 15 March - 30 November	Release at a constant rate of 300 c.f.s. Release at a constant rate of 300 c.f.s. when pool is at or above elevations prescribed by Rule Curve. When below elevation prescribed by Rule Curve, release only the minimum requirement of 50 c.f.s.
D	——— Same as Schedule C ———			550 - 560	All year	Release all inflow provided release indicated in Maximum Release table is not exceeded and outflows are never reduced to less than 300 c.f.s.
E	Control stations no longer considered			At 560 and above	All year	Release inflow up to capacity of conduit. If pool exceeds elevation 560 keep conduit open until pool returns to elevation 560. Maintain pool at elevation 560 by passing inflow until downstream conditions permit return to Schedule B. (At such times, the Reservoir Regulation Section will evaluate weather and river conditions to determine feasibility of releasing on recession of downstream stages to regain storage capacity for possible storm recurrence.)

MAXIMUM RELEASE

Munfordville Stage (feet)	Release (c.f.s.)
Below 20.0	10,000
20.0 - 22.0	8,000
22.0 - 24.0	6,100
24.0 - 26.0	4,200
26.0 - 28.0	2,100
Above 28.0	300

MINIMUM LOW FLOW RELEASE

50 c.f.s.

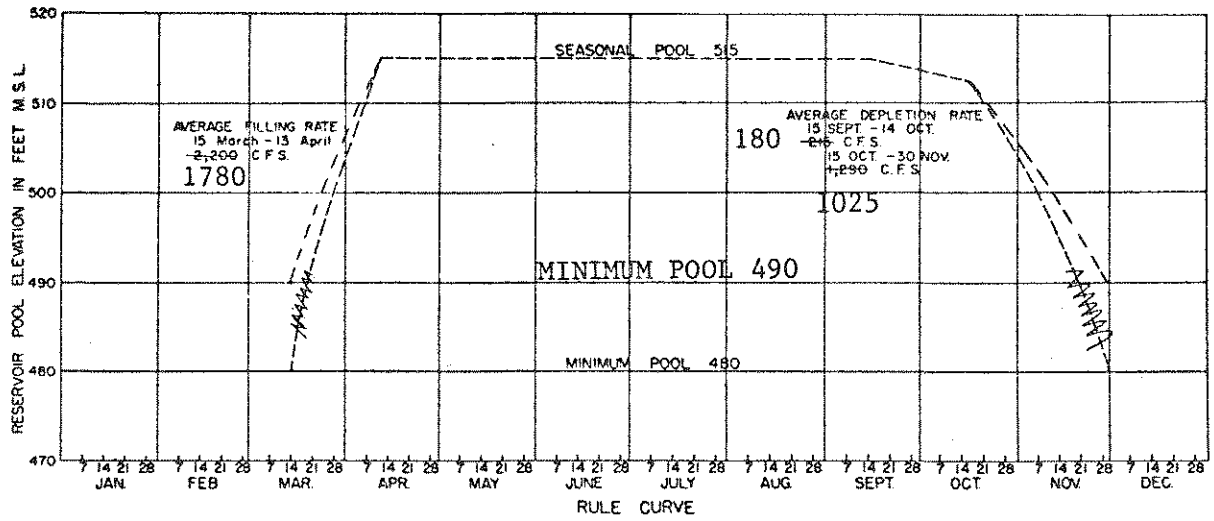

BARREN RIVER RESERVOIR

SCHEDULE OF REGULATION

FLOOD CONTROL AND LOW FLOW REGULATION

Schedule	Controlling Stages (feet): Ohio River Evansville	Green River Lock 2, Upper Gage	Green River Lock 4, Upper Gage	Range in Pool Elevation (feet)	Time of Year	Regulation
	(All stages must exist)			525		
A	Below 37 or Below 46F	Below 19 or Below 29F	Below 17 or Below 22F	Minimum Pool (~~520~~)	1 December - 14 March	Release inflow necessary to maintain pool, provided release indicated in Maximum Release table is not exceeded.
B	Same as Schedule A			525 ~~520~~ - Spillway Crest (590)	1 December - 14 March 15 March - 30 November	Release at rate indicated in Maximum Release table. Maintain pool as near Rule Curve as possible while meeting minimum flow and flood control requirements.
	(Any one condition to exist for application of Schedule C)			525		
C	At or above 37R or 6 days before 42	At or above 19R or 5 days before 23	At or above 17R	~~520~~ - 590	1 December - 14 March 15 March - 30 November	Release at a constant rate of 300 c.f.s. Release at a constant rate of 300 c.f.s. when pool is at or above elevation prescribed by Rule Curve. When below elevation prescribed by Rule Curve release only the minimum requirement of 50 c.f.s.
D	Control stations no longer considered			At 590 and above	All year	Release inflow up to capacity of conduit. If pool exceeds elevation 590 keep conduit open until pool returns to elevation 590. Maintain pool at elevation 590 by passing inflow until downstream conditions permit return to Schedule B. (At such a time the Reservoir Regulation Section will evaluate weather and river conditions to determine feasibility of releasing on recession of downstream stages to regain storage capacity for possible storm recurrence.)

MAXIMUM RELEASE

Elevation (Stage in Feet)	Allowable Release (c.f.s.) December thru March		April thru November	
Below 16.0	4000	~~6,000~~	~~4,000~~	3200
16.0 - 17.0	3250	~~5,500~~	~~3,500~~	2500
17.0 - 18.0	2750	~~4,500~~ ~~3,500~~	~~3,000~~ ~~2,500~~	2000
18.0 - 19.0	2250	~~2,500~~ 1,500	~~1,500~~ ~~1,000~~	1500
19.0 - 20.0	1750		700	1000
20.0 - 21.0	1000			500
21.0 - 22.0	300			300
Above 22.0	300			300

MINIMUM LOW FLOW RELEASE

50 c.f.s.

MINIMUM LOW FLOW OBJECTIVE

Bowling Green . 100 c.f.s.

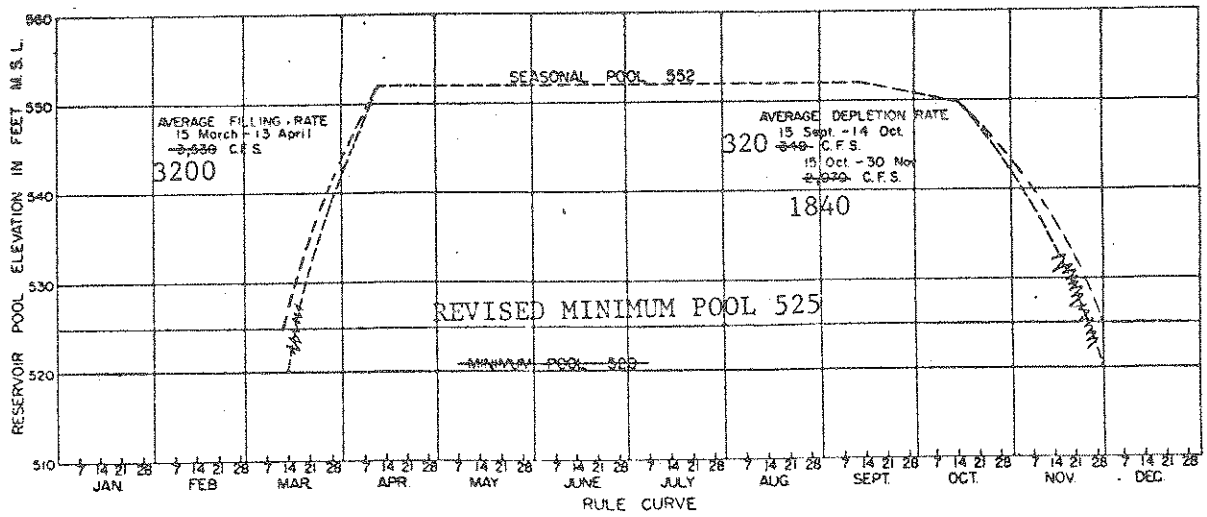

ROUGH RIVER RESERVOIR

SCHEDULE OF REGULATION

FLOOD CONTROL AND LOW FLOW REGULATION

Schedule	Controlling Stages (feet): Ohio River Evansville	Green River Lock 2, Upper Gage	Green River Lock 4, Upper Gage	Range in Pool Elevation (feet)	Time of Year	Regulation
	(All stages must exist)					
A	Below 37 or Below 46F	Below 19 or Below 29F	Below 17 or Below 22F	Minimum Pool, ~~465~~ 470	1 December - 14 March	Release inflow necessary to maintain pool, provided release indicated in Maximum Release table is not exceeded.
B	Same as in Schedule A			~~465.0~~ 470 - Spillway Crest (524)	1 December - 14 March	Release at rate indicated in Maximum Release table.
					15 March - 30 November	Maintain pool as near rule curve as possible while meeting minimum flow and flood control requirements.
	(Any one condition to exist for application of Schedule C)					
C	At or above 37R or 3 days before 42	At or above 19R or 2 days before 23	At or above 17R	~~465~~ 470 - 514	1 December - 14 March 15 March - 30 November	Release at a constant rate of 100 c.f.s. Release at a constant rate of 100 c.f.s. when pool is at or above elevations prescribed by Rule Curve. When below elevation prescribed by rule curve release only the minimum requirement of 50 c.f.s.
D	Same as Schedule C			514 - 524	All year	When precipitation forecasts indicate need to retain storage capacity for local Rough River control, pass inflow only, up to a rate indicated in Maximum Release table. However, unless a regulation based on such a forecast can prevent significant damages in Rough River, regulate so as not to increase flood crests on Green or Ohio Rivers, subject only to releasing at a minimum rate of 100 c.f.s.
E	Control stations no longer considered			At 524 and above	All year	Release inflow up to capacity of conduit. If pool exceeds elevation 524 keep conduit open until pool returns to elevation 524. Maintain pool at elevation 524 by passing inflow until downstream conditions permit return to Schedule B. (At such a time, the Reservoir Regulation Section will evaluate weather and river conditions to determine feasibility of releasing on recession of downstream stages to regain storage capacity for possible storm recurrence.)

MAXIMUM RELEASE

Combined Flow Glen Dean and Horse Branch c.f.s.		Allowable Release c.f.s.*	
~~Below 100~~	Below 100	~~1,000~~	2,000
~~100-200~~	100-200	~~2,800~~	1,800
~~200-300~~	200-500	~~2,500~~	1,600
~~300-500~~	500-800	~~2,100~~	1,400
~~500-800~~	800-1,100	~~1,700~~	1,000
~~800-1,000~~	1,100-1,400	~~1,400~~	700
~~1,000-1,200~~	1,400-1,600	~~1,000~~	300
~~1,200-1,400~~	1,600-	~~700~~	100
~~1,400-1,600~~		~~300~~	
~~Above 1,600~~		~~100~~	

* Subject to limiting stage of 20 feet at Dundee

MINIMUM LOW FLOW RELEASE

50 c.f.s.

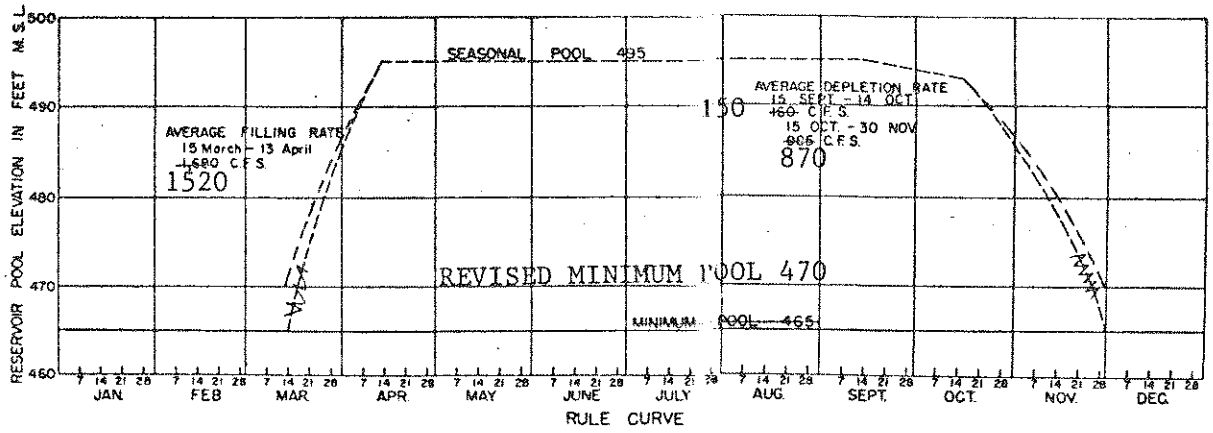

APPENDIX B

BALANCED HYDROGRAPH COMPOSITION SCHEME

GENERAL STEPS:

The maximum average flow-frequency duration curves such as shown in Figure 5.41 are used to obtain from a representative hydrograph a balanced hydrograph. The steps are as follows:

(1) For a selected exceedence frequency p, obtain the maximum average flow rates, $\overline{Q} = \overline{Q}(T_b, p)$, for various T_b-durations from the flow-frequency-duration curves. For the work reported herein T_b = 1, 3, t, ..., $(T_b)_{max}$.

(2) Consider periods that are T_b in duration starting with T_b = 1[day]. For the representative hydrograph, $Q_r(t)$, determine the T_b-period with the largest sum of ordinates. Call this sum of ordinates $SUM(T_b)$.

(3) Let $\Delta SUM = SUM(T_b) - SUM(T_b')$, where T_b' is the next smaller duration than T_b. If T_b equals 1-day, then $\overline{Q}(T_b', p) = 0.0$.

(4) Let $\Delta V = T_b * \overline{Q}(T_b, p) - T_b' * \overline{Q}(T_b', p)$. If T_b equals 1-day, then $\overline{Q}(T_b', p) = 0.0$.

(5) For each day in the T_b-set but not in the T_b'-set, the balanced hydrograph ordinate $Q_b(t)$ equals the product of $(\Delta V/\Delta SUM)$ and the corresponding representative hydrograph ordinate $Q_r(t)$, i.e.:

$$Q_b(t) = \frac{\Delta V}{\Delta SUM} * Q_r(t)$$

(6) If $T_b = (T_b)_{max}$, stop; the balanced hydrograph is then complete. Otherwise return to step 2 while increasing T_b.

EXAMPLE:

By way of an example, consider the following representative hydrograph ordinates:

Table B.1 Representative Hydrograph Ordinates

$Q_r(t)$ (cfs)	4100	5200	7000	6400	5900	5500	5100	4800	4600	4500
t(days	1	2	3	4	5	6	7	8	9	10

Let us further assume that the desired balance is specified by the following $\bar{Q} = \bar{Q}(T_b, p)$ values obtained from flow-frequency-duration curves for a given exceedence frequency p.

Table B.2 Maximum Average Flow Rates for a Given Probability, p, and for Various T_b-Durations

T_b-Days	1	3	5	10
$\bar{Q} = \bar{Q}(T_b, p)$ cfs	6000	5400	5000	4300

Iteration 1:

Step 2 (a) Set $T_b = 1$

(b) $SUM(T_b) = SUM(1) = Q_r(3) = 7000$

Step 3. $\Delta SUM = SUM(T_b) - SUM(T_b') = SUM(1) - 0 = 7000$

Step 4. $\Delta V = T_b * \bar{Q}(T_b, p) - T_b' * \bar{Q}(T_b', p) = 1 * 6000 - 0 = 6000$

Step 5. $Q_b(3) = \frac{\Delta V}{\Delta SUM} * Q_r(3) = \frac{6000}{7000} * 7000 = 6000$

Step 6. Since T_b is not equal to 10, the balanced hydrograph is not complete. Set $T_b = 3$ and return to step 2-b.

Iteration 2:

Step 2b. $SUM(T_b) = SUM(3) = Q_r(3) + Q_r(4) + Q_r(5) = 19300$

Step 3. $\Delta SUM = SUM(T_b) - SUM(T_b') = SUM(3) - SUM(1) = 13900 - 7000 = 12300$

Step 4. $\Delta V = T_b * \overline{Q}(T_b, p) - T_b' * \overline{Q}(T_b', p) = 3 * 5400 - 1 * 6000 = 102000$

Step 5. $Q_b(4) = \frac{\Delta V}{\Delta SUM} * Q_r(4) = \frac{10200}{12300} * 6400 = 5307$

$Q_b(5) = \frac{\Delta V}{\Delta SUM} * Q_r(5) = \frac{10200}{12300} * 5900 = 4893$

Step 6. Since T_b is not equal to 10, the balanced hydrograph is not complete. Set $T_b = 5$ and go to step 2-b.

Iteration 3:

Step 2b. $SUM(T_b) = SUM(5) = Q_r(2) + Q_r(3) + Q_r(4) + Q_r(5) + Q_r(6) = 30000$

Step 3. $\Delta SUM = SUM(T_b) - SUM(T_b') = SUM(5) - SUM(3) = 30000 - 19300 = 10700$

Step 4. $\Delta V = T_b * \overline{Q}(T_b, p) - T_b' * \overline{Q}(T_b', p) = 5 * 5000 - 3 * 5400 = 8800$

Step 5. $Q_b(2) = \frac{\Delta V}{\Delta SUM} * Q_r(2) = \frac{8800}{10700} * 5200 = 4277$

$Q_b(6) = \frac{\Delta V}{\Delta SUM} * Q_r(6) = \frac{8800}{10700} * 5500 = 4699$

Step 6. Since T_b is not equal to 10, set $T_b = 10$ and go to step 2-b.

Iteration 4:

Step 2b. $SUM(T_b) = SUM(10) = \sum_{t=1}^{10} Q_r(t) = 53100$

Step 3. $\Delta SUM = SUM(T_b) - SUM(T_b') = SUM(10) - SUM(5) = 53100 - 30000 = 23100$

Step 4. $\Delta V = T_b * \overline{Q}(T_b, p) - T_b' * \overline{Q}(T_b', p) = 10 * 4300 - 5 * 5000 = 18000$

Step 5. $Q_b(1) = \frac{\Delta V}{\Delta SUM} * Q_r(1) = \frac{18000}{23100} * 4100 = 3195$

$Q_b(7) = \frac{\Delta V}{\Delta SUM} * Q_r(7) = \frac{18000}{23100} * 5100 = 3974$

$Q_b(8) = \frac{\Delta V}{\Delta SUM} * Q_r(8) = \frac{18000}{23100} * 4800 = 3740$

$Q_b(9) = \frac{\Delta V}{\Delta SUM} * Q_r(9) = \frac{18000}{23100} * 4600 = 3584$

$Q_b(10) = \frac{\Delta V}{\Delta SUM} * Q_r(10) = \frac{18000}{23100} * 4500 = 3507$

Step 6. Since T_b equals 10, stop; balanced hydrograph is complete. The ordinates of the balanced hydrograph is shown in Table B.3.

Table B.3 Balanced Hydrograph Ordinates

$Q_b(t)$ (cfs)	3195	4277	6000	5307	4893	4699	3974	3740	3584	3507
t(days)	1	2	3	4	5	6	7	8	9	10

Water Resources Research Center
Lilly Hall of Life Sciences
Purdue University
West Lafayette, Indiana 47907